

**SYNTHESIS AND CHARACTERIZATION OF THERMOSETTING POLYIMIDE  
OLIGOMERS FOR MICROELECTRONICS PACKAGING**

by

Debra Lynn Dunson

Dissertation submitted to faculty of the Virginia Polytechnic Institute  
and State University in partial fulfillment of the requirements for the degree of

DOCTOR OF PHILOSOPHY

in

Chemistry

APPROVED:

Dr. James E. McGrath, Chairman

Dr. Edward R. Covington

Dr. Harry W. Gibson

Dr. Allan R. Shultz

Dr. John G. Dillard

Dr. Judy S. Riffle

April 21, 2000

Blacksburg, Virginia

**Keywords:** polyimides, crosslinking, dielectric films, thermosetting oligomers, fluorinated  
polyimides, phenylethynyl endcapped polyimides

Copyright 2000, Debra L. Dunson

# SYNTHESIS AND CHARACTERIZATION OF THERMOSETTING POLYIMIDE OLIGOMERS FOR MICROELECTRONICS PACKAGING

Debra L. Dunson

(ABSTRACT)

A series of reactive phenylethynyl endcapped imide oligomers has been prepared in either fully cyclized or amic acid precursor form. Soluble oligomers have been synthesized with controlled molecular weights ranging from 2- to 12 Kg/mol. Molecular weight characterization was performed using SEC (size exclusion chromatography) and  $^{13}\text{C}$ -NMR, revealing good agreement between the theoretical and experimental ( $M_n$ ) values. Crosslinked polyimides were obtained by solution or melt processing the oligomers into films and gradually heating in a programmed temperature manner up to the appropriate reaction temperature for the phenylethynyl groups, which is approximately 350-400°C. Thermal analysis of the resulting films showed high glass transition temperatures (>300°C) and excellent thermal stability, comparable to those found for thermoplastic control polyimides. The crosslinked films also had exceptional solvent resistance as evidenced by a high gel fraction ( $\geq 95\%$ ) following extraction in common solvents for several days. This was in contrast to the amorphous thermoplastic controls, which quickly dissolved upon immersion in solvents.

The monomers used for synthesizing the polyimide oligomers were varied systematically within the series to study the influence of both molecular structure and molecular weight on the physical and film-forming properties. The incorporation of fluorinated monomers, such as 4,4'-(hexafluoroisopropylidene)diphthalic anhydride (6FDA), reduced water absorption and lowered the dielectric constant relative to non-fluorinated polyimides in the series. When flexible ether linkages were incorporated in the repeat unit by using 4,4'-oxydianiline (ODA), relatively more

ductile solvent-cast films were obtained from oligomers having  $M_n$  values as low as 10 Kg/mol. Additionally, oligomer  $M_n$  and the relative rigidity/symmetry of the repeat unit structure greatly influenced the solubility of polyimides in NMP. For example, even 6FDA/p-phenylenediamine based oligomers with  $M_n$  values targeted below 10 Kg/mol precipitated from NMP at 180°C during solution imidization.

The relationship between solution viscosities of polyimide and poly(amic acid) thermosetting oligomers and wetting/spreading ability to form continuous films during spin casting was elucidated. Employing o-dimethoxybenzene (DMB) as a cosolvent with NMP improved the film-forming ability of the fully imidized 6FDA/ODA oligomer series. This was evidenced by a decrease in viscosity (via suppression of physical-type gel formation) and better overall coverage and clarity of the films. Humidity was found to have a detrimental effect, causing the polyimide oligomers to phase separate to form cloudy or porous films. When moisture was reduced, oligomers having  $M_n \geq 6$  Kg/mol formed spin cast films of  $<20\mu\text{m}$  thickness with good qualitative adhesion to several inorganic substrates.

Dielectric constants ( $\epsilon$ ) were estimated for several of the polyimides by measuring the refractive indices ( $n$ ) of the films and using Maxwell's relationship ( $\epsilon \cong n^2$ ). The apparent dielectric constants were low, ranging from 2.47 to 2.75.

The novel combination of low dielectric constant, solvent resistance and isotropic physical properties inherent in the thermosetting polyimide oligomers makes these materials excellent candidates for use as thin film insulating layers in microelectronics packaging applications.

Key words: polyimides, crosslinking, dielectric films, thermosetting oligomers, fluorinated polyimides, phenylethynyl endcapped polyimides.

## Acknowledgements

Virginia Tech has an abundance of deeply committed professional individuals who have been instrumental in my success in the doctoral program and to whom I am indebted. Foremost among these is my major advisor, Dr. Jim McGrath, who has been a constant source of inspiration, encouragement, understanding and knowledge. He is truly unique among educators and his energy/enthusiasm are unsurpassed.

I also wish to express my appreciation to my committee members, Dr. Judy Riffle, Dr. Harry Gibson, Dr. John Dillard and Dr. Allan Shultz, who are among Virginia Tech's finest chemistry faculty members. I especially appreciate Dr. Riffle's effort in recruiting me for the doctoral program at VT. Additionally, I owe the greatest debt of gratitude to my master's thesis advisor, Dr. Edward R. Covington (formerly at Tennessee State University), who inspired me to become a polymer chemist and to begin my doctoral program.

The best part of my success in the graduate program has been the work and social times shared with my fellow research group members. Each of them has, in their own way, helped and encouraged me during my stay at VT. I especially want to thank Dr. M. Sankarapandian (Sankar) and Dr. Charles Tchatchoua for the many hours they invested in assisting me. My appreciation is also extended to Dr. Qing Ji and Dr. H. Shobha for their GPC expertise and related discussions.

I would like to acknowledge the invaluable assistance of Mr. Tom Glass, NMR Spectroscopist for his assistance and expert knowledge. Additionally, I wish to thank the instructors in the Chemistry and Engineering Departments who shared their wealth of knowledge with me through numerous lectures, seminars and discussions in the classrooms of VT.

## List of Abbreviations and Definitions

6F	Hexafluoroisopropylidene group
6FDA	4,4'-(hexafluoroisopropylidene)diphthalic anhydride
6FDA:BPDA/DABTF	Copolyimide prepared from 6FDA and BPDA and DABTF
6FDA:BPDA/m-PDA	Copolyimide prepared from 6FDA and BPDA and m-PDA
6FDA/DABTF	Polyimide prepared from 6FDA and DABTF
6FDA/DAPI	Polyimide prepared from 6FDA and DAPI
6FDA/m-PDA	Polyimide prepared from 6FDA and m-PDA
6FDA/ODA	Polyimide prepared from 6FDA and ODA
6FDA/p-PDA	Polyimide prepared from 6FDA and p-PDA
6FDA/p-PDA:DABTF	Copolyimide prepared from 6FDA and p-PDA and DABTF
6FDA/p-PDA:DAPI	Copolyimide prepared from 6FDA and p-PDA and DAPI
6FDA/p-PDA:m-PDA	Copolyimide prepared from 6FDA and p-PDA and m-PDA
3FDAM	1,1-bis(4-aminophenyl)-1-phenyl-2,2,2-trifluoroethane
3FEDAM	1,1-bis[4-(4-aminophenoxy)phenyl]-1-phenyl-2,2,2-trifluoroethane
3FET	1,1-bis(4-aminophenyl)-1-(4-ethynylphenyl)-2,2,2-trifluoroethane
B3FB	2,2'-bis(trifluoromethyl)-benzidine
4-BDAF	2,2-bis[4-(4-aminophenoxy)phenyl]hexafluoropropane
BPDA	3,4,3',4'-biphenyltetracarboxylic dianhydride
BPDA/DAPI	Polyimide prepared from BPDA and DAPI
BPDA/p-PDA	Polyimide prepared from BPDA and p-PDA
CTE ( $\alpha$ )	Coefficient of Thermal Expansion
DABTF	3,5-Diaminobenzotrifluoride
DAPI	5(6)-Amino-1-(4-aminophenyl)-1,3,3-trimethylindane
DCB	o-Dichlorobenzene
Dielectric	Material that does not conduct electricity <sup>192</sup> .
Dielectric constant ( $\epsilon$ )	Term used to describe a material's ability to store charge when used as a capacitor device. It is the ratio of the charge that would be stored with free space to that stored with the material in question as the dielectric <sup>192</sup> .

Dielectric loss ( $\epsilon''$ )	Power dissipated by a dielectric as molecular friction opposes the molecular motion produced by an AC electric field <sup>192</sup> .
DMB	1,2-Dimethoxybenzene
DMSO	Dimethyl sulfoxide
EB	Elongation at break
Et <sub>3</sub> N	Triethylamine
Kapton™ (H-type)	Polyimide film from imidized poly(amic acid) prepared from PMDA and ODA
MCM-C	Multichip module ceramic electronic packaging
MCM-D	Multichip module deposited electronic packaging
$\langle M_n \rangle$	Number average molecular weight of polymers
NMP	N-Methyl-2-pyrrolidone
ODA	4,4'-Oxydianiline
4,4'-ODA/ODPA	Polyimide prepared from ODA and ODPA
ODPA	4,4'-Oxydiphthalic anhydride
PAA	Poly(amic acid)
PAE	Poly(amic ester)
m-PDA	1,3-Phenylenediamine
p-PDA	1,4-Phenylenediamine
PEPA or 4-PEPA	4-Phenylethynylphthalic anhydride
PFAAE	Perfluoroalkylene arylene ether
PI	Polyimide
PMDA	Pyromellitic dianhydride
PMDA/4-BDAF	Polyimide prepared from PMDA and 4-BDAF
PMDA/ODA	Polyimide prepared from PMDA and ODA; Kapton™ (H-type)
RI ( $n$ )	Refractive index
TFML	Thin film multilayer electronics packaging
Upilex S™	Polyimide prepared from BPDA and p-PDA

## Table of Contents

<b>Chapter 1 Introduction</b>	<b>1</b>
<b>Chapter 2 Literature Review</b>	<b>5</b>
2.1 Introduction	5
2.2 Synthesis of Polyimides	6
2.2.1 Classic Two-step Method of Polyimide Synthesis	6
2.2.1.1 Mechanism for Poly(amic acid) Formation	8
2.2.1.2 Monomer and Reaction Condition Effects: Poly(amic acid) Formation	8
2.2.1.2.1 Monomer Structure and Reactivity	10
2.2.1.2.2 Reaction Conditions: Temperature and Solvent Effects	12
2.2.1.3 Side Reactions	15
2.2.1.4 Thermal (Bulk) Imidization	17
2.2.1.4.1 Methods for Determining Residual Amide-Acid Groups in Insoluble Polyimides	19
2.2.1.5 Chemical Imidization	22
2.2.2 Synthesis of Polyimides via Derivatives of Poly(amic acid)s	24
2.2.3 One-step Method for High Temperature Solution Polymerization	24
2.2.3.1 Kinetics and Mechanism of High Temperature Solution Imidization	27
2.2.4 Synthesis of Polyimides via Diester-diacid Derivatives	32
2.2.4.1 Ester-Acid Solution Imidization Route Using Aliphatic Diamines	33
2.2.4.2 Mechanism of Ester-Acid Solution Imidization Route Using Aromatic Diamines	37

2.2.5 Other Synthetic Routes to Polyimides	39
2.2.5.1 Aromatic Nucleophilic Displacement Polymerization	39
2.2.5.2 Polymerization of Diisocyanates and Dianhydrides	42
2.2.5.3 Synthesis of Polyimides by Transimidization	46
2.3 Introduction to Structure-property Relationships of Polyimides	48
2.3.1 Microelectronics Packaging	48
2.3.1.1 Multilayer Interconnect Packaging	50
2.3.2 MCM-D Packaging Technology Based on Thin Film Multilayers (TFML)	51
2.3.2.1 Fabrication of MCM-D Packaging	56
2.3.2.1.1 Spin Coating	56
2.3.2.1.2 Building Thin Film Multilayers Using the Subtractive Process	57
2.3.2.1.3 Building Thin Film Multilayers Using Additive Processes	61
2.3.2.1.4 Bonding Integrated Circuit Chips to TFML Packaging	65
2.3.3 Property Considerations and Requirements for Interlayer Dielectrics	66
2.3.3.1 Electrical Properties	66
2.3.3.1.1 Dielectric Constant	66
2.3.3.1.2 Dissipation Factor	67
2.3.3.1.3 Dielectric Strength	68
2.3.3.2 Thermal Properties	69
2.3.3.2.1 Coefficient of Thermal Expansion	69
2.3.3.2.2 Thermal Stability	69
2.3.3.2.3 Glass Transition Temperature	71
2.3.3.3 Adhesive and Material Strength	72

2.3.3.3.1 Mechanical Properties	72
2.3.3.3.2 Adhesion	73
2.3.3.4 Properties in the Presence of Moisture, Solvents and Chemicals	76
2.3.3.4.1 Effect of Moisture	76
2.3.3.4.2 Effect of Solvent and Chemical Processes	77
2.4 Literature Review on Structure-property Relationships of Polyimides	77
2.4.1 Two-phase Linear Thermoplastic Polyimides	77
2.4.1.1 Polyimides Based on PMDA/ODA	78
2.4.1.2 Modified Kapton-type Polyimides for Tailoring Physical Properties	86
2.4.1.2.1 Poly(amic alkyl ester) Derivatives of PMDA/ODA for Improved Properties	88
2.4.1.2.1.1 PMDA/ODA-based Polyimides with Improved Adhesion	88
2.4.1.2.1.2 PMDA/ODA-based Low Stress Polyimides	91
2.4.1.2.1.3 PMDA/ODA-based Polyimides with Lower Dielectric Constant/Water Uptake	91
2.4.1.3 Polyimides Based on BPDA/p-PDA	97
2.4.2 Linear Thermoplastic Amorphous Polyimides	105
2.4.2.1 Linear Thermoplastic Amorphous Polyimides Based on Fluorinated Monomers	105
2.4.2.1.1 Structure/property Considerations for Dielectrics	105
2.4.2.1.2 Review of Thermoplastic Amorphous Fluorinated Polyimides	106
2.4.3 Crosslinked Amorphous Polyimides	109
2.4.3.1 Thermosetting Polyimides for Use as Interlayer Dielectrics	112

2.4.3.1.1 Trialkoxysilyl Functionalized Poly(amic ester) Oligomers	112
2.4.3.1.2 Bismaleimides and Maleimide Functionalized Oligomers	114
2.4.3.1.2.1 Maleimide Functionalized Oligomers for Microelectronics	116
2.4.3.1.3 Acetylene-containing Thermosetting Polyimides	118
2.4.3.1.3.1 Phenylethynyl Endcapped Polyimide Oligomers	119
2.4.3.1.3.2 Acetylene Functionalized Oligomers for Microelectronics	121
<b>Chapter 3 Experimental</b>	<b>123</b>
3.1 Materials Utilized in Synthesis and Characterization Experiments	123
3.1.1 Solvents	123
3.1.2 Monomers	124
3.1.2.1 Diamines	124
3.1.2.2 Dianhydrides	127
3.1.2.3 Endcappers	128
3.2 Characterization Methods	129
3.2.1 Gel Permeation Chromatography (GPC)	129
3.2.2 Nuclear Magnetic Resonance Spectroscopy (NMR)	129
3.2.3 Fourier Transform Infrared Spectroscopy (FTIR)	129
3.2.4 Thermogravimetric Analysis (TGA)	130
3.2.4.1 Dynamic TGA	130
3.2.4.2 Isothermal TGA	130
3.2.5 Differential Scanning Calorimetry (DSC)	130
3.2.6 Dynamic Mechanical Analysis (DMA)	131
3.2.7 Rotational Viscometry	131

3.2.8 Film Sample Preparation	132
3.2.8.1 Melt-pressed Films	132
3.2.8.2 Solvent-cast Free-standing Films	132
3.2.8.3 Spin-cast Films on Inorganic Substrates	133
3.2.9 Extraction Experiments	134
3.2.9.1 Soxhlet Extractions in Chloroform	134
3.2.9.2 Extractions in NMP at 60°C	134
3.2.10 Refractive Index (RI) Measurement	136
3.2.11 Water Absorption	136
3.3 Polyimide Oligomer Synthesis	136
3.3.1 Molecular Weight Control in Step Growth Polymerization	137
3.3.2 Polyimide Oligomer Synthesis by the Classic Two-step Route	139
3.3.2.1 Poly(amic acid) Formation	140
3.3.2.2 Thermal Imidization of Poly(amic acid)	140
3.3.3 Polyimide Oligomer Synthesis by the Ester-Acid Route	140
3.3.3.1 Example of Polyimide Oligomer Synthesis by the Ester-Acid Route	141
<b>Chapter 4 Results and Discussion</b>	<b>142</b>
4.1 Introduction	142
4.1.1 Low Molecular Weight Fluorinated Thermosetting Polyimide Oligomers	142
4.1.1.1 Thermosetting Polyimide Oligomers Based on 6FDA and m-PDA	145
4.1.1.2 Thermosetting Polyimide Oligomers with Target $\langle M_n \rangle$ Values of 3 Kg/mol	154
4.1.1.2.1 Polyimide Oligomers Based on 6FDA/p-PDA:m-PDA	157

4.1.1.3 Polyimide Oligomers Based on 6FDA/p-PDA_____	160
4.1.1.4 Polyimide Oligomers Based on 6FDA/p-PDA:DABTF_____	163
4.1.1.5 Oligomers Containing p-PDA:m-PDA with Target $\langle M_n \rangle$ Values of 6-12 Kg/mole_____	164
4.1.1.6 Polyimide Oligomers Based on 6FDA:BPDA and m-PDA or DABTF____	169
4.1.1.6.1 Copolyimides Based on 80:20 6FDA:BPDA_____	169
4.1.1.6.2 Copolyimides Based on 90:10 6FDA:BPDA_____	171
4.1.1.6.2.1 Characterization of Polyimides Based on 90:10 6FDA:BPDA__	173
4.1.1.7 Polyimide Oligomers Based on 6FDA/DAPI_____	175
4.1.1.7.1 Polyimide Oligomer Based on 6FDA/DAPI;p-PDA/PEPA_____	179
4.2 Properties of Soluble, Low $\langle M_n \rangle$ Fluorinated Thermosetting Polyimide Oligomers__	180
4.2.1 Introduction_____	180
4.2.1.1 Solution Viscosity of Low $\langle M_n \rangle$ Fluorinated Thermosetting Polyimide Oligomers_____	180
4.2.1.2 Water Absorption of Low $\langle M_n \rangle$ Fluorinated Thermosetting Polyimide Oligomers_____	185
4.2.1.3 Refractive Index of Fluorinated Polyimides_____	189
4.2.1.4 CTE of Low $\langle M_n \rangle$ Fluorinated Thermosetting Polyimide Oligomers____	191
4.3 Film Forming Series of Thermosetting Polyimide Oligomers_____	193
4.3.1 Thermosetting Polyimide Oligomers Based on 6FDA/ODA/PEPA_____	193
4.3.1.1 Synthesis and Characterization of 6FDA/ODA Polyimides and Poly(amic acid)s_____	194
4.3.1.2 Solvent Cast Films of 6FDA/ODA/PEPA Polyimide and Poly(amic acid)	

Oligomers_____	194
4.3.1.2.1 Thick (7-10 mil) Solution Cast Films_____	194
4.3.1.2.1.1 Thick (7-10 mil) Solution Cast Films from 6FDA/ODA/PEPA	
Polyimides_____	196
4.3.1.2.1.2 Thick (7-10 mil) Solution Cast Films from 6FDA/ODA/PEPA	
Poly(amic acid)s_____	199
4.3.2 Thermosetting Polyimide Oligomers Based on BPDA/DAPI/PEPA_____	202
4.3.2.1 Synthesis and Characterization of BPDA/DAPI/PEPA Polyimides_____	202
4.3.2.2. Solvent Cast Films of BPDA/DAPI/PEPA Polyimide Oligomers_____	202
4.3.2.2.1 Thick (7-10 mil) Solution Cast Films from BPDA/DAPI/PEPA	
Polyimides_____	202
4.3.3. Properties of 6FDA/ODA and BPDA/DAPI Polyimide Oligomers_____	204
4.3.3.1 Introduction_____	204
4.3.3.1.1 Glass Transition Temperatures of 6FDA/ODA and BPDA/DAPI Thermoset	
Films_____	206
4.3.3.1.2 Isothermal Weight Loss of 6FDA/ODA and BPDA/DAPI Thermoset	
Films_____	206
4.3.3.1.3 Solvent Resistance Studies of 6FDA/ODA and BPDA/DAPI Thermoset	
Films_____	209
4.3.3.1.4 Refractive Index of 6FDA/ODA and BPDA/DAPI Thermoset Films_	211
4.3.4 Spin Cast Films of 6FDA/ODA/PEPA and BPDA/DAPI Polyimide Oligomers_	211
4.3.4.1 Spin Cast Films of 6FDA/ODA/PEPA Polyimide and Poly(amic acid)	
Oligomers_____	214

4.3.4.1.1 Spin Cast Films of 6FDA/ODA/PEPA Polyimide Oligomers	214
4.3.4.1.2 Spin Cast Films of 6FDA/ODA/PEPA Poly(amic acid) Oligomers	217
4.3.4.1.3 Spin Cast Films of BPDA/DAPI/PEPA Polyimide Oligomers	219
<b>Chapter 5 Conclusions</b>	<b>222</b>
<b>References</b>	<b>227</b>
<b>Vita</b>	<b>241</b>

## List of Figures

2.2.1	Commonly used dianhydride and diamine monomers_____	11
2.2.2	Kapton™ repeat unit structure_____	20
2.2.3	Remaining amic acid content and intrinsic viscosity as a function of imidization reaction time_____	30
2.2.4	<sup>1</sup> H-NMR spectrum of 4,4'-ODA/ODPA poly(amic acid/imide) at different imidization stages_____	31
2.2.5	Diester dicarboxylic acids formed by the reaction of dianhydride and alcohol_____	35
2.2.6	Intramolecular poly(amide acid) salt from aliphatic amino group_____	36
2.2.7	Delocalization of negative charge in Meisenheimer transition state in imide system_____	41
2.2.8	Proposed 7-membered cyclic intermediate in the reaction of isocyanate with anhydride_____	45
2.3.1	Polyimide planarization advantage over silicon dioxide films_____	55
2.3.2	Plot of empirical thickness versus spin speed for polyimide film obtained from a commercial poly(amic acid) solution_____	58
2.3.3	Thermal processing of polyimide films for interlayer dielectrics_____	59
2.3.4	Photolithographic process and dry etching of planarized film_____	62
2.3.5	Comparison of wet etching processing for a conventional and a photosensitive polyimide_____	64
2.4.1	Interactions between polyimide chains_____	79

2.4.2	WAXD patterns of PMDA/ODA polyimide films_____	82
2.4.3	Representation of the smectic-like order of PMDA/ODA polyimide films_____	83
2.4.4	Dissipation factor vs. frequency for PMDA/ODA containing capacitor devices_____	87
2.4.5.	Dynamic mechanical behavior for poly(imide-co-arylene ether phenyl quinoxaline) (PI/PQE) block copolymer as a function of temperature_____	90
2.4.6	Residual stress versus temperature plots for polyimide/polydimethylsiloxane copolymers_____	92
2.4.7	Structure of perfluoroalkylene arylene ethers (PFAAEs)_____	93
2.4.8	Repeat unit structure of PMDA/4-BDAF polyimide_____	96
2.4.9	Structure of PMDA/3FDAM/3FET copolyimide_____	98
2.4.10	Repeat unit structure of BPDA/p-PDA polyimide_____	100
2.4.11	Repeat unit structure of copolymer of BPDA/p-PDA/B3FB_____	103
2.4.12	Fluorinated monomers commonly used for linear amorphous thermoplastic polyimides_____	107
2.4.13	WAXS spectra of 3FEDAM-6FDA/PMDA copolyimides_____	110
2.4.14	Trialkoxysilyl endcapped poly(amic ester) oligomers_____	113
2.4.15	General formula for bismaleimide_____	115
2.4.16	General formula for phenylethynyl-terminated polyimides_____	120
3.2.1	Glassware apparatus for extraction of cured polyimide films_____	135
4.1.1	Monomers used for synthesis of ~3 Kg/mol polyimide oligomer series_____	143
4.1.2	FTIR spectrum of ~2 Kg/mol 6FDA/m-PDA polyimide oligomer_____	146
4.1.3	<sup>13</sup> C-NMR spectrum of ~2 Kg/mol 6FDA/m-PDA imide oligomer_____	149

4.1.4	GPC chromatogram of ~10 Kg/mol 6FDA/m-PDA imide oligomer_____	150
4.1.5	DSC thermogram of ~2 Kg/mol 6FDA/m-PDA imide oligomer_____	151
4.1.6	Solvent resistance study of 6FDA/m-PDA polyimide films in NMP_____	155
4.1.7	Repeat unit structures of series of ~3 Kg/mol polyimide oligomers_____	156
4.1.8	<sup>13</sup> C-NMR spectra of 6FDA:BPDA 90:10 /m-PDA/PEPA imide oligomer_____	172
4.1.9	Molecular structure of diaminophenylindane (DAPI)_____	176
4.1.10	Viscosity as a function of concentration for solutions of polyimide oligomers in NMP_____	181
4.1.11	Viscosity as a function of concentration for solutions of ~7 Kg/mol 6FDA/DAPI oligomer in NMP_____	183
4.1.12	Weight increase (%) from absorbed water as a function of humidity exposure time ( $t^{1/2}$ ) for crosslinked polyimide films_____	186
4.1.13	Weight increase (%) from absorbed water as a function of humidity exposure time ( $t^{1/2}$ ) for crosslinked polyimide films with BPDA content_____	187
4.1.14	DMA thermogram of crosslinked polyimide film obtained from ~7 Kg/mol 6FDA/ODA/PEPA oligomeric precursor_____	207
4.1.15	Isothermal TGA data for a thermoset film of 6FDA/ODA polyimide and for a Kapton film at 400°C under nitrogen_____	210

## List of Schemes

2.2.1	Classic two-step method of polyimide synthesis_____	7
2.2.2	Mechanism for formation of poly(amic acid)_____	9
2.2.3	Hydrolytic degradation of poly(amic acid)_____	16
2.2.4	Conformations of poly(amic acid) during cyclodehydration_____	18
2.2.5	Mechanism of chemical imidization_____	23
2.2.6	Ultem™ --high temperature solution polymerization_____	26
2.2.7	Mechanism of high temperature solution imidization_____	29
2.2.8	Synthesis of polyimides via ester-acid solution imidization route_____	34
2.2.9	Mechanism of anhydride formation during ester-acid solution imidization route to polyimides_____	38
2.2.10	Reaction of activated bisnitroimide monomer with bisphenoxide_____	40
2.2.11	Mechanism of water catalyzed reaction of diisocyanates and dianhydrides_____	44
2.2.12	Schematic of the imide-amine interchange or transimidization reaction_____	47
2.4.1	Synthesis of poly(imide-co-arylene ether phenylquinoxaline)_____	89
2.4.2	Crosslinking of bismaleimides_____	117
4.1.1	Ester-acid route for synthesizing PEPA-encapped polyimide oligomers_____	144

## List of Tables

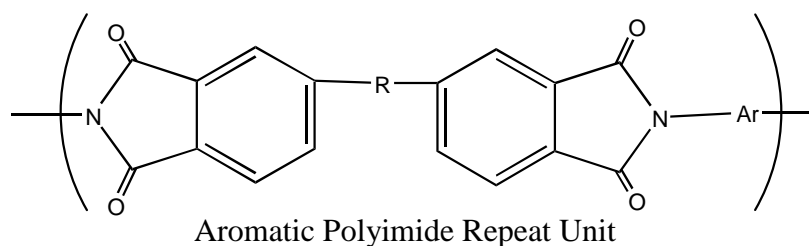
2.2.1	Electron Affinity and Log Rate Constant Values for Aromatic Dianhydrides	13
2.2.2	Log Rate Constant and pK <sub>a</sub> Values for Aromatic Diamines	14
2.2.3	Infrared Absorption Bands of Imides and Related Compounds	21
2.3.1	Multichip Module Wiring Characteristics	52
2.3.2	Comparison of Properties of Polyimide and Silicon Dioxide Dielectrics	54
2.3.3	Thermal Expansion Coefficient Values	70
2.3.4	Adhesion Characteristics of the Three Classes of Polyimides	75
2.4.1	Selected Properties of PMDA/ODA Polyimide	80
2.4.2	Imide-PFAAE Mechanical, Thermal and Dielectric Properties	94
2.4.3	Properties of Kapton (H-type) and Upilex S Films	102
2.4.4	Properties of BPDA/p-PDA/B3FB Polyimides	104
2.4.5	Properties of Fluorinated Polyimides Based on B3FB	108
2.4.6	Dielectric Properties of 6FDA-based Polyimides	111
4.1.1	Molecular Weight and Thermal Analysis Data for 6FDA/m-PDA-based Oligomers	148
4.1.2	Gel Fractions of Crosslinked 6FDA/m-PDA Oligomers	153
4.1.3	Molecular Weight and Thermal Analysis Data for 6FDA/p-PDA:m-PDA/PEPA Imide Oligomers	159
4.1.4	Molecular Weight and Thermal Analysis Data for 6FDA/p-PDA/PEPA Homopolyimide Oligomers	162

4.1.5	Molecular Weight and Thermal Analysis Data for 6FDA/DABTF:p-PDA and 6FDA/DABTF PEPA-encapped Polyimide Oligomers_____	165
4.1.6	Solubility of 6FDA/p-PDA:m-PDA/PEPA Oligomers in Organic Solvents_____	167
4.1.7	Molecular Weight and Thermal Analysis Data for 6FDA/p-PDA:m-PDA 90:10 PEPA-encapped Oligomers_____	168
4.1.8	Molecular Weight and Thermal Analysis Data for 6FDA:BPDA 90:10 Polymerized with m-PDA and PEPA_____	174
4.1.9	Molecular Weight and Thermal Analysis Data for 6FDA/DAPI/PEPA Imide Oligomers_____	178
4.1.10	Total Water Absorbed (%) of Cured Polyimide Films_____	188
4.1.11	Refractive Index and Estimated Dielectric Constant of Polyimides_____	190
4.1.12	Thermal Expansion Coefficients of Crosslinked Polyimide Films_____	192
4.1.13	Characterization of Molecular Weight of 6FDA/ODA/PEPA Polyimides and Poly(amic acid)s_____	195
4.1.14	Qualitative Results of Thick (7-9 mil) Films from Solution Casting Fully Imidized 6FDA/ODA/PEPA Thermosetting Oligomers_____	198
4.1.15	Qualitative Results of Thick (7-9 mil) Films from Solution Casting Amic-acid 6FDA/ODA/PEPA Thermosetting Oligomers_____	201
4.1.16	Characterization of Molecular Weight of BPDA/DAPI/PEPA Polyimides_____	203
4.1.17	Qualitative Results of Thick (7-9 mil) Films from Solution Casting Fully Imidized BPDA/DAPI/PEPA Thermosetting Oligomers_____	205
4.1.18	Results of Thermal Analysis of Crosslinked Polyimide Films_____	208
4.1.19	Gel Fractions of Cured Polyimide Films Exposed to NMP at 60°C_____	212

4.1.20	Refractive Index and Estimated Dielectric Constant of 6FDA/ODA and BPDA/DAPI Thermoset Films_____	213
4.1.21	Qualitative Results of Spin Cast Films from Fully Imidized 6FDA/ODA/PEPA Thermosetting Oligomers_____	216
4.1.22	Qualitative Results of Spin Cast Films from Amic-acid 6FDA/ODA/PEPA Thermosetting Oligomers_____	218
4.1.23	Qualitative Results of Spin Cast Films from Fully Imidized BPDA/DAPI/ PEPA Thermosetting Oligomers_____	220

## Chapter 1 Introduction

Polyimides belong to the important class of organic materials known as “high performance” polymers due to their exceptionally high thermo-oxidative stability<sup>1</sup>. The structural composition of aromatic polyimides consists primarily of heterocyclic imide and aryl groups, which are linked sequentially by simple atoms or groups<sup>1</sup>, as shown in the generic repeat unit below.



The comparatively rigid structure of polyimides provides high glass transition temperatures ( $T_g > 300^\circ\text{C}$ ) and imparts good mechanical strength and high modulus<sup>2-4</sup>. The linearity and stiffness of the cyclic backbone allow for molecular ordering. This phenomenon results in lower coefficients of thermal expansion (CTE) than those found for thermoplastic polymers having coiled, flexible chains<sup>5-6</sup>. Additionally, the morphology of long, linear ordered chains provides solvent resistance to the aromatic polyimides.

The outstanding thermal and chemical resistance of polyimides has promoted their use as spin-on dielectric films for isolating metal lines in multilevel electronics packaging. One important function of the dielectric film is to block electromagnetic interaction between parallel metal conducting lines that are operating independently (called “cross talk” noise)<sup>7</sup>. For effective blocking ability the film must have low electrical conductivity/permittivity. Thus,

minimal electrical signal interaction occurs with the dielectric medium and both “cross-talk” and signal transmission delays are decreased<sup>7-8</sup>. The measure of the film’s insulating ability is its dielectric constant ( $\epsilon$ ). Materials having dielectric constants of less than 4.0, the value of the standard SiO<sub>2</sub> insulator, have been recognized by the electronics industry as being superior in electrical performance to ceramic materials<sup>9</sup>. The dielectric constants of aromatic polyimides, such as Kapton-H, approach 3.0 (when dry), which has led to widespread use of these materials as thin film insulators.

Although the properties of wholly aromatic polyimides are apparently ideal for microelectronics applications, there are several problems inherent in these systems. The intractable/insoluble aromatic polyimides must be prepared initially in the form of a soluble precursor, poly(amic acid), which is obtained from solution polycondensation of an aromatic diamine with a dianhydride. The solution of poly(amic acid) is then used for spin casting films that are subsequently imidized on the substrate. The poly(amic acid) precursor is hydrolytically unstable which can result in degradation and chain scission under humid conditions<sup>10</sup>. Additionally, release of water during imidization of the poly(amic acid) causes film shrinkage that may result in delamination and voids.

Further problems encountered with wholly aromatic rigid polyimides involve their anisotropic physical properties, which arise from the large degree of molecular packing of the rigid-rod like chains<sup>5</sup>. Anisotropy in CTE and dielectric constant are particularly undesirable because the values are significantly higher with respect to the out-of-plane and the in-plane direction of chain alignment, respectively<sup>7</sup>.

To eliminate the use of poly(amic acid) precursors, amorphous polyimides have been designed which are soluble in common organic solvents<sup>11-13</sup>. This has been achieved by

incorporating flexible stable linking groups, such as oxygen, hexafluoroisopropylidene and sulfone, between aromatic rings. Also, asymmetrical, non-planar and kinked moieties have been introduced into the polyimide backbone without sacrificing the thermo-oxidative stability of the materials. The solubility of the resulting systems allows them to be fully-imidized in homogeneous solutions. The polyimide solids can be isolated following reaction by precipitating, filtering and drying.

The amorphous polyimides are easily stored and processed because, unlike poly(amic acid)s, they are hydrolytically stable. Since the solid materials fully dissolve in common solvents, solutions of the desired concentration can be prepared as needed for spin-casting films. The amorphous morphology of the polyimide results in films that normally exhibit isotropic physical properties. However, soluble polyimides pose a problem when creating the multi-layered film structures in microelectronics packaging: the solvent attacks existing films as successive dielectric layers are spin-cast on top of them.

To alleviate this problem, soluble polyimide oligomers have been designed with phenylethynyl endgroups that react to form crosslinked films upon heating in the temperature range 350-380°C<sup>14-17</sup>. The amorphous crosslinked materials display excellent solvent resistance and afford thermal stability comparable to that of rigid ordered polyimides, such as Kapton-H.

The research described in this dissertation has involved the synthesis and characterization of controlled molecular weight thermosetting polyimide oligomers with reactive phenylethynyl endgroups. The objective was to obtain soluble oligomers that would exhibit good film-forming properties during spin casting and achieve excellent adhesion upon crosslinking to form solvent-resistant films. A series of polyimide oligomers of similar molecular weight, but differing in

repeat unit, was prepared and characterized to enable a comparison with respect to thermal, solution and film properties.

Oligomers in the series displaying relatively better properties for electronics applications were subjected to further investigations with regard to film formation. A systematic study was conducted using three different polyimide oligomers to elucidate the influence of molecular structure/molecular weight on the film forming ability. This was achieved by preparing a series of oligomers in which the molecular weight was increased for a given repeat unit structure. To further study structural influences on film formation, a series of poly(amic acid)s comprised of the same monomers as the fully imidized counterparts was synthesized and characterized. It was projected that the poly(amic acid)s might behave differently during the film forming process due to intermolecular hydrogen bonding of amide and acid groups along the chains.

A primary goal of this research was to produce polyimides having lower dielectric constants than those currently used in microelectronics applications. To determine whether this had been achieved, the dielectric constants of several of the polyimide films were estimated using refractive index measurements.

## **Chapter 2 Literature Review**

### **2.1 Introduction**

The growth of modern technology has posed a constantly increasing need for materials that can perform well under harsh conditions, such as elevated temperatures. Indeed, the initial excitement generated upon introduction of polyimides by DuPont in the 1960s resulted from the outstanding thermo-oxidative stability of these materials<sup>1</sup>. Early investigations revealed the aromatic polyimides to possess a desirable array of other outstanding characteristics, such as radiation/chemical resistance, low dielectric constant, selective permeability to gases, film toughness under rigorous conditions of air aging, and retention of high mechanical strength over a wide temperature range<sup>18</sup>. These versatile properties have stimulated interest in expanding the applications for polyimides in the manufacturing of modern aerospace/automotive transportation vehicles and microelectronics devices. It is the interest of academic and industrial research to elucidate the optimum methods for producing polyimide materials tailored to these growing manufacturing interests.

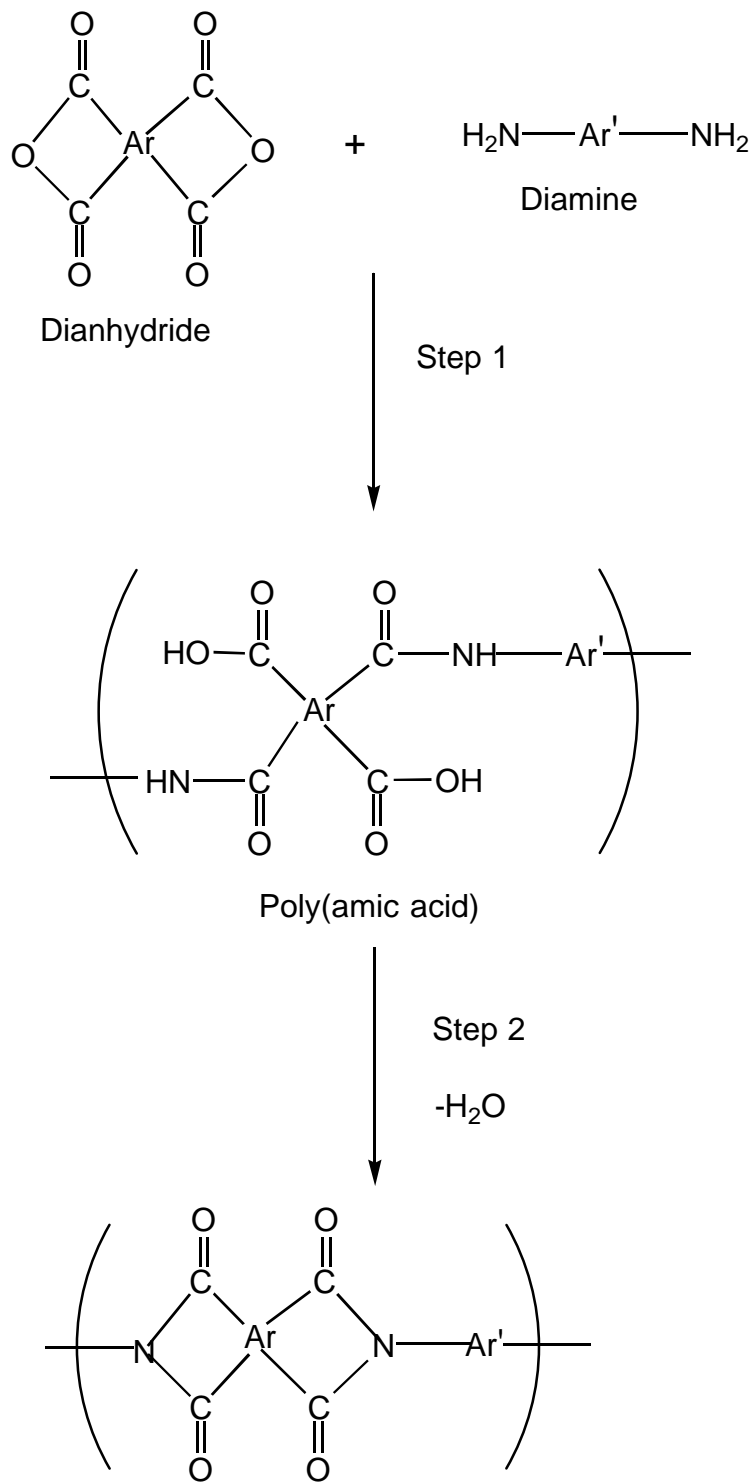
This dissertation is a contributing research segment with regard to synthesis and characterization of thermosetting polyimide oligomers targeted for use as dielectric thin films in electronics applications. This chapter will review developments in polyimide synthesis and structure/property modifications as revealed in the published literature. The following sections will provide the background information to assist the reader in understanding the fundamental approaches utilized in the dissertation research.

## 2.2 Synthesis of Polyimides

Aromatic polyimides, in general, are comprised of five-membered heterocyclic imide units and aromatic rings. The structure of these “cyclic chain” systems makes polyimides insoluble/intractable and, thus, not amenable to traditional solution/melt polycondensation reactions. Early attempts made at DuPont R & D in the 1950s utilizing direct reaction of dianhydrides and aromatic diamines in the melt or in solution resulted in precipitation of intractable low molecular weight polyimides<sup>3-4</sup>. However, by 1956, Dr. A. Endrey at DuPont had successfully pioneered the invention of obtaining polyimides through reaction of soluble/processable intermediates known as poly(amic acid)s. This type of reaction consisted of two steps: the solution polycondensation of an aromatic diamine and a dianhydride to form poly(amic acid) which could be processed into a useful shape, followed by cyclodehydration of the amide-acid to form polyimide<sup>18-19</sup>.

### 2.2.1 Classic Two-step Method of Polyimide Synthesis

In the classic two-step method of synthesizing aromatic polyimides, the initial step consists of preparing a solution of the aromatic diamine in a polar aprotic solvent, such as N-methylpyrrolidone (NMP), to which is added a tetracarboxylic dianhydride. The formation of poly(amic acid) occurs during this step at ambient temperature and is complete within 24 hours, depending on monomer reactivity. The high molecular weight poly(amic acid) produced is fully soluble in the reaction solvent and, thus, the solution may be cast into a film on a suitable substrate. The second step in this synthetic method is the cyclodehydration reaction (imidization) that is accomplished by heating the film to elevated temperatures, or by incorporating a chemical dehydrating agent<sup>20</sup>. The overall reaction scheme for the two-step method is depicted in Scheme 2.2.1.



Scheme 2.2.1 Classic two-step method of polyimide synthesis.

### 2.2.1.1 Mechanism for Poly(amic acid) Formation

The reaction mechanism for forming poly(amic acid) is shown in Scheme 2.2.2. Nucleophilic acyl substitution occurs at one of the carbonyl carbons of a phthalic anhydride unit comprising the tetracarboxylic acid anhydride. The attacking nucleophile consists of a nitrogen from the aromatic diamine with its unshared pair of electrons.

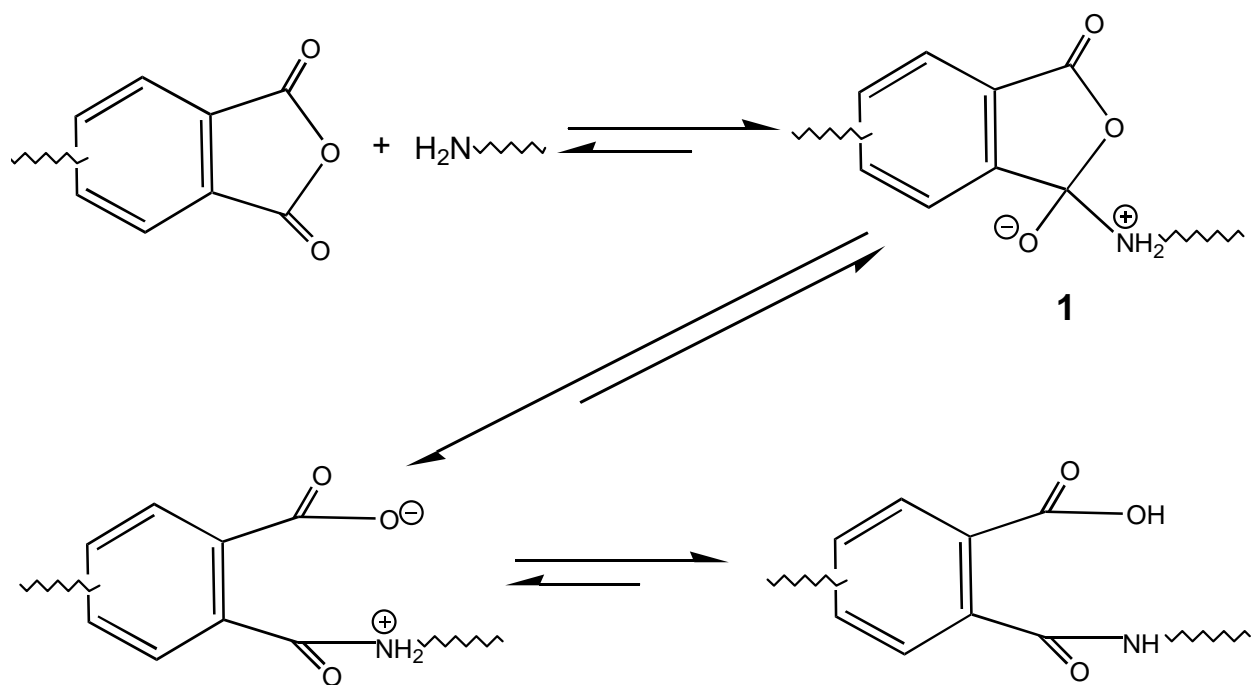
Bonding between the carbonyl carbon and the nitrogen results in formation of a cyclic intermediate, 1, with the pi electrons shifted onto the oxygen. This intermediate is short lived because the displaced electron pair shifts back to reform the carbonyl double bond and simultaneous bond-breaking occurs between the carbon and a “leaving group”.

The bond that must break in this ejection step to give linear amide-acid is that which releases the central oxygen of the cyclic intermediate 1, thereby giving a carboxylate leaving group. However, if instead the bond breaks between the nitrogen and the developing  $sp^2$  carbon, the reaction is reversed to give the starting species – free amine and anhydride groups. The rate of the forward reaction must be more rapid than the reverse to achieve high molecular weight poly(amic acid). Since the carboxylate group is chemically bonded, it cannot be systematically removed to drive equilibrium in the forward direction. However, it can be “deactivated” through hydrogen bonding with a basic solvent, such as NMP<sup>26, 29-31</sup>.

### 2.2.1.2 Monomer and Reaction Condition Effects: Poly(amic acid) Formation

To obtain high molecular weight linear poly(amic acid) the typical requirements for step-growth polycondensation reactions must be met<sup>21</sup>:

- (1) monomers must be highly pure (>99.9%)
- (2) one-to-one stoichiometry of monomers must be employed



Scheme 2.2.2 Mechanism for formation of poly(amic acid).

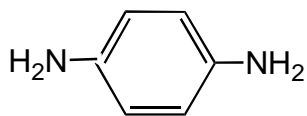
- (3) monomers must be difunctional and reacting groups must be mutually accessible
- (4) length of reaction time must be sufficient for high conversion
- (5) side reactions must be minimal or absent.

An equilibrium polycondensation reaction must satisfy an additional requirement for providing high molecular weight polymer: the forward reaction must be significantly faster than the reverse. Many studies have been published concerning reaction rate and how it is affected by various factors, including monomer-structure, temperature, solvent composition and side reactions. The relevant literature findings will be reviewed to provide a fundamental understanding. Figure 2.2.1 contains structures, names and acronyms of monomers commonly used for poly(amic acid) synthesis to aid this discussion.

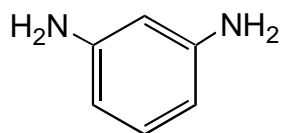
#### **2.2.1.2.1 Monomer Structure and Reactivity**

The phthalic anhydride groups, which comprise aromatic tetracarboxylic acid anhydrides, are highly electrophilic acylating agents toward amines<sup>22</sup>. The enhanced electrophilicity results from strong electron-withdrawing effects exerted by the ortho-placement of the carbonyl groups<sup>4</sup>. However, nearly all tetracarboxylic acid anhydrides contain bridging groups or atoms between the two phthalic anhydride units that can affect the electron-accepting ability of the carbonyl carbons.

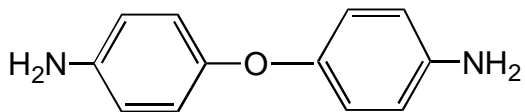
The ability to accept an incoming electron pair from a nucleophile has been found to be contingent on the electron affinity ( $E_A$ ) of the dianhydride. Early work has demonstrated the correlation between  $E_A$ , measured for a series of aromatic dianhydrides, and the log of the reaction rate constant ( $\log k_r$ ) for acylation of ODA (Table 2.2.1)<sup>23</sup>. From this data, it can be surmised that both  $E_A$  and reaction rate vary significantly according to the electronic environment of the carbonyl carbons as influenced by dianhydride bridging groups.



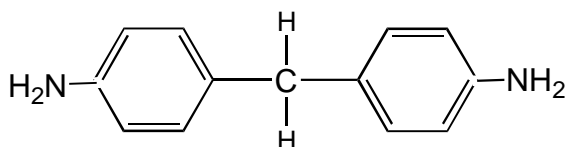
p-phenylene diamine  
p-PDA



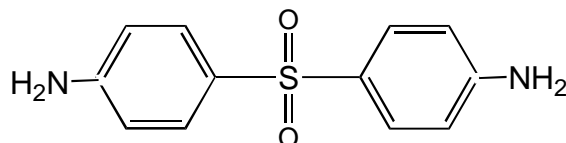
m-phenylene diamine  
m-PDA



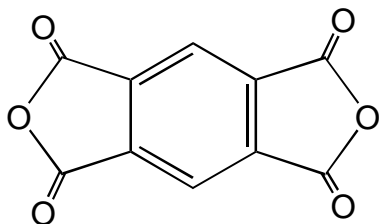
4,4'-diaminodiphenyl ether ODA



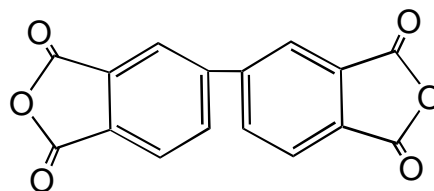
4,4'-methylene dianiline MDA



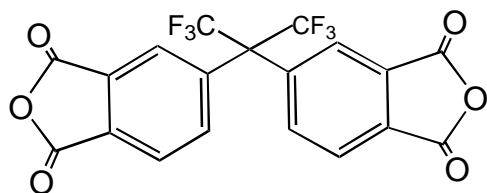
4,4'-diaminodiphenyl sulfone DDS



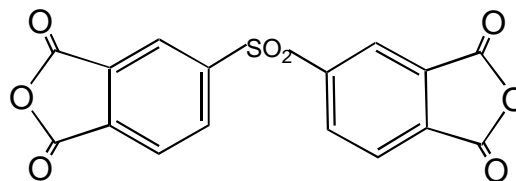
pyromellitic dianhydride PMDA



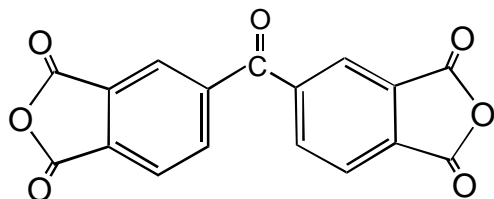
3,3',4,4'-biphenyltetracarboxylic  
dianhydride BPDA



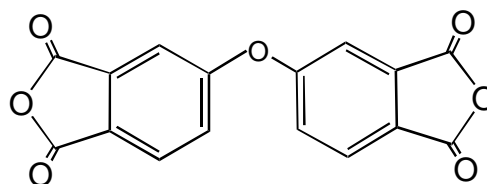
4,4'-hexafluoroisopropylidenebis(phthalic anhydride)  
6FDA



4,4',5,5'-sulfonyldiphthalic anhydride DSDA



3,3',4,4'-benzophenonetetracarboxylic dianhydride  
BTDA



3,3',4,4'-oxydiphthalic anhydride ODPA

Figure 2.2.1 Commonly used dianhydride and diamine monomers.

Sulfone and carbonyl bridging groups decrease the electron density of the anhydride carbonyl carbon by delocalization of electrons through the pi orbitals. Thus,  $E_A$  and  $\log k_r$  are relatively higher for DSDA and BTDA than those found for ODPa, which has an electron-donating ether bridging group.

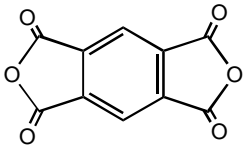
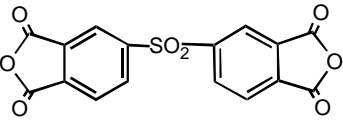
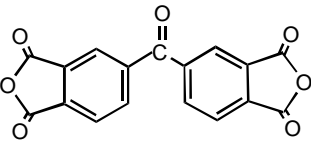
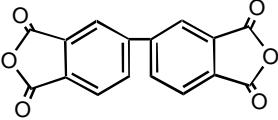
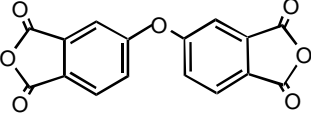
The relative nucleophilicity of diamine monomers correlates with their basicity<sup>24-26</sup>. Early investigations demonstrated the direct relationship between  $pK_a$  values and the rate constants ( $k_r$ ) determined for a series of diamines reacted with PMDA (Table 2.2.2)<sup>24</sup>. The more basic diamines, such as p-PDA and ODA, showed relatively higher reaction rates. The electron-withdrawing nature of the bridge group also affected the acylation rate of diamines. Both the  $pK_a$  and acylation rate of 4,4'-diaminobenzophenone were relatively low due to the electron-withdrawing carbonyl bridge.

Monomer reactivity is important in controlling equilibrium to favor the formation of poly(amic acid). High molecular weight poly(amic acid) is obtained when the electron affinity of the dianhydride and the basicity of the diamine are both high.

#### **2.2.1.2.2 Reaction Conditions: Temperature and Solvent Effects**

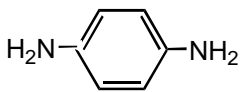
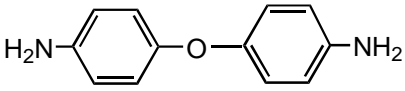
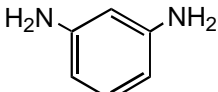
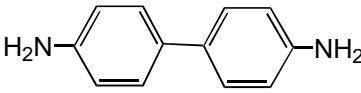
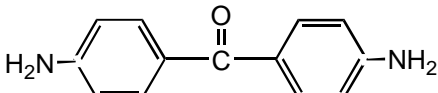
It has been reported that higher molecular weight poly(amic acid)s are obtained at lower reaction temperatures<sup>18, 27-28</sup>. These results are not surprising considering the exothermic nature of poly(amic acid) formation ( $-\Delta H_{rxn}$ ). The effect of equilibration temperature on molecular weight was systematically tested<sup>28</sup>. This was accomplished by preparing a poly(amic acid) at room temperature and removing aliquots for equilibrating individually at a given temperature. After a fixed equilibration time, the individual samples were chemically imidized and isolated to enable GPC measurement of the molecular weight. Comparison of the data showed a corresponding decrease in  $M_w$  with increasing equilibration temperature. However, since  $M_w$

Table 2.2.1 Electron Affinity and Log Rate Constant Values for Aromatic Dianhydrides<sup>23</sup>.

Dianhydrides	$E_A$ , eV	Log $k_r^*$
	0.85	0.78
	0.52	1.05
	0.48	0.49
	0.21	0.13
	0.18	-0.06

\* Reaction with ODA.

Table 2.2.2 Log Rate Constant and pK<sub>a</sub> Values for Aromatic Diamines<sup>24</sup>.

Diamine	pK <sub>a</sub>	Log k <sub>r</sub> *
	6.08	2.12
	5.20	0.78
	4.80	0
	4.60	0.37
	3.10	-2.15

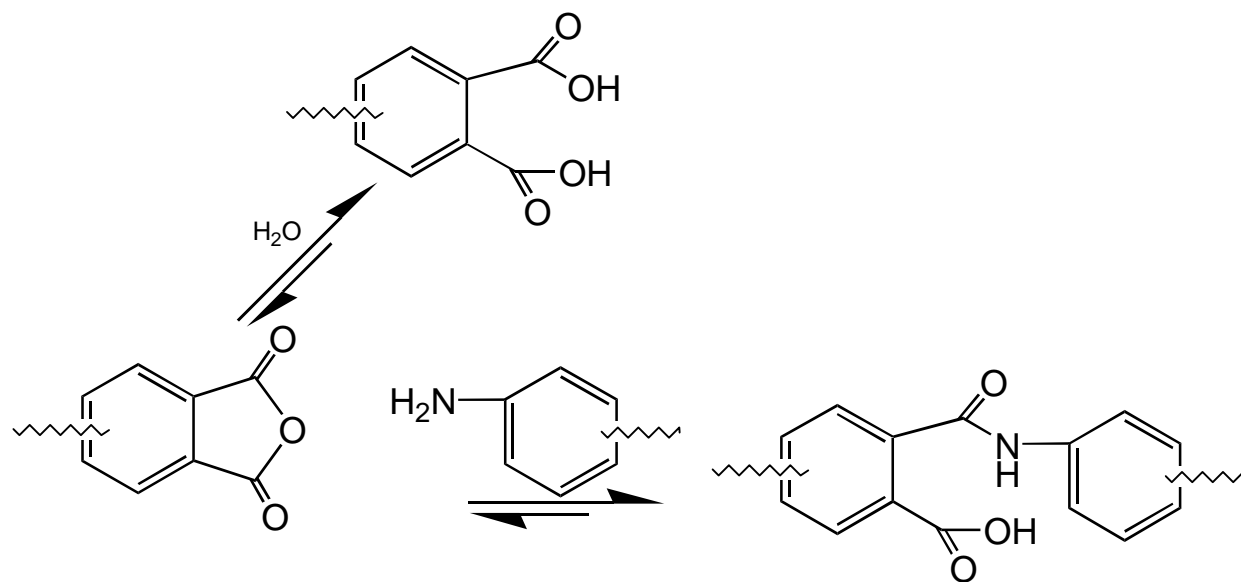
\* Reaction with PMDA.

was used as the basis for comparison, another factor must be taken into consideration: the dissolution of solid dianhydride in the reaction solution is slower at lower temperatures. This means that polymerization can occur at the solid-liquid interface more extensively at lower temperatures. Thus, high molecular weight poly(amic acid) can be rapidly attained by this interfacial-type reaction before all of the dianhydride has dissolved and stoichiometric balance is achieved<sup>10</sup>. The outcome is higher  $M_w$  and a broad molecular weight distribution.

The basicity of the reaction solvent has been found to influence the reaction rate and molecular weight of the product obtained during poly(amic acid) formation<sup>26, 29-31</sup>. In general, the use of dipolar aprotic amide solvents, such as DMAc and NMP, increases the rate of the forward reaction due to hydrogen bonding of the o-carboxamide group with the solvent. As suggested earlier, the acid-base interaction prevents dissociation of the carboxyl proton, which can reverse the reaction. Ether solvents, which are less polar and basic than the amides, lack the ability to form tight H-bonded complexes with the carboxyl group. Thus, the reaction rate is slower in THF. However, it has been suggested that the free carboxyl proton also participates in catalyzing the forward reaction by protonation of the carbonyl group of the dianhydride<sup>28</sup>.

### **2.2.1.3 Side Reactions**

The most deleterious side reaction is hydrolysis, which degrades the poly(amic acid) and decreases its molecular weight<sup>32-33</sup>. During synthesis, small amounts of water are introduced by solvents and monomers. Hydrolysis of anhydride endgroups results, converting them to dicarboxylic acids. This upsets the stoichiometric balance of anhydride and amine endgroups and, consequently, amide-acid linkages degrade to reform them (Scheme 2.2.3)<sup>10</sup>. The o-dicarboxylic acid is unreactive with aromatic diamines under the conditions of poly(amic acid) synthesis and, thus, the molecular weight is limited. The low molecular weight can reduce the



Scheme 2.2.3 Hydrolytic degradation of poly(amic acid).

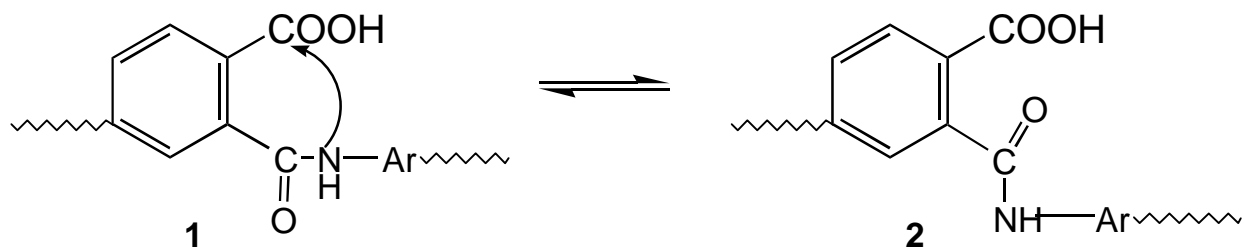
film-forming ability of the poly(amic acid) when cast from solution and thermally imidized<sup>32</sup>. When sufficient heat is applied to the bulk film, o-dicarboxylic acid groups cyclodehydrate to form anhydride and these can acylate neighboring free amine endgroups to increase the molecular weight<sup>10, 33</sup>. However, the water liberated during subsequent imidization cannot be quickly removed from the bulk film and could cause the deleterious hydrolysis cycle to be repeated<sup>36</sup>.

#### 2.2.1.4 Thermal (Bulk) Imidization

Thermal imidization consists of casting the poly(amic acid) solution onto a suitable substrate, followed by gradual heating to effect solvent removal and the cyclodehydration reaction to form polyimide. Heating is performed in a programmed manner, such as that outlined in the following sequence:

- (1) one hour at 100°C
- (2) one hour at 200°C
- (3) one hour at 300°C
- (4) one-half to one hour at a temperature just above  $T_g$ .

As the rigid cyclic imide structure is formed during the cyclodehydration, the  $T_g$  increases dramatically and can rise above the reaction temperature<sup>4, 36</sup>. The resulting decrease in chain mobility hinders attainment of the intramolecular conformation favoring the cyclodehydration reaction<sup>10, 34</sup> (Scheme 2.2.4, Structure **1**)<sup>4</sup>. Since the entropy is decreased, conformations unfavorable to imide formation, such as Structure **2**, remain rigidly fixed and the rate of cyclization decreases<sup>31, 38</sup>. In the glassy state, residual solvent molecules, such as NMP, also hinder attainment of imidization-favoring conformations by forming intermolecular hydrogen bonds with the reactive groups<sup>35</sup>. Hence, the final polyimide film contains residual



Scheme 2.2.4 Conformations of poly(amic acid) during cyclodehydration<sup>4</sup>.

uncyclized amic-acid structures, which are hydrolytically unstable and ultimately cause chain degradation<sup>3</sup>.

Other negative effects of bulk thermal imidization arise from release of volatiles, especially water, which causes degradation, voids and film shrinkage<sup>10, 33</sup>.

Despite the disadvantages, the bulk method is utilized for processing poly(amic acid) films which form insoluble, rigid polyimides that align and pack into ordered/crystalline regions. This process is used commercially to prepare DuPont's Kapton™ film, comprised of the unit structure shown in Figure 2.2.2.

#### **2.2.1.4.1 Methods for Determining Residual Amide-Acid Groups in Insoluble Polyimides**

The degree of imidization affects the stability and physical properties of the polyimide film during use<sup>2</sup>. Consequently, analytical techniques have been developed for measuring the quantity of residual amic-acid groups. However, the methods are few due to the insoluble nature of the films.

The most commonly used method has been infrared spectroscopy<sup>2, 4, 34, 37-40</sup>. Several of the absorption bands used for quantitative and qualitative analysis of polyimides and poly(amic acid)s are shown in Table 2.2.4.

During cyclodehydration of poly(amic acid), the imide absorption bands grow in intensity. Determination of the degree of imidization can be accomplished by comparing the imide band intensities ( $I$ ) in a reacted sample to those in the spectrum of a fully imidized "standard" film ( $I^0$ ). A normalization factor must be used to correct for variations in film thickness. This consists of a band in the spectrum whose intensity remains constant throughout the imidization process, such as the aromatic absorption band at  $1500\text{ cm}^{-1}$ .

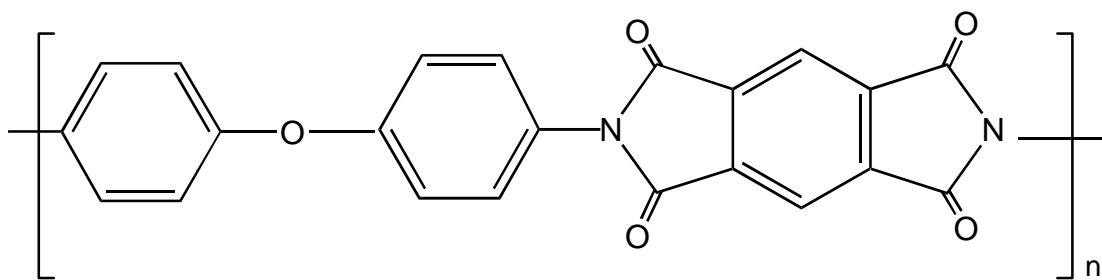


Figure 2.2.2 Kapton™ repeat unit structure.

Table 2.2.3 Infrared Absorption Bands of Imides and Related Compounds.

	Absorption Band (cm <sup>-1</sup> )	Intensity	Origin
Aromatic Imides	1780	s	C=O asymmetrical stretch
	1720	vs	C=O symmetrical stretch
	1380	s	C–N stretch
	725		C=O bending
Amic Acids	2900-3200	m	COOH and NH <sub>2</sub>
	1710	s	C=O (COOH)
	1660 amide I	s	C=O (CONH)
	1550 amide II	m	C–NH
Anhydrides	1820	m	C=O
	1780	s	C=O
	720	s	C=O
Amines	~3200 two bands	w	NH <sub>2</sub> symmetrical structure NH <sub>2</sub> asymmetrical structure

The degree of imidization is then given by the following equation:

$$P = \frac{I(\text{imide}) / I(\text{ref})}{I^0(\text{imide}) / I^0(\text{ref})}$$

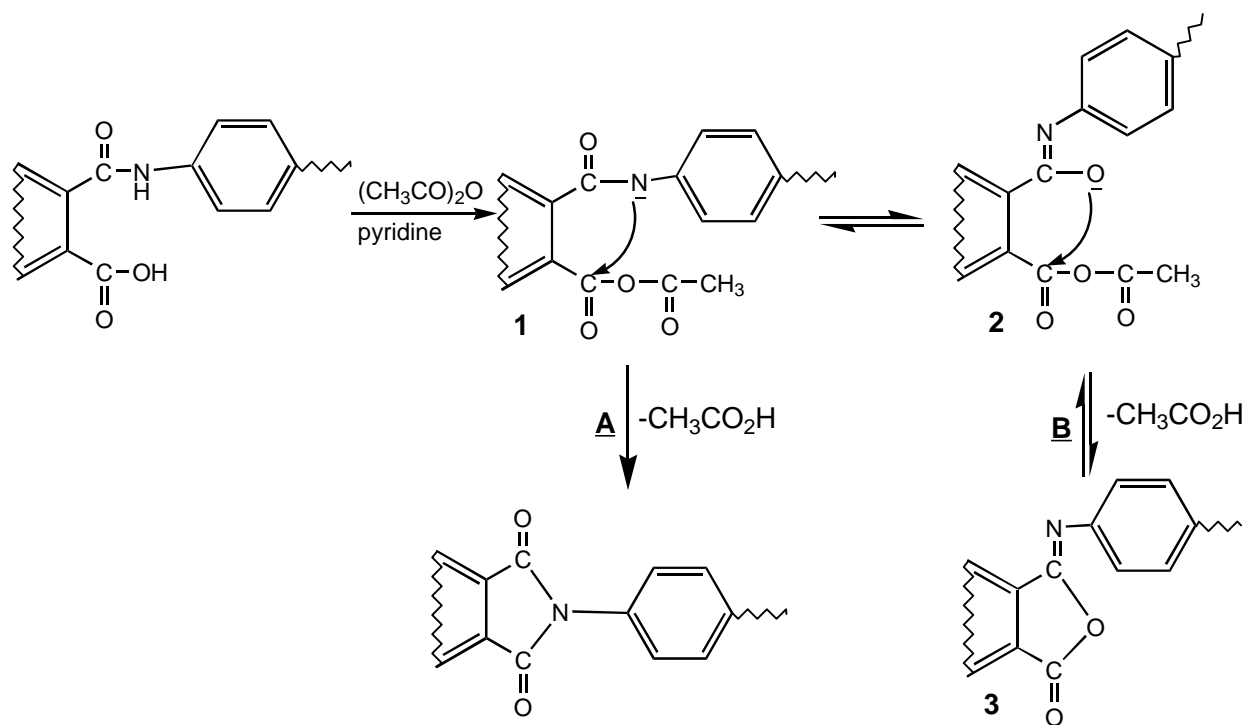
Drawbacks to utilizing this method for quantitation include:

- (1) accuracy depends upon the true extent of imidization of the “standard” film
- (2) imide absorbances at 1780 and 720  $\text{cm}^{-1}$  can be affected by overlapping anhydride absorptions and by anisotropy
- (3) low sensitivity.

### 2.2.1.5 Chemical Imidization

Although used less frequently than the thermal method, chemical imidization can be utilized for cyclization when the polyimide product is insoluble. The usual procedure involves preparing a solution of acetic anhydride and pyridine or triethyl amine in which the poly(amic acid) film is immersed<sup>10, 20</sup>. Diffusion of the chemical agents into the film effects conversion to polyimide by the mechanism shown in Scheme 2.2.5. However, once the film has swollen, it must be removed from the mixture and heat-treated to obtain complete conversion to imide.

The formation of the mixed anhydride intermediate leads to resonance structures **1** and **2**<sup>41-42</sup>. The existence of deprotonated anionic intermediates, rather than the tautomeric forms originally proposed<sup>37</sup>, was surmised when faster reaction rates were observed with increased basicity of the amine catalyst<sup>42</sup>. The cyclization of **1** to polyimide, or **2** to isoimide (**3**), leads to the subsequent release of acetic acid (or acetate ion) rather than water<sup>36, 41-42</sup>. The amount of isoimide obtained is relatively low, which has been attributed to the better nucleophilicity of negatively charged nitrogen versus the negatively charged oxygen<sup>41</sup>. Additionally, a significant amount of isoimide is attacked by acetate ion, thereby regenerating the mixed anhydride that can cyclize to imide via resonance structure **1**.



Scheme 2.2.5 Mechanism of chemical imidization.

Since water is not released during chemical imidization, the main advantage over the thermal method is elimination of hydrolytic degradation. However, the additional expense and environmental impact of using organic reagents make this method less attractive for commercial use.

### **2.2.2 Synthesis of Polyimides via Derivatives of Poly(amic acid)s**

During classic poly(amic acid) synthesis, proton transfer by the o-carboxylic acid group initiates reversal of the polycondensation reaction. Derivatization has been utilized to convert the acid to a species incapable of releasing an acidic proton, such as an ester, under the standard reaction conditions. Ester-amide derivatives have been successfully prepared by utilizing diester-diacyl chloride monomers in solution polycondensation reactions with diamines<sup>36, 43-44, 46</sup>. These derivatized polymers are useful as thin film dielectrics<sup>45-47</sup> and as photosensitive polyimide precursors<sup>48-49</sup> in electronics applications. The improved hydrolytic stability and solubility of the poly(ester-amide) precursors allow for the isolated product to be stored and then reformulated in suitable solvents as needed for spin casting<sup>46</sup>.

Imidization processing of the films is similar to that of poly(amic acid)s: (1) thermal, which requires somewhat higher temperatures than used for amide-acids, and, (2) chemical, using a base such as triethylamine to remove the amide proton<sup>36</sup>. FTIR studies indicate that chain scission side reactions involving decomposition of ester-amide to anhydride and amine groups are absent during thermal imidization of poly(amide ester)s<sup>45</sup>. This results in retention of high molecular weight and hydrolytic stability of the films.

### **2.2.3 One-step Method for High Temperature Solution Polymerization**

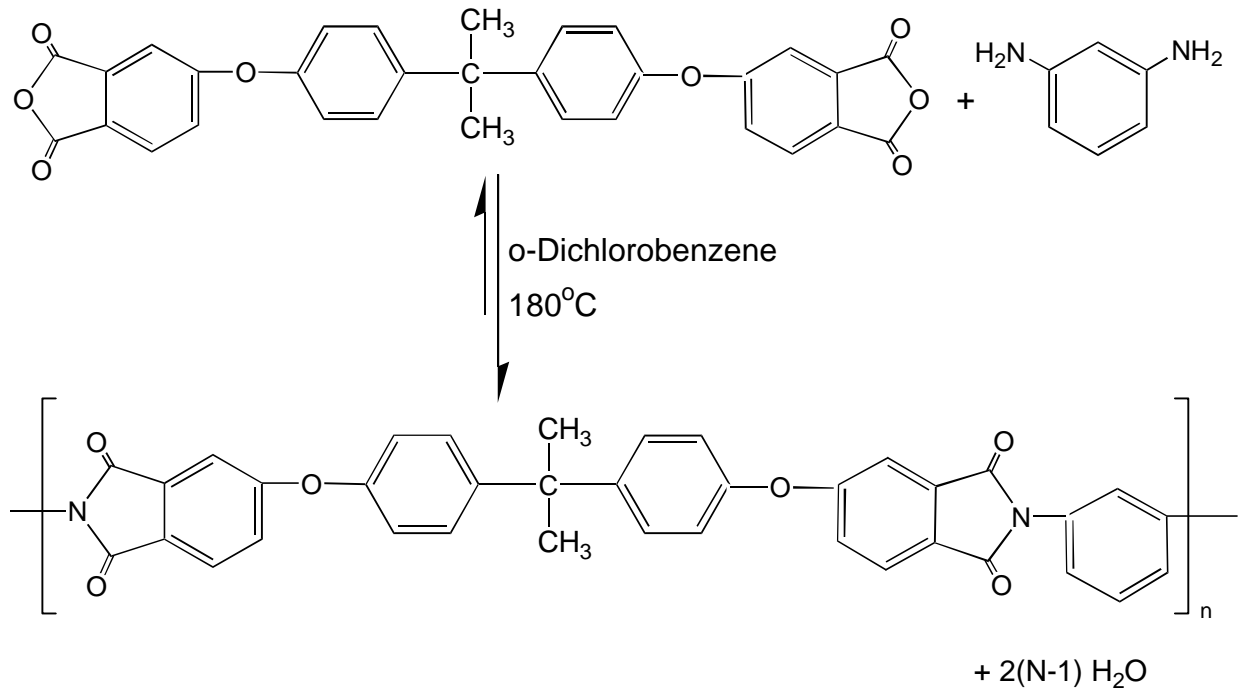
To overcome difficulties in processing and handling poly(amic acid)s, the development of soluble fully-cyclized polyimides has become important. When the polyimide is soluble in

organic solvents at polymerization temperatures, it is possible to react dianhydrides and diamines using one-step high-temperature methods in which polycondensation and imidization occur in the homogeneous solution<sup>50-62</sup>. Alternately, a solution of poly(amic acid) which has been allowed to equilibrate in a suitable solvent can be subsequently heated to effect cyclodehydration to soluble polyimide<sup>63-68</sup>. This is known as a “one-pot” procedure and differs from the classic two-stage methods because the polyimide is fully soluble in the solvents employed.

Although there are variations in the one-pot procedure, the most common involve the synthesis from diamine and dianhydride in NMP containing an azeotroping agent such as N-cyclohexylpyrrolidone (CHP) or o-dichlorobenzene (DCB). The reaction is heated to high temperatures (160-190°C) over several hours, which allows the water generated by imidization to azeotropically distill into a Dean-Stark trap<sup>12</sup>. A procedural modification developed for less reactive diamines involves dissolving the reactants in m-cresol and heating the solution for several hours at temperatures near 200°C. Due to the high temperature, the water evolved during imidization can be removed easily by distillation into a trap, or by passing an inert gas stream through the system. A widely known example of a commercial polyimide prepared by the one-pot procedure is General Electric’s Ultem™, obtained by reacting diamine and dianhydride in DCB (Scheme 2.2.6).

To prepare soluble fully-cyclized polyimides containing aryl groups, the rigid-rod structure must be modified to reduce stiffness and interchain ordering. Several strategies have been used for making soluble amorphous polyimides without sacrificing the excellent physical properties<sup>3, 12-13</sup>:

- (1) incorporating flexible bridging units between aryl groups, such as ether, CH<sub>2</sub>, SO<sub>2</sub>, C=O, C(CF<sub>3</sub>)<sub>2</sub>, thioether, phosphine oxide



Scheme 2.2.6 Ultem™ -- high temperature solution polymerization.

- (2) utilizing “kinked” linkages, such as meta- or orthocatenation, between rings
- (3) introduction of asymmetrical and cardo (loop) structures along the backbone
- (4) incorporating bulky pendant groups along the chain
- (5) limiting molecular weight and endcapping with monofunctional endcappers.

Molecular weight must be sufficiently high to attain good mechanical properties, but it must not be so high that it leads to solubility/processing problems. Therefore, the reactive amine or anhydride endgroups can be endcapped to prevent further reaction and buildup of extremely long chains.

The effects of using one or several of these strategies on polyimide physical properties will be discussed in a separate section entitled “Structures and Properties”.

The advantages of soluble amorphous polyimides include the following:

- (1) the reaction requires only a single step: homogeneous solution imidization
- (2) usually fewer than 1% of the amic-acid groups remain unimidized
- (3) polyimides are hydrolytically stable compared to poly(amic acid)s and, therefore, may be stored under ambient conditions for long periods of time
- (4) polyimide solids may be dissolved in polar solvents suitable for spin casting films
- (5) when heat processing films, there is no release of water to form voids and cause shrinkage
- (6) amorphous polyimides usually exhibit isotropic physical properties.

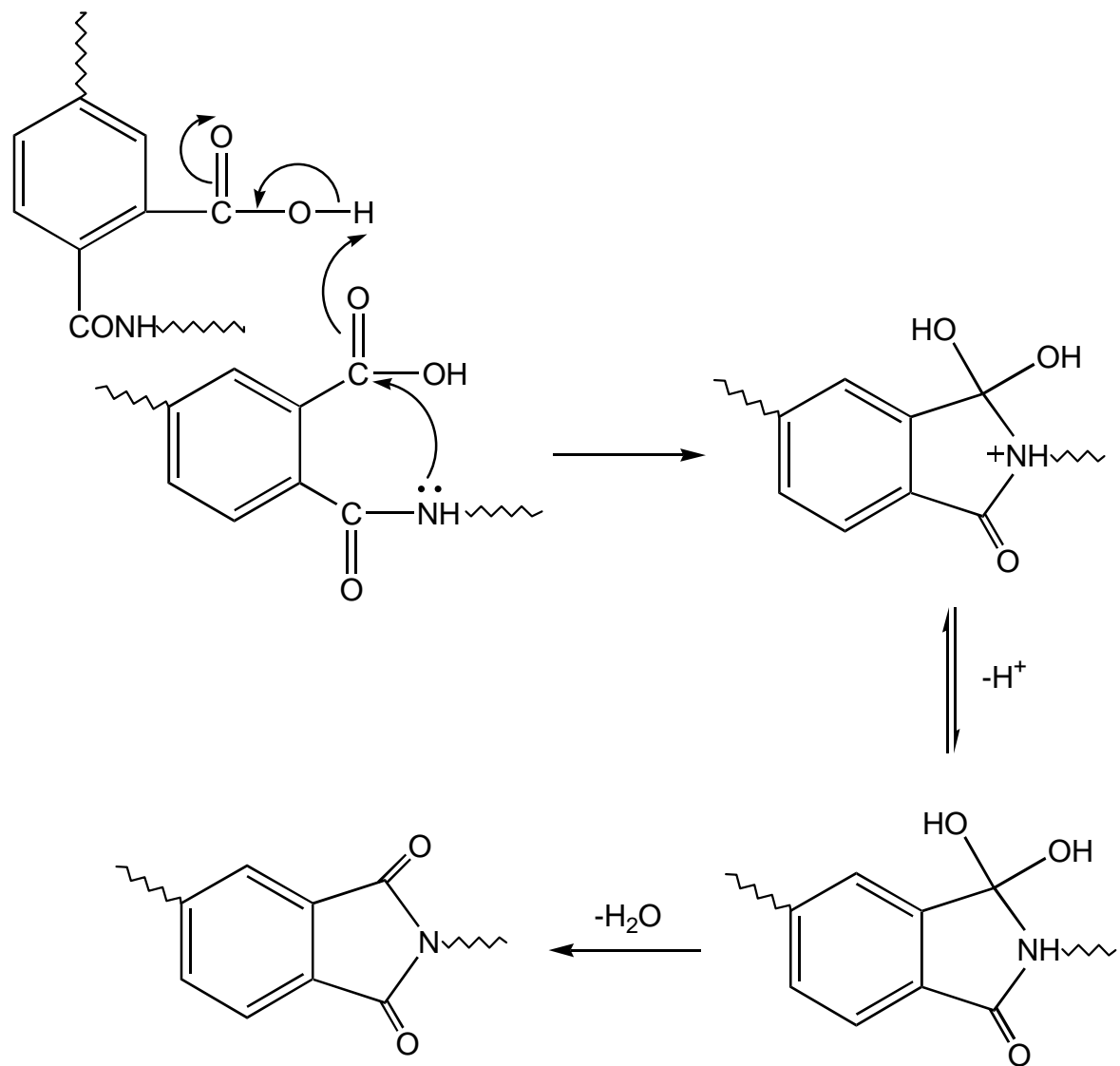
#### **2.2.3.1 Kinetics and Mechanism of High Temperature Solution Imidization**

During thermal imidization of solid poly(amic acid) films there is an increase in  $T_g$  and a simultaneous decrease in molecular motion which prevents complete conversion to imide. In contrast, the increased entropy of high-temperature solution imidization provides adequate chain

mobility throughout the reaction. Homogeneous solution conditions and elevated temperatures are believed to facilitate the rapid exchange of kinetically non-equivalent conformations<sup>69</sup>. In this case, the kinetics would be governed by the chemical reactivity of the amide-acid groups and not by the limited mutual accessibility of reacting groups resulting from unfavorable conformations.

Extensive studies conducted by Kim et al. have elucidated the kinetics of high-temperature solution imidization<sup>69</sup>. The percentage of unreacted acid groups was followed as a function of reaction time by non-aqueous potentiometric titrations using a standardized base (tetramethylammonium hydroxide). The degree of imidization was calculated and provided a linear fit when utilized in second-order kinetic equations. Second-order kinetics were also confirmed by demonstrating that the rate of imidization depended on the initial amic-acid concentration. Additionally, reaction rates were increased after introducing small amounts of monofunctional acid. This information led to the proposed reaction mechanism shown in Scheme 2.2.7, which was consistent with a second-order, auto-acid-catalyzed nucleophilic acyl substitution. Indeed, the nucleophilicity of the amide nitrogen influenced the reaction rate: electron-donating bridge units, incorporated from relatively more basic diamines such as ODA, resulted in faster rates.

Kim et al. monitored residual amic-acid content and intrinsic viscosities as a function of imidization time at a given temperature. The results revealed the effect of temperature and time in attaining fully-cyclized high molecular weight polyimides (Figure 2.2.3). During the initial stages of imidization, the intrinsic viscosity decreased dramatically. This was attributed to chain-scission of the amic-acid. The degradation was confirmed by <sup>1</sup>H-NMR where the appearance of new peaks at 6.67 and 6.85 ppm were attributed to aromatic protons adjacent



Scheme 2.2.7 Mechanism of high temperature solution imidization<sup>69</sup>.

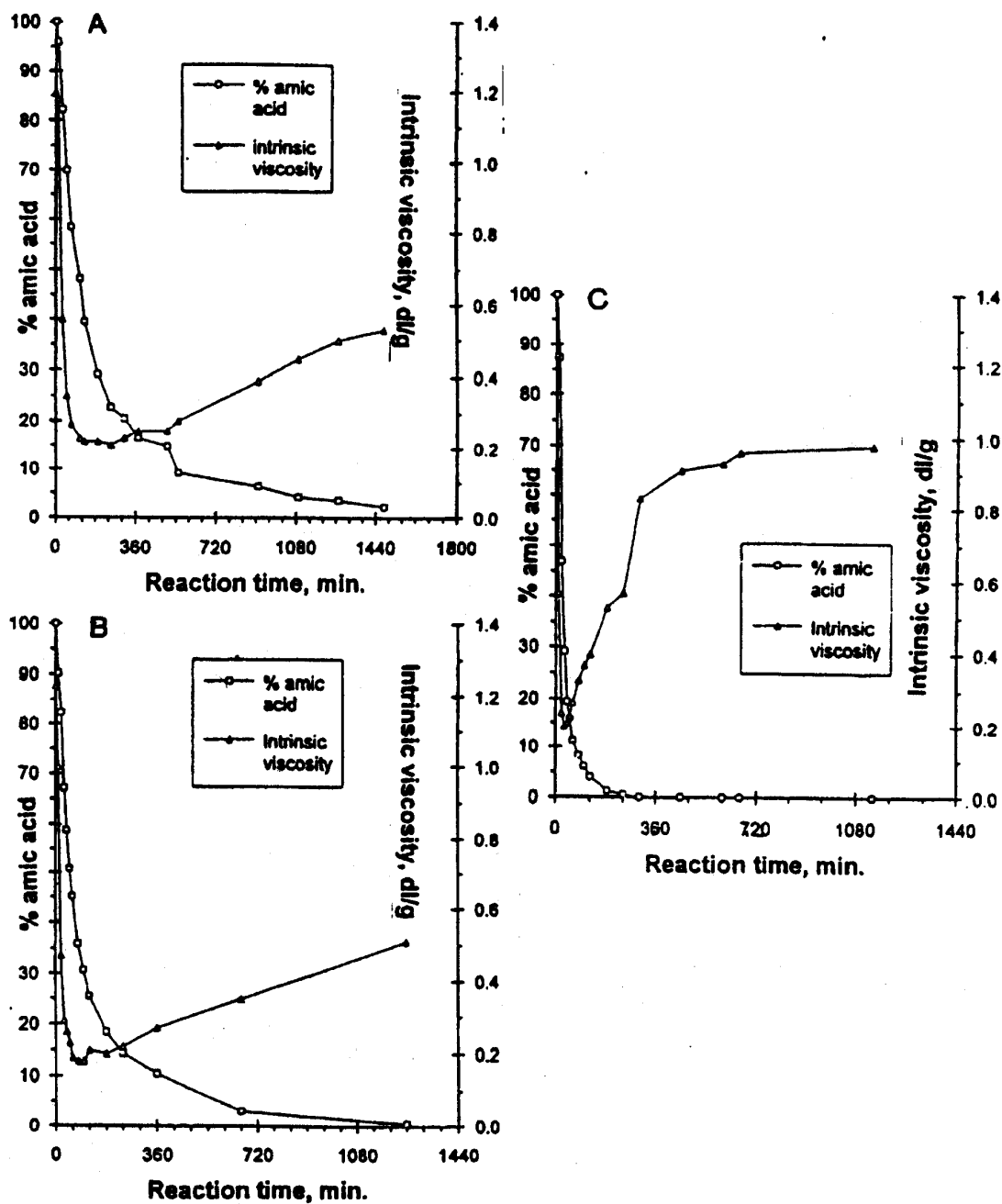


Figure 2.2.3 Remaining amic acid content and intrinsic viscosity as a function of imidization reaction time: (A) at 140°C; (B) at 150°C; (C) at 180°C<sup>69</sup>.

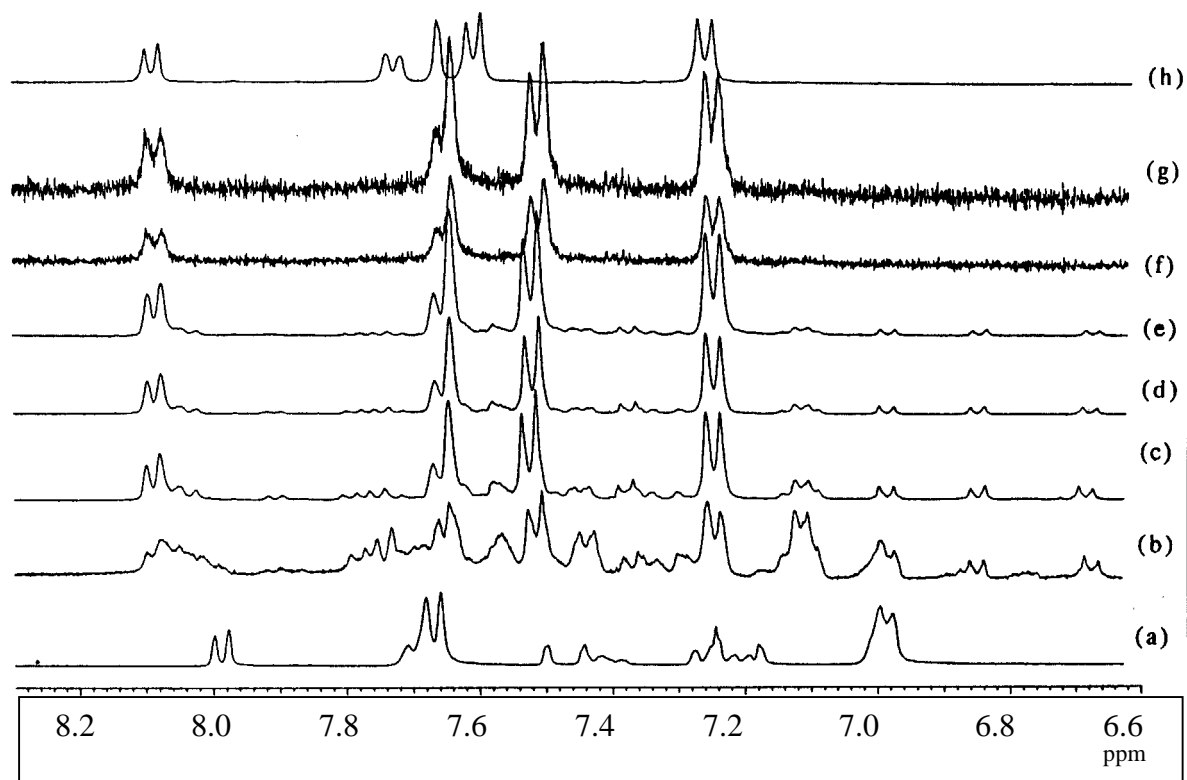
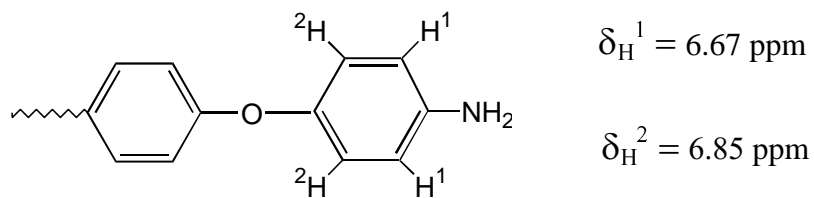


Figure 2.2.4  $^1\text{H}$ -NMR (400 MHz) spectrum of 4,4'-ODA/ODPA poly(amic acid/imide) at different imidization stages (180°C): (a) 0 h, poly(amic acid); (b) 0.33 h; (c) 0.66 h; (d) 1 h; (e) 1.66 h; (f) 3h; (g) 11 h; (h) 11 h, diluted with dry NMP<sup>69</sup>.

to terminal amino groups (Figure 2.2.4). The gradual disappearance of these extraneous peaks, as well as the increase in intrinsic viscosity with increasing reaction time, indicated re-healing of the chains. The extent of the re-healing and subsequent imidization reactions were a function of the reaction temperature at a given time: higher temperatures resulted in fewer residual amic-acid functionalities and higher intrinsic viscosities (Figure 2.2.3). These results imply that proper conditions must be employed during high-temperature solution imidization to achieve complete cyclization and maintain high molecular weight, which are important for maximizing thermal and hydrolytic stability.

#### **2.2.4 Synthesis of Polyimides via Diester-diacid Derivatives**

During the 1970s, NASA modified the reactivity of dianhydrides by preparing diester-diacid derivatives using aliphatic alcohols<sup>70</sup>. The modified structure imparted hydrolytic stability, thereby improving handling. Additionally, the tetracarboxylic acid diesters were unreactive when combined with diamines at ambient temperatures. This allowed the formulation of stable solutions containing both monomers, which were used to impregnate carbon fiber composites. A staged heating process was applied to effect *in situ* polycondensation and imidization. Thermosetting resins, called PMR-15, were prepared by incorporating an endcapping group for crosslinking via addition polymerization during thermal post-cure<sup>70-71</sup>. Advantages of this method included prolonged shelf life and low solution viscosities at high monomer concentrations. The thermal and mechanical properties of the cured resins were comparable to those of control polyimides prepared by the classic method.

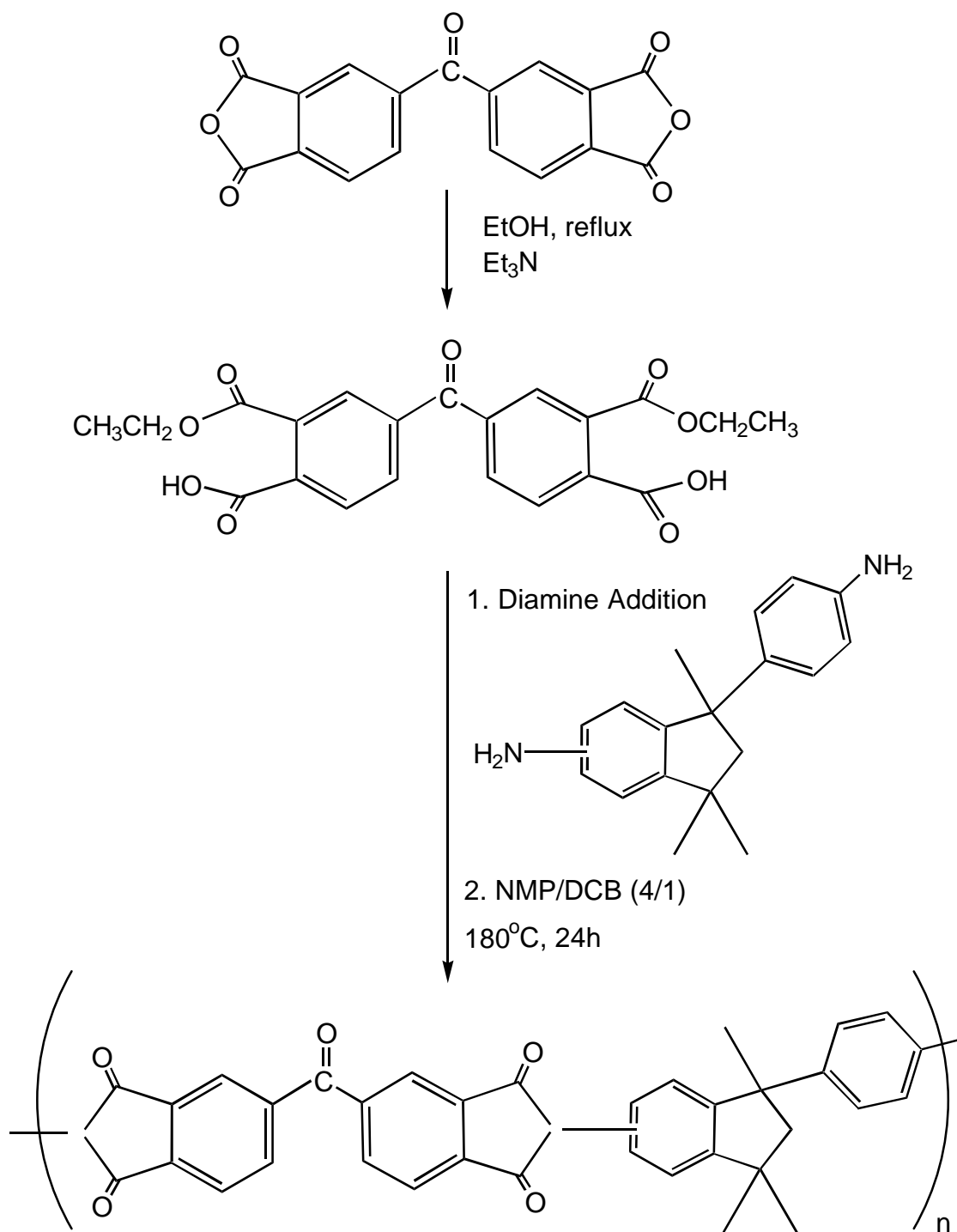
The chemistry of tetracarboxylic diesters has led to an alternative high temperature solution imidization route for preparing soluble polyimides<sup>72-77</sup>. This one-pot method involved initial reaction of the dianhydride with an aliphatic alcohol, usually ethanol, in the presence of an

amine catalyst. Excess alcohol, used as the solvent, was sequentially distilled from the reaction flask leaving a viscous mixture of dialkylester-diacid. The next step involved the addition of diamine with a solvent such as NMP, which contained an azeotroping agent (Scheme 2.28)<sup>77</sup>. When the solution was heated to high temperature (170-185°C), the monomers reacted to form poly(amic acid) with evolution of alcohol. Due to the high temperature and the effective removal of water as an azeotrope, both chain growth and imidization could proceed to high levels in the homogeneous solution.

It has been shown that tetracarboxylic acid diesters consist of a mixture of three position isomers relative to the bridge unit of the parent dianhydride (Figure 2.2.5)<sup>4</sup>. Thus, not only does the derivative possess superior hydrolytic stability, but it is more soluble than the dianhydride. The ester-acid route is more versatile than classic amic-acid synthesis for the following reasons: (1) it eliminates the necessity for drying the solvents or apparatus, (2) the monomers are readily dissolved which prevents interfacial-type reactions, and (3) the imidization is performed in a one-pot process.

#### **2.2.4.1 Ester-Acid Solution Imidization Route Using Aliphatic Diamines**

There is further advantage to using the ester-acid route when one of the monomers is an aliphatic diamine. During classic amide-acid synthesis, the higher basicity of aliphatic diamines caused intra- and inter-molecular salt formation by abstraction of carboxyl protons by amino endgroups<sup>78-79</sup> (Figure 2.2.6). The amide-acid salts had low reactivity under normal conditions at room temperature and, thus, only low molecular weight amic-acids could be obtained. When the ester-acid method was employed, high molecular weight polyimides were obtained using aliphatic diamines<sup>80</sup>. It has been surmised that the intermediate consists of an amide-ester, which lacks the highly acidic carboxyl protons. However, recalling that carboxylic acids are relatively



Scheme 2.2.8 Synthesis of polyimides via ester-acid solution imidization route<sup>77</sup>.

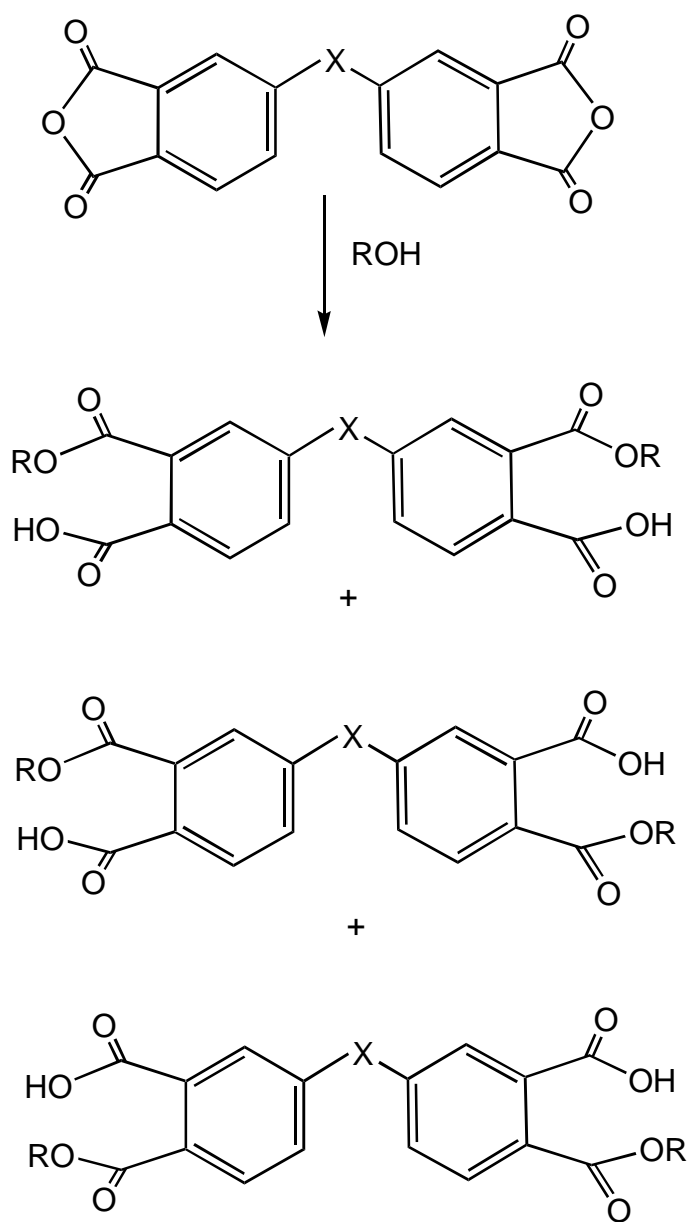


Figure 2.2.5 Diester dicarboxylic acids formed by the reaction of dianhydride and alcohol. R = methyl, ethyl, etc.; X = bridging unit<sup>4</sup>.

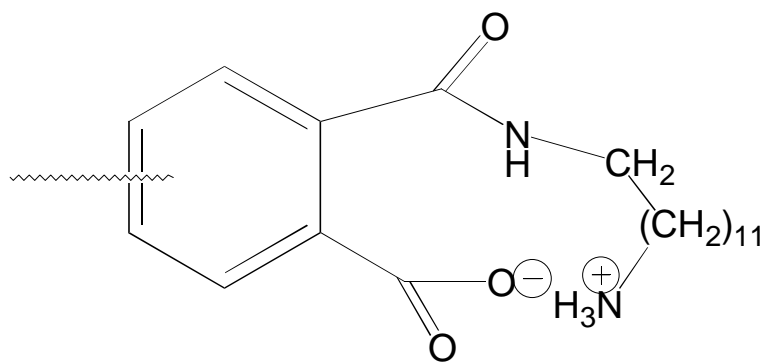


Figure 2.2.6 Intramolecular poly(amide acid) salt from aliphatic amino group.

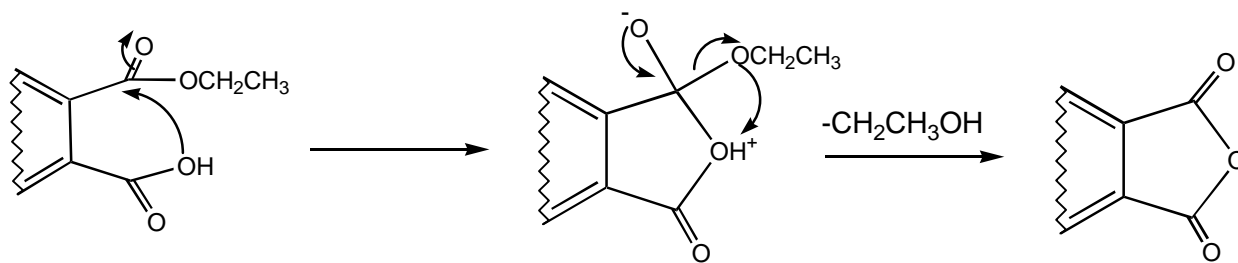
weak acylating agents toward amines<sup>\*</sup>, further work needs to be performed to elucidate the nature of the propagating species in the reaction. Since they are relatively more basic, it is plausible that aliphatic diamines are sufficiently nucleophilic to effect acyl substitution at the carboxyl carbon.

#### 2.2.4.2 Mechanism of Ester-Acid Solution Imidization Route Using Aromatic Diamines

During early studies utilizing FTIR, the formation of poly(amic acid) was not detected as a reaction intermediate using diester-diacids and aromatic diamines<sup>81-82</sup>. Therefore, the acylation of the diamine by the ester functionality appeared to be either negligible or fleeting under the conditions employed. Instead, it was noticed that significant amounts of anhydride appeared which did not arise from hydrolytic degradation. FTIR studies conducted by Moy et al. revealed that the diester-diacid derivative of BTDA readily formed the dianhydride during heating in NMP/DCB to 120-140°C<sup>73</sup>. Model reactions showed that acylation of aniline did not occur under the same conditions using either diethyl phthalate or benzoic acid. However, when the monoester of phthalic acid was refluxed in toluene, the corresponding phthalimide was obtained. This suggested that the mechanism for ester-acid solution imidization involved *in situ* generation of anhydride which became the acylating agent for the aromatic diamine (Scheme 2.2.9)<sup>81</sup>. Since amic-acid would be an intermediate in this case, it seems reasonable to conjecture that its lifetime is extremely short and that immediate cyclization to imide occurs. The low concentration would render corresponding amic-acid vibrations in the FTIR below the detection limits.

---

\* Poly(amide esters) are prepared from reacting diester-diacid chloride monomers with diamines<sup>43-46</sup>.



Scheme 2.2.9 Mechanism of anhydride formation during ester- acid solution imidization route to polyimides.

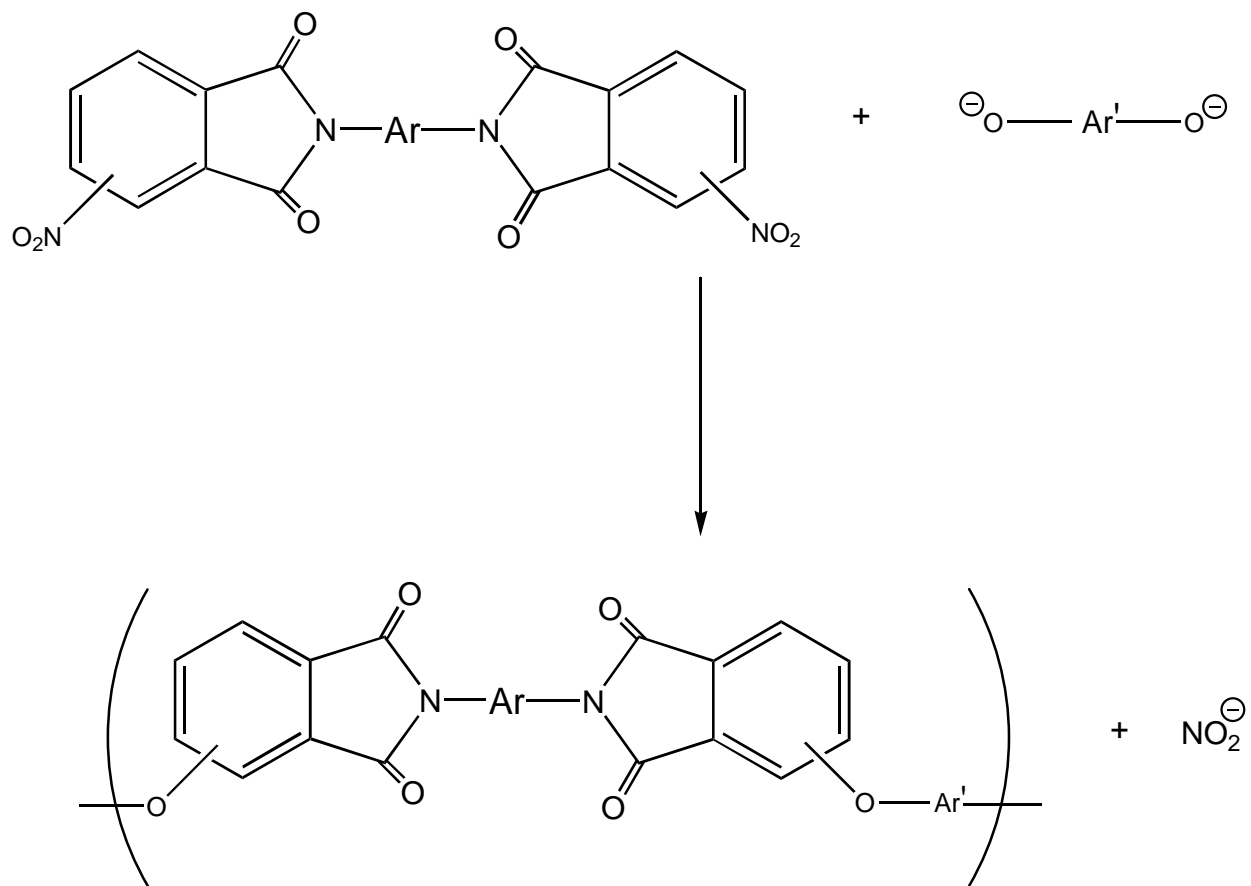
## 2.2.5 Other Synthetic Routes to Polyimides

### 2.2.5.1 Aromatic Nucleophilic Displacement Polymerization

It was recognized during the 1970s that the insertion of ether linkages into the polyimide main chain provided increased flexibility, which greatly enhanced solubility and processing characteristics<sup>82</sup>. As described above concerning production of G.E.'s Ultem, it is possible to synthesize soluble polyetherimides by direct solution polymerization of ether-containing dianhydrides with aromatic diamines. However, during the early development of Ultem, G.E.'s chemists performed a new type of synthesis involving nucleophilic aromatic substitution reactions. This involved the development of new bisnitroimide monomers, which were capable of undergoing nucleophilic displacement reactions with bisphenolates in dipolar aprotic solvents (Scheme 2.2.10).

Bisnitroimide monomers have been obtained in high yields by reaction of either 3- or 4-nitrophthalic anhydride with aromatic diamines, such as m-PDA, in acetic acid solvent. Utilization of reflux temperatures and azeotroping agents afforded fully imidized monomers<sup>83</sup>. Bisphenoxide monomer preparation consisted of heating a bisphenol, dissolved in DMSO, with an aqueous sodium hydroxide solution in the presence of toluene to azeotropically dehydrate the product<sup>84</sup>.

During polymerization of these monomers, attack of the phenoxide at the nitro-substituted aryl carbon resulted in a resonance stabilized Meisenheimer transition state (Figure 2.2.7)<sup>4</sup>. The reaction was favored with strongly nucleophilic bisphenoxides giving high molecular weight polyimides<sup>82</sup>. When the phenolate salts of benzenediols were utilized, such as resorcinol and hydroquinone, a competing redox side reaction occurred, which resulted in



Scheme 2.2.10 Reaction of activated bisnitroimide monomer with bisphenoxide.

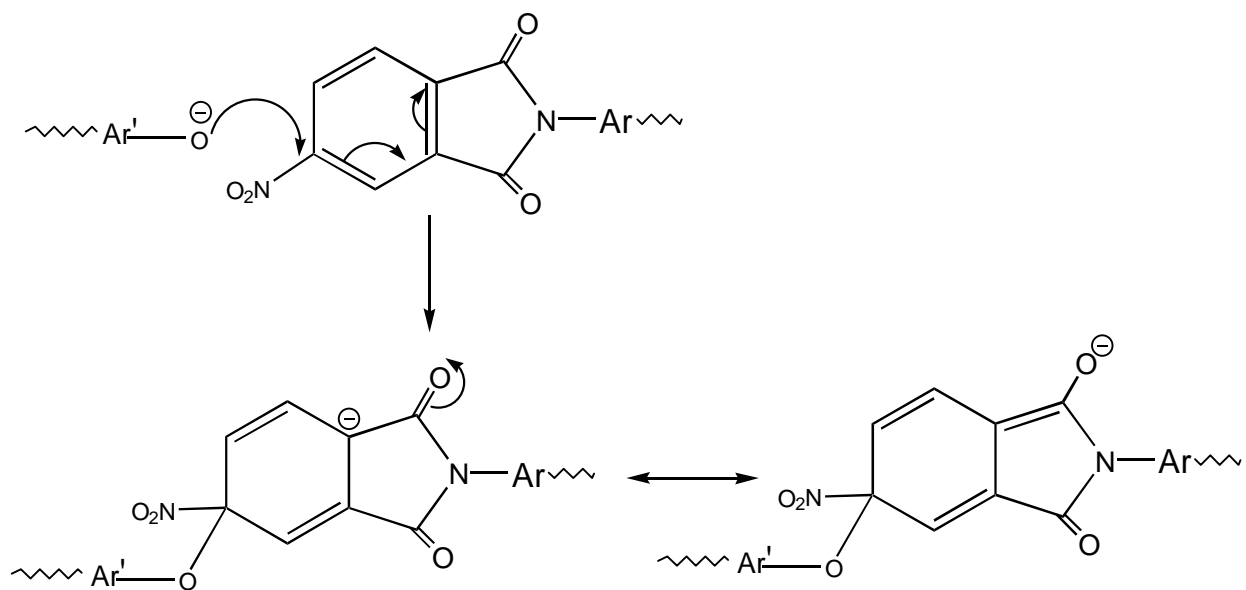


Figure 2.2.7 Delocalization of negative charge in Meisenheimer transition state in imide system.

lower molecular-weight polyimides<sup>83</sup>.

In the presence of water, only low molecular weight polyimides were obtained<sup>84</sup>. Hydrolytic ring opening of the imide caused bisphenoxide to become inactivated due to its ready acceptance of carboxyl protons from amide-acid groups.

### **2.2.5.2 Polymerization of Diisocyanates and Dianhydrides**

The reaction of aromatic diisocyanates with dianhydrides has been utilized to synthesize polyimides<sup>85-96</sup>. The chemistry, developed during the late 1960s, was subsequently investigated to elucidate the reaction mechanism and the effect of conditions on product yields. It was found that the imidization path depended on the reaction conditions.

There has been a lack of consensus over the exact stoichiometry and reaction conditions required to obtain high molecular weight polyimides using this route. It has been observed that the reaction of diisocyanates and dianhydrides proceeds at relatively moderate temperatures in dipolar aprotic solvents in the presence of alcohols, water or tertiary amines.

In the case of alcohol it was proposed that a urethane, formed by reaction of alcohol and isocyanate, underwent slow reaction with anhydride to form imide<sup>85</sup>. Consequently, regeneration of alcohol and evolution of carbon dioxide occurred as a result.

The mechanism with water catalyst has been thought to proceed through the hydrolysis-reaction product of isocyanates, urea, which decomposes to amine and carbon dioxide<sup>86</sup>. In this case, the amine reacts with anhydride to give amic-acid, which subsequently imidizes by releasing water. It may be supposed that the preferential hydrolysis of isocyanate groups by the water of imidization would enhance the rate of cyclization.

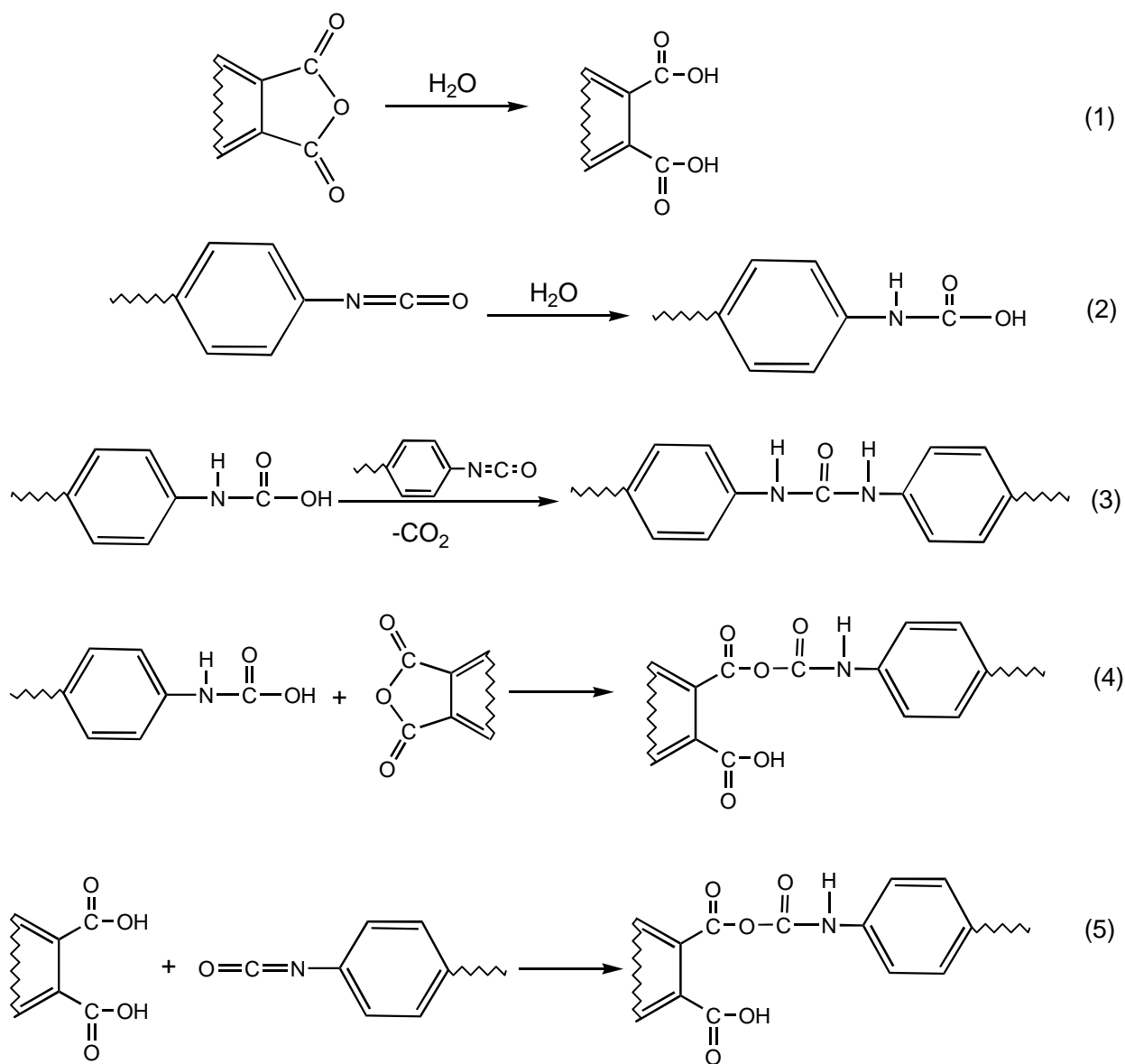
It was also reported that high molecular weight polyimides were obtained using mixtures of anhydrides and their corresponding tetracarboxylic acids with diisocyanates in the presence of

tertiary amines<sup>87</sup>. The authors could not suggest a mechanistic role for carboxylic acid groups in the reaction of diisocyanates with dianhydrides. However, since high molecular weights had been obtained, it was apparent that the stoichiometry was not upset by the presence of hydrolyzed anhydrides as it would have been in classic polyimide synthesis via amic-acids.

In Volksen's review<sup>36</sup>, a mechanism has been proposed to address the role of the hydrolyzed species (Scheme 2.2.11). In the presence of water, the anhydride and isocyanate hydrolyze simultaneously to dicarboxylic and carbamic acids, respectively (Reactions 1 and 2). Some of the carbamic acid reacts with isocyanate to form urea (Reaction 3). It has been suggested that the urea is capable of reacting slowly with anhydride to form imide<sup>86</sup>, so the presence of urea would not limit molecular weight. Additionally, either product of the hydrolysis, carbamic acid or diacid, is capable of reacting to form a mixed carbamic carboxylic anhydride (Reactions 4 and 5, respectively). Subsequent heating causes the mixed anhydride to cyclize to imide with the loss of carbon dioxide and water.

To complicate matters further, a cyclic 7-membered intermediate has been proposed for uncatalyzed reactions in the melt or in anhydrous solutions, which is directly formed by anhydride and isocyanate groups (Figure 2.2.8)<sup>36,95</sup>. This intermediate is believed to split out carbon dioxide when heated to form the 5-membered imide rings.

Lack of understanding of the precise conditions required for quantitative conversion of diisocyanates and dianhydrides to polyimides has delayed wider application and potential commercialization of this synthetic method. Further work needs to be addressed before it becomes a viable alternative route to the classic amic-acid or the one-pot solution imidization methods.



Scheme 2.2.11 Mechanism of water-catalyzed reaction of diisocyanates and dianhydrides<sup>36</sup>.

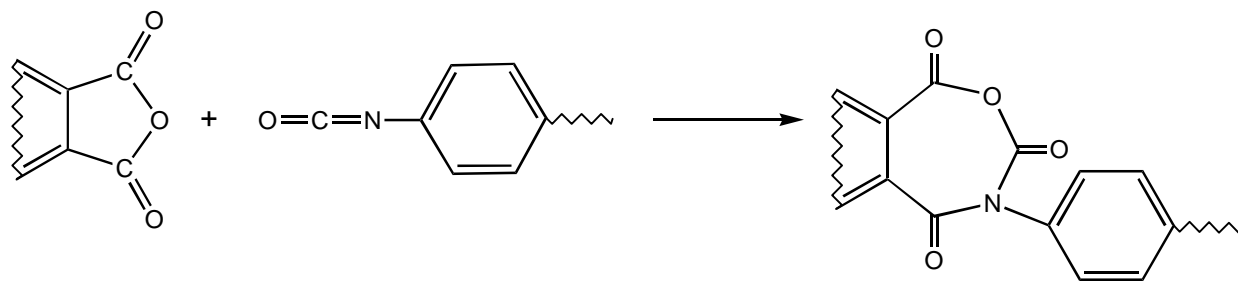


Figure 2.2.8 Proposed 7-membered cyclic intermediate in the reaction of isocyanate with anhydride.

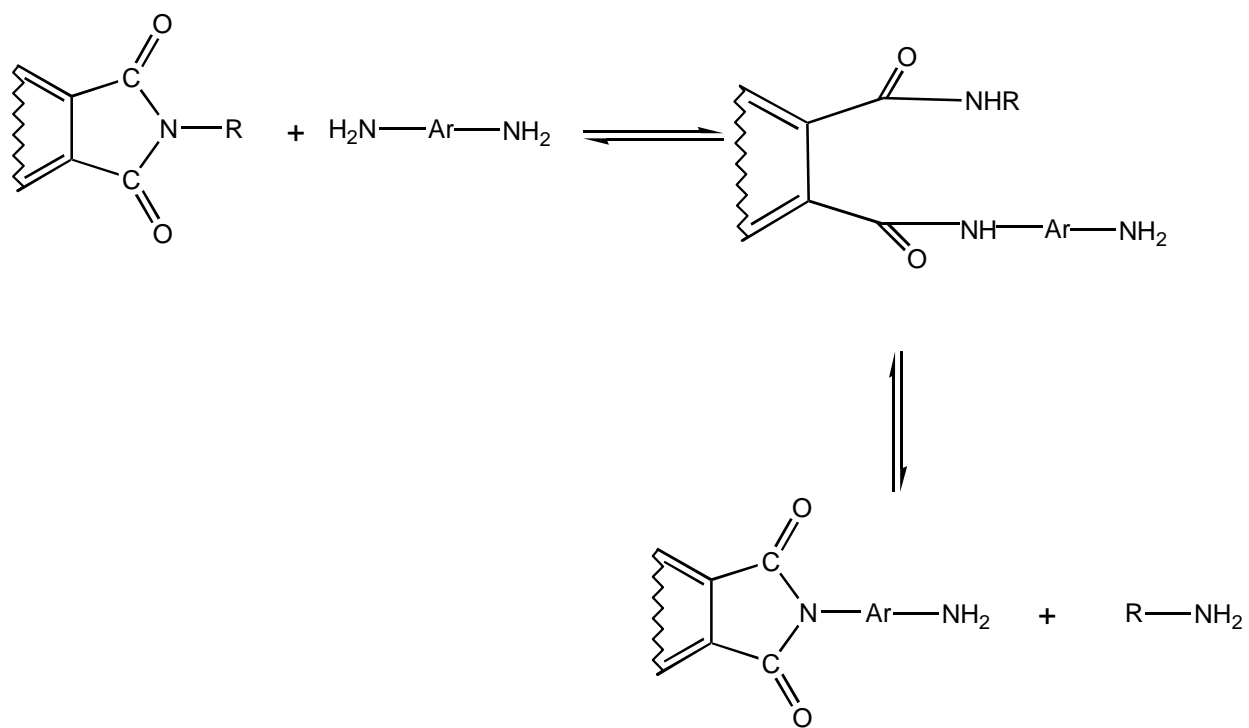
### 2.2.5.3 Synthesis of Polyimides by Transimidization

An amine-imide exchange method called transimidization has been employed to synthesize high molecular weight polyimides<sup>97</sup>. This one-step method is used for soluble/tractable polyimides, which polymerize in solution or in the melt.

At high temperatures, N,N'-substituted bisimide monomers can undergo nucleophilic attack by diamines at the imide carbonyl carbon (Scheme 2.2.12). This generates an amic-amide intermediate, which can re-cyclize to form imide. Ejection of a monoamine leaving-group during cyclization provides polymer chain growth. However, since this is an equilibrium process, the leaving group can also consist of the diamine.

Distillation of the volatile monoamine from the reaction assists in polymer formation by driving equilibrium to the right. Another strategy is to reduce the basicity/nucleophilicity of the monoamine leaving-group. Bisimides derived from heteroaromatic amines such as 2-aminopyridine, readily undergo exchange reactions with aromatic diamines<sup>98</sup>. When the transimidization reaction involves aromatic amines of similar nucleophilicity, organo-metallic catalysts containing zinc, lead or cadmium can be utilized<sup>99</sup>.

Compared with the conventional amic-acid route, the primary advantage of this method is the lack of water evolution during cyclization. Hence, this technique can be employed with monomers containing groups that are easily hydrolyzed, such as siloxane or ester groups. Rogers et al. utilized the transimidization method to synthesize perfectly alternating polyimide-polydimethyl siloxane copolymers<sup>100-101</sup>. Polyimide oligomers, having N-(2-pyrimidyl)phthalimide endgroups, were reacted with aminopropyl-terminated (dimethyl siloxane) oligomers in polar solvents at relatively low temperatures. This afforded high molecular weight polymers containing sequentially alternating hard- and soft-segments.



Scheme 2.2.12 Schematic of the imide-amine interchange or transimidization reaction.

## **2.3 Introduction to Structure-property Relationships of Polyimides**

The properties of polyimides, as for polymers in general, are governed by three fundamental characteristics: chemical structure, average molecular weight and molecular weight distribution<sup>102</sup>. The chemical structure relates to the chemical composition of the repeat unit and endgroups. It also encompasses the composition of any branches, crosslinks or defects in the structural sequence. The average molecular weight describes the average polymer chain size. The molecular weight distribution relates to the degree of regularity in the molecular size.

Extensive literature has been published describing alterations in the structure and size of the polyimide backbone and how these changes affect the physical and mechanical properties. In the following sections, a sampling of this literature will be reviewed with particular emphasis on properties applicable to microelectronics packaging devices.

To provide background information, the subject of microelectronics packaging is first addressed with regard to function, fabrication and the performance/property requirements for polymer dielectrics. The subsequent discussions on structure-property relationships of polyimides are divided into three major areas:

- (1) linear thermoplastic two-phase polyimides
- (2) linear thermoplastic amorphous polyimides
- (3) crosslinked amorphous polyimides.

### **2.3.1 Microelectronics Packaging**

Electronic devices, such as computers, contain a large number of integrated circuit chips<sup>192</sup>. Driven by electrical power, each chip performs particular operations that are transmitted as electrical signals. The chips operate as a cooperative unit by “interchip communication” which involves receiving and transmitting signals within a chip network<sup>192</sup>. Network

communication is achieved by external circuitry which connects chips to each other and to the input/output devices (keyboards, displays, printers, etc.)<sup>7</sup>. The structure that serves to connect the chips is called the electronic package.

The chips are bonded to the “first level” of the electronic package, which is called a multichip substrate<sup>103, 192</sup>. High-speed and/or high-density integrated circuits are achieved by closely spacing the chips on the substrate thereby minimizing the length of the interconnections in the packaging. Relatively shorter interconnections minimize signal transmission delays and resistive losses<sup>104</sup>.

To minimize the distance traversed by electrical signals, the packaging contains closely spaced, multiple layers of high-resolution conductor patterns (metal lines). These metal lines run horizontally (in-plane) through the packaging, with vertical connections being supplied between lines and chips by metal contact vias<sup>7</sup>.

The high density of signal lines within the packaging requires that the lines be electrically insulated from each other<sup>193</sup>. Layers of insulating material, deposited between metal lines, ensure minimal electrical interaction between signals traveling in adjacent lines, called crosstalk noise<sup>7, 192</sup>. Optimum insulation is achieved when the material has extremely low electrical conductivity, which is consistent with a low dielectric constant. Materials with relatively low dielectric constants provide effective electrical barrier properties, and this behavior has led them to be referred to as “dielectrics”.

The primary role of multichip packaging is to provide an electrical pathway for connecting the chips to each other and to the peripheral devices. As discussed above, this function includes maintaining the integrity of the electrical signals traveling through the lines by proper insulation. Additionally, the insulating material must also protect the chips and the wiring

structure from environmental influences and mechanical damage<sup>7, 103, 192</sup>. Further, it must provide connections for electrical power distribution to operate the chips and to remove heat generated by the chips during operation<sup>103</sup>.

### **2.3.1.1 Multilayer Interconnect Packaging**

The following types of multilayer interconnect packaging have been developed for microelectronics applications<sup>105-106, 192</sup>:

- (1) Ceramic substrates in which the metal wiring is imbedded in ceramic or glass-ceramic dielectrics (Multi Chip Module –Ceramic, MCM-C).
- (2) Thin film multi-layer (TFML) substrates, consisting of metal lines imbedded in organic polymer or inorganic silicon dielectric thin films. The TFML is deposited on a supporting substrate, such as ceramic (Multi Chip Module –Deposited, MCM-D).

Production of MCM-C packaging is achieved by stacking precursor ceramic sheets that have been screen-printed with precursor metal pastes and cofiring these at temperatures  $>1,000^{\circ}\text{C}$ <sup>106</sup>. The product consists of alternating layers of metal conductor lines and ceramic dielectric. Ceramics exhibit properties that have proved beneficial in electronic packaging<sup>7, 192</sup>:

- (1) High modulus, to afford good mechanical protection to the metal lines
- (2) Low moisture absorption, to protect metals from corrosion
- (3) Good heat dissipation, to prevent overheating and distortion
- (4) Low coefficients of thermal expansion (CTEs), to limit stress build-up during thermal processing/cycling of silicon semi-conductor chips bonded to the ceramic.

The major disadvantage of MCM-C packaging is the relatively high dielectric constant of ceramics ( $\epsilon$  ranges from 7 – 10, depending on the type of ceramic)<sup>106, 192</sup>. This drawback has been addressed by utilizing mixtures of ceramic and glass<sup>192</sup>, which has reduced the dielectric

constant to as low as 3.9. However, the thermal conductivity of these hybrids is relatively poor, so their usefulness is limited to lower operating temperatures.

To address the low heat dissipation, ceramic-glass hybrid films have been utilized as thin film insulators around wiring, with the resulting layered structure being supported on a ceramic substrate (similar to TFML)<sup>106</sup>. The ceramic base acts as a heat sink, and thus, the device can operate safely at higher temperatures.

### **2.3.2 MCM-D Packaging Technology Based on Thin Film Multilayers (TFML)**

The MCM-Deposited technology was initially developed utilizing chemical vapor deposition (CVD) of silicon dioxide as the thin film interlayer dielectric<sup>193, 194</sup>. This inorganic film has a dielectric constant ranging from 3.5-4.0, which is much lower than that of ceramics<sup>109</sup>. This has led to its widespread use in TFML applications and its reputation as being the “workhorse” of the electronics industry<sup>107-108</sup>.

As shown in Table 2.3.1, MCM-D technology allows for a higher wiring density, including much narrower line widths and closer line spacing, compared with ceramics<sup>106, 192</sup>. Thus, MCM-D allows greater chip density per unit area of substrate and reduction in interconnect length, which are crucial for reducing the delay time and power consumption in driving the signals between chips<sup>107</sup>. This makes MCM-D ideal for high-performance systems, such as computers.

The newest packaging to evolve using MCM-D technology employs polymeric thin films as the dielectric medium<sup>192</sup>. Polymers provide an attractive alternative to ceramics due to their significantly lower dielectric constants. Among the choices of polymers for MCM-D, polyimides have become of prime interest<sup>194</sup>. Compared with most thermoplastic organic polymers, polyimides have extremely high thermal stability<sup>195</sup>. As discussed in Section 2.2.1,

Table 2.3.1 Multichip Module Wiring Characteristics<sup>106</sup>.

Wiring Characteristics	Packaging Type	
	MCM-C	MCM-D
Line density (cm/cm <sup>2</sup> )	200 - 400	>400
Line width/separation (μm)	125/125-375	10/10-30

the rigid, ordered polyimide films prepared from amic-acids are resistant to attack by organic solvents and acids. Additionally, these materials have high  $T_g$ , outstanding mechanical strength and resistance to decomposition at high voltages.

Selected properties of polyimides and inorganic silicon dioxide are compared in Table 2.3.2. As shown, many of the important properties of silicon dioxide and polyimides are comparable. However, the thermal stability and Young's modulus of silicon dioxide are higher than those of polyimides. Additionally, silicon dioxide exhibits a much lower CTE, which may prevent stress build-up during thermal processing/cycling of silicon semi-conductor chips bonded to this substrate.

The dielectric constant of polyimides tends to be lower than that of silicon dioxide, but the main advantage offered by the polymer is its "planarization" property<sup>110</sup>. Planarization is the ability of the film to provide a planar surface over the underlying topography, consisting of metal wires and vias<sup>192</sup>. Relatively more planar and smooth topographies provide better surfaces for photolithography utilized to define etching sites for contact vias in the TFML<sup>107, 109-110, 192</sup>.

The planarization concept is illustrated in Figure 2.3.1<sup>110</sup>. As shown in the upper schematic, CVD silicon dioxide film conforms to the underlying topography of metal substrate (1), and, thus, the metal (2) deposited on top has "steps". The film formed by the polyimide, shown in the lower diagram, has been made sufficiently thick to cover the topography with a relatively planar surface. Thus, on a micron-scale level, the step height of the underlying metal lines is reduced, sidewall angles are reduced and sharp corners are more rounded<sup>107</sup>.

In the quest to improve planarization, relatively thicker silicon dioxide films have been prepared using CVD technology. It has been found that crack- and defect-free films cannot be produced above 3  $\mu\text{m}$  thickness<sup>110, 194</sup>.

Table 2.3.2 Comparison of Properties of Polyimide and Silicon Dioxide Dielectrics<sup>107, 109</sup>.

	Polyimide	SiO <sub>2</sub>
Process temperature, °C	300-350	350-450 <sup>a</sup>
Decomposition temperature, °C	>450	1710 <sup>b</sup>
Dielectric strength, V/cm	10 <sup>6</sup>	10 <sup>6</sup> -10 <sup>7</sup>
Volume resistivity, ohm-cm	10 <sup>15</sup> -10 <sup>16</sup>	>10 <sup>16</sup>
Dielectric constant	3.2-3.8	3.5-4.0
Dissipation factor	0.001-0.002	0.001
Coefficient of thermal expansion (CTE), 10 <sup>-6</sup> /°C	20-70	0.3-0.5
Thermal conductivity, W/cm-°C	0.0017	0.021
Young's modulus, GPa	3	70
Tensile strength, GPa	0.1-0.2	0.2
Planarization, %	60-100	0

a = Deposition temperature

b = Melting point

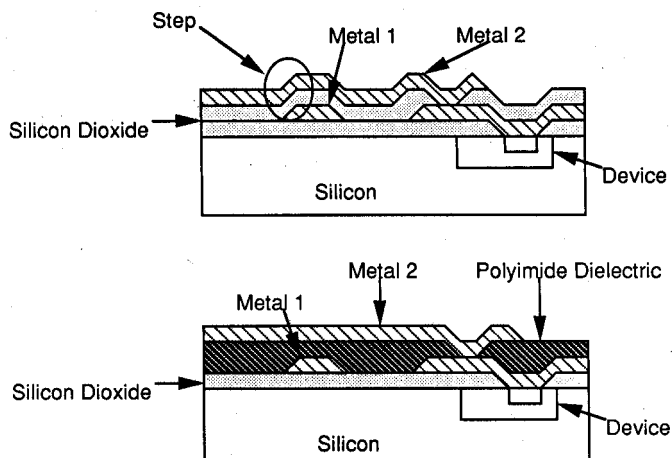


Figure 2.3.1 Polyimide planarization advantage over silicon dioxide films<sup>110</sup>.

### 2.3.2.1 Fabrication of MCM-D Packaging

The process used for fabricating MCM-D packaging consists of three basic steps, which can be repeated sequentially to create several alternating layers of conductor and dielectric. The following is a simplified outline of the steps<sup>106</sup>:

- (1) Deposition of material, either dielectric film or metal, on the substrate
- (2) Definition of a pattern on the material using photolithography
- (3) Etching the material in the form of the pattern.

As mentioned above, chemical vapor deposition (CVD) has been used to apply silicon dioxide during the first step. This technique produces very thin SiO<sub>2</sub> films, which conform to the topography and provide relatively poor planarization<sup>194</sup>. Conversely, much thicker films providing good planarization can be obtained from polyimides<sup>194</sup>. This is due to the better available techniques for their deposition<sup>105, 192, 194</sup>. The following sections discuss the basic fabrication steps used for MCM-D with regard to polyimide dielectrics, beginning with the method commonly used for applying polyimides to the substrate.

#### 2.3.2.1.1 Spin Coating

Spin coating is the most common method for depositing polyimide films in TFML packaging<sup>192</sup>. Typically, a poly(amic acid) solution is dispensed on the surface of the substrate, followed by rapidly spinning on a vacuum chuck at high speeds (up to 6,000 rpm). The solution is evenly distributed over the surface during spinning. Concomitant solvent evaporation, which is induced by the rapid spinning motion, results in formation of a semi-solid film.

The thickness of the deposited film is a function of the viscosity of the precursor solution, the solids/solvent concentration and the spin speed<sup>111</sup>. Using spin-on technology, polyimide film thickness in the range of submicron to 10 $\mu$ m or more can be obtained<sup>192</sup>. For a polyimide

solution of a given viscosity, the film thickness decreases with increasing spin rate, as illustrated in the plot of empirical thickness versus spin speed (Figure 2.3.2)<sup>110</sup>.

Following deposition, the poly(amic acid) film is subjected to heating in a programmed manner to effect imidization and solvent removal. Figure 2.3.3 illustrates the typical heating sequence employed by the electronics industry<sup>112</sup>. This thermal processing is known as “curing” in industry jargon, but actually consists of cyclodehydration of the poly(amic acid) to form linear, stiff, ordered polyimide chains.

The main process steps used to build thin film multilayer structures are described in the following section. The purpose is to reveal the types of conditions that polyimides are subjected to during processing.

#### **2.3.2.1.2 Building Thin Film Multilayers Using the Subtractive Process**

One method of fabricating TFML packaging is called the subtractive etching process<sup>7</sup>,

192.

The steps of the subtractive process are as follows:

- (1) A blanket metal is deposited onto the substrate by sputtering.
- (2) A pattern is transferred to the metal, which defines the desired line structures. The pattern is transferred by:
  - (a) Depositing a photoresist material, then softbaking it.
  - (b) Exposing the resist to UV radiation through a photomask with the desired pattern.
  - (c) Developing in a solvent to remove resist material (making the pattern in the resist).
  - (d) Hardbaking the remaining resist material.
- (3) The metal is then etched into the desired pattern using a chemical etchant that removes any metal not covered by the resist. The resist is then stripped off.

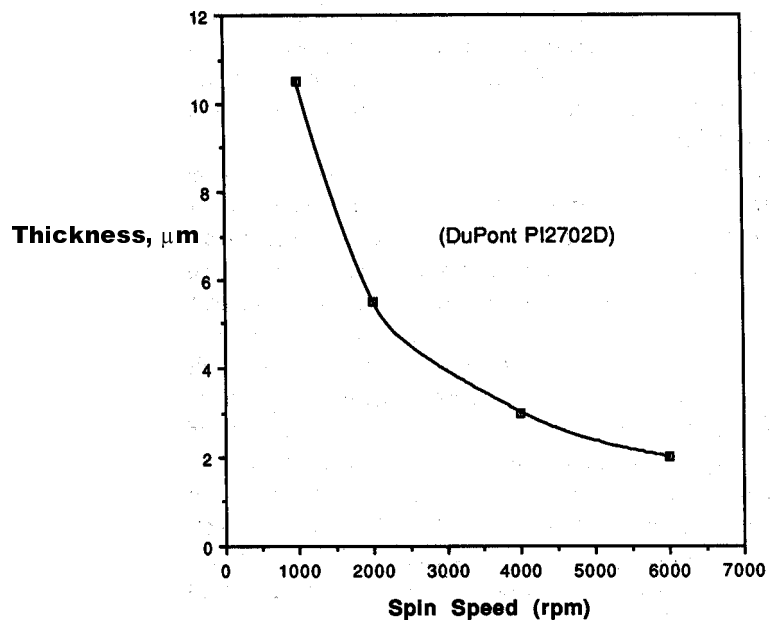
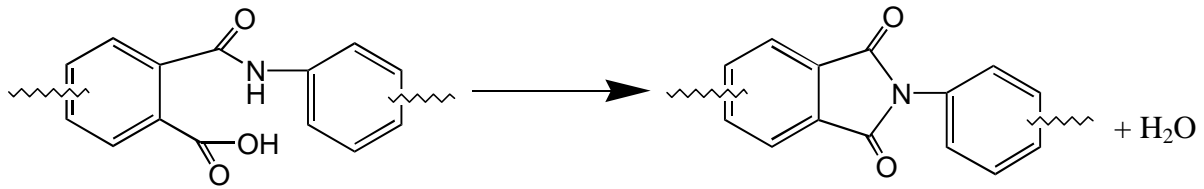


Figure 2.3.2 Plot of empirical thickness versus spin speed for polyimide film obtained from a commercial poly(amic acid) solution<sup>110</sup>.



“Cure” involves thermal imidization of PAA film, forming linear stiff “ordered” chains

General Cure Conditions\*

B-stage bake	30 min. @ 90-120°C	Solvent partially removed and imidization is initiated
Hardbake	30 min. – 1 h @ 350 – 420°C	(1) Imidization reaction is nearly complete and, (2) nearly all solvent has evaporated

Figure 2.3.3 Thermal processing of polyimide films for interlayer dielectrics<sup>112</sup>.

(4) A dielectric film is cast on top of the defined metal lines by spin-coating the poly(amic acid) solution and curing it to obtain polyimide.

The planarization ability of the polyimide film becomes important at this point in the process. This is because steps 1 through 4 must be repeated to give multi-layers of metal and dielectric. To provide an optimum surface for the next level of metal to be deposited and defined, the film must be relatively planar over the rough topography of underlying metal.

It is not possible for a polyimide film to perfectly planarize a metal pattern<sup>109</sup>. The initial coat of poly(amic acid) will provide a planar surface over any topographical feature whose height is less than the thickness of the deposited film<sup>107</sup>. However, as the solvent evaporates the solution viscosity increases until flow is minimized<sup>196</sup>. Even during curing there is a reduction in flow as  $T_g$  increases. Reduced flow and the release of volatiles during curing (water of imidization, solvent) cause the film to shrink<sup>196</sup>. This shrinkage causes the film to partially conform to the shape of the underlying topography<sup>107, 113</sup>.

The quantitative measurement of planarization over a step or conductor line of initial height,  $t_i$ , is called the degree of planarization given as<sup>107</sup>:

$$\text{DOP} = 1 - t_f / t_i$$

The variable  $t_f$  is the final step height in the cured polyimide film.

To create multi-layers, the process of sequentially depositing metal-dielectric must be repeated on top of the first planarized film. Prior to this process, holes must be etched in the film for making contact vias. This can be accomplished by the steps described below<sup>7, 192</sup>:

- (a) Depositing photoresist on top of the polyimide film.
- (b) Using photolithography for defining via patterns on the film.
- (c) Developing and subsequently hardbaking the photoresist.

- (d) Etching the patterns in the polyimide film using a laser.
- (e) Stripping off the photoresist.

Figure 2.3.4 represents a schematic drawing of the steps, although the resulting shape of the etched feature is not that of a via<sup>106</sup>.

Following via etching, the four sequential steps in building the TFML can be performed. The via holes are filled with metal during the first step (i.e. depositing the blanket of metal on the polyimide film)<sup>113</sup>. The metal is applied by plating (electro- or electroless plating), or by sputtering<sup>7</sup>. If plating is used, the polyimide film is exposed to the plating solution.

### **2.3.2.1.3 Building Thin Film Multilayers Using Additive Processes**

Other methods for building TFML packaging involve what are known as “additive” processes<sup>7</sup>. The processing steps can be carried out using two different types of etching techniques<sup>7</sup>. In the outline below, these have been designated option (a) for “wet etch” and option (b) for “dry etch”:

- (1) Depositing and heat-treating a poly(amic acid) (PAA) as a blanket film.
  - (a) If using “wet etch” process, softbaking PAA to partially cure.
  - (b) If using “dry etch” process, soft- and hard-baking PAA to imidize completely.
- (2) Depositing the process materials on film, as appropriate to etch method:
  - (a) Applying a photoresist (for “wet” etch).
  - (b) Applying an etch “mask” and, subsequently, a photoresist (for “dry” etch).
- (3) Defining the pattern by photolithography and development of photoresist.
- (4) Etching the pattern:
  - (a) in the film for “wet” etch (concomitantly during photoresist development).
  - (b) in both the “mask” and film for “dry” etch.

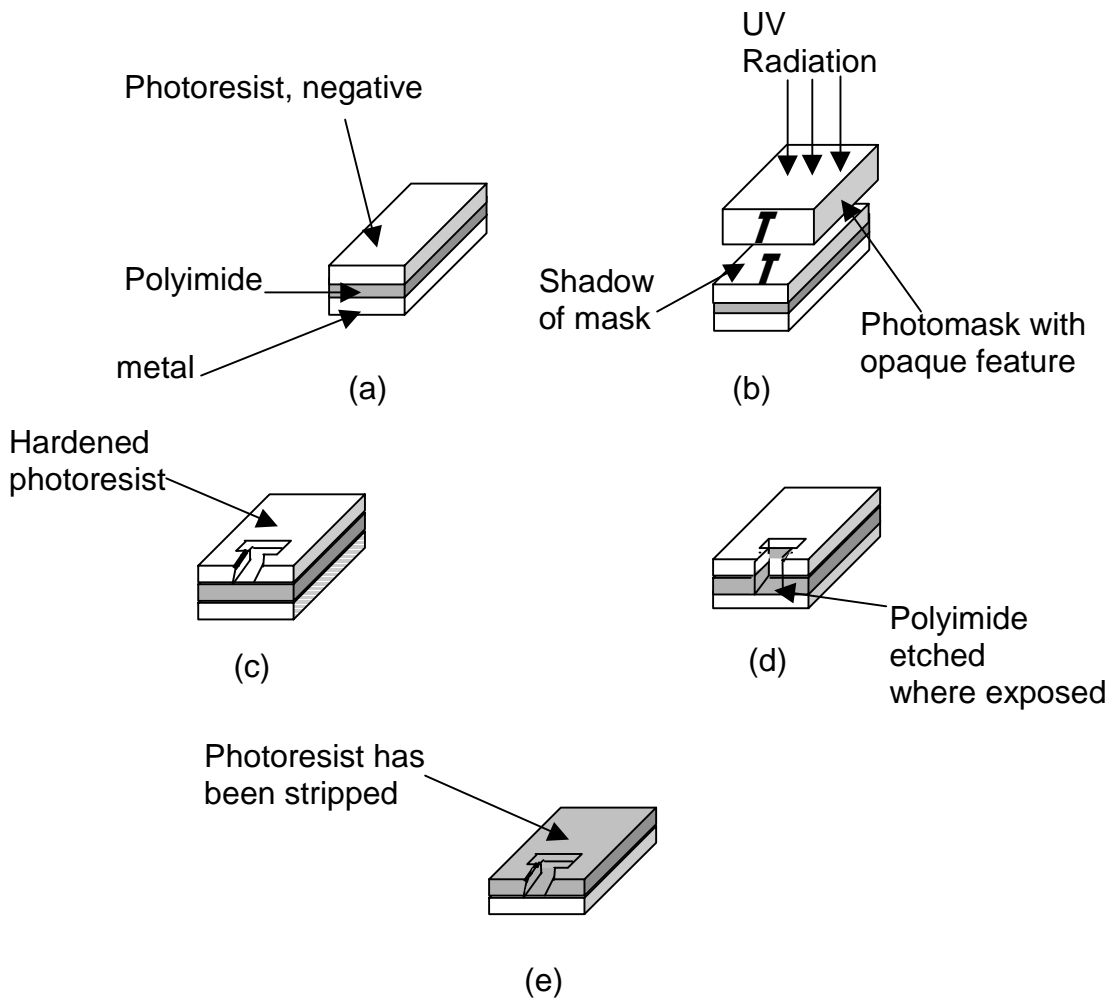


Figure 2.3.4 Photolithographic process and dry etching of planarized film<sup>106</sup>.

- (5) Stripping off the process materials (i.e. “mask”, resist).
  - (a) After stripping, the “wet” etched PAA film must be imidized (hard-baking).
  - (b) After stripping, no post-curing is required for the “dry” etched polyimide film.
- (6) Plating the patterned film with metal.

The “wet” etch process has relatively fewer steps than the “dry” method<sup>7, 192, 193</sup>. In particular, deposition of a protective mask is eliminated<sup>192</sup>. Additionally, a step is eliminated because the development of the photoresist and wet etching of the film occur simultaneously<sup>193</sup>.

Wet chemical etching methods take advantage of the high concentration of residual carboxyl moieties in the partially imidized film after soft-bake. The carboxyl functionalities render the polymer chains soluble in aqueous and other solvents<sup>110</sup>. Upon exposure to UV light, positive-type photoresists undergo transformation to chemical species that are soluble in dilute aqueous base, such as KOH and (usually) TMAH<sup>107, 194</sup>. The UV light-exposed portion of the resist and the underlying polymer film, dissolve during development in dilute basic solutions. The unexposed portion of the photoresist is hard and chemically inert and, thus, protects the remainder of the underlying PAA film from exposure to the chemical solution<sup>194</sup>.

When using photosensitive (PS) polyimides, the number of steps in wet etching can be reduced still further (Figure 2.3.5)<sup>7, 192-194</sup>. Incorporation of UV reactive groups along the polymer chain enables PS polyimides to serve as their own photoresists<sup>193</sup>. The soft-baking step is still carried out, but subsequent deposition of a separate resist material is not required<sup>192</sup>. The pattern is transferred to the PS-PAA film directly, using UV light and a photomask. The photocrosslinking groups in the PAA react to form an insoluble network in the UV-exposed areas (negative-type photoresist)<sup>193</sup>. Following crosslinking, unexposed areas of the film are chemically developed to remove them<sup>192-193</sup>.

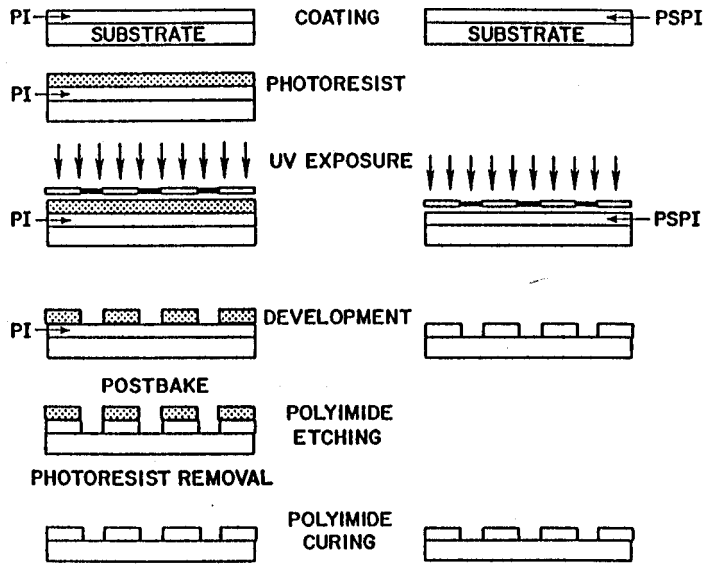


Figure 2.3.5 Comparison of wet etching processing for a conventional polyimide (PI) and a photosensitive polyimide (PSPI)<sup>7</sup>.

The final hardbake step causes the PAA groups to imidize with simultaneous evolution of the crosslinking groups<sup>104</sup>. The cure step results in larger film shrinkage than that of conventional poly(amic acid)s, which is a potential problem<sup>104, 193-194</sup>.

#### **2.3.2.1.4 Bonding Integrated Circuit Chips to TFML Packaging**

After fabricating the TFML packaging, the integrated circuit chips must be attached to its surface. There are several options for performing this bonding process. Since these require bonding metal-to-metal, the implication is that the polyimide films in the package will be exposed to high temperatures.

The technique known as “wire bonding” employs ultrasonic movement of a thin gold wire, which has been pressed into a gold pad<sup>107, 192</sup>. The frictional heat generated by the movement causes a metallic bond to form<sup>7</sup>. For gold or copper wire, thermosonic welding is used in which external heat is applied simultaneously to ultrasonic movement<sup>192-193</sup>. During these processes, very high temperatures (150-200°C) are reached under considerably high pressure and shear force. Polyimide films in the TFML substrate experience these conditions, but only for a short period of time (~20 ms)<sup>192</sup>.

Tape automated bonding, TAB, utilizes thermocompression to effect bonding between the chip bond pad and a prefabricated copper lead frame<sup>107</sup>. Once the chip has been joined to the tab tape, the outer lead pads on the tape are aligned with those on the TFML substrate<sup>193</sup>. Then metal-to-metal joining is usually accomplished using melt/reflow or thermocompression techniques, which can subject the TFML substrate to temperatures  $\geq 375^\circ\text{C}$  for a few seconds<sup>193</sup>.

In flip-chip technology, bonding is achieved by using melt/reflow solder and direct attachment of the chip to the TFML packaging<sup>110, 193</sup>. The system components, including the TFML substrate, can experience temperatures up to 370°C, or higher<sup>7</sup>. Even though the duration

of bonding time is usually 1-2 minutes, the need to exchange faulty chips will require at least 10 chip join cycles<sup>7</sup>. This results in more high temperature excursions for the packaging material.

### **2.3.3 Property Considerations and Requirements for Interlayer Dielectrics**

Polyimides are prime candidates for high performance dielectrics due to the ease with which their thermal, electrical and mechanical properties can be tailored to specific requirements. The facile modification of polyimides arises not only from the large selection of monomeric structures and combinations, but also from the wide variety of macromolecular sizes and architectures (i.e. branched, network, linear, etc.). Discussions of particular polyimide structures and their influence on physical properties will be provided in subsequent sections. First, however, a background description of the property considerations and requirements for interlayer dielectrics in MCM-D packaging will be provided.

#### **2.3.3.1 Electrical Properties**

##### **2.3.3.1.1 Dielectric Constant**

A dielectric material becomes polarized by alignment of induced- and permanent-type electric dipoles when subjected to an externally applied electric field<sup>7, 117</sup>. In order for the dielectric to inhibit or block transmission of electrical current, the mobility of the dipolar charges must be low. The insulating ability of a dielectric is described by its dielectric constant,  $\epsilon'$ . The  $\epsilon'$  is defined as the ratio of the measured capacitance of a capacitor filled with the dielectric material to the capacitance of an identical capacitor measured using a vacuum as the dielectric medium<sup>110, 192</sup>. The  $\epsilon'$  values for polyimides vary according structure, but typically range between 3.0 and 3.8<sup>104, 192</sup>.

The manifestation of a low  $\epsilon'$  value is of primary importance in using polyimides for dielectric films. If interaction of the electrical signal with the film is minimized by low  $\epsilon'$ , the

speed with which the signal traverses the conductor is maximized. This is shown by the following equation<sup>107</sup>:

$$V_p = c / \epsilon'^{1/2}$$

Where  $V_p$  is the propagation velocity of an electromagnetic sine-wave,  $c$  is the speed of light and  $\epsilon'$  is the dielectric constant of the surrounding medium (dielectric film)<sup>107</sup>.

The utilization of numerous, relatively short conductor lines in the packaging increases the speed of signal transmission between chips<sup>104</sup>. Packaging design for these systems involves selecting the thickness of the intervening dielectric layers<sup>105</sup>. To keep connection lengths short, it is desired that the lines be placed as closely as possible<sup>193</sup>. However, close proximity can allow an electromagnetic signal passing through one line to “cross-over” and induce a signal in a parallel conductor<sup>192</sup>. This phenomenon is known as “cross-talk” noise. The dielectric constant of the polyimide insulator governs the maximum conductor line density in the packaging. The lower the dielectric constant, the closer the signal lines can be placed<sup>193</sup>. Films that are better dielectric insulators reduce the magnitude of induced signals and, thus, lower the noise in the circuit.

For reliable performance under various operating conditions, the dielectric constant of a polyimide should be invariant with respect to changing electrical frequency and temperatures<sup>105</sup>. Additionally, for optimum electrical behavior, the dielectric constant should be isotropic<sup>7</sup>. This means that it is invariant with respect to the direction in which it is measured. For example, the value of  $\epsilon'$  obtained by in-plane capacitance measurements should match that obtained for capacitance measurements conducted normal to the film surface.

#### **2.3.3.1.2 Dissipation Factor**

During application of an alternating current electrical field (AC), the dielectric material

absorbs some of the electrical energy as it becomes polarized<sup>117</sup>. Some of this energy can be lost by conversion to heat in the material and, thus, the dielectric constant (or “permittivity”) is comprised of a complex value consisting of two components: the real component,  $\epsilon'$  (the dielectric constant), and the imaginary component,  $\epsilon''$ , the dielectric loss component (or dissipation factor)<sup>7</sup>. The ratio of these values is designated as the dielectric loss tangent or dissipation factor:

$$\tan \delta = \epsilon''/\epsilon'$$

The typical value for the dissipation factor of polyimides is 0.002<sup>7, 192</sup>. Low values of  $\tan \delta$  are indicative of minimal conversion of electrical energy to heat and, thus, signify minimal overall power loss in the dielectric<sup>105</sup>. It is advantageous to have low values for both the dissipation factor and the dielectric constant because electrical signals will lose less of their intensity in the dielectric medium.

### **2.3.3.1.3 Dielectric Strength**

The dielectric strength of a material measures its ability to withstand high voltages without breakdown or the passage of considerable amounts of current<sup>110</sup>. It is determined as the minimum value in the applied voltage ( $V_b$ ) at which breakdown occurs. The value of  $V_b$  can vary with respect to temperature, humidity, structure and the presence of impurities<sup>105, 110</sup>.

Most polyimides have dielectric strengths of  $10^5 - 10^6$  V/mm<sup>192</sup>. Since the maximum voltage in the TFML system is 10 volts<sup>7</sup>, polyimide dielectrics have no problem in maintaining low electrical losses in packaging applications. However, if the polyimide is utilized as a chip insulator, where film thicknesses drop below 1  $\mu\text{m}$ , there is potential for breakdown<sup>7</sup>. This particularly applies to manufacturing-type environments, where improper grounding of electronic devices can generate static charges capable of releasing currents of many thousands of

amps.

### **2.3.3.2 Thermal Properties**

#### **2.3.3.2.1 Coefficient of Thermal Expansion**

The coefficient of thermal expansion, CTE, of a material is defined as its change in dimension per unit dimension per 1°C rise in temperature<sup>192</sup>. The ideal situation is to have closely matching CTEs for all materials in the TFML<sup>192</sup>. However, as shown in Table 2.3.3, polyimides have relatively higher CTE values than the inorganic materials<sup>110, 192</sup>.

The problem with CTE mismatch occurs during high temperature processing/cycling when the polyimide film expands at a faster rate than the inorganics with which it is in contact. Internal tensile stresses build up in the film as the system returns to ambient temperature, resulting from insufficient stress relaxation of rigid aromatic polyimide chains<sup>5, 110, 113</sup>. To further complicate the problem, the out-of-plane CTE for these systems has been found to be about one order of magnitude higher than the in-plane CTE<sup>114</sup>.

The tensile internal stress typically ranges between 30-50 MPa for aromatic polyimide films<sup>113, 192</sup>. These internal stresses can result in warpage of the substrate and loss of adhesion<sup>7</sup>. These defects can greatly affect the long-term performance reliability of electronic packaging.

#### **2.3.3.2.2 Thermal Stability**

As described in a previous section, the process steps for chip attachment utilizing reflow soldering can subject the dielectric to temperatures  $\geq 370^\circ\text{C}$ . Polyimides also undergo numerous excursions to  $400^\circ\text{C}$  during the imidization processing of subsequently deposited poly(amic acid) layers. Additionally, laser ablation, metal deposition and plasma cleaning steps can generate high temperatures in the polyimide materials<sup>7</sup>.

Table 2.3.3 Thermal Expansion Coefficient Values<sup>110, 192</sup>.

Material	Thermal Expansion Coefficient Values (Approximate ) ppm/°C
SiO <sub>2</sub>	4
Si <sub>3</sub> N <sub>4</sub>	1
Si, SiC	3
Alumina	6
Gold	14
Copper	17
Aluminum	24
Polyimide	40-50

Aromatic polyimides typically have high thermal stability, exhibiting 5% weight loss in air at temperatures exceeding 400°C as measured by thermogravimetric analysis (TGA). This is advantageous for packaging applications. However, to be considered wholly thermally stable, the polyimide properties should remain constant at the temperature in question. During routine analyses in the electronics industry, the film is exposed to 400°C (isothermal TGA) for 2 hours under nitrogen purge<sup>192-193</sup>. These conditions emulate the imidization processing for subsequently deposited layers of dielectric. During exposure, a low weight loss (<1%) indicates acceptable thermal stability<sup>193</sup>.

Larger film samples can be baked under the same conditions, either free-standing or bonded to appropriate substrates, and inspected for changes in properties.

Undesirable property changes, which result from thermal degradation include<sup>7</sup>:

- (1) Embrittlement
- (2) Growth of carbonaceous deposits which are electrically conductive
- (3) Reduced adhesion
- (4) Lowered mechanical properties
- (5) Lowered  $T_g$ .

If these changes are evident, the polyimide in question is a poor candidate for use in TFML electronic packaging.

### **2.3.3.2.3 Glass Transition Temperature**

As discussed above, processing excursions to 400°C are routinely experienced by interlayer dielectrics. Under these conditions, the glass transition temperature ( $T_g$ ) of the polyimide film becomes critical. Single-phase thermoplastic films, in particular, can exhibit significant rubbery flow above  $T_g$ . If external stress is experienced during flow, the film can

become deformed resulting in warpage of the imbedded signal lines<sup>7</sup>.

Although the  $T_g$ s of aromatic polyimides are relatively higher than those of many polymers, there is wide variation depending on structure.  $T_g$ s usually exceed 300°C for rigid ordered polyimides, but those of 400°C or above are preferred for interlayer dielectrics<sup>194</sup>. Additionally, crosslinked systems can restrict flow above  $T_g$  and, in this respect, would prove beneficial for this application.

### **2.3.3.3 Adhesive and Material Strength**

Mechanical failure of packaging occurs as a response to high stress and serves to release that stress<sup>7, 113</sup>. However, since cracking and delamination are the two modes for releasing stress (cohesive and adhesive failure, respectively), the result is a damaged poorly functioning package.

#### **2.3.3.3.1 Mechanical Properties**

Polyimide films have been found to have relatively high mechanical strengths. From dynamic mechanical analysis (DMA) measurements, tensile strengths typically range from 100-200 MPa and the elongation at break (EB) values range from 10-25%<sup>47, 104, 113</sup>. However, these values reflect the behavior of relatively flawless, free-standing film specimens. The actual mechanical performance of polyimides in the package is significantly reduced due to metal vias and conductor lines which cause interfacial stress concentrations in the films (CTE mismatch effect)<sup>7</sup>. These defects will cause failure in the package long before reaching the maximum EB value measured for the “idealized” sample. Since the strains typically experienced by dielectrics in TFMLs are 1-3%, the films are resistant to cracking, but not to the extent predicted by DMA testing results<sup>7</sup>.

The internal stress alone will not cause cracking of the film, however, unless the film is very brittle<sup>7, 104, 113</sup>. In brittle polymers, the fracture strength is diminished to the extent where

the internal stress becomes critical. Typical values of 30-50 MPa have been measured for internal stresses developed by polyimides from CTE mismatch<sup>113, 192</sup>. Cracking occurs when the internal stress exceeds the fracture strength, resulting in defective metallization patterns and cohesive failure.

Often the effects of thermal and solvent processing will increase the brittleness of polyimide films, resulting in a decrease in the mechanical strength<sup>47</sup>. Since brittleness is related to the film stress and crack propagation rate, EB values measured for films following exposure to processing-type conditions can provide pertinent information. The polyimide is considered brittle if fracture of a film occurs during the initial steep point of the stress-strain curve and the EB is below 10% for a free-standing, flawless film<sup>7</sup>.

The mechanical properties of polyimide films are not solely influenced by cure history, but also depend on the molecular architecture. For example, glassy crosslinked polyimides are among the most brittle<sup>197</sup>. However, the degree of embrittlement depends on the crosslink density and this could be controlled by appropriate molecular design.

#### **2.3.3.3.2 Adhesion**

Good adhesion of the polyimide film to different inorganic interfaces, such as copper, silicon and aluminum, is important for reliable performance of electronic packaging. Additionally, self-adhesion is critical where subsequent layers of polyimide come in contact with each other. The issue of good adhesion extends to harsh processing conditions. Adhesion must remain intact after exposure to high baking or soldering temperatures, as well as during contact with chemicals and solvents used in TFML fabrication<sup>7, 192</sup>.

Adhesion failure of TFML packaging is manifested by delamination of the layers<sup>193</sup>. Partial delamination does not always lead to immediate electric failure of the system<sup>7</sup>. However,

eventually this type of failure results from the seepage of moisture into the metal circuitry exposed by the delamination of the dielectric insulator<sup>7</sup>. In the presence of moisture, bi-metal junctions in the circuitry can form a galvanic element, which causes metal corrosion<sup>192</sup>. Additionally, moisture itself can cause further delamination of the dielectric from the inorganic substrates<sup>113, 193-194</sup>.

A thorough understanding has not yet been achieved with regard to adhesion or adhesive failure of polyimides. However several generalizations have been proposed<sup>7, 193</sup>:

- (1) Good interfacial wetting of the substrate by the polyimide is essential for good adhesion.
- (2) High temperatures and humidity can cause significant degradation of adhesion.
- (3) Priming the inorganic substrate with an adhesion promoter before depositing/curing the polyimide promotes longer retention of adhesion strength.
- (4) Metal corrosion can lead to adhesion loss.
- (5) Polyimides exhibiting a large decrease in modulus at  $T_g$  show good adhesion to the substrate when processed above  $T_g$ . (Provides good wetting.)
- (6) Low molecular weight precursors for crosslinkable polyimides (thermosets) usually adhere well due to good wetting.
- (7) Diffusion of copper oxide from the interconnect into poly(amic acid) facilitates thermal degradation of adhesion (by metal catalysis).
- (8) Particulate contaminants, when present, can decrease adhesive strength.

Table 2.3.1 shows the adhesion characteristics among the three different classes of polyimides, amorphous, multi-phase (ordered mesophase, semi-crystalline, etc.) and thermosetting<sup>7</sup>.

Table 2.3.4 Adhesion Characteristics of the Three Classes of Polyimides<sup>7</sup>.

ADHESION CHARACTERISTICS OF POLYIMIDES

Polyimide type	Substrates				
	Copper	Chromium	Aluminum	Self	Ceramics
Amorphous	Good	Good	Good	Good	---
Multi-phase	Poor	Good	Good	Marginal	Good with aminosilane adhesion promoter
Thermosetting	Good	Good	Good	Good if first deposited layer is not fully cured	Good

### 2.3.3.4 Properties in the Presence of Moisture, Solvents and Chemicals

#### 2.3.3.4.1 Effect of Moisture

During storage and processing, poly(amic acid) precursors should be protected from humidity due to potential hydrolysis. As discussed in section 2.2, the release of water during imidization causes some chain-scission by hydrolysis, depending on temperature and chain mobility<sup>35</sup>. It is possible to control this effect by optimizing thermal cure conditions or by utilizing poly(amide esters)<sup>45-47, 115-116</sup>.

Film shrinkage, resulting from the release of water during imidization of poly(amic acid)s, decreases the planarization. However, planarization can be improved by casting thicker or layered films<sup>113, 194</sup>.

A more critical problem involves the uptake of water from air by fully-cured polyimide films. The water absorption of polyimides is typically greater than 1% at ambient temperatures<sup>105, 117</sup>. If this absorbed water is in the underlying dielectric layers, it can outgas during subsequent high-temperature processing causing blistering, voids and delamination in the top film layer as it cures<sup>193</sup>. Metal deposited on top of the film can also blister due to this effect<sup>7</sup>.

Absorbed moisture in the package has a critical effect on the electrical properties of the polyimide. Water has a very high dielectric constant ( $\sim 78$ )<sup>194</sup>, so even small absorptions can significantly raise the dielectric constant of the polyimide film<sup>105</sup>. For example, the dielectric constant of a PMDA/ODA-based polyimide had been observed to increase linearly from 3.1 at 0% humidity to 4.1 at 100% humidity<sup>113</sup>.

Relatively low moisture absorption is required for polyimides when operating under high humidity conditions. The modification of the chemical structure of polyimides can be effected to provide lower water absorption for these applications.

#### **2.3.3.4.2 Effect of Solvent and Chemical Processes**

Since many chemical processes are utilized in fabricating TFML packaging, it is important that interlayer polyimides display high resistance to attack by certain organic and inorganic substances. Examples of organic solvents typically utilized in processing include NMP, ethanol, toluene, cellosolve and diglyme<sup>7</sup>. During exposure to these, it is imperative that the polyimides remain dimensionally stable; that is, they should not dissolve or swell appreciatively. If significant attack by solvent occurs, the result is cracking or crazing of the polyimide film, which lead to adhesion loss, line distortion and breaking of signal lines<sup>7, 194</sup>.

Resistance to caustic solutions, such as plating solutions, is also important. If the polyimide film is easily permeated by these aqueous solutions, hydrolysis degradation can occur causing chain scission. The result is decreased mechanical strength and film integrity. Additionally, strongly acidic etching solutions are often utilized to etch metals<sup>107</sup>. If the underlying polyimide film is not protected sufficiently by the resist material, exposure to this solution can cause eventual acid-catalyzed hydrolysis<sup>117</sup>.

The chemical resistance of polyimides depends on structure. Typically, rigid-rod-like two-phase polyimides and crosslinked polyimides display higher resistance to a wide variety of processing agents.

## **2.4 Literature Review on Structure-property Relationships of Polyimides**

### **2.4.1 Two-phase Linear Thermoplastic Polyimides**

Aromatic polyimide chains consist of electron-dense and relatively electron-poor regions, which arise from aromatic diamine and dianhydride moieties, respectively. It is believed that electronic polarization can occur between these groups. Intermolecular charge polarization

occurs when a group in one chain donates some of its electron density to an electron-deficient group in another chain<sup>10</sup>. This phenomenon is called “charge transfer complexation”.

Due to the stiffness of linear rigid-rod and segmented rigid-rod polyimides, chain-chain interactions can occur over several consecutive repeat units. Consequently, the segments can become aligned along their axes. It is believed that this alignment contributes to the formation of short-range order and crystallinity<sup>10</sup>. An accurate physical picture has not yet been developed for chain-chain interactions comprising charge-transfer and crystalline-type interactions. However, two abbreviated idealized depictions appear in Figure 2.4.1<sup>10</sup>.

Polyimides containing amorphous and crystalline (or “ordered”) regions are known as two-phase or semi-crystalline polymers<sup>102</sup>. Two-phase linear thermoplastic polyimides are known for high  $T_g$ s, excellent solvent resistance and resistance to thermal/mechanical distortion at temperatures just above  $T_g$ <sup>78, 118-119</sup>. Due to these outstanding properties, several commercially available polyimides in this category have found widespread use as interlayer dielectrics in electronic packaging<sup>7</sup>. The following sections discuss the structure-property relationships of these materials, including recent modifications for tailoring the physical properties.

#### **2.4.1.1 Polyimides Based on PMDA/ODA**

The DuPont Company manufactures polyimides based on PMDA/ODA, which are known under the following trade names<sup>7</sup>: (1) Kapton (in imidized film form), and (2) Pyralin 2540 or 2545 (poly(amic acid) in solution). As mentioned in Section 2.2.1.4, bulk thermal imidization of the soluble poly(amic acid) precursor is used for making films in the desired shape due to the insoluble/intractable nature of the polyimide. Kapton polyimide exhibits a combination of outstanding physical properties for microelectronics applications (Table 2.4.1).

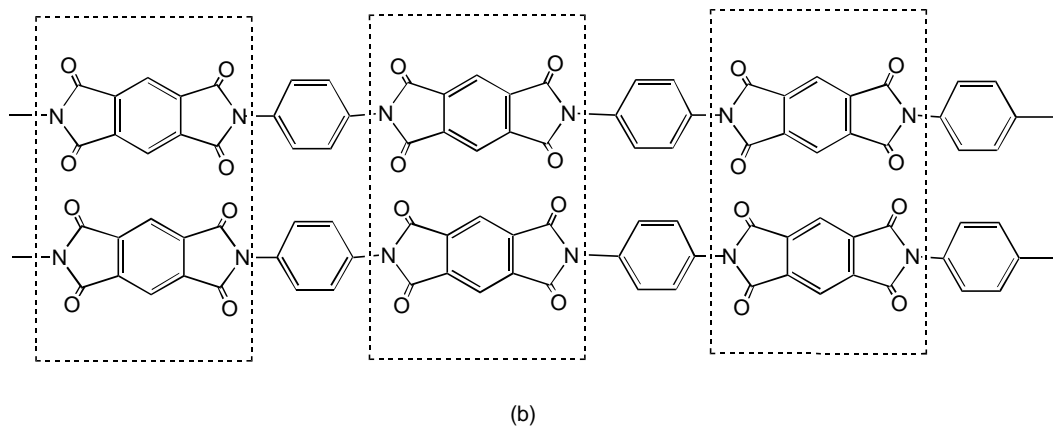
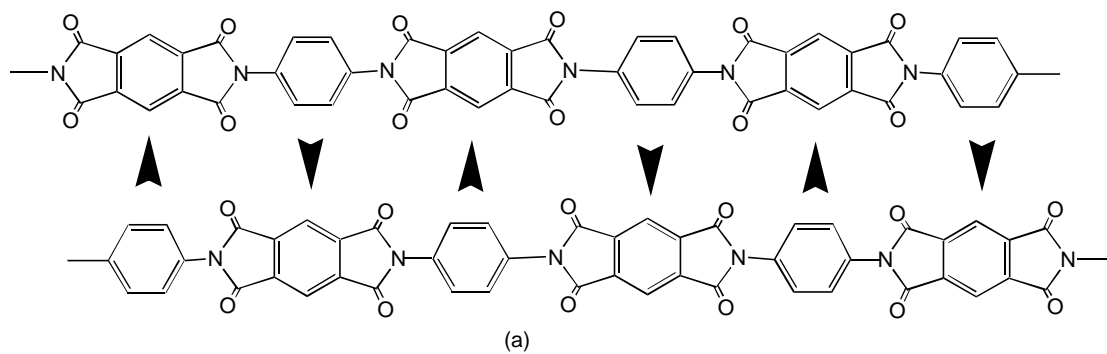


Figure 2.4.1 Interactions between polyimide chains (a) charge polarization; (b) crystalline interaction<sup>10</sup>.

Table 2.4.1 Selected Properties of PMDA/ODA Polyimide<sup>7</sup>.

Dielectric constant	3.1 dry, 3.5 wet
Dielectric loss factor	0.0012
T <sub>g</sub> (by DMA @ 5°C/min, 1 Hz)	400°C
Beta relaxation	120°C
Gamma relaxation (obs. only in presence of H <sub>2</sub> O)	-70°C
Isothermal weight loss @ 400°C in N <sub>2</sub>	0.04 wt % /h
Thermal conductivity	0.361 W/m K
Modulus / Modulus after 8h @ 400°C	3 x 10 <sup>9</sup> Pa / unchanged
Strain at break (S <sub>β</sub> ) / S <sub>β</sub> after 8h @ 400°C	60-70% / decreased from 3.0 GPa to 1.9 GPa
Tensile strength (T <sub>s</sub> ) / T <sub>s</sub> after 8h @ 400°C	1.4 x 10 <sup>8</sup> Pa / increased from 140 to 160 MPa
CTE (50 μm film thickness)	35-40 ppm/K
Crack resistance	excellent
Solvent induced crazing	not observed in films under 100μm thick
Self-adhesion (fully cured)	6-10 g/mm
Adhesion as top layer over copper (a) without and (b) with adhesion promoters	(a) 6-10 g/mm (b) 72 g/mm (Cr and silane adhesion promoter)
Adhesion as top layer over chromium	60 g/mm
Planarization	0.17

In addition to high thermo-oxidative stability and low dielectric constant, the most useful properties for electronics applications have been: (1) high chemical resistance, (2) continuing film toughness under rigorous conditions of air and thermal aging at 400°C ( $T_g$ ), and (3) retention of high mechanical strength over a wide temperature range<sup>18</sup>. Research efforts have focused on elucidating the molecular/structural origin of these properties.

Initially, PMDA/ODA was considered to be semicrystalline<sup>18, 120-121</sup>. This was based on the results of wide-angle x-ray scattering (WAXS) experiments, which showed intensified reflections for Kapton films that had been annealed at temperatures above 350°C. Additionally, evidence of chain segment aggregation was obtained using small angle x-ray scattering (SAXS)<sup>121</sup>. Since the WAXS diffraction patterns were not sharp, increased ordering at temperatures above 350° was attributed to formation of highly disordered crystals by further lateral chain alignment. Decreased chain mobility, resulting from the simultaneous increase in  $T_g$ , was believed to prohibit higher degrees of chain reorganization and therefore to interrupt the formation of sharply defined crystalline regions<sup>121</sup>.

The nature of the “disordered” crystalline morphology has been defined<sup>122-123</sup>. Transmission-type WAXD experiments conducted on PMDA/ODA polyimide films gave a symmetrical and sharp peak at 5.7 ( $2\theta$ ), which indicated a Bragg ( $d$ ) spacing of 15.0Å (Figure 2.4.2)<sup>122-123</sup>. This value was close to the calculated 15.4Å repeat unit spacing along the axis of a fully extended chain. From these results, the authors concluded that chain units in the ordered regions were nearly fully extended and were in “register” with corresponding units of neighboring chains giving a smectic liquid crystal layering (Figure 2.4.3)<sup>123</sup>. The lack of sharp diffraction patterns in the lateral direction (higher angles) indicated that the lateral distance between neighboring chains was not equal, which confirmed the two-dimensional order of a

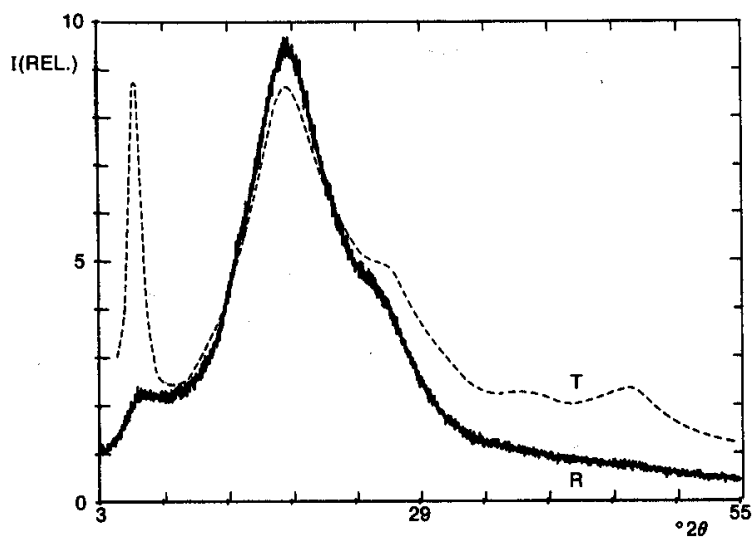


Figure 2.4.2 WAXD patterns of PMDA/ODA polyimide films in transmission (dashed trace line) and in reflection (normal signal line) runs<sup>123</sup>.

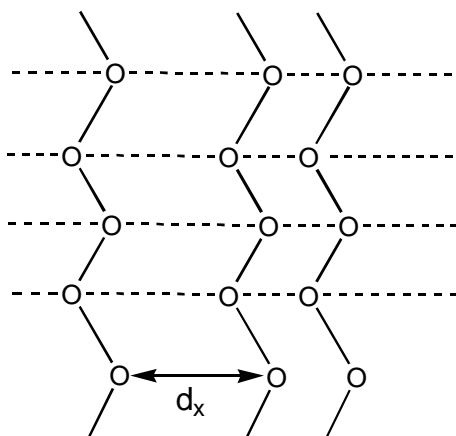


Figure 2.4.3 Representation of the smectic-like order of PMDA/ODA polyimide films

smectic type mesophase<sup>122</sup>. The smectic packing of bundles of chain units has been attributed to intermolecular charge-transfer interactions promoted by chain rigidity and high aromaticity<sup>124</sup>

Annealing (or slow incremental heating) at temperatures above 300°C increased the density of PMDA/ODA films<sup>124</sup>, as well as increasing the modulus and the  $T_g$ <sup>116</sup>.

FTIR studies revealed that PMDA/ODA films, which had been partially imidized (ca. 85%) at lower temperatures, did not afford complete imidization when heated to ~400°C<sup>115</sup>. Thus, in many cases, the hardbaking step of the cure cycle (350-420°C) may serve mainly to promote further ordering/packing of the polyimide chains. In the ordered regions, chains are capable of strong intermolecular interactions and may behave as if “bound” to one another. The presence of these “physical-type” crosslinks in the film greatly influences the physical properties. Some of the effects manifested by such a system include: (1) reduced penetration by small solvent molecules<sup>126</sup>, (2) high tensile strength and increased elongation at break values<sup>124</sup> and, (3) retention of mechanical strength and high modulus at temperatures near  $T_g$ <sup>125</sup>.

The problems posed by the two-phase morphology are related to anisotropic behavior with respect to several crucial properties, such as refractive index, dielectric constant and CTE. The anisotropy is particularly pronounced in films cast on substrates, where the polyimide chains preferentially align parallel to the substrate surface<sup>120-123</sup>.

The phenomenon of electronic polarization occurs in all materials at optical frequencies and is responsible for the refraction of light<sup>117</sup>. In polyimides, ordering/alignment and charge-transfer complexation of the chains significantly alters the directional polarizability of the molecules. Specifically, the distribution of molecular dipoles or electronic charges in the parallel direction can differ from that perpendicular to the chain axis. Consequently, the optical properties, such as the refraction of light measured at a given wavelength, become anisotropic.

PMDA/ODA films, which have been cast on substrates, are known to have the ordered regions oriented parallel to the film surface<sup>120</sup>. Due to the preferential in-plane chain alignment, the refractive index measured in the plane of the film ( $n_{\parallel}$ ) is significantly higher than the value of the refractive index measured perpendicular to the film surface ( $n_{\perp}$ )<sup>120</sup>. This phenomenon, is known as negative birefringence, and is described by the following equation<sup>114</sup>:

$$\Delta n = n_{\perp} - n_{\parallel} < 0$$

The  $\Delta n$  values for various thicknesses of thermally imidized PMDA/ODA films have been measured as ca. -0.08 at 633nm<sup>120</sup>. Since the refractive indices are anisotropic, the net polarizability of the polyimide chain system is also anisotropic.

The anisotropic polarization of two-phase polyimides at optical frequencies implies that the relative electrical permittivity also depends upon the direction in which the signal is traveling through the film. In fact, the in-plane dielectric constant ( $\epsilon'_{\parallel}$ ) becomes significant when considering the potential for cross-talk noise between signal lines in the same wiring plane within the dielectric film<sup>127</sup>. In the methods currently used for measuring the dielectric constant, the electrical field is applied normal to the film plane. Consequently,  $\epsilon'_{\perp}$  is the only value that can be directly measured.

The estimation of the dielectric constant,  $\epsilon'$ , at optical frequencies is based upon the Maxwell relationship:

$$\epsilon' \cong n^2$$

Performing the calculations using in-plane ( $n_{\parallel}=1.72$ ) and out-of-plane ( $n_{\perp}= 1.64$ ) refractive indices gives estimated dielectric constants of 2.96 and 2.69, respectively for PMDA/ODA films annealed at 400°C<sup>120</sup>. Thus, the estimated dielectric anisotropy is about 10%, which may substantially affect the electrical insulating properties of these films.

As mentioned in Section 2.3.3.4.1, the dielectric constant of PMDA/ODA has been observed to increase linearly from 3.1 at 0% humidity to 4.1 at 100% humidity<sup>113</sup>. Since this polyimide absorbs between 2.5 and 4% of its own weight at high relative humidity levels<sup>117</sup>, a substantial increase in  $\epsilon'_{\parallel}$  would be anticipated under these conditions as well.

Moisture has detrimental effects on PMDA/ODA dielectrics. DeSouza-Machado et al. utilized these films in capacitors and periodically measured the capacitance and dissipation factor at different relative humidity values (RH)<sup>117</sup>. The electrical dissipation factor was observed to increase substantially at low frequencies after aging PMDA/ODA imide films for 6 weeks at 85°C/85% RH (Figure 2.4.4). Surface analysis of the aged films using x-ray photoelectron spectroscopy (XPS) showed partial hydrolysis of the imide groups on the surface to form amide-acid. The dielectric behavior was not completely recovered after subjecting the aged samples to re-curing conditions. Thus, hydrolyzed chains and residual amide-acid groups were believed to be a problematical defect in these films.

The reasons for seeking upgraded or replacement polyimides for PMDA/ODA should be apparent from the above discussions. In addition to the drawbacks already mentioned, there are further problems due to the poor adhesion of PMDA/ODA film to itself and to copper. Additionally, the in-plane CTE (ca. 40 ppm/K) is relatively higher than that of inorganic substrates, such as silicon (CTE ca. 3 ppm/K)<sup>7</sup>.

#### **2.4.1.2 Modified Kapton-type Polyimides for Tailoring Physical Properties**

Several strategies have been investigated for improving the physical properties of Kapton-type polyimides for microelectronics applications. In the following sections, the structural modifications and resulting property improvements will be reviewed.

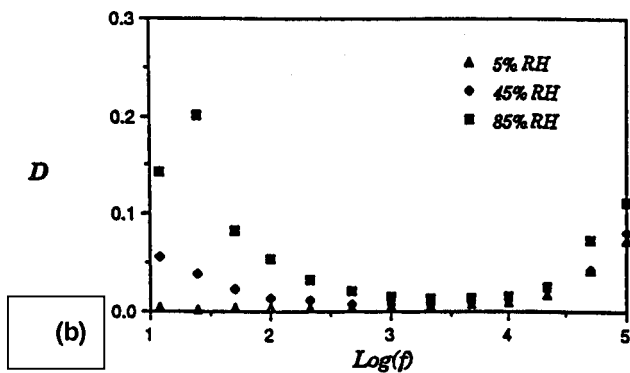
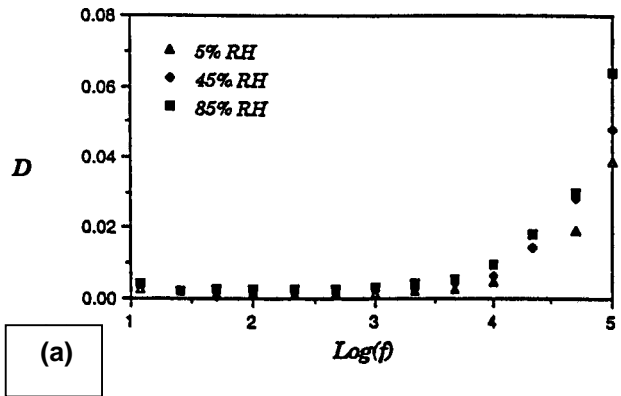


Figure 2.4.4 Dissipation factor vs. frequency (12 Hz-100 kHz) for PMDA/ODA containing capacitor devices (a) virgin device and (b) device aged for 6 weeks at 85°C/85% RH. Data taken for three RH values<sup>117</sup>.

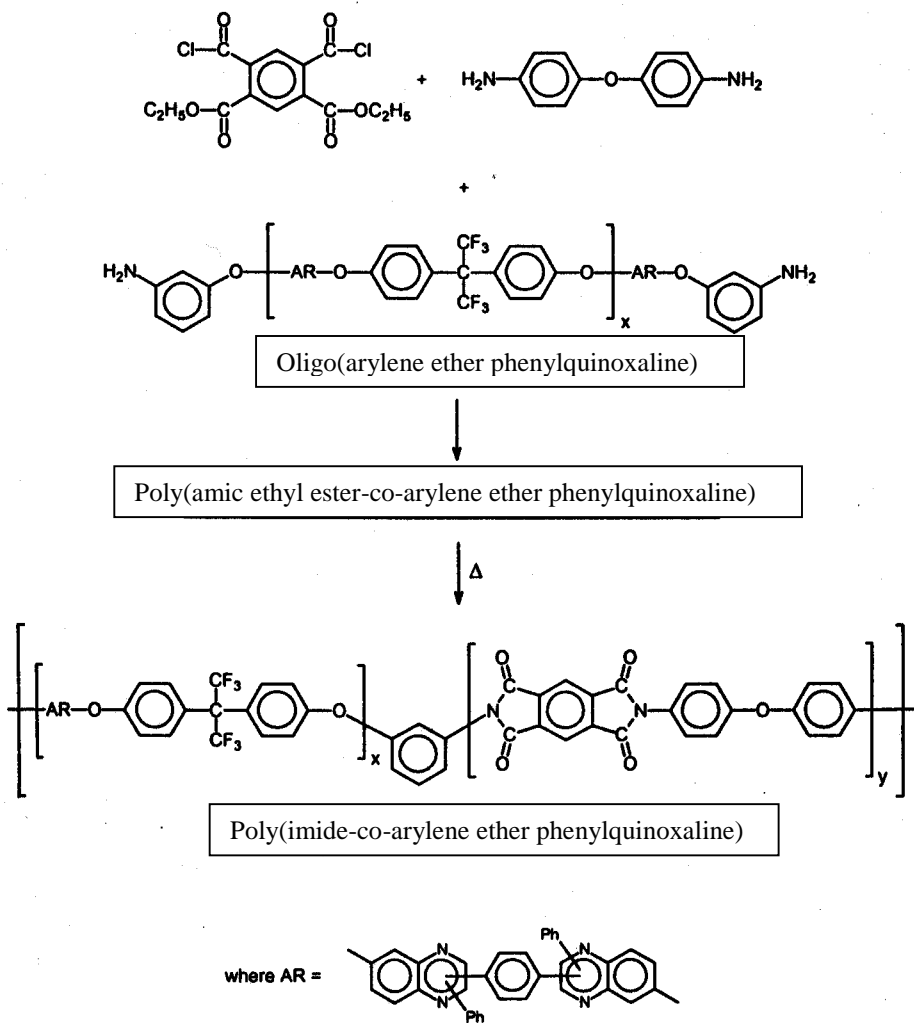
#### **2.4.1.2.1 Poly(amic alkyl ester) Derivatives of PMDA/ODA for Improved Properties**

As explained in Section 2.2.2, poly(amic alkyl ester) (PAE) derivatives are much more hydrolytically stable than their poly(amic acid) counterparts. Also, chain scission side reactions are absent during thermal imidization of PAEs<sup>45</sup>. In addition to process-type improvements, PAEs offer further benefits for dielectric applications.

##### **2.4.1.2.1.1 PMDA/ODA-based Polyimides with Improved Adhesion**

IBM developed a recrystallization process for isolating the meta isomer of the diester-diacid derivative of PMDA, which was then converted to the diester-diacid chloride<sup>47</sup>. This monomer was reacted with ODA in the usual manner. The spin-cast cured films obtained from this PAE exhibited self-adhesion values exceeding 100 g/mm<sup>47</sup>. This was at least a 10-fold improvement over Kapton's self-adhesion of 6-10 g/mm<sup>7</sup>. Adhesion of the PAE-generated polyimide to chromium was 80-90 g/mm versus Kapton's value of 60 g/mm. The improved adhesion was attributed to the relatively lower solution viscosity<sup>47</sup> and increased softening<sup>7</sup> of the PAE during the thermal cure cycle compared to the corresponding poly(amic acid). The PAE-generated polyimide exhibited solvent resistance and mechanical properties comparable to those of Kapton.

An alternative method for improving adhesion without sacrificing ordered morphology was to prepare segmented block copolymers of PMDA/ODA PAE with an engineering thermoplastic<sup>36, 128-129</sup>. To provide superior self-adhesion, the IBM research group incorporated an amine-terminated arylene ether phenylquinoxaline (PQE) (Scheme 2.4.1). Statistical incorporation of the PQE afforded the segmented block copolymer. Figure 2.4.5 shows two tan  $\delta$  peaks at the  $T_g$ s of PQE (~250°C) and of PMDA/ODA (~390°C), respectively. The retention of the ordered morphology is shown by minimal decrease in modulus ( $E'$ ) at high temperatures.



Scheme 2.4.1 Synthesis of poly(imide-co-arylene ether phenylquinoxaline)<sup>36</sup>.

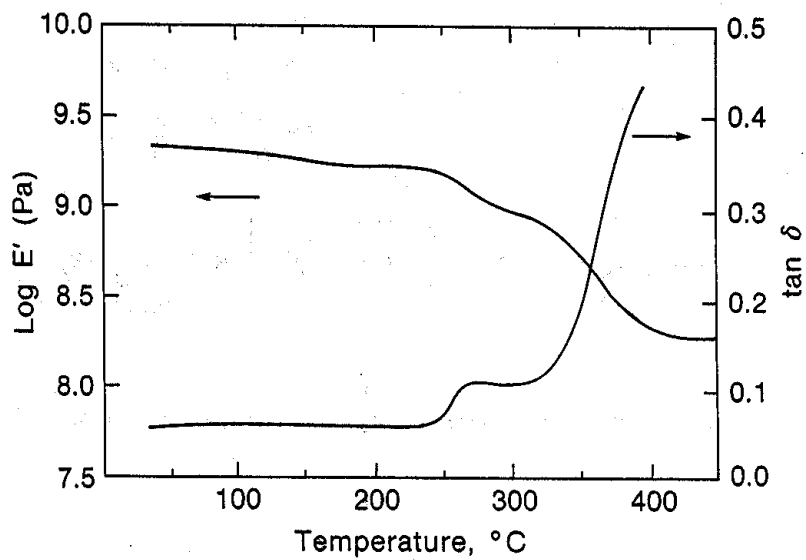


Figure 2.4.5. Dynamic mechanical behavior for poly(imide-co-arylene ether phenyl quinoxaline (PI/PQE) block copolymer as a function of temperature. PQE content is 29 wt% with a block size of 15,500<sup>128</sup>.

#### **2.4.1.2.1.2 PMDA/ODA-based Low Stress Polyimides**

As discussed in Section 2.3.3.2, internal stress buildup resulting from CTE mismatch can result in warpage of the substrate and loss of adhesion during thermal processing<sup>7</sup>. To improve stress-relaxation of the rigid PMDA/ODA polyimide, workers at IBM have prepared block copolymers containing relatively small amounts (e.g. 20% or less) of rubber-like polydimethylsiloxane (PDMS)<sup>5</sup>. The PAE synthetic route was used, with an amine-terminated PDMS oligomer serving as comonomer.

Significant reduction in residual stress was found for the PDMS-containing films (Figure 2.4.6)<sup>5</sup>. In fact, the copolymer containing 20 wt% of ~5 Kg/mol molecular weight PDMS showed zero residual stress. The polyimide containing PDMS of ~1 Kg/mol molecular weight showed moderately lower residual stress (ca. 25%) than the homopolymer.

PDMS-containing polyimides are not as thermally stable as their wholly aromatic counterparts<sup>130</sup>. Thus, the copolymers would be useful as dielectrics only if moderately lower thermal stability could be tolerated.

#### **2.4.1.2.1.3 PMDA/ODA-based Polyimides with Lower Dielectric Constant/Water Uptake**

IBM scientists have developed a method for obtaining thermally stable block copolymers with lower dielectric constants and less water uptake by incorporating oligomers of perfluoroalkylene arylene ethers (PFAAEs) in PMDA/ODA polyimide<sup>131</sup>. Figure 2.4.7 shows the structures of PFAAEs used in copolymer synthesis. As shown in Table 2.4.2, the block copolymers exhibited a reduction in dielectric constant relative to that of PMDA/ODA. Additionally, minimal increase in the dielectric constant as a function of humidity was observed for PFAAE copolymers compared to that of PMDA/ODA. The mechanical properties of Kapton were retained, indicating that the rigid block comprised the matrix of the phase-separated system.

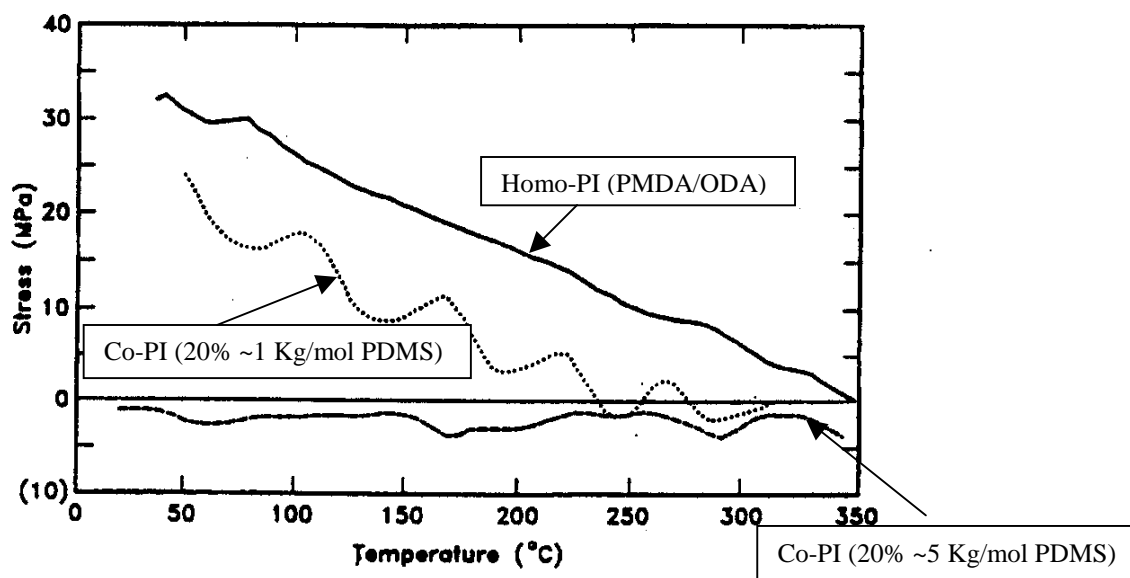


Figure 2.4.6 Residual stress versus temperature plots for polyimide/polydimethylsiloxane copolymers<sup>5</sup>.

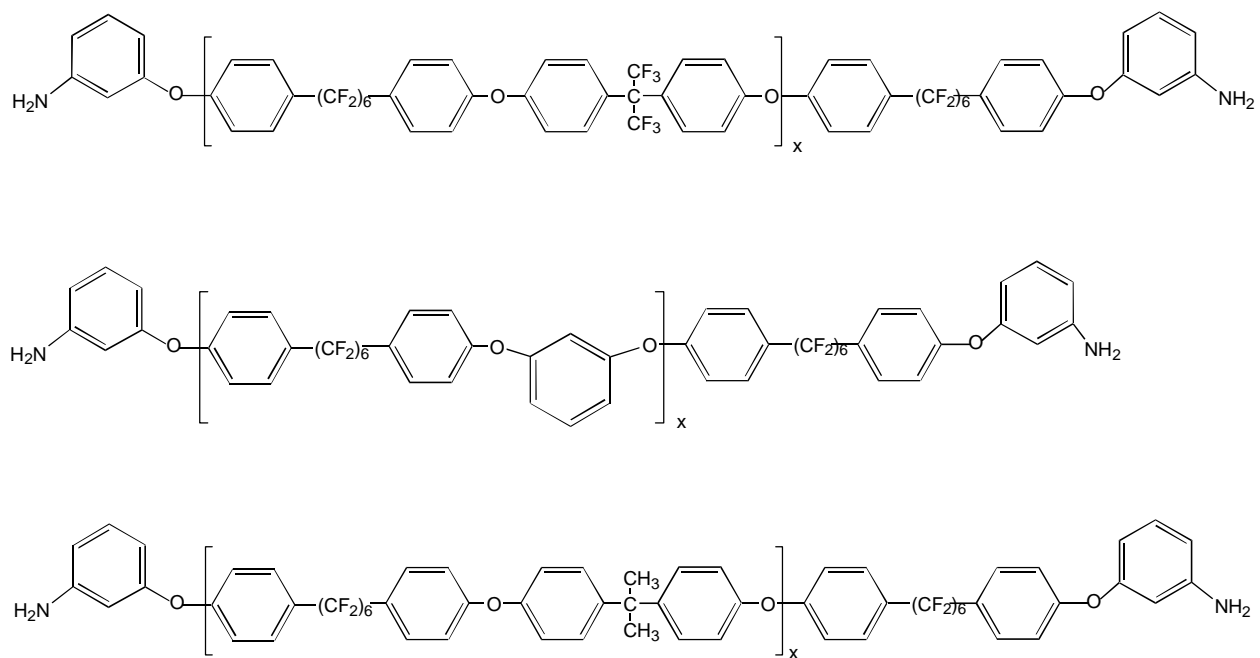


Figure 2.4.7 Structure of perfluoroalkylene arylene ethers (PFAAEs)<sup>131</sup>.

Table 2.4.2 Imide-PFAAE Mechanical, Thermal and Dielectric Properties<sup>131</sup>.

Composition		PFAAE M <sub>n</sub> (Kg/mol) (DP)	Modulus (MPa)	σ (%)	Wt% Fluorine	ε' at 1MHz Dry/Ambient	Isothermal weight loss @ 400°C in N <sub>2</sub>
Imide	PFAAE (6F <sub>2</sub> -BisAF)						
100	0	---	2.0 x 10 <sup>3</sup>	50	0	3.1/3.4	0.04wt% /h
45	55	7.7 (9.7)	2.0 x 10 <sup>3</sup>	72	24	3.0/3.2	0.20wt% /h
45	55	11.9 (15)	1.7 x 10 <sup>3</sup>	62	24	2.9/3.0	0.20wt% /h
0	100	---	1.4 x 10 <sup>3</sup>	35	43.5	2.6/2.6	---

Another strategy for reducing dielectric constants involved phase separated block copolymers in which the major phase consisted of a rigid polyimide and the dispersed phase was comprised of a thermally labile block<sup>132, 133</sup>. The formation of “nanopores” was accomplished by thermo-oxidative degradation with concomitant outgassing of the dispersed phase, which consisted of either poly(propylene oxide) (PO) or poly(methyl methacrylate) (PMMA).

To meet solvent resistance criteria, the researchers at IBM originally utilized PMDA/ODA as the matrix material for the “nanofoams”<sup>134-135</sup>. However, collapse of the foams occurred upon heating to temperatures above 300°C, which was well below the  $T_g$  of ~400°C. Hence, another rigid polyimide became the matrix material of interest for continuing this work<sup>132</sup>. This was based on PMDA and 2,2-bis[4-(4-aminophenoxy)phenyl]hexafluoropropane (4-BDAF), which was chosen because of the low water uptake and low dielectric constant of the homopolymer (Figure 2.4.8). Additionally, PMDA/4-BDAF polyimide had shown good solvent resistance and high thermal stability, which had been ascribed, in part, to its semicrystalline morphology<sup>153</sup>.

Block copolymers using pyromellitate diacyl chloride, 4-BDAF and amine-functionalized PO were prepared via the PAE route. Spin-cast PAE block copolymers were imidized under an argon atmosphere, which afforded insoluble, semi-crystalline films. Subsequent foaming reactions were carried out in air by heating to 250°C for several hours, affording nanofoam films with  $T_g$  values between 275 and 300°C.

Refractive indices ( $n$ ) of the foams were anisotropic ( $\Delta n = 0.05$ ). The  $n_{\parallel}$  values were used to estimate in-plane dielectric constants ( $\epsilon'_{\parallel}$ ). The  $\epsilon'_{\parallel}$  value of 2.4, obtained for one of the nanofoams, was significantly lower than the value of 2.7 estimated for the nonfoamed polymer.

During thermal treatments, significant foam collapse occurred above 350°C.

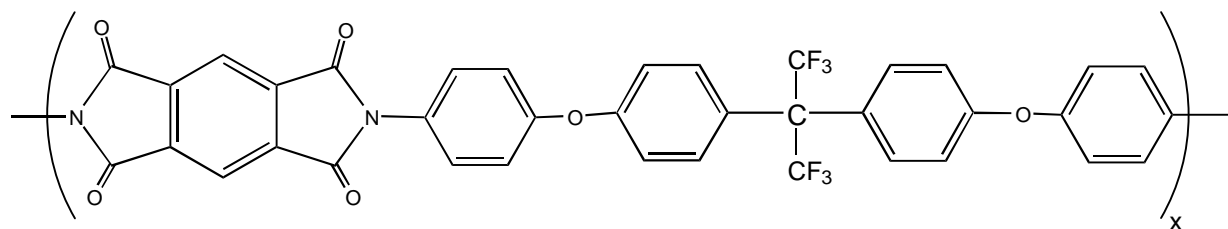


Figure 2.4.8 Repeat unit structure of PMDA/4-BDAF polyimide.

Consequently, the foams would be useful as dielectric materials only at moderately lower processing temperatures.

To prevent collapse of the nanopores at high temperatures, the strategy of functionalizing PAE/PO block copolymers with 1,1-bis(4-aminophenyl)-1-(4-ethynylphenyl)-2,2,2-trifluoroethane (3FET) has been utilized<sup>133, 159</sup>. The ethynyl groups crosslink at temperatures typically used for imidizing PAEs (ca. 200°C). Copolyimides containing controlled amounts of pendant ethynyl groups were prepared from pyromellitate diacyl chloride and 1,1-bis(4-aminophenyl)-1-phenyl-2,2,2-trifluoroethane (3FDAM) with 3FET and amine-terminated PO as comonomers (Figure 2.4.9). Subsequent thermal treatments afforded foams with high crosslink density, which provided good solvent resistance. A further advantage was evident in utilizing thermosetting-type nanofoams: the rigid matrix need not consist of a semi-crystalline polyimide. Matrices based on PMDA/3FDAM/3FET polyimides were fully amorphous. Although the refractive indices were not reported, it is possible that the values would be isotropic for amorphous crosslinked nanofoam films.

#### **2.4.1.3 Polyimides Based on BPDA/p-PDA**

Extensive research has revealed that aromatic two-phase rigid polyimides, such as PMDA/ODA, offer superior high temperature mechanical properties. However, improvements to these materials are always being sought, such as reducing the thermal mismatch stress. An outcome of this quest has been the commercial development of rigid-rod type polyimides based on BPDA/p-PDA. This polymer has been made available in film form, known as Upilex S from Hitachi, and as poly(amic acid) solutions (Hitachi's PIQ L100 and PIX L100, plus DuPont's Pyralin 2610 and 2611)<sup>7</sup>.



Unlike PMDA/ODA polyimide, Upilex S does not contain flexible linking groups (Figure 2.4.10). Consequently, it is rigid-rod-like, having a large persistence length in the chain direction and low chain flexibility. This results in a high modulus and a low CTE in the chain direction. In-plane CTE values typically range between 5 and 8 ppm, depending on the extent of parallel chain alignment attained during a given cure schedule<sup>7, 136-137</sup>. The low CTE is comparable to CTE values of metals and ceramics used in electronic packaging, resulting in minimal stress buildup during thermal processing. Residual stress measurement of BPDA/p-PDA film on a silicon substrate gave a value of 4 MPa following thermal cycling from 25°C to 400°C and cooling back to 25°C<sup>137</sup>. This is significantly lower than the residual stress typically observed for PMDA/ODA polyimides, which ranges from 30-50 MPa<sup>47</sup>.

The CTE of the highly ordered BPDA/p-PDA is anisotropic, having a much higher value in the vertical direction ( $\alpha_{\perp}$ ) than in the lateral film-plane direction ( $\alpha_{\parallel}$ ). The  $\alpha_{\perp}$  value (measured perpendicular to the film plane using laser interferometry) is as high as 150 ppm/°C at temperatures between 25°C and 300°C and to jump to 400 ppm/°C above  $T_g$ <sup>138</sup>. This high  $\alpha_{\perp}$  value is problematical because of potentially high internal stress resulting from CTE mismatch in the vertical direction, which may disrupt vertical electrical connections (metal vias) in the TFML packaging<sup>7</sup>.

The origin of the anisotropic physical properties of BPDA/p-PDA polyimides is comparable to that discussed for PMDA/ODA systems. WAXS transmission patterns of BPDA/p-PDA films showed smectic-type liquid crystalline packing order, with preferential orientation of the chains along the film plane<sup>123, 140</sup>. The WAXS experiments also revealed a relatively better intermolecular packing order in the lateral direction than that of Kapton. Thus, the BPDA/p-PDA films exhibit higher density than Kapton films<sup>136</sup>.

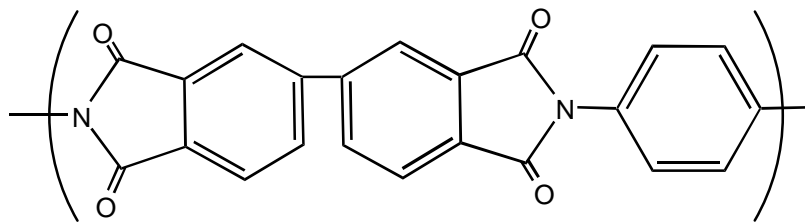


Figure 2.4.10 Repeat unit structure of BPDA/p-PDA polyimide.

Comparison of the properties of Kapton (H-type) and Upilex S has revealed that water uptake and organic solvent absorption are both significantly lower for the latter (Table 2.4.3)<sup>136</sup>. This has been attributed to the relatively higher rigidity and denser packing of the Upilex system.

Capacitance measurements have shown that Upilex S film has improved reliability in maintaining low dielectric constant in humid environments<sup>147</sup>. However, the magnitude of dielectric anisotropy in BPDA/p-PDA films is significantly higher than that of Kapton<sup>127</sup>. Using refractive index measurements, the difference ( $\Delta n$ ) between  $n_{\perp}$  and  $n_{\parallel}$  was found to be 0.24 at 633 nm. This is remarkable considering that the negative birefringence for Kapton was only 0.078 at the same wavelength<sup>127</sup>.

To reduce anisotropy in the optical/dielectric properties, BPDA/p-PDA has been copolymerized with non-coplanar diamines, such as 2,2-bis(trifluoromethyl)-benzidine (B3FB) (Figure 2.4.11)<sup>141</sup>. Copolyimides containing up to 20% of B3FB exhibited low CTE values and minimal residual stress, which were comparable to those of the BPDA/p-PDA homopolymer (Table 2.4.4). As shown in the table, the birefringence was significantly reduced for the B3FB containing polyimides. Additionally, the measured dielectric constants ( $\epsilon'_{\perp}$ ) at 100 KHz were between 3.0 and 3.2 for copolyimides containing up to 30% B3FB<sup>141</sup>. The physical properties of the copolymers became more isotropic as B3FB content increased in the series, due to increasing concentration of pendant fluoro groups and non-coplanar structure. In fact, the homopolymer containing 100% B3FB showed little anisotropy, with the lowest birefringence and  $\epsilon'_{\perp}$  values of 0.06 and 2.7-2.8, respectively.

Other workers had found that BPDA/B3FB homopolymer could be solution imidized due to solubility in hot m-cresol<sup>142-144</sup>. However, WAXS patterns of BPDA/B3FB films indicated some ordering, presumably due to solvent-promoted crystallization during drying<sup>142</sup>. Annealing

Table 2.4.3 Properties of Kapton (H-type) and Upilex S Films<sup>136</sup>.

Film Type	Density (g/cm <sup>3</sup> )	Moisture Regain (%)	Dielectric Constant ( $\epsilon'_{\perp}$ )	Tensile Modulus @25°C (MPa)	Uptake of CH <sub>2</sub> Cl <sub>2</sub> at 25°C (wt%)
Kapton H	1.42	2.8	3.5	300	22
Upilex S	1.47	1.2	3.5	900	<1

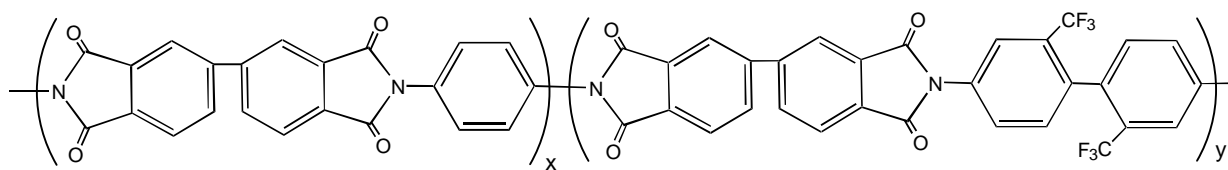


Figure 2.4.11 Repeat unit structure of copolymer of BPDA/p-PDA/B3FB

Table 2.4.4 Properties of BPDA/p-PDA/B3FB Polyimides<sup>141</sup>.

Polyimide/ Copolyimide	CTE, ppm/°C @ 100°C	Residual Stress on Si (MPa)	Refractive Index In-plane	Refractive Index Out-of-plane	Birefringence
BPDA/p- PDA	5	<3.4	1.84	1.61	0.23
BPDA/B3FB	24	17.65	1.65	1.59	0.06
p-PDA/B3FB ratio					
90/10	7	0 – 6.8	1.81	1.61	0.2
80/20	10	0 – 6.8	1.79	1.61	0.18
70/30	11	-----	1.76	1.60	0.16
50/50	11	-----	1.73	1.59	0.14

at high temperatures enhanced the order, resulting in a lower CTE of 7 ppm/°C in the 50-200°C temperature range. The rigid structure in combination with fluorine content resulted in high thermal stability, indicated by ~1% weight loss at 460°C in nitrogen during a 2 hour period.

## **2.4.2 Linear Thermoplastic Amorphous Polyimides**

As discussed in Section 2.4.1, chain-chain packing through intermolecular electronic interactions (charge transfer complexation) has imparted semi-crystalline morphology to rigid aromatic polyimides. To produce isotropic amorphous polyimides from predominantly aromatic structures, this behavior must be suppressed. Strategies which have been utilized for this purpose include: incorporating kinks in the polyimide backbone using ortho or meta catenation or crankshaft-type linkages<sup>147-149</sup>; introducing electron-withdrawing groups in the diamine and electron-donating groups in the dianhydride<sup>65, 148-149, 152-153</sup>; incorporating bulky units along the chain<sup>52-53, 55-60, 62, 67-68</sup>; introducing non-coplanar, asymmetric groups along the chain<sup>51, 54, 66, 146, 150-151</sup>; incorporating flexible linking groups<sup>63-64, 148-149</sup>; and combinations of these techniques.

One very effective method for reducing chain-chain interaction is to utilize monomers that have substituent or linking groups consisting of perfluoro-alkylene groups<sup>14, 63-65, 152-153</sup>. Such groups can impart steric and/or flexibilizing effects to the polyimide backbone, thus inhibiting intermolecular packing. As a further benefit, fluorinated polyimides usually afford lower dielectric constants, easier processability and reduced water absorption relative to the non-fluorinated rigid-rod or segmented rigid-rod polyimides.

### **2.4.2.1 Linear Thermoplastic Amorphous Polyimides Based on Fluorinated Monomers**

#### **2.4.2.1.1 Structure/property Considerations for Dielectrics**

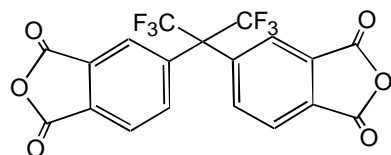
Poor solvent resistance is the main drawback in utilizing thermoplastic amorphous fluorinated polyimides as dielectric film. This means that dimensional stability of a pre-existing

dielectric film cannot be retained when subsequent polyimide layers are spin-cast on top of it, or when it is exposed to cleaning/stripping by organic solvents. Additionally, amorphous fluorinated polyimides have reduced adhesion strength due to low surface energy<sup>145</sup>. However, it is anticipated that new film processing technologies, such as melt-extrusion coating, will increase the possibility for using this type of polyimide for interlayer dielectrics. Consequently, a selected review of the literature with respect to structure/property relationships of thermoplastic amorphous fluorinated imides follows.

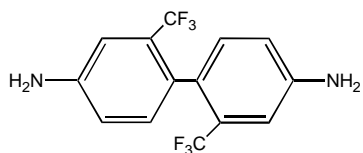
#### **2.4.2.1.2 Review of Thermoplastic Amorphous Fluorinated Polyimides**

Some of the fluorinated monomers commonly used for synthesizing thermoplastic amorphous fluorinated polyimides appear in Figure 2.4.12. The 4,4'-hexafluoroisopropylidene bis(phthalic anhydride) (6FDA) is commercially available, which has led to its widespread use<sup>154</sup>. In general, polyimides containing 6FDA have amorphous character with excellent solubility in polar solvents and  $T_g$ s that are relatively lower than those of rigid two-phase polyimides<sup>13</sup>. This has been attributed to the presence of the hexafluoroisopropylidene (6F) linking group, which imparts flexibility to the backbone and hinders intermolecular packing.

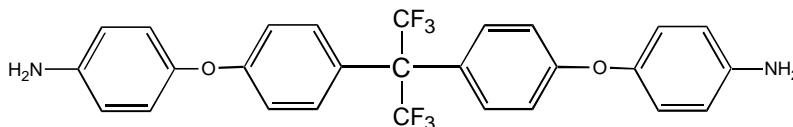
The improved solubility and other characteristics imparted by 6FDA can be illustrated by the work of Matsuura et al.<sup>155-156</sup>. These workers prepared B3FB containing homopolymers, one consisting of 6FDA and the other of PMDA<sup>155</sup>. The polyimide based on 6FDA/B3FB dissolved completely in a wide variety of solvents, including DMAc, acetone, THF and ethyl acetate at 70°C. In contrast, the PMDA/B3FB based polyimide was insoluble in all solvents except DMAc. Comparison of the physical properties (Table 2.4.5) revealed the relatively lower values of 6FDA/B3FB with respect to  $T_g$ , dielectric constant, refractive index and water absorption rate. Additionally, the greater entropy of the 6F polyimide resulted in higher CTE.



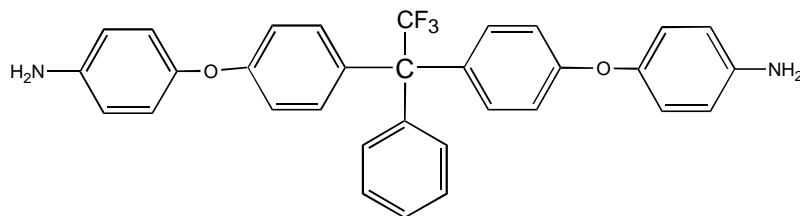
4,4'-hexafluoroisopropylidenebis(phthalic anhydride)  
6FDA



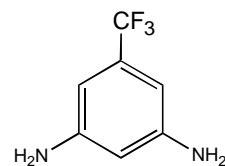
2,2-bis(trifluoromethyl)-benzidine B3FB



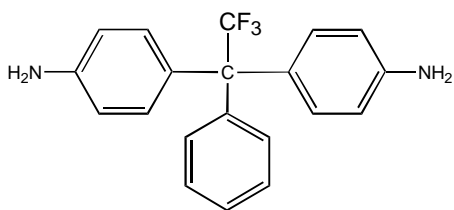
2,2-bis[4-(4-aminophenoxy)phenyl]hexafluoropropane 4-BDAF



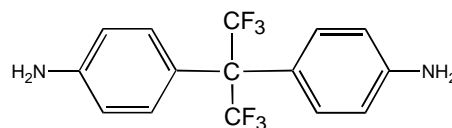
1,1-bis[4-(4-aminophenoxy)phenyl]-1-phenyl-2,2,2-trifluoroethane 3FEDAM



3,5-diaminobenzotrifluoride  
DABTF



1,1-bis(4-aminophenyl)-1-phenyl-2,2,2-trifluoroethane  
3FDAM



1,1-bis(4-aminophenyl)-1-methyl-2,2,2-trifluoroethane  
6FDAM

Figure 2.4.12 Fluorinated monomers commonly used for linear amorphous thermoplastic polyimides.

Table 2.4.5 Properties of Fluorinated Polyimides Based on B3FB<sup>155</sup>.

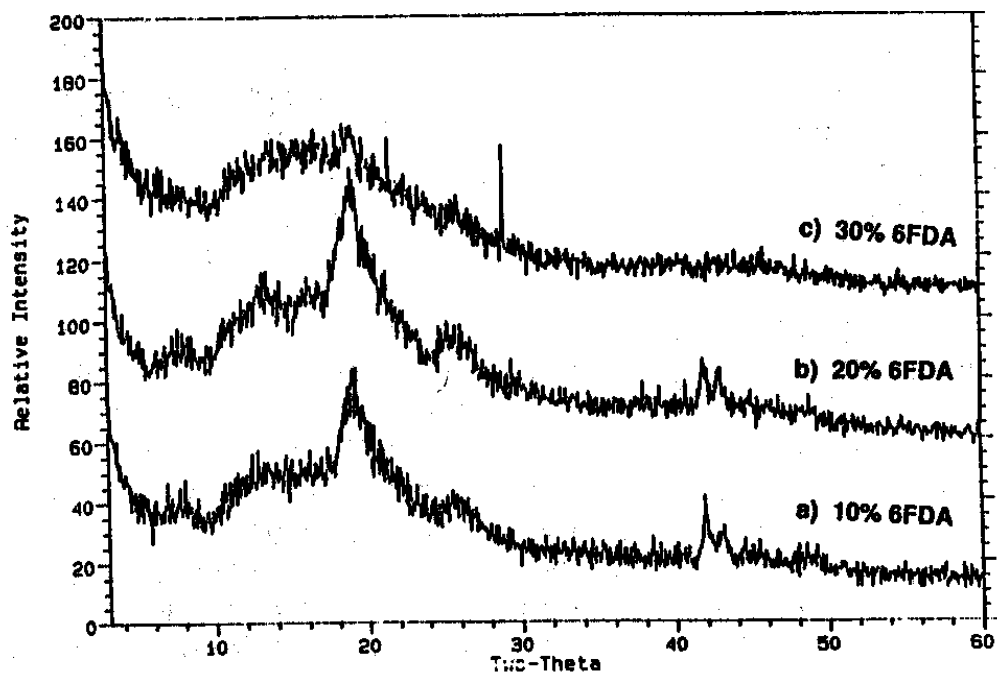
	6FDA/B3FB	PMDA/B3FB
Fluorine content, %	31.2	23.0
T <sub>g</sub> , °C	335	>400
Dielectric constant (@ 1MHz) Dry	2.8	3.2
	Wet (50% RH)	3.0
Refractive index (@ 589.6nm)	1.556	1.647
Water absorption rate, % after 3 days	0.2	0.7
CTE ppm/°C (50-300°C)	48	3

Work by Brink et al. illustrated the suppression of ordered morphology by 6FDA when incorporated in rigid polyimides comprised of PMDA and 1,1'-bis[4-(4-aminophenoxy)phenyl]-1-phenyl-2,2,2-trifluoroethane (3FEDAM)<sup>157</sup>. Sharp peaks in the WAXS spectra (Figure 2.4.13) indicated crystallinity in the copolymers of 3FEDAM-6FDA/PMDA at lower concentrations of 6FDA (e.g. 10- or 20%). The 30% 6FDA containing copolyimide showed only a broad amorphous peak. Thus, moderately low amounts of 6FDA prevented ordering and packing in these systems.

Hougham et al. studied homopolymers of 6FDA containing a series of fluorinated and non-fluorinated diamines<sup>158</sup>. A trend of decreasing dielectric constant with increasing fluorine content was observed (Table 2.4.6). Since absorbed water raises the dielectric constant significantly, the authors surmised that the increase in hydrophobicity with increasing fluorine content was mainly responsible for the observed trend. The 6FDA-containing polyimides had comparable  $T_g$  and thermal decomposition values. Additionally, the refractive indices of the series exhibited birefringence values  $<0.01$ , indicating that all of the homopolymers were essentially amorphous.

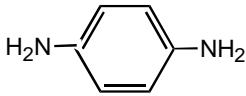
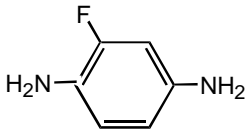
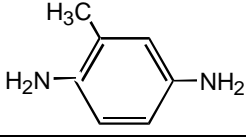
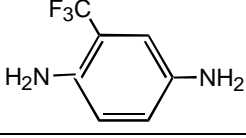
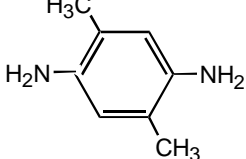
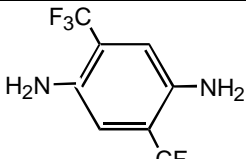
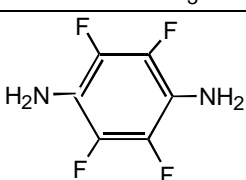
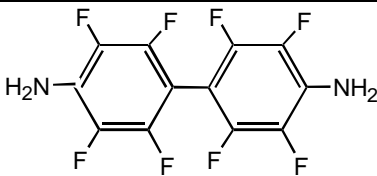
### **2.4.3 Crosslinked Amorphous Polyimides**

Due to the advantages of fluorinated polyimides, researchers have sought methods for imparting solvent resistance to these amorphous systems. The method of choice has been the utilization of crosslinking groups, which form solvent-resistant networks at temperatures above those used for thermal imidization. These types of polyimides are known as thermosetting polyimides. Thermosetting polyimides consist of imide moieties in low molecular weight prepolymers that have reactive terminal or pendant groups, which undergo homo- and/or copolymerization by thermal or catalytic means<sup>10</sup>. Historically, the main application for



2.4.13 WAXS spectra of 3FEDAM-6FDA/PMDA copolyimides<sup>157</sup>.

Table 2.4.6 Dielectric Properties of 6FDA-based Polyimides<sup>158</sup>.

Diamine structure	$\epsilon'$ dry, 1kHz	$\epsilon'$ wet, 1kHz
	$2.81 \pm 0.024$	$3.22 \pm 0.028$
	$2.85 \pm 0.041$	$3.19 \pm 0.014$
	$2.75 \pm 0.023$	$3.16 \pm 0.000$
	$2.72 \pm 0.005$	$3.05 \pm 0.042$
	$2.74 \pm 0.039$	$3.21 \pm 0.075$
	$2.59 \pm 0.030$	$2.87 \pm 0.080$
	$2.68 \pm 0.046$	$2.91 \pm 0.027$
	$2.55 \pm 0.020$	$2.73 \pm 0.024$

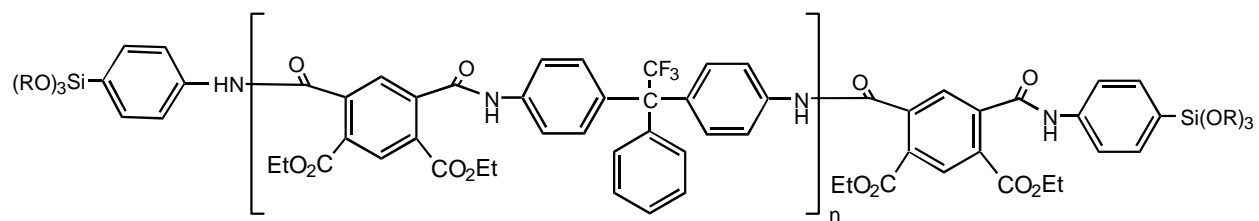
thermosetting polyimides has been as matrices in advanced composites. This has resulted from ease of processing due to their relatively low melt viscosities and the ability to tailor specific rheological properties by controlling the molecular weight. Additionally, crosslinked thermosetting polyimides have excellent retention of physical properties at high temperatures, in wet environments and in the presence of solvents and lubricating fluids.

#### **2.4.3.1 Thermosetting Polyimides for Use as Interlayer Dielectrics**

Thermosetting polyimides are usually pre-imidized and can be designed with crosslinking groups that cure into three-dimensional networks without evolution of volatiles. This eliminates several problems encountered with poly(amic acid)s, such as hydrolytic instability and outgassing of water vapor during cyclodehydration, which causes decomposition, blistering and voids in multilayer electronics packaging. Additionally, low molecular weight precursors have relatively lower solution viscosities, which means that they can be spin-cast from more highly concentrated solutions. Due to this feature, thermosetting polyimides are expected to provide better wetting/adhesion, lower film shrinkage and better planarization when coated on the inorganic substrates used in microelectronics. Unlike the rigid-rod or segmented rigid-rod type polyimides, such as Kapton or BPDA/p-PDA, the amorphous thermosets commonly exhibit isotropic physical properties, which further endorses their use in electronics packaging.

##### **2.4.3.1.1 Trialkoxysilyl Functionalized Poly(amic ester) Oligomers**

Crosslinking chemistry for most thermosetting polyimides has usually involved reactive endgroups that form networks via thermal addition polymerization<sup>10</sup>. However, a different approach was recently taken by scientists at IBM<sup>46</sup>. These workers incorporated trialkoxysilyl endgroups in fluorinated poly(amic ester)s as a means for providing crosslinking sites (Figure 2.4.14). The soluble pre-polymers have been found to undergo simultaneous imidization and



2.4.14 Trialkoxysilyl endcapped poly(amic ester) oligomers

crosslinking at temperatures  $>250^{\circ}\text{C}$ . The crosslinking reaction was thought to occur by hydrolysis of the silyl ether functionalities to silanol groups, followed by silanol condensation.

The primary reason for choosing this chemistry for thermosetting polyimides was to achieve substantial linear chain extension via condensation-type crosslinking. This was anticipated to produce less brittle films than those obtained with addition-type thermosetting polyimides, which often contain stiff aromatic/polyaromatic crosslinks and/or high crosslink density.

The inherent drawback in this method was the use of moisture-sensitive alkoxy-silyl groups, which required workup and storage under anhydrous conditions. Additionally, the precursor was not pre-imidized, which resulted in greater volatile evolution during thermal processing of the film. However, good solvent resistance was evidenced in NMP for the crosslinked materials. Additionally, the  $T_g$ s, thermal stability and tensile mechanical properties were found to be comparable to those of the high molecular weight thermoplastic controls.

#### **2.4.3.1.2 Bismaleimides and Maleimide Functionalized Oligomers**

Bismaleimides have comprised an important class of thermosetting polyimides. They have become exceedingly important in composite and electronics applications because of excellent processability and a good balance of thermal and mechanical properties<sup>10</sup>. The general structure of a bismaleimide is shown in Figure 2.4.15.

The double bond of the maleimide endgroup is highly electron deficient due to the adjacent electron-withdrawing carbonyl groups. Hence, low molecular weight bismaleimide precursors can undergo homo- and copolymerization at the carbon-carbon double bond to provide a crosslinked network. Additionally, the unsaturated alkenyl group is a very reactive dienophile and, therefore, can undergo Diels Alder-type cycloaddition reactions.

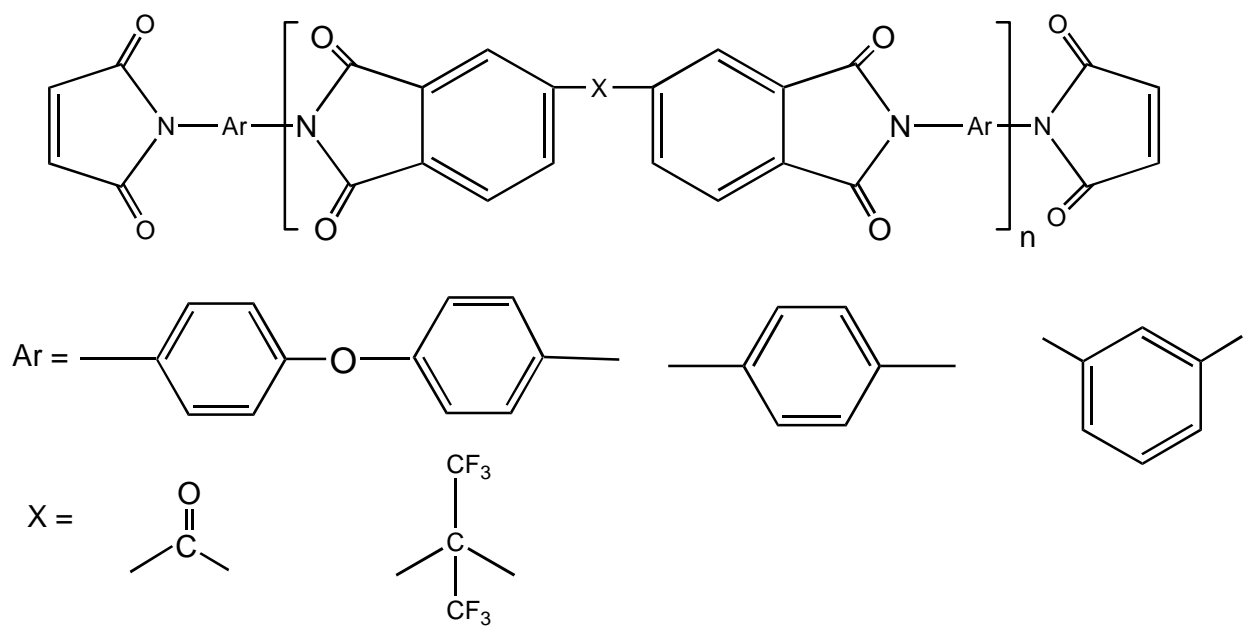


Figure 2.4.15 General formula for a bismaleimide.

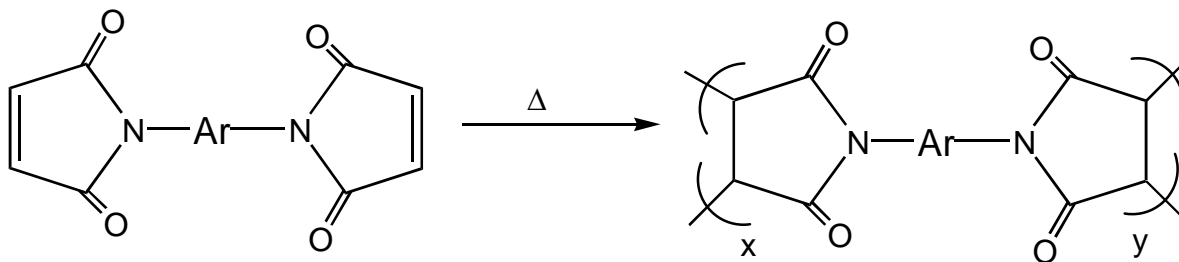
Bismaleimides (BMIs) are produced by reacting a diamine with an excess of maleic anhydride in organic solvents to obtain a bismaleamic acid intermediate<sup>161</sup>. Bismaleamic acids are cyclodehydrated to bismaleimide by heating in N,N-dimethylformamide (DMF) or acetic acid<sup>162-163</sup>. Alternatively, the bismaleamic acid may be chemically dehydrated using acetic anhydride with sodium acetate catalyst<sup>10</sup>.

The facile crosslinking reaction of BMI occurs upon heating it to temperatures near 200°C or higher. The free-radical type thermally-induced homopolymerization occurs to yield a crosslinked system (Scheme 2.4.2). The resulting thermoset network is usually very brittle due to a high crosslink density, which adversely affects its mechanical properties.

BMI-type chemistry has been extended to include maleimide-terminated prepolymers. These have been prepared by reacting amine-terminated fully imidized oligomers with maleic anhydride, which is incorporated as reactive endcapper<sup>160, 164</sup>. Phenylmaleic anhydride (PMA) has also been utilized to synthesize maleimide-functionalized polyimide oligomers<sup>14, 164-165</sup>. One pot-solution imidization and simultaneous endcapping were used in oligomer synthesis due to PMA's relatively higher onset temperature for crosslinking. Maleimide-encapped oligomers have been processed into films by melt or solution techniques. By controlling the molecular weight of the pre-polymer, the crosslink density of the thermoset film can be tailored to reduce some of the brittleness.

#### **2.4.3.1.2.1 Maleimide Functionalized Oligomers for Microelectronics**

Arnold et al. investigated the dielectric behavior of thermosetting 6FDA/bisaniline A-based imide oligomers, which had been endcapped with maleic anhydride (MA)<sup>160</sup>. The attractive features of this system included the incorporation of fluorine groups for lowering



Scheme 2.4.2 Crosslinking of bismaleimides.

the dielectric constant and water uptake in the solvent-resistant crosslinked film. The cured thermosetting polyimide films had significantly lower dielectric constants at 15 GHz than that measured for Kapton film at the same frequency (2.52-2.56 and 3.16, respectively).

One point that may be made here is that preparation of imide oligomers having reactive crosslinking groups allows tailoring of physical properties through judicious monomer selection. Thus, highly fluorinated imides can be obtained by reacting fluorinated diamines with fluorine-containing dianhydrides to further reduce dielectric constant and water absorption. Since the film is crosslinked in the final curing step, the resulting enhanced solubility of the pre-polymer is advantageous. Thus, the increased entropy imparted by incorporating numerous perfluoro-alkylene groups is not detrimental to the film's integrity in its final form.

#### **2.4.3.1.3 Acetylene-containing Thermosetting Polyimides**

Like BMIs, thermosetting ethynyl-encapped imide oligomers were originally developed for use as matrices in fiber composites<sup>10</sup>. The processing of so-called "pre-pregs" involved melt-infusion of the fibers with imide prepolymer above its  $T_g$ . An obvious requirement is that the temperature at which the polymer flows ( $T_g$ ) and the temperature at which the acetylene groups crosslink must be widely separated (e.g. wide "processing window"). This observation holds true for any high temperature processing of polyimide oligomers having thermosetting endgroups: since the crosslinked networks are insoluble/infusible, the curing reaction must not occur prior to shaping the polyimide into its desired form.

Preimidized acetylene-encapped oligomers have been developed and marketed as Theramid 600 (National Starch)<sup>10</sup>. The onset of cure coincided with flow ( $T_g \sim 200^\circ\text{C}$  and  $T_{\text{cure}} \sim 283^\circ\text{C}$ )<sup>167</sup> and, thus, Theramid 600 has a narrow processing window. Modification of the  $T_g$  of the thermosetting imide prepolymers is relatively easy. By judicious selection from a variety of

monomers, the backbone structure has been altered to tailor both the solubility and the flow temperature, thereby changing the processing characteristics<sup>72-73</sup>.

#### **2.4.3.1.3.1 Phenylethynyl Endcapped Polyimide Oligomers**

One strategy for widening the processing window has been the use of phenyl-substituted acetylenes for reactive endcappers<sup>14-17, 74-75, 164, 166, 168, 170-175</sup>. The general structures for the phenylethynyl-terminated imide oligomers are shown in (Figure 2.4.16). The peak value for the crosslinking reaction exotherm is near 380°C. Typically, the  $T_g$ s of the prepolymers are near 200°C, resulting in substantially large windows for melt processing.

Following crosslinking, the  $T_g$ s of phenylacetylene endcapped imides increase by 30-100°C, depending on backbone rigidity and oligomer molecular weight. This illustrates an important advantage in utilizing acetylene-functionalized thermosetting polyimides: the  $T_g$ s of the thermosets are usually comparable to, or they exceed, the  $T_g$ s of the corresponding thermoplastic systems. This feature is applicable to films that have been solvent-cast, as well as to the melt-processed systems.

Ethynyl-containing imide oligomers have been synthesized by the classic “two step” poly(amic acid) route<sup>166-167</sup> and by one-step solution imidization via the ester-acid route<sup>14-17, 72-75, 164, 168</sup>. To achieve endcapping with an ethynyl-substituted aromatic amine, such as 3-ethynyl aniline, the monomer stoichiometry must be offset to provide anhydride endgroups. When utilizing an ethynyl-substituted anhydride as endcapper, such as 4-phenylethynyl phthalic anhydride (4-PEPA), the amine endgroups must predominate. The difference in these two types of endgroups is shown in Figure 2.4.16. Similar thermoset properties are achieved using either type of endcapper<sup>169</sup>.

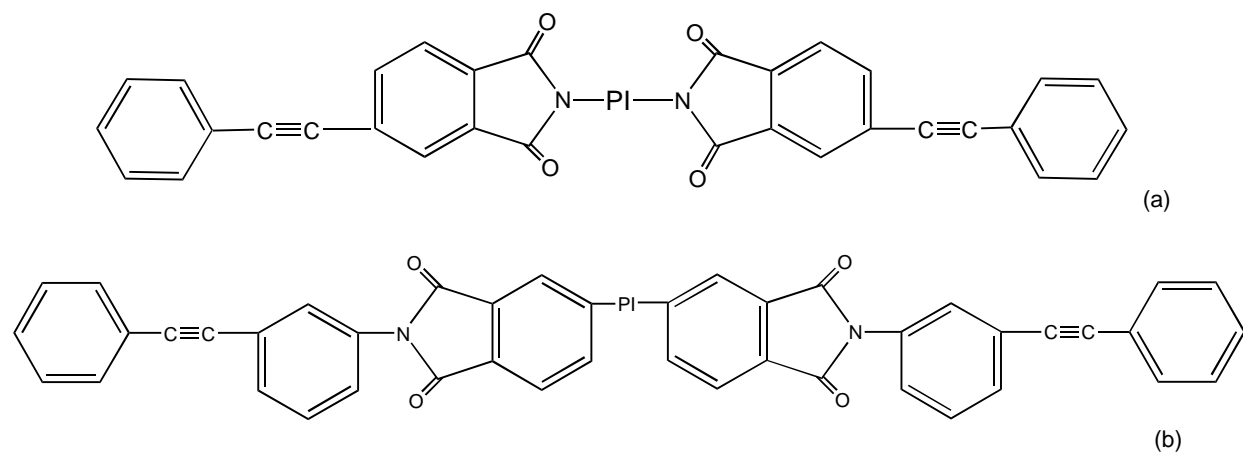


Figure 2.4.16 General formula for phenylethynyl-terminated polyimides (a) endcapped with 4-phenylethynyl phthalic anhydride and (b) endcapped with 3-ethynyl aniline.

The chemistry involved in the crosslinking reaction of acetylene-functionalized polyimides has not been well elucidated. DSC experiments have shown that the reaction is exothermic<sup>167</sup>. Also, the absence of volatile by-products has been ascertained<sup>74</sup>. The crosslinking has been suggested to proceed through a free-radical type ethynyl endgroup coupling<sup>176</sup>. The resulting conjugated yne-yne or ene-yne systems are then proposed to rearrange and/or react intermolecularly to form aromatic linkages<sup>177-178</sup>.

Since the final products are insoluble, identification of the crosslinked species using solution spectroscopy is impossible. Recent studies of isotopically labeled ethynyl-functionalized imides using solid-state <sup>13</sup>C magic-angle spinning NMR have been conducted to identify some of the structures obtained during cure<sup>179</sup>. These results have supported the proposed bimolecular and trimolecular aromatization, as well as Diels-Alder addition-type mechanisms. The major products of the reaction have been shown to be aromatic and bridged aromatic systems, such as benzene, naphthalene and phenanthrene.

#### **2.4.3.1.3.2 Acetylene Functionalized Oligomers for Microelectronics**

The primary thrust of this dissertation research has been the investigation of phenylethynyl endcapped polyimide oligomers as possible candidates for thin film interlayer dielectrics in electronics packaging. This proposed application is a fairly recent extension to McGrath and Meyers's patented work<sup>15</sup> involving thermosetting polyimide oligomers endcapped with 4-phenylethynylphthalic anhydride (4-PEPA). However, early work by Harris et al.<sup>170-171</sup> indicated the developing concept that these types of thermosets might be useful in electronics applications.

Several years ago, Harris et al. investigated fluorinated thermosetting polyimide oligomers proposed for use as "planarizing coatings" in electronics<sup>170-171</sup>. It was proposed that

the coatings would be applied from the melt, presumably to planarize the metal topography underlying the silicon dioxide dielectric film. This feature made these systems dissimilar to spin-cast polyimide thin films typically utilized as dielectrics.

These authors sought to provide a wider processing window between  $T_g$  and  $T_{cure}$  than that of Theramid 600 bismaleimide, which had been previously investigated. They were able to achieve this goal through judicious choice of monomers and endcapper, as well as controlling the molecular weights between 1.0- and 1.5 Kg/mol.

The end-capping agent 3-phenylethynyl aniline (3-PEA) was among those chosen for polyimides based on 6FDA and 1,3-bis(3-aminophenoxy)benzene (APB). For the 3-PEA endcapped system, the processing window was found to exceed  $105^{\circ}\text{C}$  and the  $T_g$  following cure had risen  $70^{\circ}\text{C}$ . Additionally, the long-term isothermal aging of the cured film at  $316^{\circ}\text{C}$  in air showed minimal weight loss ( $\sim 20\%$ ) after 723 hours.

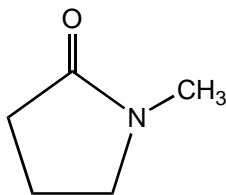
The potential for obtaining relatively thick planarizing coatings with good adhesion was a primary factor in selecting the phenylethynyl functionalized imide oligomers for this dissertation research. The low molecular weight of the precursors was expected to provide low solution viscosities at relatively higher concentrations for solution casting films, resulting in thicker coatings and better wetting of the substrate. The ability to incorporate fluorine in the backbone without compromising solvent resistance of the cured film was anticipated to provide many benefits for dielectric applications. These included relatively lower dielectric constants and water absorption compared with non-fluorinated polyimides. The primary objective of this dissertation research was to synthesize thermosetting polyimide oligomers, which would exhibit good film forming properties and adhesion, and which would also meet the requirements of high  $T_g$  and thermal stability for dielectric applications.

## Chapter 3 Experimental

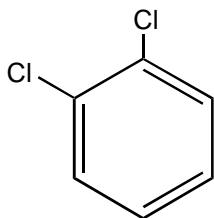
### 3.1 Materials Utilized in Synthesis and Characterization Experiments

#### 3.1.1 Solvents

1-Methyl-2-pyrrolidinone (NMP: Fisher Scientific). NMP was purified for use in poly(amic acid) synthesis by drying over calcium hydride for at least 12 hours, followed by distillation under reduced pressure (using a vacuum pump) (b.p. 202°C/760mmHg).



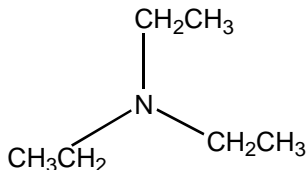
o-Dichlorobenzene (o-DCB: Fisher Scientific) was used as received (b.p. 80°C/760mmHg).



Methanol (Fisher Scientific) was received as an HPLC grade solvent and was used without further purification (b.p. 65°C/760mmHg).

Ethanol (100% AAPER Alcohol and Chemical) was used as received (b.p. 78.5°C/760mmHg).

Triethylamine (TEA or Et<sub>3</sub>N: Fisher Scientific) was used as received (b.p. 89°C/760mmHg).

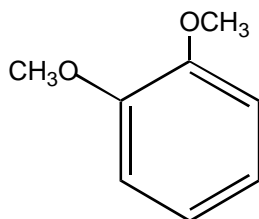


Diethyl ether (Anhydrous, Mallinckrodt) was used as received (b.p. 89°C/760mmHg).

Chloroform (Burdick and Jackson) was received as an HPLC grade solvent and was used without

further purification (b.p. 61-62°C/760mmHg).

o-Dimethoxybenzene (o-DMB: Acros Organics). o-DMB was purified for use in poly(amic acid) synthesis by drying over calcium hydride for at least 12 hours, followed by distillation under reduced pressure (using a vacuum pump) (b.p. 204-206°C/760mmHg).



Deuterated Chloroform (CDCl<sub>3</sub>: Cambridge Isotope Laboratories) was used as received.

### 3.1.2 Monomers

#### 3.1.2.1 Diamines

##### 1,3-Phenylenediamine (m-PDA)

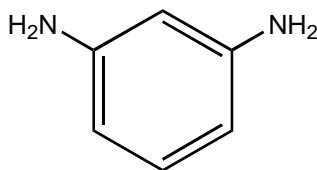
Supplier: Acros Organics

Empirical Formula: C<sub>6</sub>H<sub>8</sub>N<sub>2</sub>

Molecular Weight (g/mol): 108.14

m.p., °C: 66

Structure:



Purification: m-PDA was sublimed under vacuum (~5 torr) at ~61°C. This monomer oxidizes readily in air and must be used soon after sublimation. It must be stored in the dark under vacuum to prevent oxidation.

### 1,4-Phenylenediamine (p-PDA)

Supplier: Acros Organics

Empirical Formula:  $C_6H_8N_2$

Molecular Weight (g/mol): 108.14

m.p., °C: 145

Structure:



Purification: p-PDA was sublimed under vacuum (~5 torr) at ~110°C, successively two times.

This monomer is air and photo-sensitive and must be used soon after sublimation. It must be stored in the dark under vacuum.

### 3,5-Diaminobenzotrifluoroide (3,5-DABTF)

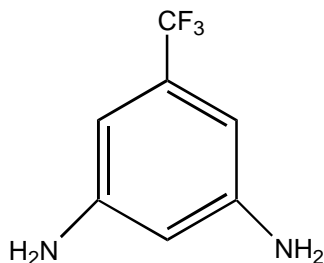
Supplier: Marshalton Research Labs

Empirical Formula:  $C_7H_5F_3$

Molecular Weight (g/mol): 176.14

m.p., °C: 85

Structure:



Purification: 3,5-DABTF was sublimed under vacuum (~5 torr) at ~80°C. This monomer is air and photo-sensitive and must be used soon after sublimation. It must be stored under vacuum in the dark.

### 4,4'-Oxydianiline (4,4'-ODA)

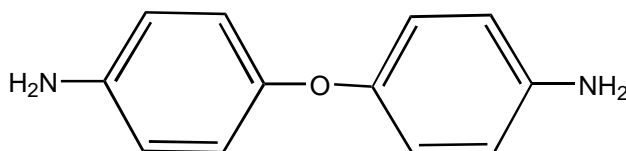
Supplier: Kennedy and Klim

Empirical Formula:  $C_{12}H_{12}N_2O$

Molecular Weight (g/mol): 200.24

m.p., °C: 192

Structure:



Purification: 4,4'-ODA was sublimed under vacuum (~5 torr) at ~155°C.

### 5(6)-Amino-1-(4-aminophenyl)-1,3,3-trimethylindane (diaminophenylindane or DAPI)

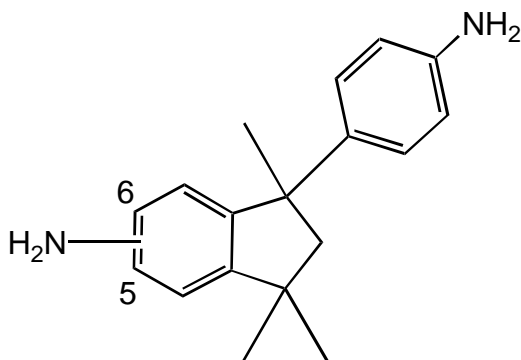
Supplier: Ciba

Empirical Formula:  $C_{18}H_{22}N_2$

Molecular Weight (g/mol): 266.39

m.p., °C: 78-112

Structure: Equimolar mixture of C-5 and C-6 isomers as determined by HPLC.



Purification: DAPI was received as a polymer grade material. To remove moisture, it was dried under vacuum at 50-60°C for at least 12 hours.

### 3.1.2.2 Dianhydrides

#### 4,4'-Hexafluoroisopropylidenebis(phthalic anhydride) (6FDA)

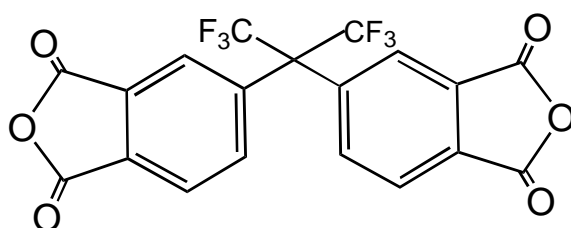
Supplier: Clariant

Empirical Formula:  $C_{19}H_6F_6O_6$

Molecular Weight (g/mol): 444.243

m.p., °C: 247

Structure:



Purification: Electronic grade 6FDA was dried at  $\sim 180^\circ\text{C}$  under vacuum for at least 12 hours prior to use.

#### 3,4,3',4'-Biphenyltetracarboxylic dianhydride (BPDA)

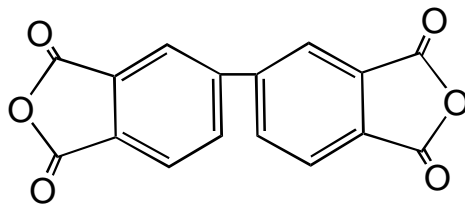
Supplier: Chriskev

Empirical Formula:  $C_{16}H_6O_6$

Molecular Weight (g/mol): 294.224

m.p., °C: 300

Structure:



Purification: BPDA was obtained in polymer grade purity and was dried at  $\sim 180^\circ\text{C}$  under vacuum for at least 12 hours prior to use.

### 3.1.2.3 Endcappers

#### Phthalic anhydride (PA)

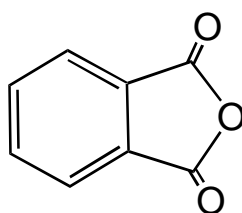
Supplier: Acros Organics

Empirical Formula:  $C_8H_4O_3$

Molecular Weight (g/mol): 148.117

m.p., °C: 134

Structure:



Purification: PA was purified by subliming under vacuum (~5 torr) at ~120°C.

#### 4-Phenylethynylphthalic anhydride (4-PEPA)

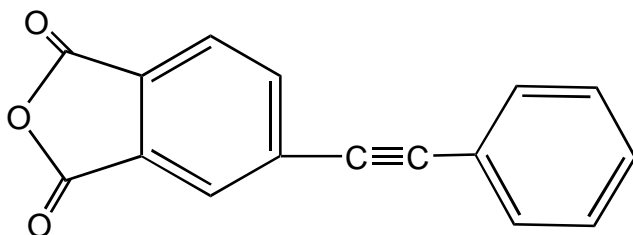
Supplier: Daychem Labs

Empirical Formula:  $C_{16}H_8O_3$

Molecular Weight (g/mol): 248.24

m.p., °C: 150-151

Structure:



Purification: 4-PEPA was purified using vacuum sublimation (~5 torr) at ~145°C.

## **3.2 Characterization Methods**

### **3.2.1 Gel Permeation Chromatography (GPC)**

GPC was conducted with a Waters GPC/ALC 150C chromatograph equipped with a differential refractometer detector and an on-line differential viscometric detector (Viscotek 150R) coupled in parallel. GPC measurements were performed using an NMP mobile phase, containing 0.02M P<sub>2</sub>O<sub>5</sub>, at a flow rate of 1.0 ml/min. The stationary phase consisted of Waters Styragel HT3 + HT4 columns, maintained at a temperature of 60°C. A series of polystyrene standards having narrow molecular weight distributions (Polymer Laboratory) were employed to generate a universal calibration curve<sup>180-181</sup>. This allowed calculation of absolute values of  $\langle M_n \rangle$ ,  $\langle M_w \rangle$  and  $\langle M_v \rangle$  for the polyimides being evaluated.

### **3.2.2 Nuclear Magnetic Resonance Spectroscopy (NMR)**

NMR spectra (<sup>13</sup>C) were obtained using a Varian Unity 400 MHz Spectrometer. Quantitative <sup>13</sup>C-NMR experiments using polyimide solutions were conducted to enable calculation of  $\langle M_n \rangle$  using endgroup analysis for the lower molecular weight oligomers.

### **3.2.3 Fourier Transform Infrared Spectroscopy (FTIR)**

FTIR was utilized to confirm the functional groups in the polyimide oligomers. Measurements were conducted on a Nicolet Impact 400 FTIR Spectrometer using thin polymer films cast on salt plates from dilute chloroform solutions. FTIR bands occurring at approximately 1780-, 1730-, 1375- and 720 cm<sup>-1</sup> confirmed the presence of imide functional groups in polyimide oligomers.

### **3.2.4 Thermogravimetric Analysis (TGA)**

#### **3.2.4.1 Dynamic TGA**

Prior to conducting TGA measurements, the polyimides were carefully dried under vacuum at elevated temperatures to remove residual solvent/moisture. Dynamic TGA was performed in air to assess the thermal stability of polyimide oligomers and crosslinked polyimide films. The samples were heated at a rate of 10°C/min in a Perkin Elmer TGA 7 instrument. The sample weight loss was measured as a function of temperature. The thermal stability of the polyimides was generally reported as the temperature at which 5% weight loss was observed.

#### **3.2.4.2 Isothermal TGA**

Rigorously dried crosslinked polyimide films were analyzed using an isothermal heating program in the Perkin Elmer TGA 7. The experiments were run in nitrogen at 400°C for 2 hours. These conditions emulated processing conditions typically used for processing polyimide thin films in multilayer electronics packaging. Hence, the comparison of overall weight loss during the 2 hour period with that of a commercially available control (Kapton) provided valuable information on thermal stability.

### **3.2.5 Differential Scanning Calorimetry (DSC)**

DSC was used to ascertain the thermal transition temperatures of the polyimide oligomers and the crosslinked polyimide films. A Perkin Elmer DSC 7 instrument was programmed to heat the samples under nitrogen at a heating rate of 10°C/min.

For the oligomer samples (in powdered form), two scans were used: the first heat was to a final temperature just above the  $T_g$ , but significantly below  $T_{cure}$ ; the second heat was to a temperature above  $T_{cure}$ . The  $T_g$  was calculated from the endothermic shift in the baseline occurring during the second heating scan.

For the cured polyimide film samples,  $T_g$  was determined from the first heating scan, since no difference in calculated  $T_g$  values had been evidenced when using successive scans.

### **3.2.6 Dynamic Mechanical Analysis (DMA)**

DMA was utilized to analyze crosslinked polyimides to determine storage and loss modulus values, as well as  $\tan \delta$ . The instrument used was a Perkin Elmer DMA 7. For 1 mm thick melt-pressed cured films, the 3-point bend deformation mode was used at a frequency of 1 Hz. These samples were dynamically heated at a rate of 5°C/min under nitrogen. The maximum value of  $\tan \delta$  obtained during the scan was taken as the  $T_g$  of the cured polyimides.

For ~7-10 mil thick crosslinked films, the extension-mode deformation was used at a frequency of 1 Hz and a heating rate of 5°C/minute under nitrogen. The maximum  $\tan \delta$  value for these samples was taken to represent  $T_g$  for these materials as well.

A quartz expansion probe was utilized to determine the CTE values of a series of 1 mm thick melt-pressed cured films. Probe displacement distance as a function of temperature was measured at a heating rate of 5°C/min. The CTE was calculated from the slope of the best fit line for the data collected between 50 and 300°C.

### **3.2.7 Rotational Viscometry**

Rotational viscometry measurements were utilized to determine the viscosity of a series of imide oligomer solutions prepared using NMP. A Brookfield Digital cone-and-plate viscometer (DV-II) was used for the experiments, which were performed at room temperature.

The viscosity values for each solution were obtained at various rotation rates (rpm) and were subsequently plotted and extrapolated to zero rpm to provide corrected viscosities.

### **3.2.8 Film Sample Preparation**

#### **3.2.8.1 Melt-pressed Films**

Melt pressed films of 1 mm thickness were prepared using compression molding at temperatures 20-50°C above  $T_g$ . First, the powdered oligomers were placed in an aluminum mold pre-heated by resting on the lower heated platen of a smart press. The polyimides were allowed to become molten and, subsequently, the mold was covered by an aluminum plate. A contact pressure of 0.2 kpsi was applied to the plate-mold assembly between the platens. The temperature of the smart press was then ramped to 380°C and held there for 1 hour to cure the polyimides. Following cure, the temperature was gradually decreased to room temperature before removing the sample mold from the smart press. The melt-pressed films were used in DMA (3-point bend and CTE), moisture-absorption studies and Soxhlet extraction experiments.

#### **3.2.8.2 Solvent-cast Free-standing Films**

Free-standing polyimide films were prepared by casting solutions of the oligomers prepared in solvents consisting of either NMP or in NMP/o-DMB. Prior to casting, the solutions were filtered to remove particles using syringe Acrodisc filters having porosities of 0.45 and 0.22  $\mu\text{m}$ .

Approximately 4 ml of each solution was placed inside a 2.5" diameter area on a clean glass plate being heated to ~85°C on a hot plate. To confine the solution to this area, a 2.5" diameter stainless steel ring was used on top of the glass plate to function as a mold. The films were then heated on a hot plate at 85°C under a cardboard cover until solid to the touch.

Following solidification, the films were placed under vacuum at 85°C overnight, after which time they were peeled from the glass plate. After re-placing the films loosely on the glass plate, they were then heated gradually (over an 8 h period) under vacuum from 85-200°C. To

ensure complete dryness, the vacuum oven was gradually heated to a final temperature of  $\sim 10^{\circ}\text{C}$  above the  $T_g$  of the oligomer.

Following drying, the films were heated in a furnace under nitrogen at  $380^{\circ}\text{C}$  for 1 hour to provide crosslinked materials. The film samples were used for extraction experiments, for DMA studies (tension-mode) and for refractive index measurements.

### **3.2.8.3 Spin-cast Films on Inorganic Substrates**

Films, with thicknesses in the micrometer range, were produced by spin-coating various substrates using a Headway Photo-resist Spinner (Model 1-EC101D-R485). The solutions were prepared and filtered as described above for free-standing films. Pre-cleaned and dried inorganic substrates (e.g. silicon wafers, glass microscope slides, aluminum plates and ferrochromium-coated steel plates) were placed on the chuck of the spin-coating apparatus. The polyimide oligomer solutions were then applied and the chuck was subsequently rotated at speeds ranging from 1,000-6,000 rpm, depending on the desired film thickness.

Spin-coated films were immediately placed under a nitrogen atmosphere supplied by a gas inlet on a covered hot plate. Using a programmable temperature controller (Omega CN2011), the hot plate temperature was gradually ramped (rate = 1 to  $1.5^{\circ}\text{C}/\text{min.}$ ) and held at a predetermined temperature. The following heating schedule was used: 1 hour at  $100^{\circ}\text{C}$ , then 1 hour at  $200^{\circ}\text{C}$  and, finally, 1 hour at  $300^{\circ}\text{C}$ . The high molecular weight polyimide control films were further subjected to 30 min at a temperature just above  $T_g$  to ensure dryness. The oligomeric imide films were cooled and transferred to a furnace, where they were heated under nitrogen at  $380^{\circ}\text{C}$  to effect crosslinking.

### **3.2.9 Extraction Experiments**

#### **3.2.9.1 Soxhlet Extractions in Chloroform**

Free-standing melt-produced films were subjected to Soxhlet extractions in refluxing chloroform for a period of 5 days, followed by drying under vacuum at 200°C for 1 day and at 300°C for 1 hour. The gel fraction was determined gravimetrically using an analytical balance.

#### **3.2.9.2 Extractions in NMP at 60°C**

Free-standing solution-cast films were extracted with NMP using a specially designed glass apparatus (Figure 3.2.1). The inner perforated-tube of the apparatus held the sample inside an extraction thimble. The NMP circulated continuously from the outer jacket to the inner perforated-tube with stirring. The apparatus was constantly heated by immersion in an oil bath at 60°C. The samples were heated under nitrogen to protect NMP from oxygen and humidity.

Pre-treated fiberglass thimbles were utilized to contain the samples during heating. The thimbles had been carefully extracted and dried under “sample” conditions by themselves prior to weighing and using for film extraction experiments.

Before immersion in the NMP, the films were thoroughly dried under vacuum to remove moisture and were carefully weighed using an analytical balance. The ratio of solvent to dry film sample used for the immersion experiments was approximately 500:1.

After heating the films/thimbles for 3 days in NMP at 60°C, the samples were removed and air-dried overnight. Subsequently, they were heated under vacuum at 200°C for 1 day and at 300°C for several hours to remove NMP. The gel fractions were determined gravimetrically using an analytical balance. Two samples of each polyimide were used to calculate an average % gel value.

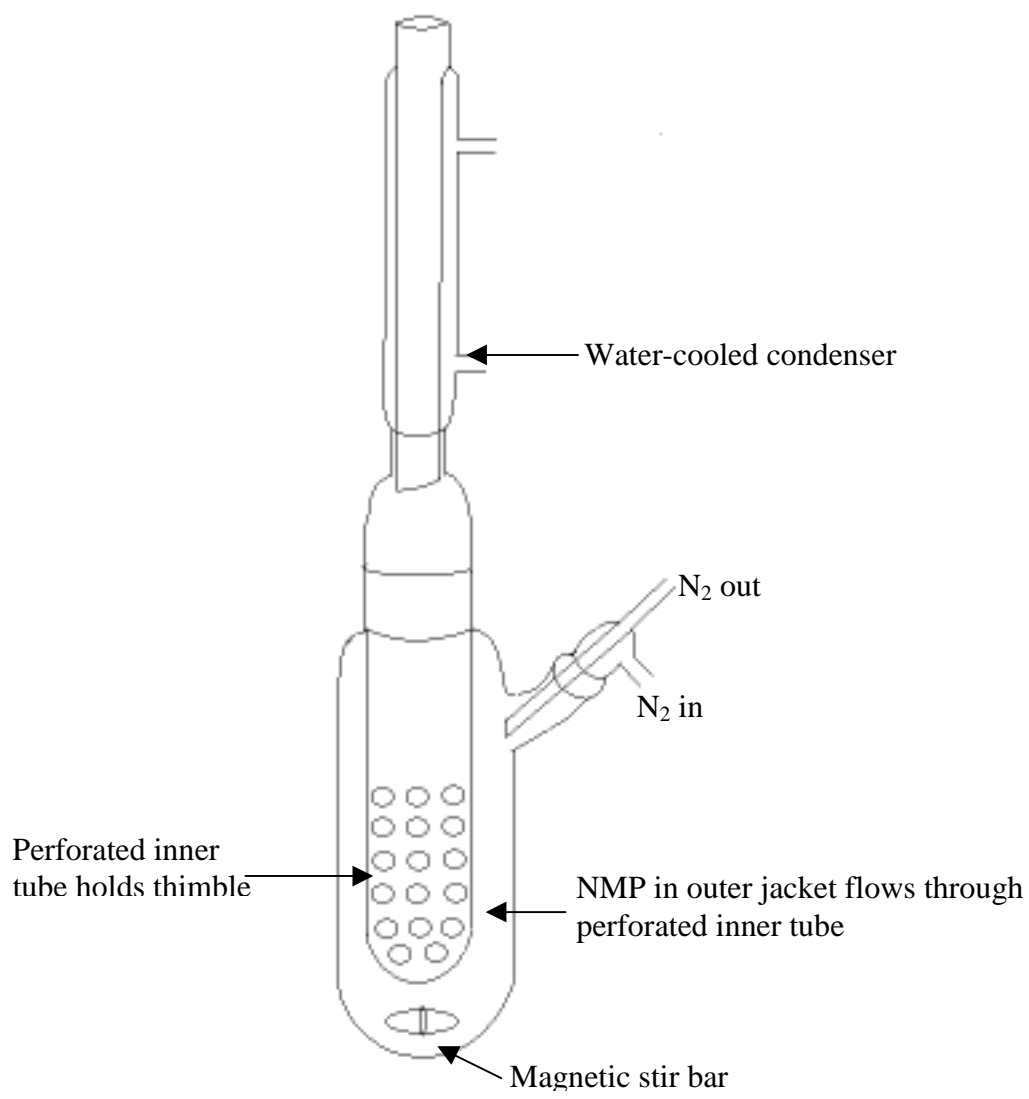


Figure 3.2.1 Glassware apparatus for extraction of cured polyimide films.

### **3.2.10 Refractive Index (RI) Measurement**

RI of thin solution-cast polymer films were determined using a Metricon™ Model 2010 prism coupler-type refractive index measuring device. The instrument featured an index accuracy of  $\pm 0.001$  and an index resolution of  $\pm 0.0005$ . RI measurements of the polyimide films were performed at an operating wavelength of 633 nm using a prism of type 200-P-4.

### **3.2.11 Water Absorption**

Water absorption of melt-pressed cured polyimide films was determined during exposure to 85% relative humidity (RH) in air at 85°Fahrenheit (F) for a period of 1 week. Prior to the exposure, the samples were rigorously dried under vacuum for 1 week and then were carefully weighed using an analytical balance. Two samples of each polyimide were then placed in a Blue M Humid Flow™ Environmental Temperature and Humidity Chamber (CFR-400 Series, Model 7652C-2), which had been pre-regulated to 85% RH/85°F.

Periodically, the samples were removed and weighed. They were then quickly returned to the chamber, which effectively provided RH conditions to within  $\pm 5\%$  of 85% as indicated by an electronic digital hygrometer. The weight of the water absorbed by a given polyimide sample during periodic measurements was determined by taking an average of the data for the two samples.

## **3.3 Polyimide Oligomer Synthesis**

Important prerequisites for obtaining polyimides having well-defined structures and good molecular weight control involve purification of the starting materials and control of stoichiometry. For the series of polyimides prepared, target values for number average molecular weights ( $\langle M_n \rangle$ ) ranged from 2.0 to 12.0 Kg/mol. Additionally, it was desired that the monomer stoichiometry be offset to favor the diamine to enable endcapping with monofunctional

anhydrides. The stoichiometric calculations utilized for achieving  $\langle M_n \rangle$  values that were close to the target range will be discussed in the following section.

### 3.3.1 Molecular Weight Control in Step Growth Polymerization

In step growth polymerization, the proper monomer stoichiometry for achieving a desired  $\langle M_n \rangle$  is determined by utilizing the Carothers equation:

$$\langle X_n \rangle = \frac{N_0}{\frac{1}{2}(2N_0 - N_0 p f_{av})} = \frac{2}{2 - p f_{av}} = \frac{2}{2 - f_{av}} \quad (\text{when } p=1) \quad \text{Eq. 3-1}$$

where,

$\langle X_n \rangle$  = the number average degree of polymerization,

$p$  = the extent of reaction of the functional groups, and

$f_{av}$  = the average number of functional groups per monomer molecule.

When a monofunctional molecular weight limiting reagent (endcapper) is to be utilized, the difunctional monomer stoichiometry must be controlled in such a way as to provide the appropriate endgroups for reaction with the endcapper. When using difunctional monomers, called generically AA and BB, the step growth polymerization will result in formation of A-B type links. If the BB difunctional monomer is utilized as an excess component, then B type functional endgroups will be produced. In this case  $f_{av}$  would be defined as:

$$f_{av} = \frac{4N_A}{N_A + N_B} = \frac{4r}{r + 1} \quad \text{Eq. 3-2}$$

where,

$$r = N_A / N_B \quad \text{Eq. 3-3}$$

and,  $N_A < N_B$ , representing the stoichiometric imbalance of difunctional monomers with BB as the excess component.

Plugging the redefined equation for  $f_{av}$  into Equation 3-1 and rearranging gives:

$$\langle X_n \rangle = (1 + r) / (1 - r) \quad \text{Eq. 3-4}$$

When an A-type monofunctional endcapper is used to control the molecular weight by reacting with B type endgroups, the stoichiometric imbalance in the reacting system is further defined as:

$$r = N_B / (N_A + N_{A'}) \quad \text{Eq. 3-5}$$

where  $N_A + N_{A'} > N_B$ . The combination of monomer AA with the monofunctional A-type endcapper provides the desired stoichiometric excess.

A sample calculation of monomer/endcapper stoichiometry using the above equations will be provided below to help illustrate the method used in this research.

The Carothers equation was utilized to calculate the reaction stoichiometry for a 6FDA/ODA polyimide with an endcapper comprised of 4-PEPA. The target number average molecular weight ( $\langle M_n \rangle$ ) was 10 Kg/mol. Designations for the ODA diamine, the 6FDA dianhydride and the PEPA endcapper were assigned as BB, AA and A, respectively. Thus, the polyimide product would have the structure A(BBAA) $_n$ BBA.

$\langle X_n \rangle$  is related to the polymer molecular weight as follows:

$$\langle X_n \rangle = 2 M_d / M_{ru} \quad \text{Eq. 3-6}$$

where,  $M_d$  is the desired molecular weight of the polyimide and  $M_{ru}$  is the repeat unit molecular weight. Correcting the  $M_d$  by subtracting the contribution of the endgroups gives:

$$\langle X_n \rangle = 2 \frac{M_d - 2 \times \text{Endgroup(A) - Mol. weight}_{BB} \text{ residue}}{M_{ru}} \quad \text{Eq. 3-7}$$

For our case:  $M_d = 10,000 \text{ g/mol}$

Endgroup(A) mol. weight = 246.248 g/mol (phenylethynyl phthalimido group)

Mol. weight<sub>BB</sub> residue = C<sub>12</sub>H<sub>8</sub>O = 168.195 g/mol

$M_{ru} = 608.45 \text{ g/mol}$

Thus, the value for  $\langle X_n \rangle$  in this case is 30.7. Equation 3-4 can be solved for  $r$  to give:

$$r = \frac{\langle X_n \rangle - 1}{\langle X_n \rangle + 1} \quad \text{Eq. 3-8}$$

Application of this equation gives  $r = 0.937$ .

The stoichiometric amount ( $N_B$ ) of monomer BB can be obtained by first rearranging Eq. 3-3 to give:  $N_B = N_A / r$

And, setting the stoichiometric amount of monomer AA ( $N_A$ ) to 1.000, gives  $N_B = 1.067$ .

Since it has been determined that  $N_A = 1.000$  and  $N_B = 1.067$  and  $r = 0.937$ , the Equation 3-5 can be utilized to calculate the stoichiometric amount of monofunctional endcapper needed ( $N_A'$ ). First, Eq. 3-5 is rearranged to give:  $N_A' = (N_B - rN_A) / r$

And, plugging in the known values gives  $N_A' = 0.139$ .

Reactant amounts in this synthesis can be generated from these results as follow:

	Moles	Scaled moles <sup>1</sup>	Mol. wt. (g/mol)	Reactant amount (g)
6FDA	1.000	$5.000 \times 10^{-2}$	444.243	22.2122
ODA	1.067	$5.335 \times 10^{-2}$	200.241	10.6829
PEPA	0.139	$6.950 \times 10^{-3}$	248.240	1.7253

1: Scaled moles for an ~30g batch of polyimide product

### 3.3.2 Polyimide Oligomer Synthesis by the Classic Two-step Route

The classic two-step route of polyimide synthesis involves the preparation of a poly(amic acid) in the initial step, followed by cyclodehydration of the polymer in the second step. The latter step can be performed either by thermal, chemical or solution methods. The following is an example of the classic two-step method used in this research. The structure of the polymer consisted of a PEPA-endcapped 6FDA/ODA oligomer, with a targeted  $\langle M_n \rangle$  of 10 Kg/mol.

### 3.3.2.1 Poly(amic acid) Formation

A three-necked round bottom flask equipped with a mechanical stirrer and nitrogen inlet was flame dried under a steady flow of nitrogen. Then 9 ml of dry NMP and ODA (2.1366g,  $1.067 \times 10^{-2}$  mol) were charged to the flask. The mixture was stirred under nitrogen flow to completely dissolve the diamine. Then 6FDA (4.4424g,  $1.000 \times 10^{-2}$  mol) and PEPA (0.3451g,  $1.390 \times 10^{-3}$  mol) were gradually rinsed into the diamine solution using 21ml of dry NMP. The mixture was stirred under steady nitrogen flow while the anhydrides gradually dissolved (which was complete within a few hours). Once the reaction solution became homogeneous, stirring was continued under the same conditions (room temperature, nitrogen purge) for ~20 hours. The clear, yellow poly(amic acid) solution exhibited a somewhat higher viscosity than the initial monomer solution.

### 3.3.2.2 Thermal Imidization of Poly(amic acid)

The poly(amic acid) solution described above was filtered using an Acrodisc syringe filter (0.22 $\mu$ m porosity) and applied to a glass plate for film formation, as described in Section 3.2.8.2. The thermal sequence used to imidize, dry and crosslink the film has also been covered in Section 3.2.8.2. In this particular case, this process yielded a free-standing brownish film. Spin casting, followed by thermal imidization and crosslinking was also performed, as described in Section 3.2.8.3.

### 3.3.3 Polyimide Oligomer Synthesis by the Ester-Acid Route

The primary method for polyimide synthesis used in this research was the ester-acid route, which is also comprised of two steps. The first step involves the reaction of dianhydride and anhydride endcapper with ethanol to provide ester-acid intermediates. The second step consists of reacting the intermediates and diamine in solution at elevated temperatures. The

presence of an azeotroping agent ensures that imidization is achieved by preventing hydrolysis.

The following is an example of the ester-acid method used in this research. The structure of the polymer consisted of a PEPA-encapped BPDA/DAPI oligomer, with a targeted  $\langle M_n \rangle$  of 8 Kg/mol.

### 3.3.3.1 Example of Polyimide Oligomer Synthesis by the Ester-Acid Route

A three-necked round bottom flask was equipped with a mechanical stirrer, a nitrogen inlet and a reverse-type Dean Stark trap fitted with a water-cooled condenser. The flask was immersed in a silicone oil bath, which was equipped with a thermocouple-type temperature-regulating device. The BPDA (14.7112g,  $5.000 \times 10^{-2}$  mol) and PEPA (1.9363g,  $7.800 \times 10^{-3}$  mol) were rinsed into the flask using 120ml absolute ethanol and 19ml triethyl amine. The mixture was stirred under nitrogen at reflux ( $\sim 100^\circ\text{C}$ ), during which the solution became clear and ethanol distilled into the trap. Cessation of ethanol distillation and the formation of a highly viscous mixture in the flask indicated the end of the first stage of the reaction.

The trap was emptied of ethanol and it was refilled with o-DCB. Then the DAPI (14.3190g,  $5.375 \times 10^{-2}$  mol) was slowly added to the reaction mixture with stirring. To ensure quantitative transfer of the diamine, DAPI was rinsed into the flask using the reaction solvents. These consisted of 180ml NMP and 45ml o-DCB (80:20 vol:vol), which provided a final solids content of 12% wt/vol.

The reaction solution was continually stirred and heated at  $175\text{-}180^\circ\text{C}$  for 24 hours under nitrogen. Subsequently, the solution was allowed to cool to room temperature. The polyimide product was coagulated by slowly pouring the solution into stirring methanol in a blender. The polymer solids were collected using vacuum filtration and were washed with excess methanol. Solids were air-dried overnight, followed by drying under vacuum at  $\sim 160^\circ\text{C}$  for  $\sim 24$  hours.

## Chapter 4 Results and Discussion

### 4.1 Introduction

In this dissertation research, a series of polyimide oligomers having reactive endgroups was prepared. Several key characteristics were studied for comparison with thermoplastic systems and to elucidate structure/property relationships within the series. This chapter addresses the results of these experiments and the related knowledge that has been obtained from the data.

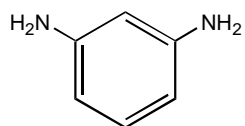
#### 4.1.1 Low Molecular Weight Series of Fluorinated Thermosetting Polyimide Oligomers

A series of fluorinated thermosetting polyimide oligomers with  $\langle M_n \rangle$  target values of 2-10 Kg/mol was prepared using 6FDA and various diamines<sup>182-183</sup>. The monomers utilized are depicted in Figure 4.1.1. In some cases, the thermoplastic analogues were prepared to enable comparison of the physical properties.

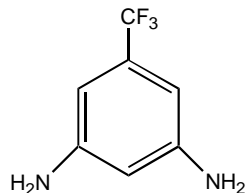
The synthetic method used to prepare this series was the ester-acid solution imidization route (Scheme 4.1.1). Due to the incorporation of 6FDA, the polyimides were anticipated to be soluble in polar solvents, such as NMP. Hence, this method was chosen because it affords fully imidized, hydrolytically-stable polyimides<sup>14-17</sup>. Indeed, the benefits of using the ester-acid route were evident during this research: in nearly all cases, fully imidized soluble oligomers with controlled molecular weights were obtained.

A further advantage was that the reaction solvents did not have to be purified to remove traces of water prior to use. A binary mixture of solvents was used for the reaction, NMP and o-DCB (4:1) with the o-DCB acting as an azeotroping agent. This system was very effective in removing water as evidenced in the synthesis of thermoplastic control polyimides. Using 1:1 stoichiometry, very high molecular weights were obtained, which in some cases

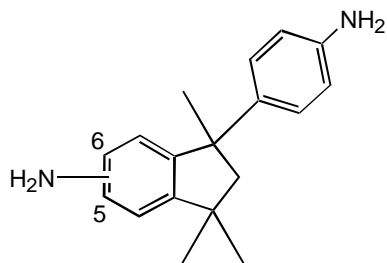
### Diamines



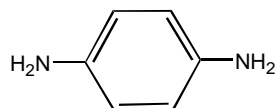
m-phenylenediamine  
m-PDA



3,5-diaminobenzotrifluoride  
DABTF

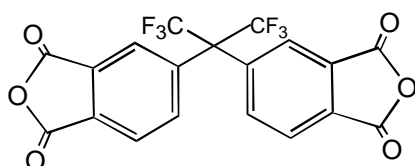


diaminophenylindane  
DAPI

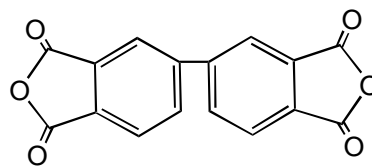


p-phenylenediamine  
p-PDA

### Dianhydrides

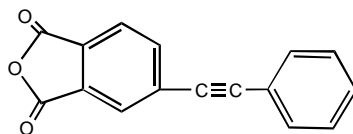


4,4'-hexafluoroisopropylidenebis(phthalic anhydride)  
6FDA



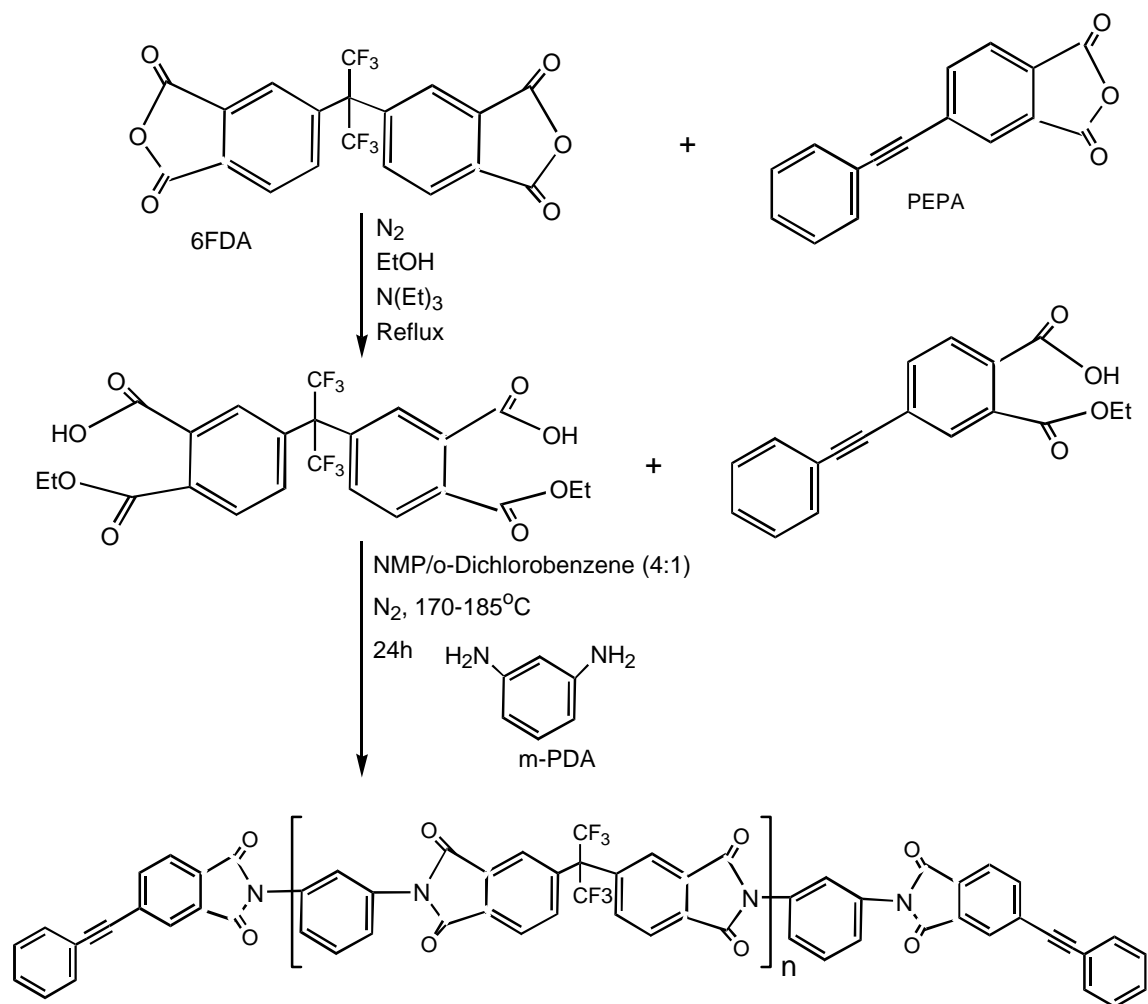
biphenyldianhydride  
BPDA

### Endcapper



4-phenylethynylphthalic anhydride (PEPA)

Figure 4.1.1 Monomers used for synthesis of  $\sim 3$  Kg/mol polyimide oligomer series.



Scheme 4.1.1 Ester-acid route for synthesizing PEPA-encapped polyimide oligomers.

exceeded 100 Kg/mol.

The discussion below provides information on specific polyimides that were synthesized and the characterization/analysis of their corresponding physical properties.

#### **4.1.1.1 Thermosetting Polyimide Oligomers Based on 6FDA and m-PDA**

In this dissertation research, the use of commercially available monomers was of primary interest due to convenience, ready availability and low cost. Manufacturers/developers of electronics packaging typically purchase polymers from a chemical company vendor<sup>184</sup>. Thus, the manufacturer's primary concerns in adopting new polyimide materials involve expense and the timeliness of polymer preparation by the chemical vendor. With this in mind, an inexpensive monomer, m-PDA, was initially chosen for combining with the more expensive fluorinated dianhydride, 6FDA.

The molecular weight series prepared using 6FDA/m-PDA consisted of 2-, 3- and 10 Kg/mol. Additionally, a high molecular weight thermoplastic polyimide control was synthesized. In each case, the ester-acid solution imidization route afforded materials that were completely soluble in polar solvents, such as NMP and chloroform. The polymer product yield was greater than 90%.

Thin films on salt plates were prepared from dilute concentrations of the oligomers in chloroform. Then FTIR spectra were obtained for analysis of the imide functional groups. A typical FTIR spectrum is shown in Figure 4.1.2. The bands appearing at approximately 1780-, 1730-, 1375- and 720  $\text{cm}^{-1}$  confirmed the presence of imide groups. Additionally, the lack of absorbances near 2900-3200  $\text{cm}^{-1}$  indicated that the polyimide did not contain significant amounts of amic-acid functional groups.

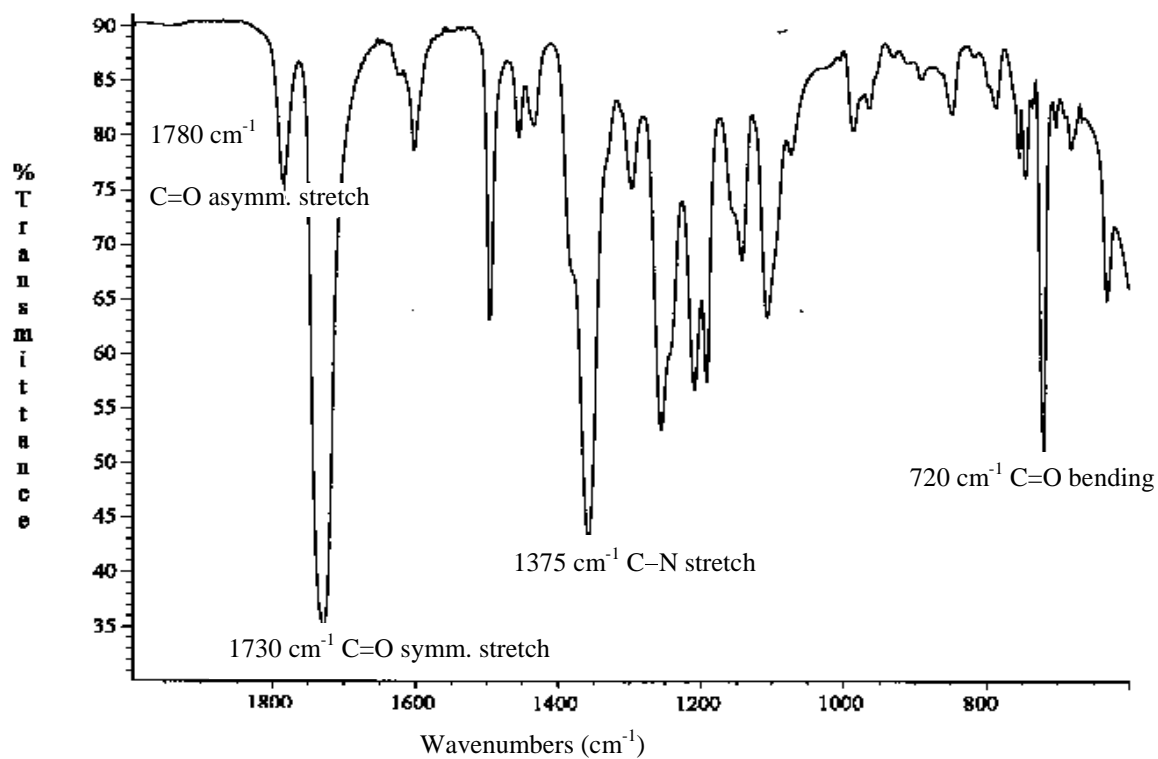


Figure 4.1.2 FTIR spectrum of ~2 Kg/mol 6FDA/m-PDA polyimide oligomer film.

Oligomer molecular weight control was achieved by offsetting the stoichiometry in favor of m-PDA and using PEPA as an endcapping agent. As shown in Table 4.1.1, the experimental number average molecular weights ( $\langle M_n \rangle_{\text{EXP}}$ ) corresponded well with the target values. For oligomers having target values less than 10 Kg/mol, the measurements were performed using  $^{13}\text{C}$ -NMR endgroup analysis. This method was chosen because GPC did not provide sufficient resolution between the elution volumes of pure solvent and polyimide at very low oligomer molecular weights.

Figure 4.1.3 shows part of a typical  $^{13}\text{C}$ -NMR spectrum of a PEPA-endcapped oligomer. The spectral region exhibits resonances at  $\sim 87$  and  $\sim 94$  ppm, which are attributed to the ethynyl carbons. The peak further upfield ( $\sim 65$  ppm) arises from resonance of the quaternary carbon of the hexafluoroisopropylidene (6F) group. The ratio of internal units to endgroups was determined using the average integral value of the endgroup peaks and the integrated area of the 6F peak. This gave the average number of repeat units in the polymer chain ( $n$ ). The  $\langle M_n \rangle_{\text{EXP}}$  was obtained by multiplying " $n$ " by the repeat unit molecular weight and adding the molecular weight contributions of the endgroups.

GPC analysis was performed for relatively higher molecular weight 6FDA/m-PDA polyimides. The GPC chromatogram for the  $\sim 10$  Kg/mol oligomer (Figure 4.1.4) showed the desired monomodal molecular weight distribution. Chromatogram resolution was sufficient to determine baseline location and, thus,  $\langle M_n \rangle_{\text{EXP}}$  was calculated from the curve within the normally expected error limits. The molecular weight distributions ( $\langle M_w \rangle / \langle M_n \rangle$ ) were around 2, which is typical for condensation polymers.

DSC thermograms of oligomers showed  $T_g$  as a broad endothermic shift in the baseline (Fig. 4.1.5). Also, the exothermic  $T_{\text{cure}}$  of reacting phenylethynyl groups peaked at  $\sim 380^\circ\text{C}$ .

Table 4.1.1 Molecular Weight and Thermal Analysis Data for 6FDA/*m*-PDA-based Oligomers.

Target MW Kg/mol	Dianhydride Ratio mol%	Diamine	$\langle M_n \rangle^a$ Kg/mol	TGA <sup>c</sup> 5% wt loss(°C)	DSC <sup>d</sup> T <sub>g</sub> (°C) uncured	DSC <sup>e</sup> T <sub>g</sub> (°C) cured	DMA <sup>f</sup> T <sub>g</sub> (°C) cured
2	6FDA 100	<i>m</i> -PDA	2.03	551	200	334	343
3	6FDA 100	<i>m</i> -PDA	3.13	543	234	327	338
10	6FDA 100	<i>m</i> -PDA	12.3 <sup>b</sup>	541	276	312	-----
1:1 stoichiometry	6FDA 100	<i>m</i> -PDA	117.4	539	293	-----	-----

a=<sup>13</sup>C-NMR in chloroform at room temperature.

b=GPC, mobile phase = NMP + 0.02 M P<sub>2</sub>O<sub>5</sub>, 60°C.

c=Heating rate of 10°C/min in air.

d=Second heating; heating rate of 10°C/min in nitrogen.

e=After cure in nitrogen; heating rate of 10°C/min in N<sub>2</sub>.

f= Melt pressed cured samples; heating rate of 5°C/min.

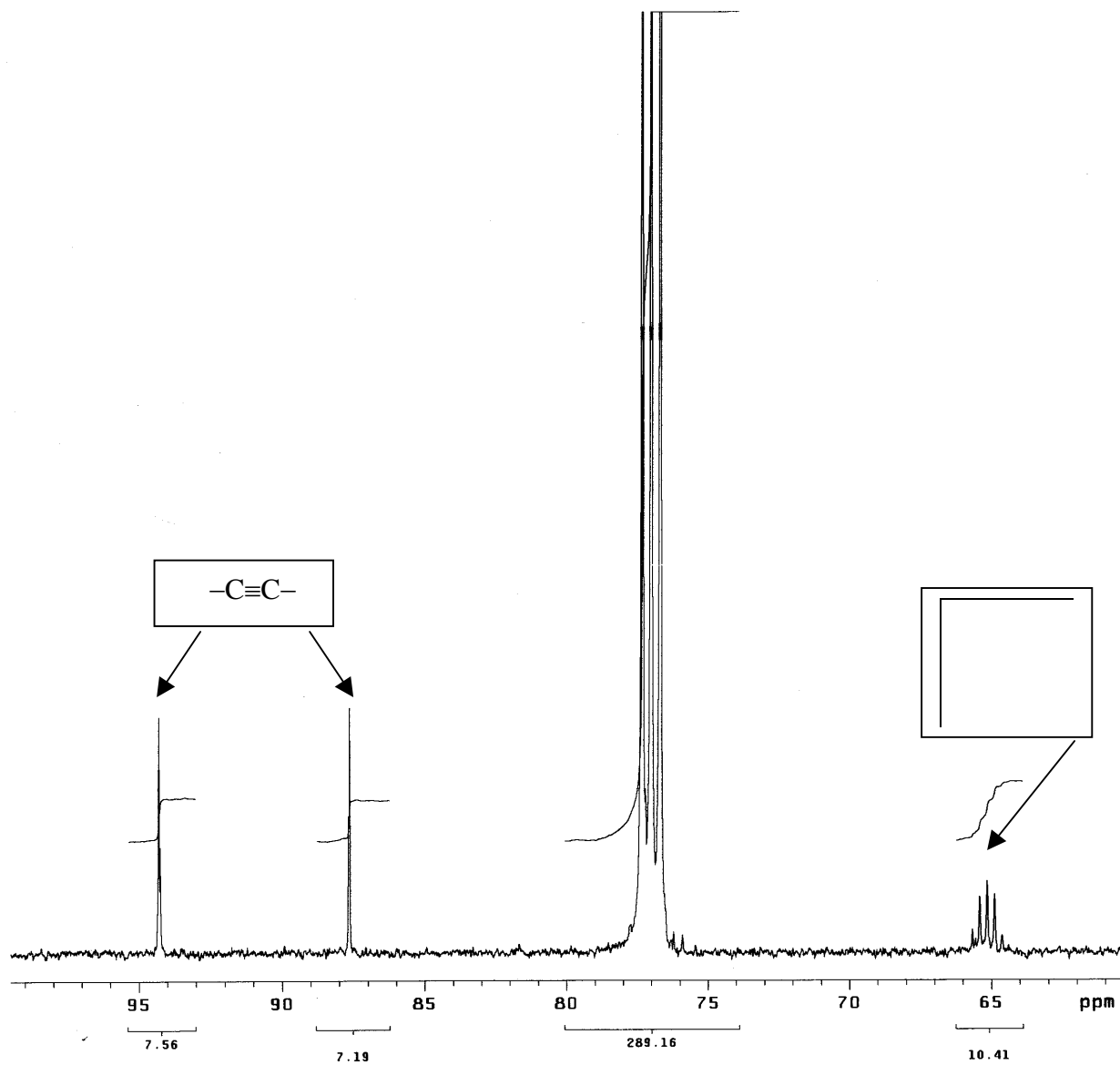


Figure 4.1.3  $^{13}\text{C}$ -NMR (100 MHz) spectrum of  $\sim 2$  Kg/mol 6FDA/m-PDA imide oligomer in d-chloroform.

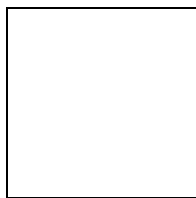


Figure 4.1.4 GPC chromatogram of ~10 Kg/mol 6FDA/m-PDA imide oligomer (mobile phase = NMP + 0.02M P<sub>2</sub>O<sub>5</sub>).

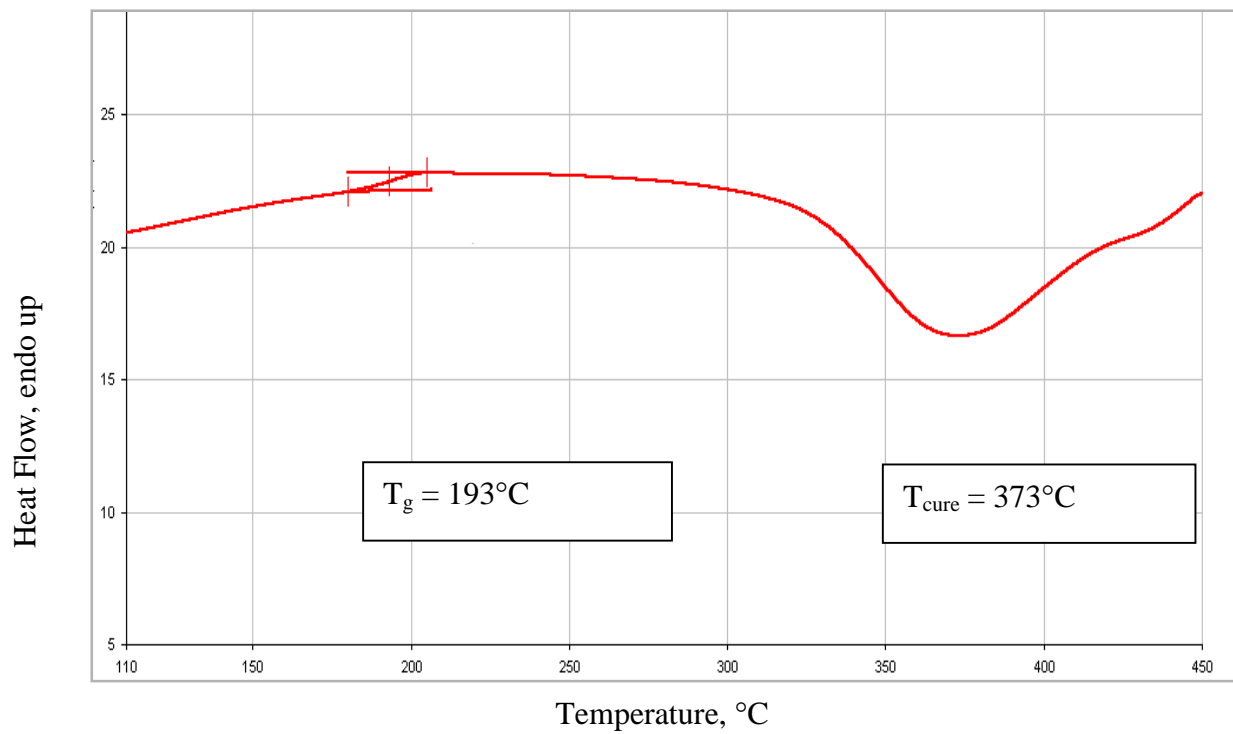


Figure 4.1.5 DSC thermogram of ~3 Kg/mol 6FDA/m-PDA imide oligomer, showing  $T_g$  and  $T_{\text{cure}}$ .

Thermal treatments at 380°C under contact pressures of 0.2 kpsi afforded crosslinked polyimide oligomers. The thermal stabilities of the thermosets were comparable to that of the thermoplastic control, exhibiting 5% weight loss in air at temperatures around 540°C (Table 4.1.1).  $T_g$ s of the crosslinked oligomers exceeded that observed for the thermoplastic polyimide and, in the cases of the ~2- and 3K polyimides, were ~35-40°C higher.

The thermoplastic and thermosetting 6FDA/m-PDA-based polyimides differed enormously in their film forming abilities. Solution-casting for obtaining free-standing films was conducted using the ~3K oligomer and the thermoplastic control, respectively. Due to lower solution viscosity, the oligomer could be prepared at relatively higher concentrations in NMP (~40% w/v). This was deemed to be advantageous from the standpoint that less solvent might result in lower film shrinkage.

All attempts to make films failed using the oligomer, despite numerous trials employing various solution concentrations and heating conditions, and regardless of whether solutions were applied by molding or blading. Long before the films were completely dry, de-lamination and massive cracking of the low molecular weight precursors were observed. Conversely, the high molecular weight thermoplastic imide formed tough, creasable transparent films when cast from ~15% w/v solution, followed by programmed drying under nitrogen. Based on these observations, it was conjectured that the failure of the oligomer to form cohesive films might have resulted from insufficient chain entanglement in the bulk of these relatively thick films.

Melt-pressing the neat oligomers using scrim cloth between aluminum plates and curing at 380°C provided relatively thin crosslinked films. Extraction of these films using chloroform enabled quantitation of the gel fraction (i. e. the amount of polyimide incorporated into the network) (Table 4.1.2). The gel contents of  $\geq 94\%$  indicated excellent solvent resistance.

Table 4.1.2 Gel Fractions of Crosslinked 6FDA/*m*-PDA Oligomers.

Target MW (Kg/mol)	Polyimide	Sample Preparation	%Gel <sup>b</sup>
10	6FDA/ <i>m</i> -PDA	Melt-pressed film cured at 380°C for 1 h	94
3	6FDA/ <i>m</i> -PDA	Melt-pressed film cured at 380°C for 1h	98
3	6FDA/ <i>m</i> -PDA	powder cured in air at 380°C for 1h	97
2	6FDA/ <i>m</i> -PDA	Melt-pressed film cured at 380°C for 1h	94
2	6FDA/ <i>m</i> -PDA	powder cured in air at 380°C for 1h	98

a=under a load of 350 psi.

b=refluxed in chloroform for 5 days, followed by drying under vacuum at 200°C for 1 day and 300°C for 1h.

A visual comparison of the solvent resistance of the thermoset film with that of the thermoplastic system was made using a digital camera to record the results. As the photographs in Figure 4.1.5 illustrate, the thermoplastic film dissolved completely within 30 minutes of immersion in NMP. The dimensions of the thermoset film did not appear to change during the same time period.

#### **4.1.1.2 Thermosetting Polyimide Oligomers with Target $\langle M_n \rangle$ Values of 3 Kg/mol**

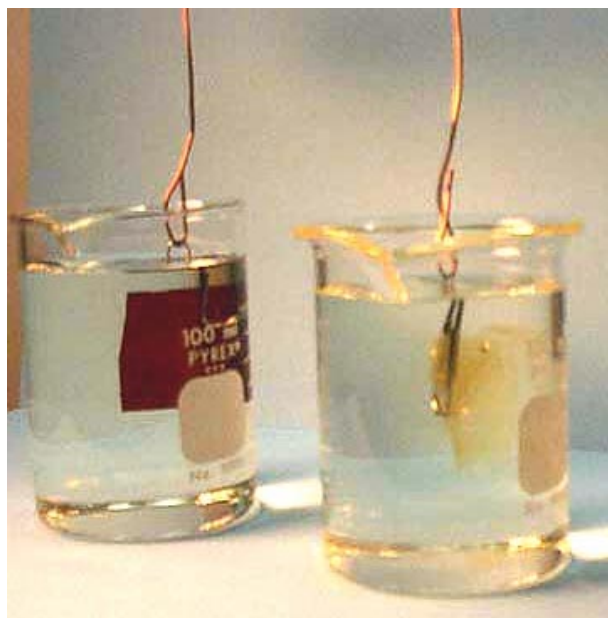
Earlier work<sup>182-183</sup> with 6FDA/m-PDA PEPA-encapped thermosetting oligomers had demonstrated the most important advantage of these materials: solvent resistance. However, it was the aim of this research to tailor key physical properties of interest in microelectronics. Hence, it was decided to produce a series of oligomers with different types of backbone units and to explore the influence of molecular structure on pertinent properties, such as water absorption,  $T_g$ , thermal stability and dielectric constant.

The target molecular weight for this series was selected as 3 Kg/mol, which was expected to produce relatively rigid thermoset materials due to high crosslink density. The dianhydride chosen was 6FDA, due to its fluoroalkylene groups, which enhance the solubility of the oligomeric precursor and cause reduction in dielectric constant and water uptake.

A series of homo- and copolymers based on 6FDA, PEPA and various diamines was produced having backbone units shown in Figure 4.1.6. Additionally, copolymers based on 6FDA and BPDA were prepared (also shown in Figure 4.1.6). This strategy was used for increasing backbone rigidity and to incorporate a relatively cheaper monomer, BPDA, for lowering the cost of the polymer.

The following sections discuss the synthesis and characterization of these polyimides.

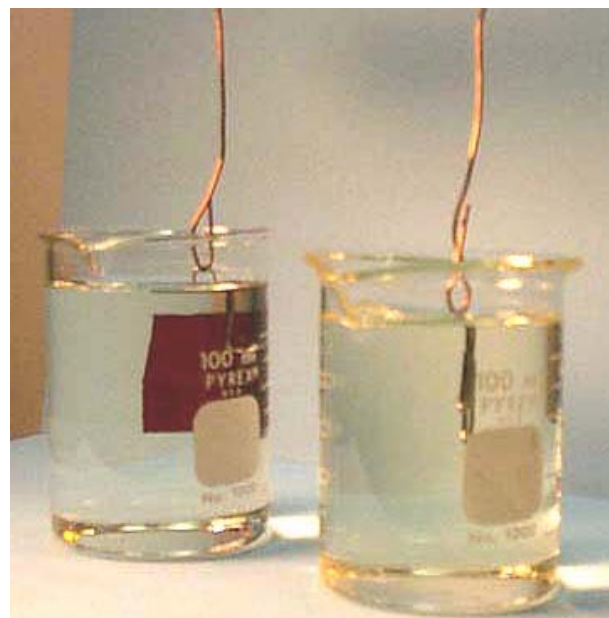
**PI Films: Initial Immersion in NMP**



Thermoset Film  
from Crosslinking  
3K oligomer

Thermoplastic  
Film

**PI Films: At 30 min. Immersion Time**



Thermoset Film  
no dimensional  
change

Thermoplastic Film  
completely dissolved

Figure 4.1.6 Solvent resistance study of 6FDA/m-PDA polyimide films in NMP.

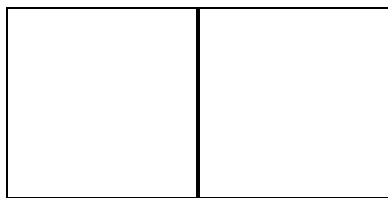


Figure 4.1.7 Repeat unit structures of series of ~3 Kg/mol polyimide oligomers.

#### 4.1.1.2.1 Polyimide Oligomers Based on 6FDA/p-PDA:m-PDA

Copolyimides based on 6FDA/p-PDA:m-PDA have been known since the early 1970s<sup>154</sup>. The Avimid N<sup>®</sup> resin, developed and marketed by DuPont as a matrix material for fiber composites, was comprised of 6FDA and p-PDA:m-PDA in a 95:5 mole % ratio<sup>10</sup>. This thermoplastic material has had a reputation of very high thermal stability and excellent high-temperature adhesion. However, its tenacious retention of the high boiling reaction solvent, NMP, has often caused void formation during melt processing. The Avimide N<sup>®</sup> backbone has also been utilized as a thermosetting PMR-type system<sup>185</sup>. Prior to infusing the carbon fibers, the alcoholic vehicle containing the monomers was charged with the appropriate amount of nadic ester to give unsaturated endgroups capable of crosslinking. The  $T_g$  value of the crosslinked material was well over 300°C.

In this research, incorporation of the p-PDA monomer in 6FDA-based polyimides was utilized as a strategy for increasing the  $T_g$  of the PEPA-encapped thermosets. Previous work by Meyer had shown that a 6FDA/p-PDA/PEPA oligomer, with a target  $\langle M_n \rangle$  of 3 Kg/mol, had become insoluble during solution imidization in NMP<sup>14</sup>. Additionally, this polymer had displayed a  $T_m$  at 452°C, thus confirming the suspected semi-crystalline morphology. Since the aim of this research was to obtain fully cyclized, soluble polyimides with high  $T_g$ s, the strategy of using m-PDA as a comonomer was used. The bent structure of m-PDA was believed to be important for breaking up chain symmetry and, thus, to provide soluble polyimide materials.

Initial preparation of a copolyimide, targeted at 3 Kg/mol  $\langle M_n \rangle$ , involved a mole % ratio of 80:20 with respect to p-PDA:m-PDA. The ester-acid solution imidization route was performed after rigorously purifying the monomers. The solution remained clear at 180°C

during the 24 hour imidization process. However, subsequent cooling to room temperature resulted in a cloudy solution, which provided evidence for insolubility. Due to the relatively scant haziness of the solution, the amount of precipitate was estimated to be <10% of the total polymer yield.

It was believed that incorporating more of the kinked m-PDA would improve solubility. Hence, two additional copolyimides were prepared using 6FDA/p-PDA:m-PDA/PEPA where the m-PDA content was increased to 30 and 40 mole %, respectively. The targeted  $\langle M_n \rangle$  values were 3 Kg/mol. The solution imidization yielded identical results for each trial: the materials were soluble at imidization temperatures, but a small amount of precipitate formed upon cooling.

The reduced solubility found in the series of p-PDA based oligomers probably arose from alignment and packing of the more rigid low molecular weight fractions. The lower solubility would result in poor processability during solution casting, although the insoluble portions could be filtered from the solutions prior to film preparation.

Molecular weight characterization of the copolymer series was conducted using quantitative  $^{13}\text{C}$ -NMR analysis. To ensure solubility, the oligomer solutions in NMP were heated to 160°C while acquiring the spectra. The results of the calculations, shown in Table 4.1.3, indicated that good molecular weight control had been achieved, giving  $\langle M_n \rangle_{\text{EXP}}$  close to target values. The close correlation suggested that the reacting species had remained completely soluble during solution imidization, thus maintaining the required stoichiometric balance.

Results of thermal analysis, using both DSC and DMA techniques, indicated that very high  $T_g$ s could be obtained with these crosslinked materials. As expected, the cured copolyimide containing 80 mol % p-PDA exhibited the highest  $T_g$  (397°C, by DMA), due to more rigidity imparted by higher p-PDA content. The  $T_g$  of this material was comparable to that of Kapton,

Table 4.1.3 Molecular Weight and Thermal Analysis Data for 6FDA/p-PDA:m-PDA/PEPA Imide Oligomers.

Target MW Kg/mol	$\langle M_n \rangle^a$ Kg/mol	<i>p</i> -PDA ratio mol %	Diamine comonomer mol %	$T_g^b$ °C	DSC <sup>c</sup> $T_{g2}$ °C	DMA <sup>d</sup> $T_{g2}$ °C
3	3.01	80	20 <i>m</i> -PDA	256	375	397
3	2.55	70	30 <i>m</i> -PDA	239	370	383
3	3.38	40	60 <i>m</i> -PDA	241	339	369

a=<sup>13</sup>C-NMR in NMP at 160-170°C.

b=Uncured oligomer; 2<sup>nd</sup> heating, heating rate of 10°C/min in N<sub>2</sub>.

c=After cure in N<sub>2</sub> at 380°C 1h; heating rate of 10°C/min in N<sub>2</sub>.

d=Melt pressed cured samples; heating rate of DMA =5°C/min.

which has been reported in the range of 380-400°C. This attribute, in particular, would make this thermosetting copolyimide very attractive for microelectronics packaging, where thermal processing temperatures typically reach 400°C.

Excellent thermo-oxidative stability was also exhibited by the p-PDA:m-PDA containing copolyimides, with 5% weight loss at temperatures >530°C.

#### **4.1.1.3 Polyimide Oligomers Based on 6FDA/p-PDA**

Since exceptionally high  $T_g$ s had been obtained with p-PDA containing polyimides, it was not deemed advantageous to further reduce the amount of p-PDA in the copolymers. It was believed, however, that the shorter chains in the ~3K system were responsible for insolubility due to intermolecular packing. Previous work by Meyer had shown that the solubility for 6FDA/p-PDA/PEPA homopolymers depends on molecular weight<sup>14</sup>. Meyer's series had consisted of oligomers with targeted  $\langle M_n \rangle$  values of 3-, 10- and 15 Kg/mol. Among these, only the 3 Kg/mol oligomer had exhibited insolubility. Hence, the next strategy for obtaining soluble polyimides was to prepare oligomers of relatively higher molecular weight consisting of 6FDA/PEPA and using p-PDA as the sole diamine. The m-PDA was not utilized because a significant decrease in  $T_g$  would be expected from incorporating a kinked monomer and simultaneously decreasing the final crosslink density by lengthening the chains.

The first homopolyimide oligomer prepared in this series had a target  $\langle M_n \rangle$  of 6 Kg/mol. The ester-acid solution imidization was conducted at a temperature of 180°C. Within a few hours of heating, the formation of a milky precipitate was observed, which gradually increased in quantity over the next several hours. The amount of insoluble material was estimated to be >90% of the total polyimide product.

The next attempt at making a soluble oligomer involved targeting the  $\langle M_n \rangle$  value at 8 Kg/mol and again using 6FDA/p-PDA/PEPA. The same result was observed during imidization as that found for the ~6K system: excessive cloudy precipitate appeared in the solution at 180°C. This result was unexpected, considering that 8 Kg/mol was near to the 10 Kg/mol value at which Meyer had obtained a soluble polyimide.

To ascertain whether Meyer's result could be reproduced, the 10 Kg/mol homopolyimide based on 6FDA/p-PDA/PEPA was prepared. During the ester-acid solution imidization, the polymer remained fully dissolved. Additionally, the solution remained clear after cooling to room temperature. Apparently, the relatively higher molecular weight provided more entropy through an increased number of chain conformations/entanglements, thus inhibiting chain packing and ordering.

Molecular weight characterization and thermal analysis data for the series appear in Table 4.1.4. Due to insolubility, determination of the  $\langle M_n \rangle_{\text{EXP}}$  of the ~6- and ~8K oligomers could not be performed. The GPC results of the ~10K system showed a very close correlation of  $\langle M_n \rangle_{\text{EXP}}$  with the target value.

$T_g$ s of the oligomers were determined by heating powdered samples of the oligomers in the DSC to 450°C. In all three cases,  $T_g$ s in excess of 320°C were obtained.  $T_g$ s of this magnitude would coincide with the temperatures at which phenylethynyl groups react<sup>74</sup>. This meant that there was an insufficient processing window between  $T_g$  and  $T_{\text{cure}}$ . This observation was supported by the lack of an exothermic peak in the DSC baseline between 320 and 400°C, which arises from the reaction of the endgroups. Additionally, samples treated at 380°C for 1 hour showed no increase in  $T_g$ , indicating that minimal crosslinking had occurred. The polymers remained in the glassy state at  $T_{\text{cure}}$ , which inhibited mutual accessibility of reactive endgroups.

Table 4.1.4 Molecular Weight and Thermal Analysis Data for 6FDA/p-PDA/PEPA Homopolyimide Oligomers.

Target MW Kg/mol	$\langle M_n \rangle$ Kg/mol	<i>p</i> -PDA ratio mol %	$T_g^b$ °C
10	10.2 <sup>a</sup>	100	351
8	insoluble	100	333
6	insoluble	100	323

a=GPC, mobile phase = NMP + 0.02 M P<sub>2</sub>O<sub>5</sub>, 60°C.

b=Uncured oligomer; DSC 2<sup>nd</sup> heating, heating rate of 10°C/min in N<sub>2</sub>.

#### 4.1.1.4 Polyimide Oligomers Based on 6FDA/p-PDA:DABTF

Insolubility had resulted from the predominant chain symmetry and low molecular weights of the p-PDA based imide oligomers. To suppress packing in the low molecular weight systems, a kinked monomer with a bulky substituent was selected for copolymerization. This was 3,5-diaminobenzotrifluoride (DABTF), which supplied meta-catenation and large pendant trifluoromethyl groups to the polyimide chains. This monomer, although costly, was commercially available from a number of sources.

The incorporation of DABTF was expected to provide two benefits: increased solubility and lower dielectric constant. Previous work at NASA Langley had produced a series of thermoplastic homopolyimides containing DABTF, using a variety of dianhydrides<sup>186</sup>. The 6FDA/DABTF-based polyimide in the series had exhibited a lower dielectric constant than the other imides, which contained non-fluorinated dianhydrides (i.e. BPDA, OPA, BTDA). Despite the higher cost, the improvements in electrical properties might justify the use of DABTF in electronics applications.

Initially, a PEPA-encapped homopolyimide control was synthesized, using 6FDA/DABTF. This thermosetting imide had a target  $\langle M_n \rangle$  of 3 Kg/mol. The ester-acid route provided ~85% polymer product yield. The  $\langle M_n \rangle_{\text{EXP}}$  determined using <sup>13</sup>C-NMR was 3.3 Kg/mol, which was in good agreement with the target value. The product yield was found to be lower than the yields produced using other monomers, which were usually >90%. This probably resulted from loss of lower molecular weight species that had failed to precipitate in methanol.

The first copolyimide was prepared, by reacting 6FDA and PEPA with p-PDA:DABTF in a molar (%) ratio of 80:20. Synthesis was performed using the ester-acid solution imidization as described above. During the imidization step at 180°C, the polymer remained in solution, as

evidenced by a clear brown liquid. However, after completion of the reaction and during the subsequent cooling process, small amounts of precipitate were observed.

Two additional sequential syntheses were attempted: the first employing a molar ratio of 70:30 p-PDA:DABTF, and the second a 60:40 molar ratio of p-PDA:DABTF. For each case, a small amount of precipitate was observed upon cooling the reaction solution. The amount of precipitated material was estimated to be <10%.

The molecular weight and thermal characterization data for the series of copolymers and the homopolymer appear in Table 4.1.5. Comparison of the  $T_g$ s of the crosslinked materials revealed the expected trend:  $T_g$  increased dramatically with increasing p-PDA content. The  $T_g$  for the copolyimide containing 80 mol% p-PDA was approximately 396°C, which was about 70°C higher than that of the 6FDA/DABTF homopolyimide. The high  $T_g$  makes this material an attractive candidate for microelectronics packaging. However, the reduced solubility of the oligomeric precursor would be detrimental to solution casting.

Thermal stability of this series was comparable to the other thermosets studied: 5% weight loss occurred at temperatures ~540°C.

#### **4.1.1.5 Oligomers Containing p-PDA:m-PDA with Target $\langle M_n \rangle$ Values of 6-12 Kg/mole**

The p-PDA based copolyimides containing pendant and/or kinked diamines exhibited better solubility than 6FDA/p-PDA homopolymers with  $\langle M_n \rangle$  values less than 10 Kg/mol. However, further work was needed to design oligomers that were completely soluble to provide better spin casting materials. Additionally, it was a primary objective to keep  $T_g$  as high as possible, in consideration of the high processing temperatures used in microelectronics.

Table 4.1.5 Molecular Weight and Thermal Analysis Data for 6FDA/DABTF:p-PDA and 6FDA/DABTF PEPA-encapped Polyimide Oligomers.

Target MW Kg/mol	$\langle M_n \rangle^a$ Kg/mol	p-PDA ratio mol %	Diamine comonomer mol %	T <sub>g</sub> <sup>b</sup> °C	DSC <sup>c</sup> T <sub>g2</sub> °C	DMA <sup>d</sup> T <sub>g2</sub> °C
3	2.88	80	20 DABTF	241	360	396
3	3.80	70	30 DABTF	247	359	385
3	2.59	40	60 DABTF	245	342	357
3	3.34	0	100 DABTF	228	314	329

a=<sup>13</sup>C-NMR in NMP at 160-170°C.

b=Uncured oligomer; 2<sup>nd</sup> heating, heating rate of 10°C/min in N<sub>2</sub>.

c=After cure in N<sub>2</sub> at 380°C 1h; heating rate of 10°C/min in N<sub>2</sub>.

d=Melt pressed cured samples; heating rate of DMA =5°C/min.

The next strategy was to simultaneously increase the molecular weight and to employ a small amount of kinked monomer. To meet this requirement, m-PDA was chosen as the comonomer to be introduced in a 10 mol% ratio with 90 mol% p-PDA. This ratio was consistently used in the series of copolymers.

The series of copolymers had four selected target  $\langle M_n \rangle$  values: 6-, 8-, 10- and 12 Kg/mol. In all cases, the ester-acid route produced very dark brown solutions during imidization at 180°C. After cooling, the reaction solutions appeared clear, but it was uncertain whether the dark color interfered with visual detection of particles. Close-up illumination of the solution with a white light-source did not reveal any particles.

After isolating and drying the oligomers, solubility experiments were conducted using NMP, chloroform and DMSO. Solubility was tested at 12% w/v concentration at room temperature. The results are shown in Table 4.1.6, and were based on visual observations, not actual quantitation. None of the copolyimides was soluble in chloroform. Conversely, the solutions in NMP and in DMSO showed a high degree of clarity as prepared for most of the polyimides tested. However, after the solutions were allowed to stand at room temperature for 24-48 hours, a small amount of precipitate was observed. The exception was the solution of the 6K oligomer in DMSO, which retained its clarity. The precipitates observed in the other solutions may have resulted from solvent induced crystallization.

Copolyimides were completely soluble in NMP containing 0.02M  $P_2O_5$  at the low concentrations used in the GPC mobile phase. Hence,  $\langle M_n \rangle$  was characterized using GPC. The results, as well as the thermal analysis data for the copolymer series, appear in Table 4.1.7.

Table 4.1.6 Solubility of 6FDA/p-PDA:m-PDA/PEPA Oligomers in Organic Solvents.

Target $\langle M_n \rangle$ Kg/mol	Diamine Ratio Mol%	Solvents		
		Chloroform	NMP	DMSO
6	p-PDA/m-PDA 90:10	insoluble	~90% soluble	Completely soluble
8	p-PDA/m-PDA 90:10	insoluble	~90% soluble	~90% soluble
10	p-PDA/m-PDA 90:10	insoluble	soluble*	soluble*
12	p-PDA/m-PDA 90:10	insoluble	soluble*	soluble*

\* After >24-48 hours of standing at room temperature, a small amount of precipitate was observed.

Table 4.1.7 Molecular Weight and Thermal Analysis Data for 6FDA/p-PDA:m-PDA 90:10 PEPA-encapped Oligomers.

Target $\langle M_n \rangle$ Kg/mol	$\langle M_n \rangle^a$ Kg/mol	Diamine Ratio Mol%	$T_g^b$ °C	$T_{g2}^c$ °C
6	8.1	p-PDA/m-PDA 90:10	286	402
8	9.5	p-PDA/m-PDA 90:10	300	365
10	10.6	p-PDA/m-PDA 90:10	305	358
12	11.7	p-PDA/m-PDA 90:10	310	353

a=GPC, mobile phase = NMP + 0.02 M  $P_2O_5$ , 60°C.

b=Uncured oligomer; DSC 2<sup>nd</sup> heating, heating rate of 10°C/min in  $N_2$ .

c=Cured film cast from NMP solution (dried and heated to 380°C for 1h in  $N_2$ ), DSC 1<sup>st</sup> heat, heating rate of 10°C/min in  $N_2$ .

For uncrosslinked 6FDA/p-PDA:m-PDA oligomers,  $T_g$  increased with increasing molecular weight, but remained near 300°C. For the crosslinked films, a trend of increasing  $T_g$  with decreasing molecular weight of the oligomeric precursor was observed. After curing,  $T_g$ s had risen by about 45-65°C, except for that of the ~6K oligomer. Remarkably, the  $T_g$  of the ~6K uncured oligomer rose from 286°C to 402°C after cure, which comprised an increase of 116°C. This probably resulted from the higher crosslink density, plus the wider processing window between  $T_g$  and  $T_{cure}$ , which facilitated the reaction of phenylethynyl groups.

Among the series of 6FDA/p-PDA:m-PDA 90:10 thermosetting oligomers, the ~6K system seemed the most attractive for use as a dielectric film. Its excellent solubility in DMSO and high  $T_g$  appeared to endorse it for this application. However, the hazardous environmental impact of using DMSO would undoubtedly detract from its overall advantages.

#### **4.1.1.6 Polyimide Oligomers Based on 6FDA:BPDA and m-PDA or DABTF**

##### **4.1.1.6.1 Copolyimides Based on 80:20 6FDA:BPDA**

The series of p-PDA based thermosetting imides had demonstrated very high  $T_g$ s, which resulted from stiffening the backbone of relatively lower molecular weight precursors. Another strategy that was utilized was incorporation of a stiff dianhydride comonomer.

Biphenyldianhydride, BPDA, was selected because of its symmetrical and rigid structure. It was thought that the benefits of using BPDA would include: high  $T_g$ s without sacrificing thermal stability and, possibly, lower CTEs. The BPDA monomer was commercially available in polymer grade purity and had the added advantage of being less costly than 6FDA.

The first copolymer synthesis consisted of using 6FDA and BPDA in an 80:20 mole% ratio. The stoichiometric amounts of the other reactants, m-PDA and PEPA, were determined based on the Carothers equation using a target  $\langle M_n \rangle$  of 3 Kg/mol. The synthesis method used

was the ester-acid route. The first step involved preparing the ester-acid derivatives of BPDA, 6FDA and PEPA. This was followed by reaction with m-PDA in NMP/o-DCB 4/1 at 180°C.

The incorporation of 20 mole% of BPDA had a dramatic effect on polyimide solubility. During solution imidization at ~180°C, a heavy colloidal dispersion of fine particles was observed. Since a relatively small amount of BPDA comonomer had been employed, it was likely that its incorporation had not been statistical with regard to 6FDA. Several rigid units of BPDA/m-PDA along the chains could probably lead to packing and, hence, insolubility.

Another synthesis method was utilized to prepare the same copolymer, the classic amic-acid route. This was done to allow equilibration of the reaction of 6FDA and BPDA with the diamine, thus obtaining a statistical copolymer. The steps in this reaction involved preparing a solution of m-PDA in dry NMP, followed by slow addition of BPDA, 6FDA and PEPA to the diamine solution. After stirring at room temperature for ~24 hours, solution imidization was carried out by adding dry o-DCB as an azeotroping agent and heating the reaction solution to 180°C. Again, during this heating period, a heavy colloidal dispersion of particles formed in the solution.

Slow dissolution of dianhydrides in the first step of classic amic-acid synthesis has been thought to result in interfacial-type polymerization between solid anhydride and dissolved diamine<sup>10</sup>. If this had occurred in this study, the stoichiometry of 6FDA/BPDA would have been incorrect in the beginning, and subsequent reaction time may have been insufficient to allow equilibration of these monomers with m-PDA. Hence, it was decided to attempt amic-acid synthesis again with the order of monomer addition reversed. A solution of 6FDA, BPDA and PEPA was prepared using dry NMP. After dissolving the anhydrides completely, the diamine was added and the reaction solution was stirred for ~24 hours. Then solution imidization was

performed as before. During heating at  $\sim 185^{\circ}\text{C}$ , a moderate amount of colloiddally dispersed particles formed. The reduced amount of precipitate indicated improved solubility, which could have arisen from a better statistical incorporation of BPDA. Since the copolyimide was not completely soluble, this conjecture could not be proved using solution spectroscopic techniques.

#### 4.1.1.6.2 Copolyimides Based on 90:10 6FDA:BPDA

To address the solubility problem, the next copolymer was prepared with a relatively lower amount of BPDA. The ester-acid route was utilized to synthesize a copolyimide consisting of 6FDA:BPDA in a 90:10 molar ratio. The other reactants, m-PDA/PEPA, were utilized in the stoichiometric quantities determined for a target  $\langle M_n \rangle$  of 3 Kg/mol. During solution imidization and after cooling, the solution remained clear, indicating good solubility of the polyimide.

The  $\langle M_n \rangle_{\text{EXP}}$  for the 90:10 6FDA/BPDA copolyimide was determined using  $^{13}\text{C}$ -NMR analysis. Applicable portions of the expanded spectra are shown in Figure 4.1.8. The average number of repeat units containing 6FDA ( $n_{6\text{F}}$ ) was determined in the manner previously described, using the peak integral ratio of the internal 6F quaternary carbon to that of the ethynyl carbons of the endgroups. Then  $n_{6\text{F}}$  was multiplied by the corresponding repeat unit molecular weight to give the contribution of this species to  $\langle M_n \rangle_{\text{EXP}}$  of the copolymer.

The average number of repeat units comprised of BPDA ( $n_{\text{BP}}$ ) was calculated in a similar manner. A peak appeared at  $\sim 145$  ppm, which was attributed to the resonance of the aromatic carbons comprising the biphenyl linking group. Determining the peak integral ratio of these internal carbons to that of the ethynyl carbons gave  $n_{\text{BP}}$ . Then  $n_{\text{BP}}$  was multiplied by the corresponding repeat unit molecular weight. Adding the molecular weight contributions of both types of repeat units, as well as the contribution of the endgroups, provided  $\langle M_n \rangle_{\text{EXP}}$ .

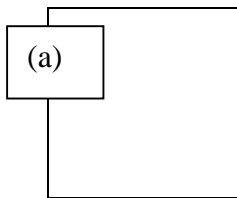
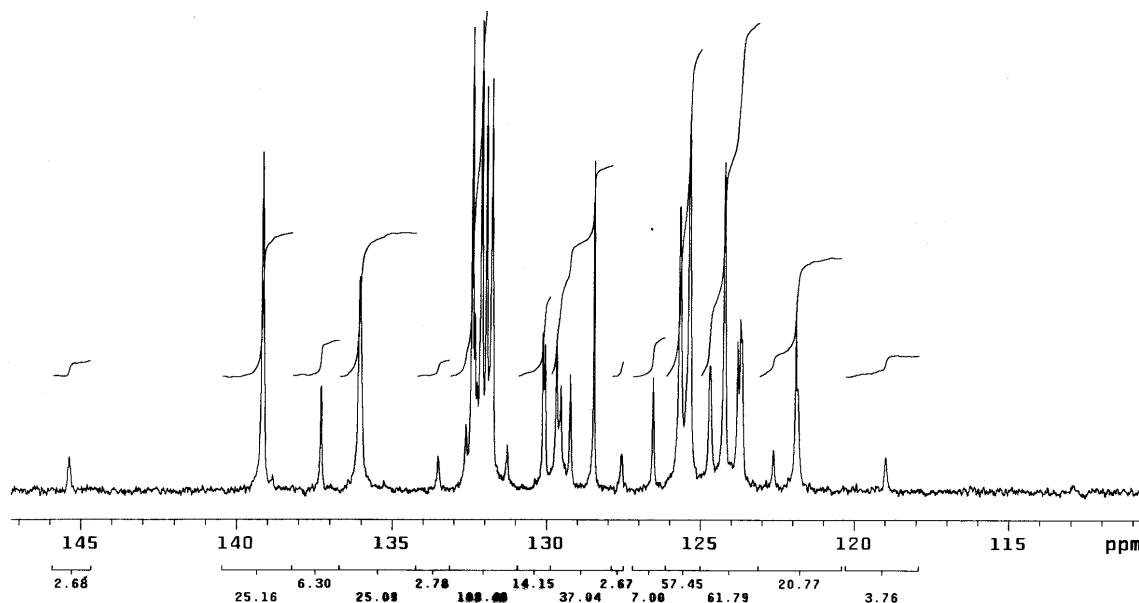


Figure 4.1.8  $^{13}\text{C}$ -NMR (100 MHz) spectra of 6FDA [ ] /m-PDA/PEPA imide oligomer (in  $\alpha$ -chloroform): (a) expanded region containing resonances of ethynyl carbons and quaternary carbon of 6F group; (b) expanded region containing resonance of aromatic biphenyl bridging carbon.



From the  $^{13}\text{C}$ -NMR integrations the ratio of 6FDA to BPDA repeat units ( $n_{6F}:n_{BP}$ ) was 4.05:0.45, which was reduced to the whole number % ratio of 90:10. This was in good agreement with the theoretical composition.

To evaluate whether a similar copolymer could be obtained using the classic synthesis method, the amic-acid route was employed using the same monomers/stoichiometry as before.

The traditional route of adding the dianhydrides to a solution of the diamine was followed. After reacting for ~24 hours at room temperature, the solution imidization was performed as described previously.

It was also of interest to prepare ~3K 6FDA/BPDA-based oligomer containing a greater concentration of fluoroalkylene groups to study the effect on the physical properties. The same ratio of 6FDA:BPDA (90:10) was polymerized with the fluorinated diamine, DABTF, using PEPA as the endcapper. The ester-acid route was utilized for the synthesis.

#### 4.1.1.6.2.1 Characterization of Copolyimides Based on 90:10 6FDA:BPDA

The thermal analysis and molecular weight characterization results of the 90:10 6FDA:BPDA copolymer series appear in Table 4.1.8. Data for ~3K 6FDA/m-PDA/PEPA and 6FDA/DABTF/PEPA homopolyimides have been included for comparison.

The two 90:10 6FDA:BPDA/m-PDA copolyimides, which had been prepared using the two different routes, had nearly identical  $T_g$ s and  $\langle M_n \rangle_{EXP}$  values. This was a good indication that their structures and compositions were the same.

The DMA results of the BPDA copolyimides were compared with those of the corresponding homopolymers. The  $T_g$  had increased only 10°C with incorporation of BPDA. This was not surprising, since only 10 mole% of BPDA had been utilized in the copolymers.

Table 4.1.8 Molecular Weight and Thermal Analysis Data for 6FDA:BPDA 90:10

Polymerized with m-PDA and PEPA.

Target $\langle M_n \rangle$ Kg/mol	Mole Ratio 6FDA/BPDA Used in synthesis	Mole Ratio 6FDA/BPDA Calculated ( $^{13}\text{C}$ -NMR)	Diamine	Synthesis Method	$\langle M_n \rangle_{EXP}^a$ Kg/mol	$T_g^b$ uncured oligomer, °C	DMA <sup>c</sup> $T_g$ after cure, °C

3	90:10	90:10	m-PDA	Ester- acid	3.04	234	347
3	90:10	86:10	m-PDA	Amic- acid	2.95	233	---
3	100:0	N/A	m-PDA	Ester- acid	3.13	234	338
3	90:10	87:10	DABTF	Ester- acid	3.34	228	340
3	100:0	N/A	DABTF	Ester- acid	3.39	228	329

a=<sup>13</sup>C-NMR in chloroform at room temperature.

b=DSC 2<sup>nd</sup> heating; heating rate of 10°C/min in nitrogen.

c= Melt pressed cured samples; heating rate of DMA =5°C/min.

#### 4.1.1.7 Polyimide Oligomers Based on 6FDA/DAPI

Marginal solubility of imide oligomers containing moderate amounts of p-PDA and BPDA had been evidenced by the systems prepared in this research. Conversely, the imides prepared from less rigid monomers, such as 6FDA/m-PDA, had demonstrated excellent solubility in a variety of solvents. However, the  $T_g$  of the cured materials of this type was lower than that desired for an interlayer dielectric material, which should be  $\sim 390^\circ\text{C}$ . Hence, it was the continuing goal of this research to obtain a soluble thermosetting polyimide with as high a  $T_g$  value as possible.

Ciba-Geigy's development of a substituted phenylindane diamine led to preparation of the first soluble polyimides containing rigid dianhydrides<sup>187-189</sup>. The monomer, 5(6)-amino-1-(4-aminophenyl)-1,3,3-trimethylindane (DAPI), was prepared by acid catalyzed dimerization of  $\alpha$ -methylstyrene, followed by nitration and reduction.

Figure 4.1.9 shows the structure of DAPI, which contains the rigid indane structure<sup>76-77</sup>. As shown, projecting out from the indane plane are four bulky groups, three methyls and one phenyl. The bent structure results from the non-coplanarity of the indane and phenyl rings. Additionally, nitration of the phenylindane precursor produces substituents at both the 5- and 6-positions in a 50:50 mixture and hence, following reduction, a 50:50 isomeric ratio of amino-groups is obtained.

Incorporating DAPI in polyimides provides solubility due to the bent structure and bulky groups, as well as the asymmetry imparted to the backbone by the isomeric mixture. Thus, molecular ordering/packing is suppressed, even when very rigid dianhydrides are incorporated. Additionally, due to the rigid nature of DAPI, polyimides with very high  $T_g$ s can be obtained using this monomer.

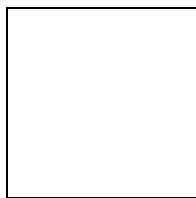


Figure 4.1.9 Molecular structure of diaminophenylindane (DAPI).

In this research, two DAPI containing polyimides were prepared using 6FDA and PEPA. The target  $\langle M_n \rangle$  values were 3- and 7 Kg/mol, respectively. The ester-acid solution imidization route was used for the synthesis. Additionally, a thermoplastic control using 1:1 stoichiometry was prepared for comparison. All of the DAPI-based polyimide products were soluble in a variety of solvents, including chloroform, NMP and DMAc.

Molecular weight and thermal analysis data are shown in Table 4.1.9. The 5% weight loss temperatures were  $>500^\circ\text{C}$  for the thermosetting imides. Compared to the thermoplastic control value ( $443^\circ\text{C}$ ), this was a significant increase. Since aliphatic bonds are relatively weaker with respect to thermo-oxidative degradation, the high thermal stability of the thermosets can be attributed to the stable aromatic crosslinks formed by reaction of phenylethynyl groups.

The  $T_g$  values of the crosslinked DAPI imides exceeded that of the thermoplastic control

by ~15-20°C. The DMA results showed an increase in  $T_g$  of ~18°C for the ~3K DAPI film compared to that of the ~3K 6FDA/m-PDA crosslinked material reported previously (338°C). Hence, rigidifying the backbone with DAPI had only a relatively minor effect in raising the  $T_g$ . This was attributed to the incorporation of a relatively flexible dianhydride, 6FDA.

DMA samples could not be produced by melt pressing the ~7K DAPI oligomer due to the narrow processing window between the  $T_g$  of the oligomer and  $T_{cure}$ .

Using solution casting techniques, film preparation was attempted using the ~3K and ~7K DAPI oligomers. A variety of solvents, heating programs and conditions were tried, but in each case the films cracked. Attempts to heal the fissures by heating to temperatures above  $T_g$  in a furnace yielded films with channels that were very brittle.

Table 4.1.9 Molecular Weight and Thermal Analysis Data for 6FDA/DAPI/PEPA

Imide Oligomers.

Target $\langle M_n \rangle$ Kg/mol	Diamine	$\langle M_n \rangle_{EXP}$ <sup>a</sup> Kg/mol	TGA <sup>c</sup> 5% weight loss, °C	$T_g^d$ uncured oligomer °C	DSC <sup>e</sup> $T_{g2}$ °C	DMA <sup>f</sup> $T_{g2}$ °C
3	DAPI	3.5 <sup>b</sup>	522	242	340	356
7	DAPI	6.0	517	266	334	*
1:1 Stoichiometry	DAPI	24.5	443	319	N/A	N/A

a=GPC, mobile phase = NMP + 0.02M P<sub>2</sub>O<sub>5</sub>, 60°C.

b=<sup>13</sup>C-NMR in chloroform at room temperature.

c=Heating rate of 10°C/min in air.

d=2<sup>nd</sup> Heating; heating rate of 10°C/min in N<sub>2</sub>.

e=After cure in N<sub>2</sub> at 380°C for 1 h; DSC heating rate of 10°C/min in N<sub>2</sub>.

f=Melt pressed cured samples; DMA heating rate of 5°C/min in N<sub>2</sub>.

\*=Inadequate melt flow for making melt-pressed DMA samples.



#### 4.1.1.7.1 Polyimide Oligomer Based on 6FDA/DAPI:p-PDA/PEPA

The increase in  $T_g$  by using DAPI in 6FDA-containing homopolyimide oligomers had been relatively minor. However, a comonomer was still desired for producing soluble p-PDA containing copolyimides. Hence, DAPI was selected for copolymerizing with p-PDA and 6FDA in order to study the effect on  $T_g$  and solubility.

The ester-acid route was utilized to synthesize an ~3 Kg/mole PEPA-encapped oligomer using 6FDA and a ratio of DAPI:p-PDA of 60:40. During high temperature solution imidization at 180°C, the polyimide remained in solution. However, after cooling to room temperature, a small amount of precipitate was observed (<10%). It was surmised that the insoluble material probably arose from alignment and packing of the rigid, low molecular weight fractions. However, the presence of precipitate was undesirable for solution film casting techniques used in dielectric film applications.

As expected, the  $T_g$  of the cured material was significantly higher than that of the ~3K 6FDA/DAPI homopolyimide (380°C compared to 356°C, as obtained from DMA). The thermal stability, as demonstrated by the 5% weight loss temperature of 522°C, was identical to that of the homopolymer.

The marginal solubility of 6FDA/DAPI:p-PDA 60:40 had been a somewhat surprising outcome. It was believed that increasing the target  $\langle M_n \rangle$  might have resulted in a completely soluble oligomer. However, no further copolymers of this type were prepared because the  $T_g$  of such a system would undoubtedly be near that of the ~3K 6FDA/DAPI homopolyimide.

## **4.2 Properties of Soluble, Low $\langle M_n \rangle$ Fluorinated Thermosetting Polyimide Oligomers**

### **4.2.1 Introduction**

In addition to the  $T_g$ s and thermal stability discussed above, several other properties were of interest with respect to dielectric applications, including water absorption, CTE and dielectric constant. Several of the imides were selected for these types of studies, using the criteria that the oligomers exhibit complete solubility in organic solvents.

Our objective was to continue working with fully imidized soluble oligomers rather than poly(amic acid) precursors typically utilized in the electronics industry. The advantages of using the amorphous thermosetting imides, such as hydrolytic stability and isotropic physical properties, were anticipated to provide an attractive alternative to the traditional rigid-rod polyimides. These thermosetting amorphous systems were also anticipated to provide essential solvent-resistance for dielectric film applications. As pointed out earlier, thermoplastic amorphous fluorinated polyimides had been shown to provide remarkably low dielectric constants. However, because of poor solvent resistance and poor adhesion, these materials would be inadequate for the electronics devices and processing techniques currently used in the industry.

#### **4.2.1.1 Solution Viscosity of Low $\langle M_n \rangle$ Fluorinated Thermosetting Polyimide Oligomers**

Viscosities in NMP solutions were determined using four of the oligomers from the soluble polyimide series: ~2- and ~3K 6FDA/m-PDA, ~3K BPDA:6FDA 90:10/m-PDA and ~3K 6FDA/DABTF. The study involved formulation of a series of solutions and measuring the viscosity as a function of systematic increase in oligomer concentration (w/v). The results are shown in Figure 4.1.10. It was observed that as the solution concentrations were increased from 15- to 50%, the solution viscosities remained low (under 0.4 P•s [SI units] or 400 cps).

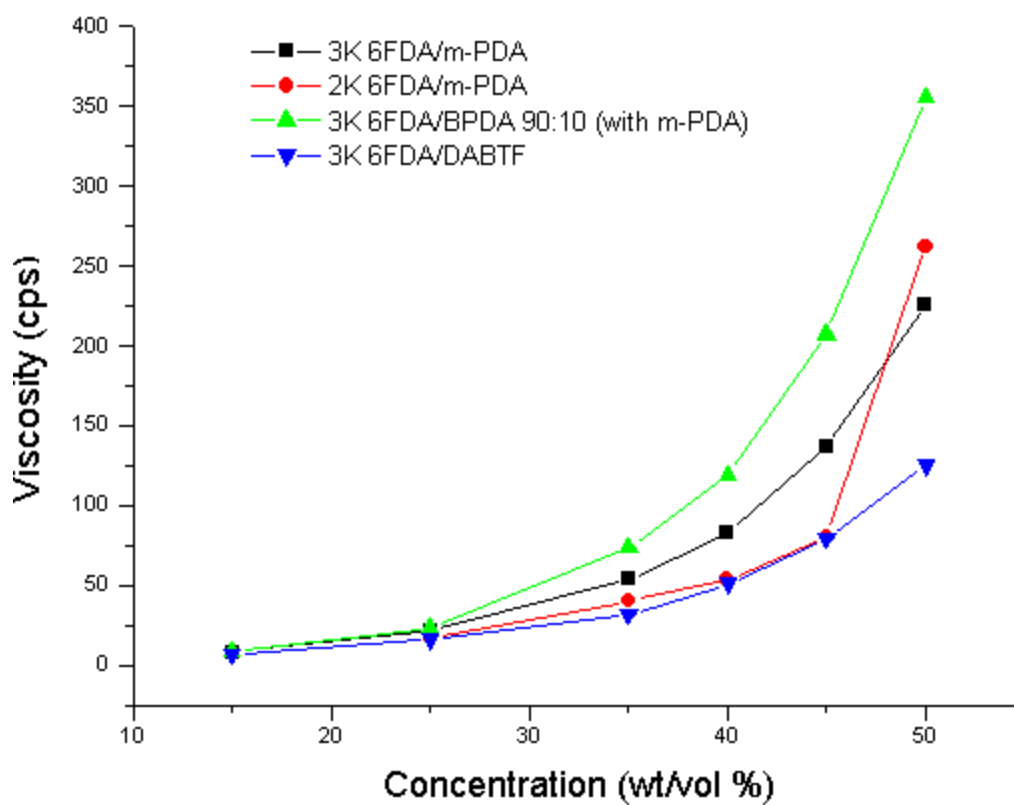


Figure 4.1.10 Viscosity as a function of concentration for solutions of polyimide oligomers in NMP.

The solution concentration of 35% (w/v) appeared to be a critical value at which noticeable increase in viscosity was observed. This was particularly true for the 6FDA:BPDA copolyimide. The stiffening effect of incorporating BPDA may have resulted in a lower density and, hence, a relatively higher viscosity.

For comparison, the ~7K 6FDA/DAPI polyimide oligomer was subjected to the same type of viscosity study. Since the solution concentration of 35% (w/v) had appeared to be a critical value, the concentrations were systematically increased from this starting point. The plotted results are shown in Figure 4.1.11. The viscosity was below 600 cps at a solution concentration of 50%, which was still remarkably low, considering the  $\langle M_n \rangle$  value was more than twice that of the other systems.

The ability to formulate solutions with low viscosity at relatively high concentrations was anticipated to provide several advantages for dielectric films. Some of these projected benefits were: lower film shrinkage due to fewer volatiles coming off during drying, better planarization, and improved flow to provide better wetting and adhesion.

An interesting effect was noted for the m-PDA containing polyimide solutions. A gel began to form after allowing them to stand overnight at room temperature in sealed vials. In this case, the term "gel" was used in the sense that steady state flow was absent and that the solution was comprised of a relatively dilute system of polymer/solvent. The gel behavior was thermally reversible because re-liquification occurred upon heating (gel-sol transition). Thus, the gel appeared to be comprised of a physical network.

Thermo-reversible gel/sol behavior of polyimide solutions has been reported in the literature<sup>12, 114, 190-191</sup>. It was noted that the tendency for gel formation increased with higher polyimide concentrations in the solution. Indeed this effect was noted during one of the

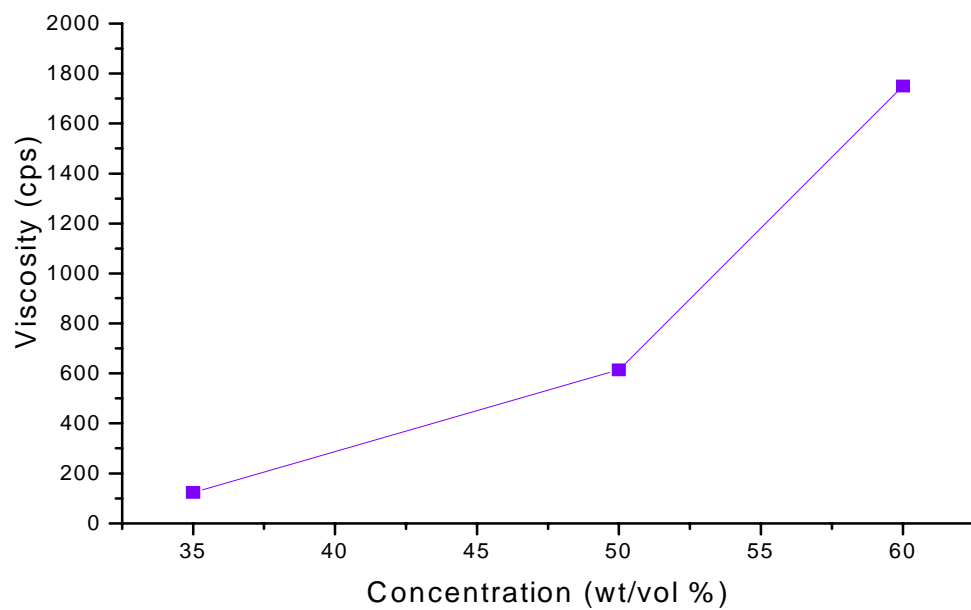


Figure 4.1.11 Viscosity as a function of concentration for solutions of ~7K 6FDA/DAPI polyimide oligomer in NMP.

viscosity experiments. Figure 4.1.10 shows the viscosity increase as a function of polyimide concentration for the ~2K 6FDA/m-PDA system. An abrupt jump to higher viscosity was seen as the concentration was sequentially increased from 45 to 50 % (w/v). This behavior was not found for the other oligomers in the series. The ~2K 6FDA/m-PDA solutions used for viscosity measurements had been prepared the previous day, while the others had been formulated a few hours prior to testing. In retrospect, it appeared that the sol-gel transformation was just beginning for the 50% solution. It was noted in the experimental record that this solution had begun to appear less transparent than other corresponding solutions in the series, which perhaps signaled the onset of gelation.

The mechanism for formation of polyimide gels has not been elucidated. It has been proposed that the gel-sol transition occurs through a liquid-liquid phase separation<sup>12, 114</sup>. The suggested composition was that of a relatively solute-rich liquid phase surrounded by another liquid phase containing relatively more solvent. It was reported that gelation of polyimide solutions was unrelated to the development of liquid crystalline order. This observation was based on experiments using polarized light microscopy and SAXS to detect the onset of crystallinity in polyimide systems that had exhibited sol-gel and disorder-order transitions in m-cresol solutions<sup>190-191</sup>.

In the experimental series, it appeared that the pendant trifluoromethyl substituent of DABTF and the asymmetric structure of DAPI each suppressed the gel formation, since neither 6FDA/DABTF nor 6FDA/DAPI polyimide solutions gelled during prolonged storage. This suggested that gel formation must consist of some type of ordering because it had been observed with the more symmetrical m-PDA containing polyimides. Further work needs to be done to elucidate the mechanism and type of molecular associations in these physical-type gels.

#### 4.2.1.2 Water Absorption of Low $\langle M_n \rangle$ Fluorinated Thermosetting Polyimide Oligomers

Water absorption of melt-pressed cured polyimide films was monitored during exposure to 85% relative humidity (RH) at 85°F for a period of 1 week. These conditions were expected to resemble actual operating environments for microelectronics in computers, etc. Gravimetric methods were utilized to determine the amount of absorbed water, which was recorded as the average percentage weight gain for two samples of each polyimide.

The results of the percentage weight increase as a function of the square root of exposure time ( $t^{1/2}$ ) appear in Figures 4.1.12 and 4.1.13. All of the crosslinked polyimides in the series had been prepared from oligomers of  $\langle M_n \rangle \sim 3\text{Kg/mole}$ . The data were plotted separately for the 6FDA homopolyimides and the 6FDA:BPDA 90:10 copolyimides for convenience in distinguishing the two polymer types. As shown, the samples containing the fluorinated diamine DABTF showed the lowest increase in water absorption. This was attributed to the relatively higher fluorine content imparted by both monomers.

As shown in the plots, the equilibrium water absorption had not been attained for the films of 6FDA/m-PDA, 6FDA/ODA or 6FDA:BPDA 90:10/m-PDA during the period of one week. It was anticipated that an additional 1-2 days would have been required, but device malfunction prevented continuation of the experiment.

The total amounts of water absorbed during the one-week exposure time are given in Table 4.1.10. The aliphatic groups in 6FDA/DAPI contributed to low water absorption for this polyimide, which was nearly as low as that of the highly fluorinated imides. The minimal water uptake of these crosslinked materials would be advantageous for dielectric performance, since absorbed water causes significant increase in dielectric constant.

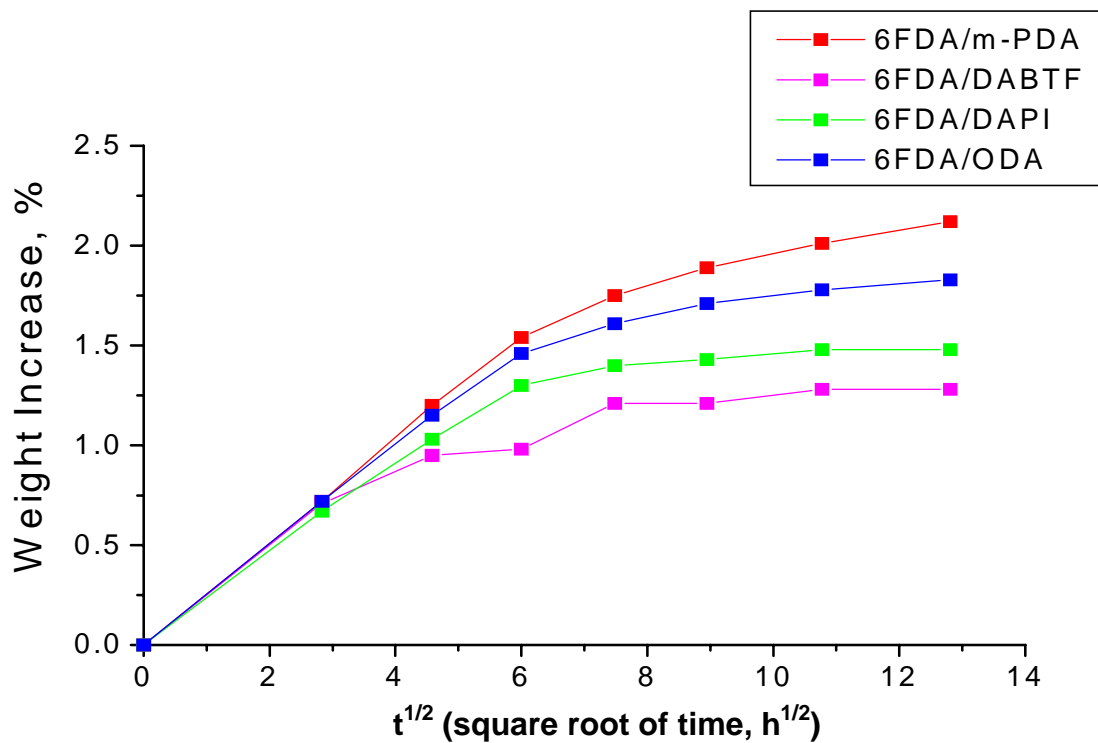


Figure 4.1.12 Weight increase (%) from absorbed water vapor as a function of humidity exposure time ( $t^{1/2}$ ) for crosslinked polyimide films. (Films exposed to 85%RH at 85°F).

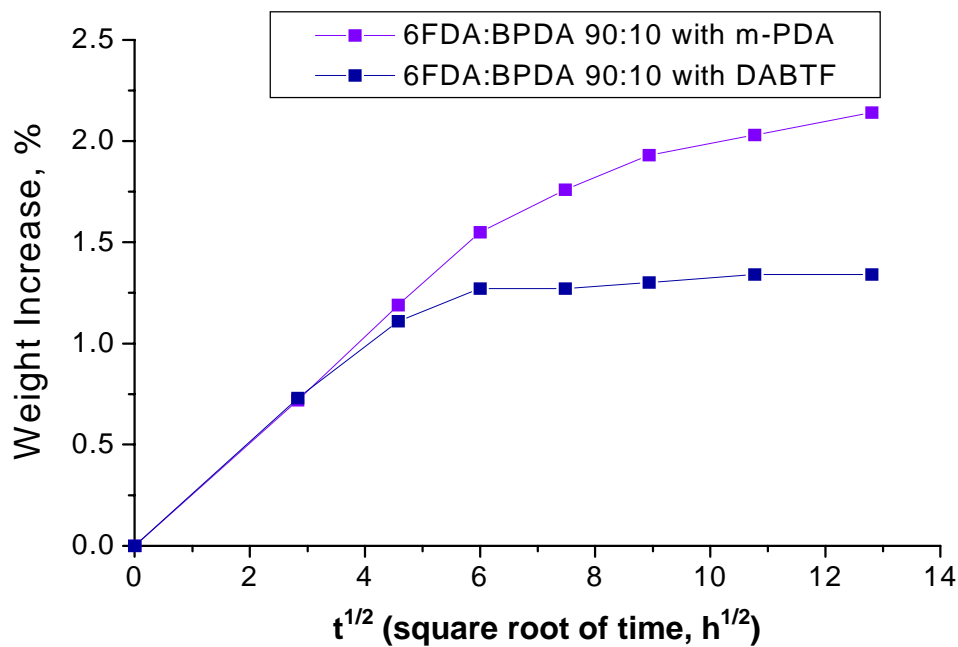


Figure 4.1.13 Weight increase (%) from absorbed water as a function of humidity exposure time ( $t^{1/2}$ ) for crosslinked polyimide films with BPDA content. (Films exposed to 85%RH at 85°F).

Table 4.1.10 Total Water Absorbed (%) of Cured Polyimide Films.

Composition of Melt-pressed, Cured Polyimide Films (Crosslinked ~3K oligomeric precursor)	Total % Water Uptake (weight increase)* After 1 Week Exposure to 85% RH @ 85°F
6FDA/m-PDA	2.1
6FDA/ODA	1.8
6FDA/DAPI	1.5
6FDA/DABTF	1.3
6FDA:BPDA 90:10/m-PDA	2.1
6FDA:BPDA 90:10/DABTF	1.3

\* standard deviation for average % weight increase of sample  $< \pm 0.1\%$

### 4.2.1.3 Refractive Index of Fluorinated Polyimides

Direct measurement of dielectric constant involves preparation of a capacitor-type sample, which is comprised of polyimide film between two metal conductors<sup>105, 192</sup>. This is often difficult and time-consuming, due to problems with obtaining uniform, defect-free films having the correct thickness<sup>105</sup>. Conversely, measurement of the refractive index of polyimide films is a relatively convenient method for estimating the dielectric properties<sup>114</sup>.

The refractive index (RI) measurements required only a very small piece of film sample. However, it was essential that the film was smooth and defect-free. As discussed previously, film preparation using solutions of the ~3- and ~7K imides had resulted in cracked, non-uniform samples. Additionally, melt-pressed films had rough surfaces due to the use of scrim cloth as a mold release. Consequently, films for RI had to be prepared from solution-casting high molecular weight thermoplastic analogues of our polyimide series. It was anticipated that the identical backbone compositions of these imides would allow valid correlation of their RI and dielectric properties.

The RI results ( $n$ ) for the 6FDA/m-PDA and 6FDA/DAPI polyimides are shown in Table 4.1.11. The Maxwell relationship ( $\epsilon \cong n^2$ ) was utilized to estimate the dielectric constants ( $\epsilon$ ) and these values are reported in the table. Included for comparison are RI values of Kapton film as reported in the literature<sup>120</sup>. The RI values obtained for the polyimides prepared in this research were significantly lower than those of Kapton and, hence, lower estimated  $\epsilon$  values were obtained (2.52 and 2.47). Additionally, Kapton film is birefringent due to ordering/alignment of the molecules in the film plane. Thus, two corresponding  $n$  values have been reported:  $n_{\perp}$  and  $n_{\parallel}$ , the out-of-plane and in-plane RIs, respectively. Kapton's estimated dielectric constant was based on this anisotropy, thus yielding two values  $\epsilon_{\perp}$  and  $\epsilon_{\parallel}$  for this film.

Table 4.1.11 Refractive Index and Estimated Dielectric Constant of Polyimides.

Polyimide Composition	Refractive Index, $n$ (@ 633 nm)**		Estimated Dielectric Constant	
6FDA/m-PDA	1.589		2.52	
6FDA/DAPI	1.571		2.47	
Kapton Control* (PMDA/ODA)	Out-of-plane 1.64	In-plane 1.72	Out-of-plane 2.69	In-plane 2.96

\* reported RI values from Ref. 120.

\*\* standard deviation for RI measurements =  $\pm 0.001$ .

#### 4.2.1.4 CTE of Low $\langle M_n \rangle$ Fluorinated Thermosetting Polyimide Oligomers

The CTE is another important property with regard to dielectric films. Unfortunately, most organic polymers have much higher CTEs than those of the inorganic substrates and conductors used in electronics<sup>192</sup>. This CTE mismatch results in residual stress buildup in the dielectric material following thermal processing<sup>113</sup>.

It was of interest to determine the CTEs of thermosetting fluorinated polyimide oligomers for comparison with that of Kapton. Since both systems were very rigid, it was unknown whether the highly crosslinked thermosetting imides would show relatively lower CTE values. The crosslinked film samples were prepared by melt-pressing and curing ~3K oligomeric polyimide precursors.

The CTE data collected for the crosslinked polyimide series are shown in Table 4.1.12. The values ranged between 44 and 51 ppm. These values were much higher than those of inorganic substrates, such as silicon with a CTE = 3 ppm<sup>192</sup>. The thermoplastic Kapton control has a CTE value between 30 and 40 ppm, as conventionally measured in the plane of the film<sup>7</sup>. However, due to Kapton's two-phase morphology, the CTE is anisotropic. Hence, a significantly higher CTE of 150 ppm has been reported<sup>7</sup> from measuring in the out-of-plane direction ( $\alpha_{\perp}$ )<sup>\*</sup>.

Incorporation of 10 mole% of the rigid BPDA comonomer in the 6FDA:BPDA/m-PDA system did not lower the CTE relative to that of 6FDA homopolyimides. This confirmed that the small amount of BPDA had not increased the rigidity significantly, which had also been suggested by the DMA analysis of  $T_g$ .

---

\* This high  $\alpha_{\perp}$  value is problematical because of potentially high internal stress resulting from CTE mismatch in the vertical direction, which may disrupt vertical electrical connections (metal vias) in the TFML packaging<sup>7</sup>.

Table 4.1.12 Thermal Expansion Coefficients of Crosslinked Polyimide Films.

Polyimide Composition / Target Mol. Weight (Kg/mol)	Linear CTE (ppm/°C)** In-Plane	Linear CTE (ppm/°C) Out-of-Plane
6FDA/m-PDA / 3.0	44	---
6FDA/DAPI / 3.0	45	---
6FDA:BPDA 90:10/m-PDA / 3.0	50	---
6FDA/DABTF / 3.0	51	---
Kapton (PMDA/ODA) / High Mol. Wt. Control	30-40*	150*

\* = from Ref. 7.

\*\* standard deviation =  $\pm 5$  ppm/°C

### **4.3 Film Forming Series of Thermosetting Polyimide Oligomers**

Film forming properties are of primary importance for interlayer dielectrics used in electronic circuitry. The method of coating substrates using solution casting is the major process used to obtain thin film multilayer structures, consisting of alternating strata of polymer and metal. Formation of a cohesive film with minimal volatile evolution and maximum adhesion/planarization is the desired outcome of such a process.

In this thesis, the initial studies of film formation have been discussed involving relatively rigid and low molecular weight thermosetting oligomers: ~3K 6FDA/m-PDA and, ~3- and ~7K 6FDA/DAPI. In the interest of the proposed application for these materials, the polyimide structure had to be tailored to achieve successful film production. Further, the technique of spin casting had to be incorporated into the research because of its applicability to the manufacture of electronics packaging.

#### **4.3.1 Thermosetting Polyimide Oligomers Based on 6FDA/ODA/PEPA**

It was believed that the failure of the low molecular weight oligomers to form cohesive films resulted from a combination of rigidity and excessively short chain length. Such a system would have minimal molecular entanglements. Thus, the chains would be less likely to maintain a coherent structure as  $T_g$  was approached and the chains began to "unravel".

The strategy for solving the problem involved the use of a more flexible monomer unit in the backbone and, simultaneously, providing longer polyimide chains. The monomer selected was 4,4'-oxydianiline (ODA), which was anticipated to impart flexibility to the polyimide through its ether linking group. For lengthening the chains, a series of target  $\langle M_n \rangle$  values was selected: 7-, 10- and 12 Kg/mol. Thus, the effect of molecular weight could be evaluated with respect to the film forming properties of 6FDA/ODA/PEPA oligomers.

An additional strategy was applied to this series of oligomers. Since poly(amic acid)s associate through intermolecular hydrogen bonding, there was a chance that such an interaction might cause the "short chains" to behave more like relatively longer molecule. Hence, a corresponding 6FDA/ODA series of poly(amic acid)s was prepared utilizing the same series of target  $\langle M_n \rangle$  values as selected for the fully imidized oligomers.

#### **4.3.1.1 Synthesis and Characterization of 6FDA/ODA Polyimides and Poly(amic acid)s**

The synthesis of 6FDA/ODA/PEPA fully imidized oligomers was performed using the ester-acid solution imidization method. A series of three of these oligomers was prepared with different target  $\langle M_n \rangle$  values: 7-, 10- and 12 Kg/mol. The isolated polyimide solids could be easily reformulated in various organic solvents, including NMP, chloroform and DMAc.

A series of poly(amic acid)s comprised of 6FDA/ODA/PEPA was prepared using the classic method of synthesis. The monomers and solvents were carefully dried prior to reaction. The target  $\langle M_n \rangle$  values were identical to those utilized for the series of fully imidized oligomers.

Molecular weight characterization was performed using GPC. The  $\langle M_n \rangle_{\text{EXP}}$  values are listed in Table 4.1.13. The results showed that good molecular weight control had been achieved for both systems. For each of the polyimides and poly(amic acid)s in the series, the  $\langle M_n \rangle_{\text{EXP}}$  corresponded well with target values.

#### **4.3.1.2 Solvent Cast Films of 6FDA/ODA/PEPA Polyimide and Poly(amic acid) Oligomers**

##### **4.3.1.2.1 Thick (7-10 mil) Solution Cast Films**

The primary objective was to determine the film forming behavior of the series of 6FDA/ODA/PEPA oligomers when cast from solutions containing NMP. The first phase of this

Table 4.1.13 Characterization of Molecular Weight of 6FDA/ODA/PEPA Polyimides and Poly(amic acid)s.

Composition/Structure	Target $\langle M_n \rangle$ , Kg/mol	$\langle M_n \rangle_{\text{EXP}}$ by GPC, Kg/mol
6FDA/ODA Polyimide	7.0	9.2
6FDA/ODA Polyimide	10.0	11.7
6FDA/ODA Polyimide	12.0	13.0
6FDA/ODA Poly(amic acid)	7.0	9.9
6FDA/ODA Poly(amic acid)	10.0	11.7
6FDA/ODA Poly(amic acid)	12.0	14.7

project involved utilizing a blade or mold for controlling thickness to 7-10 mil. Since films in this thickness range were needed for DMA analysis, the experimental objective was twofold. Specifically, these studies would determine whether the oligomers could form cohesive films of relatively thicker dimension, and, if successful, would yield the film samples needed for DMA.

#### **4.3.1.2.1.1 Thick (7-10 mil) Solution Cast Films from 6FDA/ODA/PEPA Polyimides**

Glass plates were utilized as the substrates. The polyimide solutions were either bladed directly onto the plate, or a stainless steel mold was placed on the plate and the solution was evenly poured into it. While processing the "thick" films, it became apparent that a controlled slow heating program was required. The so-called "skin" formed at the topside by rapid evaporation of solvent was relatively more solid than the interior of the film. If heating was too rapid after formation of this "skin", the rapidly evaporating solvent coming from beneath it would cause massive bubbling at the film surface.

During the early course of this work, it was suggested that employment of a co-solvent with NMP might alter the surface tension to provide more cohesive films. Based on solubility studies and boiling point compatibility, the co-solvent chosen was o-dimethoxybenzene (DMB). This solvent had a boiling point just  $\sim 4^{\circ}\text{C}$  above that of NMP and also formed clear solutions with 6FDA/ODA/PEPA. It unexpectedly provided a further benefit with these polyimides. When solutions were prepared using NMP alone, the formation of a physical gel would ensue just a few hours following preparation. Conversely, when NMP/DMB solvent mixtures were used, the onset of gelation would occur much later, usually within a day or two, depending on the concentration of DMB.

The final process developed for programmed heating of these films is described in the experimental section of this dissertation. The qualitative results obtained for film formation of

the series of fully imidized oligomers are shown in Table 4.1.14. Brief descriptions of the heating processes have been placed under the table to provide a quick reference. The table indicates the solvent ratios (NMP:DMB) employed in each trial, since these had been varied in order to determine the effect on film formation.

The film prepared from the ~12K oligomer in NMP exhibited a few cracks during drying, but produced a flexible film. Incorporation of solvent mixtures NMP:DMB of 90:10 and 80:20 resulted in intact films, but the films were somewhat less flexible. It was believed that strains developed in the films during heating arising from confinement within the stainless steel mold on the glass substrate (CTE mismatch). The films that did not crack exhibited non-uniform distortions (warping) and, thus, the strains appeared to be "frozen in". In the case where NMP alone was utilized, the cracks may have resulted from stress cracking which relieved these internal strains.

Film preparation using the ~10K 6FDA/ODA polyimide oligomer with the binary solvent mixture produced similar results to those of the ~12K system. The films remained intact during the drying process with some warpage distortion. Apparently during cure (as observed for both the ~10- and ~12K films), the distortions diminished because after taking the films from the furnace they appeared flat. Thus, stress relaxation probably occurred as a result of the temperature excursion to 380°C, which was above  $T_g$ .

The film studies of the relatively lower  $\langle M_n \rangle$  ~7K 6FDA/ODA polyimide yielded very different results than the others in the series. The initial film trial, which was conducted using NMP, produced a film which had cracked in a few places as was observed for the ~12 K system. Following cure, the material was not as brittle as expected considering the relatively low  $\langle M_n \rangle$  of the precursor. The stress-cracking phenomenon occurred with this film, but not as massively

Table 4.1.14 Qualitative Results of Thick (7-9 mil) Films from Solution Casting Fully Imidized 6FDA/ODA/PEPA Thermosetting Oligomers.

Polyimide Size/Structure	Solvent/Co-Solv. Ratio NMP:DMB	(w/v) Solution Concentration	Film Results	
			During Drying	After Curing
~12K 6FDA/ODA	100:0	20%	Cracks (few)	Flexible film
	90:10	20%	Intact	Bendable, high modulus
	80:20	20%	Intact	Bendable, high modulus
~10K 6FDA/ODA	90:10	20%	Intact	Bendable, high modulus
	80:20	20%	Intact	Bendable, high modulus
~7K 6FDA/ODA	100:0	30%	Cracks (few)	Bendable, high modulus
	90:10	20%	Cracks (many)	Brittle pieces
	80:20	30%	Cracks (many)	Brittle pieces
	60:40	25%	Cracks (many)	Brittle pieces

Solutions cast on glass plate held at 85°C; following solidification, dried film under vacuum at 85°C for ~12 h; then oven temperature was gradually ramped from 85°C to 200°C over ~12 h. Continued heating for ~12h at 200°C, then finished drying at ~10°C above T<sub>g</sub>. Cured to crosslink by heating at 380°C for 1 h under N<sub>2</sub>.

as during early attempts to prepare films from more rigid ~3- and ~7K imide oligomers (6FDA/m-PDA and 6FDA/DAPI).

However, subsequent trials utilizing the ~7K 6FDA/ODA polyimide and NMP:DMB co-solvents produced films resembling those obtained during the early work with relatively rigid systems. During drying, film cohesion was lost through massive crack formation. The apparent difference from the first trial was the presence of the DMB co-solvent. However, this was not believed to be the key effect in the changes observed.

The "anomalous" result of the first ~7K film, which did not contain DMB, might have occurred because the solution had not been confined within a steel ring during drying. During subsequent trials, the drying films were contained within the metal ring, which might have led to development of excessive strains in the films. Thus, the massive cracking might have been to relieve these strains. The strain development appeared more excessive in the ~7K system than it had in either the ~12- or ~10K polyimide films containing DMB. This was surmised because though the latter had shown warpage, they had remained intact.

From the results discussed above, the role played by the DMB co-solvent was unclear. Perhaps it improved plasticization during the drying process. In the cases of the relatively higher  $\langle M_n \rangle$  precursors, the films containing DMB had remained intact during drying. This was advantageous, but further work needed to be done to confirm this behavior.

#### **4.3.1.2.1.2 Thick (7-10 mil) Solution Cast Films from 6FDA/ODA/PEPA Poly(amic acid)s**

To study solvent effects on film forming properties, a series of poly(amic acid)s was prepared first in NMP and then was re-prepared using NMP:DMB 90:10 co-solvents. The poly(amic acid) (PAA) solutions were cast inside a stainless steel ring on a glass plate and were subjected to the same programmed heating as used for the corresponding 6FDA/ODA fully

imidized series. It was believed that the intermolecular hydrogen bonding of PAAs might induce the oligomers to behave as "longer chains" during film formation, thereby producing cohesive films without cracks.

The qualitative results of the PAA film trials are shown in Table 4.1.15. The results for the PAAs were very similar to those obtained with the corresponding imides. The film prepared using ~12K PAA in NMP had a few cracks, but was fairly flexible. When DMB co-solvent was present, the film from this PAA precursor remained intact, as had been observed for the ~12K imide.

The film prepared from the ~10K PAA in NMP underwent massive cracking during drying. However, in the subsequent trial when DMB was incorporated, the film from this precursor remained intact. Since PAAs hydrogen bond to NMP<sup>35</sup>, the complexation of solvent-polymer had probably limited the extent of PAA intermolecular association. With insufficient PAA intermolecular interactions, the "short chains" would fail to behave cohesively to emulate a relatively longer molecule. Thus, the film results for PAAs would not differ significantly from those of the fully imidized series.

This same conjecture could be made with respect to results obtained from the ~7K PAA film trials. Both trials resulted in films that cracked into numerous brittle pieces. It would be instructive to employ DMB as the only solvent in this case, thus eliminating the strong PAA-solvent complexation. This would allow extensive PAA intermolecular hydrogen bonding, which might facilitate formation of cohesive films. However, before attempting the synthesis of PAA in DMB, the solubility of the monomers would need to be tested in the pure solvent. (It is anticipated that the PAA product would be soluble in DMB, based on successful preparation of a 40% (w/v) solution consisting of DMB and ~10K 6FDA/ODA fully imidized oligomer.) An

Table 4.1.15 Qualitative Results of Thick (7-9 mil) Films from Solution Casting

Amic-acid 6FDA/ODA/PEPA Thermosetting Oligomers.

PAA Oligomer size/structure	Solvent/Co-Solv. Ratio NMP:DMB	(w/v) Solution Concentration	Film Results	
			During Drying and Imidization	After Curing
12K 6FDA/ODA	100:0	23%	Cracks (few)	Bendable, high modulus
12K 6FDA/ODA	90:10	23%	Intact	Bendable, high modulus
10K 6FDA/ODA	100:0	23%	Cracks (many)	Brittle pieces
10K 6FDA/ODA	90:10	23%	Intact	Bendable, high modulus
7K 6FDA/ODA	100:0	23%	Cracks (many)	Brittle pieces
7K 6FDA/ODA	90:10	23%	Cracks (many)	Brittle pieces

additional consideration is that the PAA equilibration reaction rate might be undesirably slow in DMB, since it is an ether solvent of relatively lower basicity than NMP.

### **4.3.2 Thermosetting Polyimide Oligomers Based on BPDA/DAPI/PEPA**

Utilizing ODA had apparently improved flexibility of the thermosetting polyimide oligomers. However, to comply with the interests of microelectronics applications, the high  $T_g$  rigid systems needed to be explored further, especially with regard to film formation.

Work by others had shown that high molecular weight thermoplastic imides comprised of BPDA/DAPI were completely soluble in common organic solvents<sup>76-77</sup>. Additionally, the  $T_g$  was reported as 368°C. The possibility of attaining high  $T_g$ s from BPDA/DAPI thermosetting PEPA-encapped oligomers was very attractive for microelectronics packaging applications.

#### **4.3.2.1 Synthesis and Characterization of BPDA/DAPI/PEPA Polyimides**

The BPDA/DAPI/PEPA fully imidized oligomers were prepared using the ester-acid solution imidization route. The target  $\langle M_n \rangle$  values utilized for the series were 6-, 8-, 10- and 12 Kg/mol, respectively. All of the oligomers prepared were completely soluble in NMP, chloroform, methylene chloride and DMAc.

Characterization of  $\langle M_n \rangle_{EXP}$  of the oligomers was performed using GPC. The results are shown in Table 4.1.16. Close agreement between  $\langle M_n \rangle_{EXP}$  and target values indicated that good molecular weight control had been achieved.

#### **4.3.2.2 Solvent Cast Films of BPDA/DAPI/PEPA Polyimide Oligomers**

##### **4.3.2.2.1 Thick (7-10 mil) Solution Cast Films from BPDA/DAPI/PEPA Polyimides**

Preparation methods used for solution casting thick (7-10 mil) films of BPDA/DAPI/PEPA oligomers were identical to those described for 6FDA/ODA polyimides. The initial film trials began with the oligomer of highest  $\langle M_n \rangle$ , based on our previous

Table 4.1.16 Characterization of Molecular Weight of BPDA/DAPI/PEPA Polyimides.

Polyimide Composition/Structure	Target $\langle M_n \rangle$ , Kg/mol	$\langle M_n \rangle_{\text{EXP}}$ by GPC, Kg/mol
BPDA/DAPI	6.0	7.2
BPDA/DAPI	8.0	8.0
BPDA/DAPI	10.0	10.9
BPDA/DAPI	12.0	11.2

experience that the higher molecular weights resulted in better films. For each film trial, the solution was applied to the glass substrate within the confines of a stainless steel ring. This method was used to control the thickness and to prevent de-wetting due to the lowered viscosity of the solution as it was initially heated. A binary solvent composition was used, consisting of NMP and DMB. This choice was based on our previous experience that DMB-containing films normally remained intact.

The qualitative results for the film trials are shown in Table 4.1.17. As shown, two different (v/v) ratios of NMP:DMB were employed for each imide: 90:10 and 80:20. The results for the ~12K BPDA/DAPI film were encouraging because both trials had yielded intact films. However, the rigidity of this system (compared to 6FDA/ODA) resulted in crosslinked films with lower flexibility. When attempts were made to fold film edges over to test for creasability, the materials cracked, showing relatively more brittleness than the 6FDA/ODA systems.

The results of film formation for the ~10K BPDA/DAPI oligomer were also indicative of a more brittle system. Each film cracked during the drying process in a few places, presumably to relieve strain. However, after crosslinking the brittle behavior increased as shown by the bending test for determining the degree of flexibility. The films each exhibited glasslike shattering when this test was applied.

Thick film experiments for the ~8- and ~6K BPDA/DAPI oligomers were not conducted. This decision was based on the brittle film behavior of the higher molecular weight counterparts.

### **4.3.3 Properties of 6FDA/ODA and BPDA/DAPI Thermosetting Polyimide Oligomers**

#### **4.3.3.1 Introduction**

Several key properties of the 6FDA/ODA and BPDA/DAPI thermoset films were of.

Table 4.1.17 Qualitative Results of Thick (7-9 mil) Films from Solution Casting Fully Imidized BPDA/DAPI/PEPA Thermosetting Oligomers.

Polyimide Oligomer/Structure	Solvent/Co-solv. NMP:DMB	(w/v) Solution Concentration	Film Results	
			During Drying	After Curing
~12K BPDA/DAPI	90:10	20%	Intact	Cracks when bent
	80:20	20%	Intact	Cracks when bent
~10K BPDA/DAPI	90:10	20%	Cracks (few)	Shatters when bent
	80:20	20%	Cracks (few)	Shatters when bent

interest with respect to dielectric applications, such as  $T_g$  and thermal stability. Especially important, however, were the considerations of solvent resistance and dielectric properties. These properties were measured for the imides in the series that had produced relatively better films.

#### **4.3.3.1.1 Glass Transition Temperatures of 6FDA/ODA and BPDA/DAPI Thermoset Films**

Uniform, defect-free film samples were subjected to DMA experiments using the extension mode of film deformation. Heating the film at a rate of  $5^\circ\text{C}/\text{min}$  during cyclic loading provided storage and loss moduli from which  $\tan \delta$  was obtained. The  $T_g$  of the film was determined as the maximum peak height in the  $\tan \delta$  curve.

A typical DMA thermogram of a crosslinked film appears in Figure 4.1.14. The  $T_g$  values obtained from the respective thermograms of the film series appear in Table 4.1.18. Included in the table are the 5% weight loss temperatures from TGA measurements and the  $T_g$ s as determined using DSC.

The  $T_g$ s for the 6FDA/ODA films did not vary much within the series, with values just above  $300^\circ\text{C}$ . As expected, the  $T_g$ s of the BPDA/DAPI series were relatively higher ( $355^\circ\text{C}$ ) due to increased backbone stiffness. Thermal stabilities of both types of imide structures were excellent, showing 5% weight loss temperatures above  $500^\circ\text{C}$ .

#### **4.3.3.1.2 Isothermal Weight Loss of 6FDA/ODA and BPDA/DAPI Thermoset Films**

The electronics industry utilizes isothermal TGA methods to evaluate the thermal stability of dielectric films. This is done by measuring the total weight loss while holding the films at  $400^\circ\text{C}$  for 2 hours in nitrogen. This experiment is intended to simulate thermal processing conditions used for thin film multilayer electronics packaging. It is obvious that negligible weight loss by degradation is desirable in this case. Therefore, the results of this test

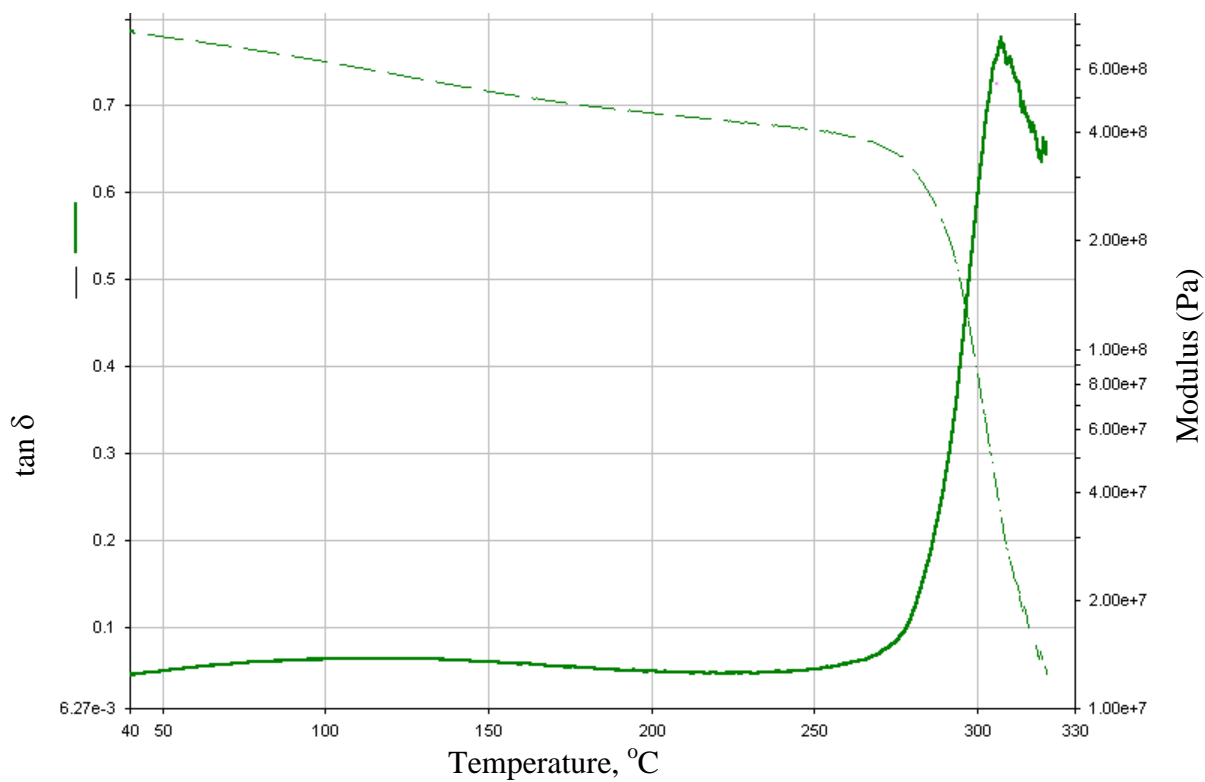


Figure 4.1.14 DMA thermogram of crosslinked polyimide film obtained from ~7K 6FDA/ODA/PEPA oligomeric precursor.

Table 4.1.18 Results of Thermal Analysis of Crosslinked Polyimide Films.

Polyimide/Mol. Wt. (Kg/mol)	T <sub>g</sub> of Film by DSC (°C)	T <sub>g</sub> of Film by DMA (°C)	TGA 5% Weight Loss Temp. (°C)
6FDA/ODA			
7	303	307	523
10	310	302	522
12	314	313	527
1:1 Stoichiometry thermoplastic control	286	-----	510
BPDA/DAPI			
10	355	-----	537
12	355	342	541
1:1 Stoichiometry thermoplastic control	368	-----	558

can determine whether a given polymer is suitable for the application. The industry standard for comparing the thermal stability of new polymers is Kapton polyimide film. This is because it has been a viable, thermally stable component of microelectronics packaging for many years.

The TGA experiments involved using Kapton film (PMDA/ODA) as a control. The total weight loss was ~0.5% for the 2 hour period. The TGA thermogram in Figure 4.1.15 depicts the results, as well as those obtained for a crosslinked film of ~7K 6FDA/ODA/PEPA polyimide. As shown, the overall weight loss of the thermosetting system was nearly as low (~0.8%) as that of Kapton. Additionally, most of the weight loss occurred in the first few minutes of heating.

The other films in the 6FDA/ODA/PEPA series exhibited comparable thermal stabilities under these conditions. Additionally, the BPDA/DAPI/PEPA polyimide films (~10- and ~12K) proved to be equally thermally stable, despite the presence of aliphatic groups. The overall weight losses ranged from 0.5-0.8% for the entire series of films, which would be satisfactory for dielectric applications.

#### **4.3.3.1.3 Solvent Resistance Studies of 6FDA/ODA and BPDA/DAPI Thermoset Films**

Another important property of dielectric films is their solvent resistance. It is vital that pre-existing films be inert to solvent attack as subsequent film solutions are spin cast over them. Since NMP is commonly used in polyimide solutions industrially, it was of interest to test solvent resistance of the thermosetting imides using this solvent. Additionally, processing conditions utilized for dielectrics are more aggressive due to elevated temperatures. Hence, it was believed that the experiments would be more meaningful if the films were exposed to hot NMP.

Traditional Soxhlet methods could not be used since NMP decomposes at its boiling point under ambient pressure. Hence, a new glassware apparatus was designed for immersing

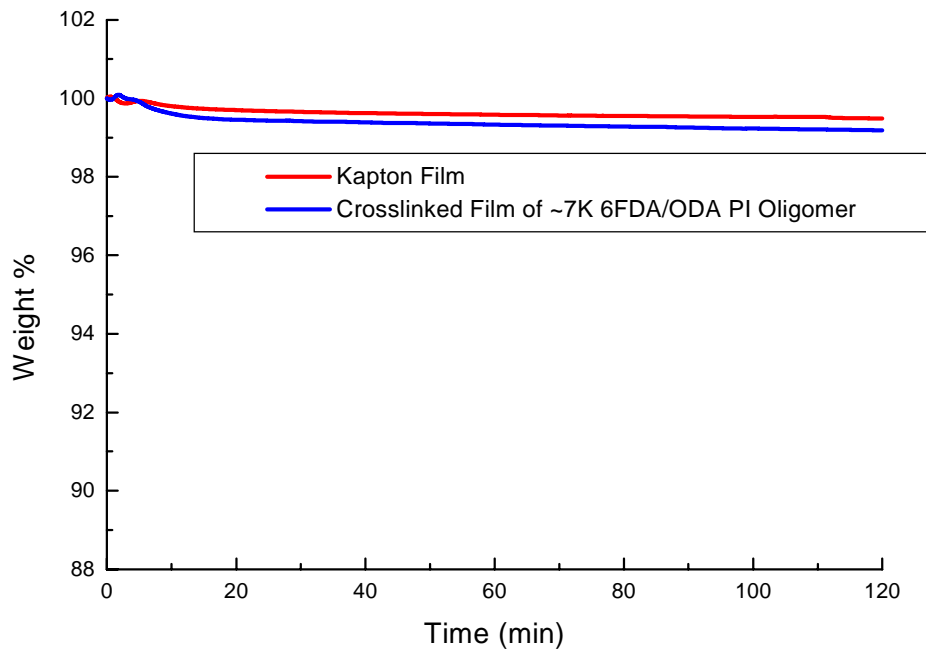


Figure 4.1.15 Isothermal TGA data for a thermoset film of 6FDA/ODA polyimide and for a Kapton film at 400°C under nitrogen.

films in NMP at 60°C, as described in the Experimental Section of this thesis. The films were continually immersed in the hot NMP for three days and were then dried thoroughly to remove residual solvent. The post-extraction weight divided by the initial weight provided the gel fraction of the material. This represented the amount of polyimide oligomer that had been incorporated in the 3-dimensional network by crosslinking. Thus, the gel fraction comprised the quantity of insoluble material in the polyimide film.

The gel fraction (%) values are reported in Table 4.1.19. The very high gel fractions obtained,  $\geq 95\%$ , for the 6FDA/ODA and BPDA/DAPI films indicated excellent solvent resistance under these conditions.

#### **4.3.3.1.4 Refractive Index of 6FDA/ODA and BPDA/DAPI Thermoset Films**

The refractive indices of the 6FDA/ODA and BPDA/DAPI cured thermoset films were utilized to estimate their respective dielectric constants. The results are shown in Table 4.1.20. The fluorine content of the 6FDA/ODA film resulted in a lower estimated value than that calculated for BPDA/DAPI (2.58 versus 2.75, respectively). Compared to the estimated values for Kapton, which reflected the anisotropic nature of the film<sup>7</sup>, the BPDA/DAPI dielectric constant was still significantly lower.

#### **4.3.4 Spin Cast Films of 6FDA/ODA/PEPA and BPDA/DAPI Polyimide Oligomers**

It was desirable to employ the technique of spin casting in this research because of its widespread use in the manufacture of electronics packaging. The 6FDA/ODA and BPDA/DAPI thermosetting oligomers were chosen for the spin casting experiments. Since extensive work in preparing free-standing films had already been completed, a comparison could be made of the results obtained from the two film casting techniques. It was anticipated that the film-forming behavior might differ greatly in the micron thickness range typically produced by spin casting.

Table 4.1.19 Gel Fractions of Cured Polyimide Films Exposed to NMP at 60°C.

Polyimide Oligomer Size/Structure	Gel Fraction
~12K 6FDA/ODA	95%
~10K 6FDA/ODA	95%
~7K 6FDA/ODA	95%
~12K BPDA/DAPI	98%

Table 4.1.20 Refractive Index and Estimated Dielectric Constant of 6FDA/ODA and BPDA/DAPI Thermoset Films.

Polyimide Composition	Refractive Index, $n^{**}$		Estimated Dielectric Constant	
6FDA/ODA	1.607		2.58	
BPDA/DAPI	1.657		2.75	
Kapton Control* (PMDA/ODA)	Out-of-plane 1.64	In-plane 1.72	Out-of-plane 2.69	In-plane 2.96

\*reported RI values from Ref. 120.

\*\*standard deviation for RI measurements =  $\pm 0.001$ .

#### **4.3.4.1 Spin Cast Films of 6FDA/ODA/PEPA Polyimide and Poly(amic acid) Oligomers**

To compare the film forming properties of the fully imidized and the poly(amic acid) 6FDA/ODA/PEPA oligomers, both were subjected to spin casting experiments. The synthesis and characterization of these oligomers was reported in the previous sections and will not be repeated here.

##### **4.3.4.1.1 Spin Cast Films of 6FDA/ODA/PEPA Polyimide Oligomers**

Spin cast films were prepared using the ~7-, ~10- and ~12K 6FDA/ODA/PEPA fully imidized oligomers. The first step involved reformulating the polymers in solutions containing either NMP or NMP with DMB co-solvent. The next step was to filter the solutions through syringe filters (0.45 and 0.22  $\mu\text{m}$  porosities) to remove undissolved particles. This was done in accordance with the standards of the electronics industry for obtaining films with minimal particle content<sup>158, 192</sup>. Solutions containing only NMP and polyimide (15-20% w/v) gelled inside the filters, thereby blocking solution flow. Hence, NMP solutions had to be abandoned in favor of solutions containing binary solvent mixtures consisting of NMP and DMB.

The solutions were applied to clean, dry 1" square glass plates, followed by rapid spinning using the spin-coating apparatus. Several different spin rates were utilized for obtaining complete coating of the substrate. The spin time for each sample was approximately 1-2 minutes. No protection from dust and/or humidity was afforded during spinning. The non-protective conditions would be considered sub-standard for processing of dielectric films in the electronics industry.

Spin-coated films were immediately placed under nitrogen atmosphere supplied by a gas inlet on a covered hot plate. Using a programmable temperature controller, the films were dried on the hot plate as described in Section 3.2.8.3. Subsequently, films were cured at 380°C for 1

hour to form crosslinked materials.

Qualitative film results for the 6FDA/ODA/PEPA imide oligomers are shown in Table 4.1.21. As indicated, film uniformity was assessed by appearance and not by quantitative thickness measurements. The designation of "rough surface" indicated uneven coverage of the substrate, much like miniscule bumps projecting from the film plane. This phenomenon had appeared in the ~7K oligomer system containing 80:20 NMP:DMB. It was suggestive of incomplete wetting of the substrate. When the NMP:DMB ratio was adjusted to 60:40 during the subsequent trial with this oligomer, the film appeared smooth and clear. This suggested that increasing the DMB content of the precursor solution had improved the film-forming ability.

Spin casting results for the ~10- and ~12K oligomers were also indicative of marginal wetting ability of the solutions containing relatively lower amounts of DMB. The trials incorporating 10- and 20% DMB in the solvent mixture resulted in films with voids or roughness in the film texture. In the trials where the DMB content was increased to 40% (v/v) and the polymer concentration was decreased to 10% (w/v), the films had relatively smooth surfaces. However, some phase separation appeared in the form of a white radial pattern within these films. This was thought to result from absorbed moisture from the surroundings and/or water impurities in the casting solvents.

To test the hypothesis that oligomer precipitation was caused by absorbed humidity, a freshly cast film was allowed to stand under the hood in ambient relative humidity (RH) at room temperature (~75% RH at ~25°C). Within several minutes, the film had turned completely white and opaque.

The fact that NMP is relatively more hygroscopic than DMB may have caused the difference in the results when solutions of higher NMP content were used. Significant amounts

Table 4.1.21 Qualitative Results of Spin Cast Films from Fully Imidized 6FDA/ODA/PEPA Thermosetting Oligomers.

Oligomer Structure / mol. wt (Kg/mol)	Spin Rate Krpm	Solv:Co-Solv NMP:o-DMB	(w/v) Solution Concentration	Uniformity of Cured Film (cured @ 380°C 1h)
PI 7K	1.0, 1.2, 1.5	80:20	25%	rough surface
	1.0	60:40	25%	smooth, clear
10K	1.5, 2.0	90:10	20%	voids
	1.5, 2.0	80:20	18%	rough surface
	3.0, 4.0, 5.0, 6.0	60:40	10%	Smooth top surface, white radial pattern within film
12K	1.5, 2.0	90:10	20%	voids
	1.0, 1.5, 2.0	80:20	15%	voids
	3.0, 4.0, 5.0, 6.0	60:40	10%	Smooth top surface, white radial pattern within film

of absorbed water from the environment would "phase separate" from the relatively hydrophobic polyimide as the solvent evaporated during spinning. The concomitant evaporation of the water from its respective domains would have left holes or "pockets" in the films.

#### **4.3.4.1.2 Spin Cast Films of 6FDA/ODA/PEPA Poly(amic acid) Oligomers**

Spin cast films were prepared using the series of ~7-, ~10- and ~12K poly(amic acid) 6FDA/ODA/PEPA oligomers. The poly(amic acid) (PAA) solutions which had been prepared using the classic synthesis method were each comprised of 23% (w/v) concentration. To ensure uniformity, the solutions were filtered through a pre-dried syringe filter just prior to casting.

The filtered solutions were applied to clean, dry glass substrates, followed by rapid spinning using the spin coating apparatus. It was observed during all trials that spinning had to be continued for ~5 minutes to get complete coating. If shorter spin times were used, the film was overly "wet" and retracted/delaminated from the glass plate. No protection from the environment was afforded to the films during the spin time. After spin casting, the films were imidized and dried under nitrogen on a temperature-programmable hot plate, followed by curing in a furnace at 380°C for 1 hour.

The qualitative results obtained from spin casting the PAA series appear in Table 4.1.22. By visual inspection, each film appeared identically smooth, clear and uniform. DMB in the PAA precursor solution (NMP:DMB 90:10) seemed to have no effect on film formation, as compared to the controls containing only NMP.

The film forming behavior of PAA contrasted significantly with that of the fully imidized complementary series. Moisture-induced phase separation was not evident in the PAA series. This was attributed to the acidic nature of the PAA in the presence of water. Due to the acid-base interactions, the PAA was relatively hydrophilic and no phase separation occurred between

Table 4.1.22 Qualitative Results of Spin Cast Films from Amic-acid 6FDA/ODA/PEPA

Thermosetting Oligomers.

Oligomer Structure / mol. wt (Kg/mol)	Spin Rate Krpm	Solv:Co-Solv NMP:o-DMB	(w/v) Solution Concentration	Uniformity of Cured Film (cured @ 380°C 1h)
PAA				
7K	1.5	90:10	23%	smooth, clear
10K	1.5	90:10	23%	smooth, clear
12K	2.0	90:10	23%	smooth clear
PAA				
10K	4.0	100:0	23%	smooth, clear
12K	4.0	100:0	23%	smooth, clear

PAA and water. Thus, voids and pitted surfaces were eliminated from the films.

The longer spin times (~5 min.) needed for PAA solutions to form continuous coatings may have resulted from the high surface tension of the solutions.

#### **4.3.4.1.3 Spin Cast Films of BPDA/DAPI/PEPA Polyimide Oligomers**

Spin cast films were prepared using the ~6-, ~8-, ~10- and ~12K fully imidized BPDA/DAPI/PEPA oligomers. To compare the influence of the solvent/co-solvent on film forming properties, the polymers were reformulated in solutions containing either NMP or NMP with DMB co-solvent. The solutions were filtered prior to spin casting as explained previously. The NMP-based solutions did not gel during filtration; hence, all solutions remained candidates for spin casting studies. The spin cast samples were prepared in the same way as the fully imidized 6FDA/ODA/PEPA oligomers described in Section 4.2.4.1.1.

The results of spin casting experiments using BPDA/DAPI imide oligomers appear in Table 4.1.23. As shown, most of the films appeared smooth and clear regardless of the solvent composition and spin rate.

Small amounts of absorbed moisture from the environment seemed to have a detrimental effect on spin casting, which was similar to that found for the 6FDA/ODA imides. This was evidenced by the slight roughness of some of the films. If relatively more DMB had been incorporated in the solutions, the moisture absorption causing phase separation might have been minimized. Films exposed to high ambient humidity for a few minutes turned opaque and yellow (the color of the polyimide solid). However, once the films were immersed in nitrogen, they returned to their original clarity. If exposure to the humid environment was prolonged, clarity of the film did not return upon immersion in nitrogen nor by heating under nitrogen. The opaque yellow color apparently consisted of an oligomer precipitate.

Table 4.1.23 Qualitative Results of Spin Cast Films from Fully Imidized BPDA/DAPI/ PEPA  
Thermosetting Oligomers.

Oligomer Structure / mol. wt (Kg/mol)	Spin Rate Krpm	Solv:Co-Solv NMP:o-DMB	(w/v) Solution Concentration	Uniformity of Cured Film (cured @ 380°C 1h)
PI				
6K	4.0, 5.0, 6.0	80:20	20%	smooth, clear
	4.0, 5.0, 6.0	100:0	20%	roughness due to moisture
8K	4.0, 5.0	80:20	20%	smooth, clear
	4.0, 5.0, 6.0	100:0	20%	roughness due to moisture
10K	4.0, 5.0	80:20	20%	smooth, clear
	4.0, 5.0, 6.0	100:0	20%	smooth, clear
12K	4.0, 5.0	80:20	20%	roughness due to moisture
	4.0, 5.0, 6.0	100:0	20%	smooth, clear

In this series, the relatively lower molecular weight precursors, such as ~6- and ~8K BPDA/DAPI oligomers, had produced coherent spin cast films, which showed good qualitative adhesion to glass substrates. This was in marked contrast to the "thick" free-standing film experiments, where oligomers with  $\langle M_n \rangle$  below 12 Kg/mol had spontaneously cracked during drying. The relatively smaller thickness dimension of spin cast films provided for more rapid solvent removal prior to  $T_g$ . Thus, the molecules were able to hold together during the drying process even in the presence of strains induced by CTE mismatch. However, whether the films contained significant residual stresses following cooling remains an area to be explored in the future.

## Chapter 5 Conclusions

The main objective of this research was to synthesize and characterize reactive phenylethynyl endcapped imide oligomers for possible use as interlayer dielectric materials. The research was aimed at providing basic structure-property correlations for a series of the oligomers comprised of various backbone units with phenylethynyl phthalic anhydride (PEPA) used as endcapper. Particular emphasis was given to tailoring the physical properties by systematic variation of monomers in order to meet the requirements for dielectric materials. The amorphous, isotropic nature of the soluble imide oligomers was thought to provide a major advantage for dielectric applications. Additionally, by using processing conditions currently employed in the electronics industry (380°C for 1h), crosslinked insoluble films could be obtained by reaction of phenylethynyl groups without evolution of volatiles.

Several soluble, amorphous imide oligomers were successfully prepared using the ester-acid solution imidization method. The reactions afforded polyimides with controlled molecular weights ranging in the series from 2 to 12 Kg/mol. Most of these imides were comprised of the fluorinated monomer 4,4'-(hexafluoroisopropylidene)diphthalic anhydride (6FDA), which was found to impart solubility to the oligomer. However, when 6FDA was combined with a kink-structured diamine (such as m-phenylenediamine), the  $T_g$  values after crosslinking were just above 300°C. This was significantly below the  $T_g$  value of ~390°C for optimum performance in dielectric applications.

Attempts to raise the  $T_g$  of 6FDA-containing imides included rigidifying the backbone by incorporating stiff monomers such as p-phenylene diamine (p-PDA), biphenyldianhydride (BPDA) or diaminophenylindane (DAPI). In the cases of p-PDA and BPDA, the solubility of the oligomers was decreased, presumably due to the ordering/packing of the lower molecular

weight fractions. The resulting two-phase materials would have an adverse effect on solution casting and might result in anisotropic properties. Conversely, the incorporation of DAPI monomer provided complete solubility and raised the  $T_g$  after cure to values of 340 to 355°C, depending on the dianhydride used and the target molecular weight.

The soluble, low molecular weight series comprised of 6FDA/PEPA-containing oligomers ( $\leq 3$  Kg/mol) produced tough ductile films after melt pressing and curing. The melt-pressed crosslinked films exhibited high thermal stability, excellent solvent resistance and low water absorption. Attempts to form free-standing films from solution casting techniques did not result in cohesive samples. However, it was observed that solutions had very low solution viscosities at polymer concentrations  $\leq 50\%$  (w/v) in NMP, which may prove useful for adhesive applications where high solids contents are desirable.

To improve the film-forming properties, the ether-linked diamine 4,4'-oxydianiline (ODA) was employed in 6FDA/PEPA based imide oligomers. Simultaneously, target values for the molecular weights were raised in order to increase chain entanglements and lead to cohesive film formation by solution casting.

Free-standing films were successfully prepared using 6FDA/ODA/PEPA polyimide oligomers of ~7-, 10- and 12 Kg/mol molecular weight. Initially, cracking had been observed with solutions containing N-methyl-2-pyrrolidone (NMP). However, later it was found that the use of a binary solvent mixture in the solution (NMP:1,2-dimethoxybenzene [DMB]) improved the ability of the film to hold together. It was thought that internal strains had developed in the heated films, which resulted in stress cracking. However, when DMB was present, the cracking rarely occurred. This may have been due to the improved plasticization by DMB. An amic-acid control series of these oligomers was prepared in NMP and in NMP:DMB for comparison. The

film results were nearly identical to those of the fully imidized series, where films were successfully obtained from the NMP:DMB solutions. Intermolecular hydrogen bonding of amic-acid precursors appeared to have no influence on the film forming behavior. Perhaps it was minimized by preferential hydrogen bonding of PAA with NMP.

Spin cast films were successfully prepared using 6FDA/ODA/PEPA imide and amic-acid series. The polyimide coatings proved to be moisture-sensitive prior to solvent removal, which was evidenced by phase-separation in the form of oligomer precipitate. Spun on coatings of the amic-acids, which were relatively hydrophilic, did not exhibit precipitation and produced clear, uniform films after imidization and curing.

A relatively rigid, high  $T_g$  oligomer series based on BPDA/DAPI/PEPA was prepared and studied with respect to film-forming properties. Free-standing films were successfully prepared using the imide oligomer of  $\sim 12$  Kg/mol and binary solvent mixtures (NMP:DMB). An attempt was made to produce a free-standing film from the BPDA/DAPI oligomer of  $\sim 10$  Kg/mol, but was less successful due to brittleness.

Spin cast films having adequate to exceptional uniformity were obtained from BPDA/DAPI/PEPA oligomers of  $\sim 6$ -, 8-, 10- and 12 Kg/mol molecular weight. These coatings also proved to be moisture-sensitive prior to solvent removal, due to humidity absorbed from the environment. In most cases, this resulted in a slightly rough surface without precipitation of the oligomer.

Free-standing crosslinked films of both 6FDA/ODA/PEPA and BPDA/DAPI/PEPA had thermal stabilities comparable to that of Kapton film using isothermal TGA at  $400^\circ\text{C}$  in nitrogen. An overall weight loss of  $\leq 0.8\%$  was observed during the 2 hour period.

The solvent-resistance of these films was also excellent. Gel fractions of  $\geq 95\%$  were obtained

after immersion for 3 days in NMP at 60°C, followed by careful drying. The estimated dielectric constants of these two materials were attractively low. The value provided by the 6FDA/ODA imide film was 2.58, which was lower than that of the BPDA/DAPI (2.75) due to the higher fluorine content of the former imide.

The novel combination of low dielectric constant, solvent resistance and isotropic physical properties inherent in the thermosetting polyimide oligomers make these materials viable candidates for use as interlayer dielectrics in microelectronics packaging.

### **Suggested Future Research**

It would be of interest to further explore the utilization of 1,2-dimethoxybenzene as a solvent for fully imidized and amic-acid type oligomers as an alternative to NMP. Film thickness could be determined as a function of the solution viscosity and spin speed for oligomer solutions. Even more relevant would be spin casting oligomer solutions onto patterned thin film conductor lines. Then the degree of planarization over the metal topography could be determined, which would provide pertinent information with regard to thin film multilayer electronic packaging.

Fabrication of capacitor-type samples with the crosslinked polyimide film between two metal conductors would enable determination of the dielectric constant. The dielectric constant and dissipation factor could be studied as a function of frequency. Determining the dielectric constant during immersion in a controlled humidity/temperature chamber would reveal the insulator's reliability under conditions that simulate actual operating environments.

The mechanical properties would be of vital interest for the proposed thin film multilayer application. Reliability in terms of thin film adhesion strength and mechanical performance needs to be determined. In particular, residual stress measurements could be conducted using

samples that have been spin cast and cured on inorganic substrates. Peel strength measurements could be performed to assess the interfacial bond strength of thermosetting polyimides that have been spin cast onto a variety of inorganic substrates, as well as polyimide itself.

It would be of interest to further develop the phenylethynyl-terminated imides to provide tougher, less brittle films. A suggested strategy for doing this would involve the incorporation of a low molecular weight reactive thermoplastic as a comonomer, such as an amine-terminated polydimethylsiloxane. Important considerations in performing such modifications would be the maintenance of thermal stability, solubility of the imide precursors and high  $T_g$ .

## References

1. Critchley, J.P.; Knight, G.J.; Wright, W.W. *Heat-Resistant Polymers: Technologically Useful Materials*; Plenum: 1983.
2. Adrova, N.A.; Bessonov, M.I.; Laius, L.A.; Rudakov, A.P. *Polyimides: A New Class of Thermally Stable Polymers*; Technomic: 1970.
3. Sroog, C. E. *Prog. Polym. Sci.* **1991**, 16, 561.
4. Ghosh, M.K.; Mittal, K.L. (eds.) *Polyimides: Fundamentals and Applications*; Marcel Dekker: 1996.
5. Hedrick, J.L.; Brown, H.R.; Volksen, W.; Sanchez, M. *Polymer* **1997**, 38(3), 605.
6. Numata, S.; Fujisaki, K.; Makino, D.; Kinjo, N. In *Recent Advances in Polyimide Science and Technology*; Weber, W.D.; Gupta, M.R. (eds.); Soc. Plast. Eng.: 1985.
7. Feger, C.; Franke, H. *Polyimides in High Performance Electronics Packaging and Optoelectronic Applications*; In *Polyimides: Fundamentals and Applications*; Ghosh, M.K.; Mittal, K.L. (eds.); Marcel Dekker: 1996.
8. Wong, C.P. (ed.) *Polymers for Electronic and Photonic Applications*; Academic Press: 1993.
9. Moore, S.K. "Low-k Hits the Road"; *Chemical Week*, June 23, 1999.
10. Wilson, D.; Stenzenberger, H.D.; Hergenrother, P.M. *Polyimides*; Chapman & Hall: 1990.
11. Johnson, R.O.; Burlhis, H.S. *J. Polym. Sci.: Polym. Symp.* **1983**, 70, 129.
12. Huang, S.J.; Hoyt, A.E. *TRIP* **1995**, 3, 262.

13. Sato, M. *Polyimides*; In *Plast. Eng.: Handbook of Thermoplastics*, V. 41; Marcel Dekker: 1997.
14. Meyer, G.W. *Ph.D. Thesis*, Virginia Tech.: 1995.
15. Meyer, G.W.; J.E. McGrath *US Patent 5,493,002* (to VPI and State University): 1996.
16. Meyer, G.W.; Pak, S.J.; Lee, Y.J.; McGrath, J.E. *Polymer* **1995**, 36(11), 2303.
17. Meyer, G.W.; Glass, T.E.; Grubbs, H.J.; McGrath, J.E. *J. Polym. Sci. Part A: Polym. Chem.* **1995**, 33, 2141.
18. Sroog, C.E.; Endrey, A.L.; Abramo, S.V.; Berr, C.E.; Edwards, W.M.; Olivier, K.L. *J. Polym. Sci. Part A* **1965**, 3, 1373.
19. Edwards, W.M. *US Patent 3,179,614* (to E.I. du Pont de Nemours and Co.): 1965.
20. Edwards, W.M. *US Patent 3,179,634* (to E.I. du Pont de Nemours and Co.): 1965.
21. McGrath, J.E. "Polymers, Synthesis" *Encyclopedia of Physical Science and Technology, Vol. 13*; Academic Press: 1992.
22. Carey, F.A.; Sundberg, R.J. *Advanced Organic Chemistry, 3<sup>rd</sup> Ed., Part A: Structure and Mechanisms*; Plenum Press: 1993.
23. Svetlichnyi, V.M.; Kalnins, K.; Kudryavtsev, V.V.; Koton, M.M. *Dokl. Akad. Nauk SSSR* (Eng. Transl.) **1977**, 237(3), 693.
24. Zubkov, V.A.; Koton, M.M.; Kudryavtsev, V.V.; Svetlichnyi, V.M. *Zh. Org. Khim.* (Engl. Transl.) **1981**, 17(8), 1501.
25. Ardashnikov, A.Y<sub>A</sub>; Kardash, I.Y<sub>E</sub>; Pravednikov, A.N. *Polym. Sci. USSR* **1971**, 13(8), 2092.
26. Koton, M.M.; Kudryavtsev, V.V.; Adrova, N.A.; Kalnin'sh, K.K.; Dubnova, A.M.; Svetlichnyi, V.M. *Polym. Sci. USSR* **1974**, 16(9), 2411.

27. Bower, G.M.; Frost, L. *J. Polym. Sci.* **1963**, A1, 3135.
28. Kaas, R.L. *J. Polym. Sci.: Polym. Chem. Ed.* **1981**, 19, 2255.
29. Solomin, V.A.; Kardash, I.E.; Snagovskii, Y<sub>u</sub>.S.; Messerle, P.E.; Zhubanov, B.A.;
30. Pravednikov, A.N. *Dokl. Akad. Nauk SSSR* (Engl. Transl.) **1977**, 236(1), 510.
31. Pravednikov, A.N.; Kardash, I.Y<sub>E</sub>.; Glukhoyedov, N.P.; Ardashnikov, A.Y<sub>A</sub>. *Polym. Sci. USSR* **1973**, 15(2), 399.
32. Dine-Hart, R.A.; Wright, W.W. *J. Appl. Polym. Sci.* **1967**, II, 609.
33. Frost, L.W.; Kesse, I. *J. Appl. Polym. Sci.* **1964**, 8, 1039.
34. Kreuz, J.A.; Endrey, A.L.; Gay, F.P.; Sroog, C.E. *J. Polym. Sci.* **1966**, A-1(4), 2607.
35. Brekner, M.J.; Feger, C. *J. Polym. Sci. Part A: Polym. Chem.* **1987**, 25, 2005.
36. Volksen, W. *Adv. Polym. Sci.* **1994**, 117, 111.
37. Koton, M.M.; Meleshko, T.K.; Kudryavtsev, V.V.; Nechayev, P.P.; Kamzolkina, Y<sub>e</sub>.V. Bogorad, N.N. *Polym. Sci. USSR* **1982**, A24(4), 791.
38. Laius, L.A.; Bessonov, M.I.; Kallistova, Y<sub>e</sub>.V.; Adrova, N.A.; Florinskii, F.S. *Polym. Sci. USSR* **1967**, A9(10), 2470.
39. Pryde, C.A. *J. Polym. Sci. Part A* **1989**, 27, 711.
40. Pryde, C.A. *Polym. Sci. Part A* **1993**, 31, 1045.
41. Kailani, M.H.; Sung, C.S.P. *Macromolecules* **1998**, 31, 5771.
42. Kailani, M.H.; Sung, C.S.P. *Macromolecules* **1998**, 31, 5779.
43. Stoffel, N.C.; Kramer, E.J.; Volksen, W.; Russell, T.P. *Polymer* **1993**, 34(21), 4524.
44. Huang, W.; Tong, Y.; Xu, J.; Ding, M. *J. Polym. Sci. Part A: Polym. Chem.* **1997**, 35, 143.

45. Stoffel, N.C.; Kramer, E.J.; Volksen, W.; Russell, T.P. *J. Polym. Sci. Part B: Polym. Phys.* **1998**, 36, 2247.
46. Carter, K.R.; Srinivasan, S.A.; Hedrick, J.L.; Miller, R.D.; Lee, V.Y.; DiPietro, R.A.; Nguyen, T. In *Advances in Polyimides and Low Dielectric Polymers*; Sachdev, H.S.; Khojasteh, M.M.; Feger, C. (eds.); Soc. Plast Eng.: 1997.
47. Czorny, G.; Chen, K.R.; Prada-Silva, G.; Arnold, A.; Souleotis, H.; Kim, S.; Ree, M.; Volksen, W.; Dawson, D.; DiPietro, R. In *Proceed. 42<sup>nd</sup> Electr. Comp. And Techn. Conference*; IEEE: 1992.
48. Yoda, N.; Hiramoto, H. *J. Macromol. Sci. Chem.* **1984**, A21(13&14), 1641.
49. McKean, D.R.; Wallraff, G.M.; Volksen, W.; Hacker, N.P.; Sanchez, M.I.; Labadie, J. *ACS Symp. Series* **1994**, 537, 482.
50. Takekoshi, T. *Adv. Polym. Sci.* **1990**, 94, 1.
51. Harris, F.W.; Lin, S.-H.; Li, F.; Cheng, S.Z.D. *Polymer* **1996**, 37(22), 5049.
52. Harris, F.W.; Hsu, S. L.-C. *High Perf. Polym.* **1989**, 1(1), 3.
53. Harris, F.W.; Sakaguchi, Y.; Shibata, M.; Cheng, S.Z.D. *High Perf. Polym.* **1997**, 9, 251.
54. Chern, Y.-T.; Shiue, H.-C. *Macromolecules* **1997**, 30, 5766.
55. Yi, M.H.; Huang, W.; Jin, M.Y.; Choi, K.-Y. *Macromolecules* **1997**, 30(19), 5606.
56. Choi, K.-Y.; Yi, M.H. *Macromol. Symp.* **1999**, 142, 193.
57. Yi, M.H.; Huang, W.; Lee, B.J.; Choi, K.-Y. *J. Polym. Sci. Part A: Polym. Chem.* **1999**, 37, 3449.
58. Yi, M.H.; Huang, W.; Jung, J.T.; Kwon, S.K.; Choi, K.-Y. *J. Macromol. Sci. Pure Appl. Chem.* **1998**, A35(5), 843.

59. Yang, C.-P.; Chen, J.-A. *J. Polym. Sci. Part A: Polym. Chem.* **1999**, 37, 1681.
60. Yang, C.-P.; Chen, J.-A. *J. Appl. Polym. Sci.* **1999**, 73, 987.
61. Furukawa, N.; Yuasa, M.; Kimura, Y. *J. Polym. Sci. Part A: Polym. Chem.* **1998**, 36, 2237.
62. Tamai, S.; Yamashita, W.; Yamaguchi, A. *J. Polym. Sci. Part A: Polym. Chem.* **1998**, 36, 971.
63. Waldbauer, R.O.; Rogers, M.E.; Arnold, C.A.; York, G.A.; McGrath, J.E. *35<sup>th</sup> Int. SAMPE Symp.* **1990**, 97.
64. McGrath, J.E.; Rogers, M.E.; Arnold, C.A.; Kim, Y.J.; Hedrick, J.C. *Makromol. Chem., Macromol. Symp.* **1991**, 51, 103.
65. Rogers, M.E.; Grubbs, H.; Brennan, A.; Rodrigues, D.; Lin, T.; Marand, H.; Wilkes, G.L.; McGrath, J.E. *37<sup>th</sup> Int. SAMPE Symp.* **1992**, 717.
66. Yagci, H.; Ostrowski, C.; Mathias, L.J. *J. Polym. Sci. Part A: Polym. Chem.* **1999**, 37, 1189.
67. Ayala, D.; Lozano, A.E.; de Abajo, J.; de la Campa, J.G. *J. Polym. Sci. Part A: Polym. Chem.* **1999**, 37, 805.
68. Yang, C.-P.; Tang, S.-Y. *J. Polym. Sci. Part A: Polym. Chem.* **1999**, 37, 455.
69. Kim, Y.J.; Glass, T.E.; Lyle, G.D.; McGrath, J.E. *Macromolecules* **1993**, 26, 1344.
70. Serafini, T.T.; Delvigs, P.; Lightsey, G.R. *J. Appl. Polym. Sci.* **1972**, 16, 905.
71. Vannucci, R.D. *Proc. 32<sup>nd</sup> Intl. SAMPE Symp.* **1987**, 602.
72. Moy, T.M. *Ph.D. Thesis*, Virginia Tech.: 1993.
73. Moy, T.M.; DePorter, C.D.; McGrath, J.E. *Polymer*, **1993**, 34(4), 819.
74. Tan, B. *Ph.D. Thesis*, Virginia Tech.: 1997.

75. Tan, B.; Tchatchoua, C.N.; Dong, L.; McGrath, J.E. *Polym. Adv. Technol.* **1998**, 9, 84.
76. Farr, I.V. *Ph.D. Thesis*, Virginia Tech.: 1999;  
Farr, I.V.; Kratzner, D.; Glass, T.E.; Dunson, D.; Ji, Q.; McGrath, J.E. *J. Polym. Sci. Part A: Polym. Chem.*(Accepted) **2000**.
77. Farr, I.V.; Glass, T.E.; Ji, Q.; McGrath, J.E. *High Perf. Polym.* **1997**, 9, 345.
78. Kreuz, J.A.; Hsiao, B.S.; Renner, C.A.; Goff, D.L. *Macromolecules*, **1995**, 28, 6926.
79. Seino, H. *J. Polym. Sci. Part A: Polym. Chem.* **1999**, 37, 3584.
80. Mecham, S.J.; Dunson, D.L.; Bagwell, M.; Farr, I.V.; Ji, Q.; McGrath, J.E.  
*Unpublished results* **1999**, Virginia Tech.
80. Johnston, J.C.; Meador, M.A.B.; Alston, W.B. *J. Polym. Sci. Part A: Polym. Chem.* **1987**, 25, 2175.
81. Garcia, D. *J. Polym. Sci. Part A: Polym. Chem.* **1987**, 25, 2275.
82. Takekoshi, T.; Kochanowski, J.E.; Manello, J.S.; Webber, M.J. *J. Polym. Sci.: Polym. Symp.* **1986**, 74, 93.
83. White, D.M.; Takekoshi, T.; Williams, F.J.; Relles, H.M.; Donahue, P.E.; Klopfer, H.J.; Loucks, G.R.; Manello, J.S.; Matthews, R.O.; Schluez, R.W. *J. Polym. Sci.: Polym. Chem. Ed.* **1981**, 19, 1635.
84. Takekoshi, T.; Wirth, J.G.; Heath, D.R.; Kochanowski, J.E.; Manello, J.S.; Webber, M.J. *J. Polym. Sci.: Polym. Chem. Ed.* **1980**, 18, 3069.
85. Farrissey, W.J.; Rose, J.S.; Carleton, P.S. *J. Appl. Polym. Sci.* **1970**, 14, 1093.
86. Carleton, P.S.; Farrissey, W.J.; Rose, J.S. *J. Appl. Polym. Sci.* **1972**, 16, 2983.
87. Alvino, W.M.; Edelman, L.E. *J. Appl. Polym. Sci.* **1975**, 19, 2961.
88. Alvino, W.M.; Edelman, L.E. *J. Appl. Polym. Sci.* **1978**, 22, 1983.

89. Ghatge, N.D.; Mulik, U.P. *J. Polym. Sci.: Polym. Chem. Ed.* **1980**, 18, 1905.
90. Shinde, B.M.; Ghatge, N.D.; Patil, N.J. *J. Appl. Polym. Sci.* **1985**, 30, 3505.
91. Wenzel, M.; Ballauff, M.; Wegner, G. *Makromol. Chem.* **1987**, 188, 2865.
92. Helmer-Metzmann, F.; Ballauff, M.; Schulz, R.C.; Wegner, G. *Makromol. Chem.* **1989**, 190, 985.
93. Kakimoto, M.-A.; Akiyama, R.; Negi, Y.S.; Imai, Y. *J. Polym. Sci. Part A: Polym. Chem.* **1988**, 26, 99.
94. Sendijarevic, A.; Sendijarevic, V.; Frisch, K.C. *J. Polym. Sci. Part A: Polym. Chem.* **1990**, 28, 3603.
95. Avadhani, C.V.; Wadgaonkar, P.P.; Vernekar, S.P. *J. Polym. Sci. Part A: Polym. Chem.* **1990**, 28, 1681.
96. Kilic, S.; Mohanty, D.K.; Yilgor, I.; McGrath, J.E. *Polym. Prepr.* **1986**, 27(1), 318.
97. Takekoshi, T. *US Patent 3,847,870* (to General Electric): 1974.
98. Takekoshi, T.; Webb, J.L.; Anderson, P.P.; Olsen, C.E. *IUPAC Abstracts: 32<sup>nd</sup> Intl. Symp. on Macromol.* **1988**, 464.
99. Takekoshi, T.; Kochanowski, E.J. *US Patent 3,850,855* (to General Electric): 1974.
100. Rogers, M.E.; McGrath, J.E. *Polym. Prepr.* **1993**, 34(2), 1993.
101. Rogers, M.E.; Glass, T.E.; Mecham, S.J.; Rodrigues, D.; Wilkes, G.L.; McGrath, J.E. *J. Polym. Sci. Part A: Polym. Chem.* **1994**, 32, 2663.
102. Van Krevelen, D.W. *Properties of Polymers: Their Estimation and Correlation with Chemical Structure*; Elsevier: 1976.
103. Tummala, R.R. *Proc. IEEE* **1992**, 80(12), 1924.
104. Jensen, R.J. *ACS Symp. Ser.* **1987**, 346, 466.

105. Webster, J.R. *MS Thesis*, Virginia Tech.: 1998.
106. Sherwani, N.; Yu, Q.; Badida, S. *Introduction to Multichip Modules*; Wiley-Interscience: 1995.
107. Lai, J.H. *Polymers for Electronic Applications*; CRC Press: 1989.
108. Carter, K.R. *Review of Ultra-Low k Materials, Ultra-Low k Workshop*; ACS Division of Polymer Chemistry; Monterey, CA: Nov. 14-17, 1999.
109. Htoo, M.S., Ed. *Microelectronics Polymers*; Marcel Dekker: 1989.
110. Wong, C.P., Ed. *Polymers for Electronic and Photonic Applications*; Academic Press: 1993.
111. Flack, W.W.; Soong, D.S.; Bell, A.T.; Hess, D.W. *J. Appl. Phys.* **1984**, 58(4), 1199.
112. Soane, D.S.; Martynenko, Z. *Polymers in Microelectronics: Fundamentals and Applications*; Elsevier: 1989.
113. Jensen, R.J.; Cummings, J.P.; Vora, H. *IEEE Trans. Components, Hybrids & Manufacturing Techn.* **1984**, CHMT-7(4), 384.
114. Cheng, S.Z.D.; Arnold, F.E.; Li, F.; Harris, F.W. *TRIP* **1993**, 1(8), 243.
115. Baise, A.I. *J. Appl. Polym. Sci.* **1986**, 32, 4043.
116. Feger, C. *Polym. Eng. Sci.* **1989**, 29(5), 347.
117. De Souza-Machado, R.; Wu, S.-Y.; Denton, D.D. *Dielectric Properties of Polyimides and Factors Influencing Such Properties*; In *Polyimides: Fundamentals and Applications*; Ghosh, M.K.; Mittal, K.L. (eds.); Marcel Dekker: 1996.
118. Srinivas, S.; Caputo, F.E.; Graham, M.; Gardner, S.; Davis, R.M.; McGrath, J.E.; Wilkes, G.L. *Macromolecules* **1997**, 30, 1012.
119. Ratta, V.; Stancik, E.J.; Ayambem, A.; Pavatareddy, H.; McGrath, J.E.; Wilkes, G.L.

- Polymer* **1999**, 40, 1889.
120. Russell, T.P.; Gugger, H.; Swalen, J.D. *J. Polym. Sci.: Polym. Phys. Ed.* **1983**, 21, 1745.
  121. Russell, T.P. *J. Polym. Sci.: Polym. Phys. Ed.* **1984**, 22, 1105.
  122. Takahashi, N.; Yoon, D. Y.; Parrish, W. *Macromolecules* **1984**, 17, 2583.
  123. Yoon, D.Y.; Parrish, W.; DePero, I.E.; Ree, M. *Mat. Res. Soc. Symp. Proc.* **1991**, 227, 387.
  124. Cho, K.; Lee, D.; Lee, M.S.; Park, C.E. *Polymer* **1997**, 38(7), 1615.
  125. Bessanov, M.I.; Koton, M.M.; Kudryavtsev, V.V.; Laius, L.A. *Polyimides: Thermally Stable Polymers*; Consultants Bureau, NY: 1987.
  126. Stevens, M.P. *Chemical Structure and Polymer Morphology*; In *Polymer Chemistry: An Introduction, 2<sup>nd</sup> Ed.*; Oxford Univ. Press: 1990.
  127. Boese, D.; Herminghaus, S.; Yoon, D.Y.; Swalen, J.D.; Rabolt, J.F. *Mat. Res. Soc. Symp. Proc.* **1991**, 227, 379.
  128. Volksen, W.; Yoon, D.Y.; Hedrick, J.L.; Hofer, D. *Mat. Res. Soc. Symp. Proc.* **1991**, 227, 23.
  129. Hedrick, J.; Labadie, J.; Volksen, W. *SAMPE Proc.* **1990**, 4, 214.
  130. McGrath, J.E.; Dunson, D.L.; Mecham, S.J.; Hedrick, J.L. *Adv. Polym. Sci.* **1999**, 140, 61.
  131. Labadie, J.W.; Sanchez, M.I.; Cheng, Y.Y.; Hedrick, J.L. *Mat. Res. Soc. Symp. Proc.* **1991**, 227, 43.
  132. Carter, K.R.; DiPietro, R.A.; Sanchez, M.I.; Russell, T.P. *Chem. Mater.* **1997**, 9, 105.
  133. Jayaraman, S. *Ph.D. Thesis*, Virginia Tech.: 1995.

134. Hedrick, J.L.; Russell, T.P.; Labadie, J.W.; Lucas, M.; Swanson, S.A. *Polymer* **1995**, 36, 2685.
135. Hedrick, J.L.; Carter, K.R.; Labadie, J.W.; Miller, R.D.; Volksen, W.; Hawker, C.J.; Yoon, D.Y.; Russell, T.P.; McGrath, J.E.; Briber, R.M. *Adv. Polym. Sci.* **1999**, 141, 1.
136. Pawlowski, W.P. *Mat. Res. Soc. Symp. Proc.* **1991**, 227, 247.
137. Nomura, H.; Eguchi, M.; Niwa, K.; Asano, M. *Mat. Res. Soc. Symp. Proc.* **1991**, 227, 195.
138. Chen, S.T. *J. Electron. Mater.* **1993**, 22(7), 797.
139. Subramanian, R.; Pottiger, M.T.; Morris, J.H.; Curilla, J.P. *Mat. Res. Soc. Symp. Proc.* **1991**, 227, 147.
140. Coburn, J.C.; Pottiger, M.T.; Nader, A.E.; Pryde, C.A. *Mat. Res. Soc. Symp. Proc.* **1992**, 264, 107.
141. Sachdev, K.G.; Graham-Ode, S.; Nunes, T.L.; Sachdev, H.S. *Advances in Polyimides and Low Dielectric Polymers: Proc. 6<sup>th</sup> Intl. Conf. Polyimides*; Society of Plastics Engineers, Mid Hudson Section: 1999.
142. Cheng, S.Z.D.; Arnold, F.E.; Zhang, A.; Hsu, S.L.-C.; Harris, F.W. *Macromolecules* **1991**, 24, 5856.
143. Arnold, F.E.; Cheng, S.Z.D.; Hsu, S.L.-C.; Lee, C.J.; Harris, F.W. *Polymer* **1992**, 33(24), 5179.
144. Harris, F.W.; Hsu, S.L.-C.; Lee, C.J.; Lee, B.S.; Arnold, F.; Cheng, S.Z.D. *Mat. Res. Soc. Symp. Proc.* **1992**, 264, 3.

145. Sasaki, S.; Nishi, S. *Synthesis of Fluorinated Polyimides*; In *Polyimides: Fundamentals and Applications*; Ghosh, M.K.; Mittal, K.L. (eds.); Marcel Dekker: 1996.
146. Hasegawa, M.; Sensui, N.; Shindo, Y.; Yokota, R. *Macromolecules* **1999**, 32(2), 387.
147. Yang, C.-P.; Lin, J.-H. *J. Polym. Sci.: Part A: Polym. Chem.* **1995**, 33, 2183.
148. Hsiao, S.-H.; Liou, G.-S.; Chen, S.-H. *J. Polym. Sci.: Part A: Polym. Chem.* **1998**, 36, 1657.
149. Hsiao, S.-H.; Yang, C.-P.; Chu, K.-Y. *Macromolecules* **1997**, 30(2), 165.
150. Liaw, D.-J.; Liaw, B.-Y.; Yang, C.-M. *Acta Polym.* **1999**, 50, 332.
151. Chern, Y.-T. *Macromolecules* **1998**, 31, 5837.
152. Hedrick, J.L.; Charlier, Y.; DiPietro, R.; Jayaraman, S.; McGrath, J.E. *J. Polym. Sci.: Part A: Polym. Chem.* **1996**, 34, 2867.
153. Rogers, M.E.; Brink, M.H.; McGrath, J.E. *Polymer* **1993**, 34(4), 849.
154. Cassidy, P.E.; Aminabhavi, T.M.; Farley, J.M. *J. Macromol. Sci.-Rev. Macromol. Chem. Phys.* **1989**, C29(2&3), 365.
155. Matsuura, T.; Hasuda, Y.; Nishi, S.; Yamada, N. *Macromolecules* **1991**, 24, 5001.
156. Sasaki, S. Matsuura, T.; Nishi, S.; Ando, S. *Mat. Res. Soc. Symp. Proc.* **1992**, 264, 49.
157. Brink, M.H. *Ph.D. Thesis*, Virginia Tech.: 1994.
158. Hougham, G.; Tesoro, G.; Shaw, J. *Macromolecules* **1994**, 27(13), 3642.
159. Hedrick, J.L.; Carter, K.; Sanchez, M.; DiPietro, R.; Swanson, S. *Macromol. Chem. Phys.* **1997**, 198, 549.
160. Arnold, C.A.; Chen, Y.P.; Rogers, M.E.; Graybeal, J.D.; McGrath, J.E. *Proc. 3<sup>rd</sup> Intl. SAMPE Electron. Conf.* **1989**, June 20-22, 198.

161. White, L. E. *Ind. Eng. Chem. Prod. Res. Dev.* **1986**, 25, 395.
162. Stenzenberger, H.; Heinen, K.V.; Hummel, R.O. *J. Polym. Sci.: Part A: Polym. Chem.* **1976**, 14, 2911.
163. Hummel, R.O.; Heinen, K.V.; Stenzenberger, H. *J. Appl. Polym. Sci.* **1974**, 18, 2015.
164. Zhuang, H. *Ph.D. Thesis*, Virginia Tech.: 1998.
165. Meyer, G.W.; Heidbrink, J.L.; Franchina, J.G.; Davis, R.M.; Gardner, S.; Vasudevan, V.; Glass, T.E.; McGrath, J.E. *Polymer* **1996**, 37(22), 5077.
166. Johnston, J.A.; Li, F.M.; Harris, F.W.; Takekoshi, T. *Polymer* **1994**, 35(2), 4866.
167. Hergenrother, P.M. *J. Macromol. Sci.-Rev. Macromol. Chem.* **1980**, C19(1), 1.
168. Meyer, G.W.; Tan, B.; McGrath, J.E. *High Perf. Polym.* **1994**, 6, 423.
169. Takekoshi, T.; Terry, J.M. *Polymer* **1994**, 35(22), 4874.
170. Harris, F.W.; Pamidimukkala, A.; Gupta, R.; Das, S.; Wu, T.; Mock, G. *Polym. Prepr.* **1983**, 24, 324.
171. Harris, F.W.; Sridhar, K.; Das, S. *Polym. Prepr.* **1984**, 25, 110.
172. Hergenrother, P.M.; Smith, J.G. *Polymer* **1994**, 35(22), 4858.
173. Meyer, G.W.; Jayaraman, S.; Lee, Y.J.; Lyle, G.D.; Glass, T.E.; McGrath, J.E. *Mat. Res. Soc. Symp. Proc.* **1993**, 305, 3.
174. Meyer, G.W.; Glass, T.E.; Grubbs, H.J.; McGrath, J.E. *Polym. Prepr.* **1994**, 35(1), 549.
175. McGrath, J.E.; Meyer, G.W.; Jayaraman, S.K.; Rogers, M.E.; Lin, Y.; Wescott, J.M.; Lakshmanan, P.; Davis, R. *39<sup>th</sup> Intl. SAMPE Symp. Proc.* **1994**, 930.
176. Pickard, J.M.; Jones, E.G.; Goldfarb, I.J. *Polym. Prepr.* **1979**, 20, 370.

177. Sefcik, M.D.; Stejskal, E.O.; McKay, R.A.; Schaefer, J. *Macromolecules* **1979**, 12, 423.
178. Kovar, R.F.; Ehlers, G.F.; Arnold, F.E. *J. Polym. Sci. Polym. Chem. Ed.* **1977**, 15, 1081.
179. Swanson, S.A.; Fleming, W.W.; Hofer, D.C. *Macromolecules* **1992**, 25(2), 582.
180. Konas, M.; Moy, T.M.; Rogers, M.E.; Shultz, A.R.; Ward, T.C.; McGrath, J.E. *J. Polym. Sci., Part B: Polym. Phys.* **1995**, 33, 1429.
181. Konas, M.; May, T.M.; Rogers, M.E.; Shultz, A.R.; Ward, T.C.; McGrath, J.E. *J. Polym. Sci., Part B: Polym. Phys.* **1995**, 33, 1441.
182. Dunson, D.L.; Sankarapandian, M.; Glass, T.E.; Oyama, H.; Farr, I.V.; McGrath, J.E. *Polym. Prepr.* **1998**, 39(2), 796.
183. Dunson, D.L.; Sankarapandian, M.; Oyama, H.; Webster, J.; Barlow, F.D.; Elshabini, A.; McGrath, J.E. *Proc. IMAPS, 31<sup>st</sup> Intl. Conf. Microelectron.* **1998**, 230.
184. Conversations with R&D group managers at Hewlett-Packard and Intel, 2/00 and 3/00.
185. Gibbs, H.H.; Myrick, D.E. *33<sup>rd</sup> Intl. SAMPE Symp.* **1988**, 1473.
186. Gerber, M.K.; Pratt, J.R.; St. Clair, A.K.; St. Clair, T.L. *Polym. Prepr.* **1990**(1), 340.
187. Bateman, J.H.; Bardonia, D.A. *US Patent 3,856,752* (to Ciba-Geigy Corp.): 1974.
188. Bateman, J.H.; Geresy, W.; Neiditch, D.S. *Coatings and Plastics Prepr., ACS Div. Org. Chem. Coatings and Plastics* **1975**, 35(2), 77.
189. Falcigno, P.; Masola, M.; Williams, D.; Jasne, S. *Polyimides: Materials, Chemistry and Characterization*; Feger, C.; Khojasteh, M.M.; McGrath, J.E. (eds.); Elsevier: 1989.

190. Lee, S.K.; Cheng, S.Z.D.; Wu, Z.; Lee, C.J.; Harris, F.W. *Polym. Intl.* **1993**, 30, 115.
191. Cheng, S.Z.D.; Lee, S.K.; Barley, J.S.; Hsu, S.L.C.; Harris, F.W. *Macromolecules* **1991**, 24, 1883.
192. Tummala, R.R.; Rymaszewski, E.J.; Klopfenstein, A.G. (eds.) *Microelectronics Packaging Handbook: Semiconductor Packaging, Pt. II (2<sup>nd</sup> Ed.)*; Chapman & Hall: 1997.
193. Messner, G.; Turlik, I.; Balde, J.W.; Garrou, P.E. *Thin Film Multichip Modules*; International Society for Hybrid Microelectronics (ISHM): 1992.
194. Horie, K.; Yamashita, T. (eds.) *Photosensitive Polyimides: Fundamentals and Applications*; Technomic: 1995.
195. Tant, M.R.; Connell, J.W.; McManus, H.L.N. (eds.) *High-Temperature Properties and Applications of Polymeric Materials; ACS Symposium Series 603*; American Chemical Society: 1995.
196. Bauer, C.L.; Farris, R.J. In *Polyimides: Materials, Chemistry and Characterization*; Feger, C.; Khojasteh, M.M.; McGrath, J.E. (eds.); Elsevier: 1989.
197. Soucek, M.D.; Pater, R.H. In *Advances in Polyimide Science and Technology, Proc. 4<sup>th</sup> Intl. Conf. on Polyimides*; Feger, C.; Khojasteh, M.M.; Htoo, M.S. (eds.); Technomic: 1991.

**Debra L. Dunson**

---

- SUMMARY**
- Expertise in polymer synthesis and thermal characterization.
  - Extensive technical writing/editing skills (undergraduate minor in English, plus recent publications and related job experience).
  - Valuable managerial/teaching experience in laboratory classes at university level.

**EDUCATION**    **Ph.D. Candidate in Synthetic Polymer Chemistry**, Virginia Polytechnic Institute and State University (**VPI & SU**), Blacksburg, VA

Expected Graduation: **May 2000**

Research Area: Synthesis and Characterization of Thermosetting Polyimide Oligomers for Microelectronics Packaging

Advisor: Professor James E. McGrath, Ph.D.

**M.S. in Polymer Chemistry**, Tennessee State University (**TSU**), Nashville, TN

May 1995

Research Area: Synthesis and Characterization of Copolymers of Vinylidene Chloride and Methyl Acrylate

Advisor: Professor Edward R. Covington, Ph.D.

**B.S. in Chemistry**, Tennessee State University, Nashville, TN

August 1990, Summa Cum Laude

**A.S. in General Technology**, Nashville State Technical Institute, Nashville, TN

May 1988, Highest Honors

**HONORS**    Member of Phi Lambda Upsilon (Alpha Theta Chapter VPI & SU) 8/96 to present

**EXPERIENCE**    **GRADUATE RESEARCH ASSISTANT:**

**Doctoral: VPI & SU (8/95 to present)**

- Planned and performed synthesis and characterization of thermosetting polyimide oligomers targeted for use as interlayer dielectrics in microelectronics packaging.

**EXPERIENCE** • Investigated influence of molecular weight/backbone structure with respect to thermal and film-forming properties of oligomeric polyimides.  
**Interdisciplinary Team Member**, Investigation of Film Adhesion for Microelectronics in Cooperation with Hewlett Packard Corporation, Corvallis, OR (7/99 to present)

- Synthesized high molecular weight thermoplastic polyimides and performed basic characterization, including preparation of thin films for adhesion tests.

**Masters: TSU (5/94 – 5/95)**

- Carried out synthesis of copolymers of vinylidene chloride and methyl acrylate by emulsion polymerization.
- Studied the variations in thermal properties with regard to amount of comonomer incorporated in the polymer.

**Laboratory Manager/Instructor Tennessee State University: (TSU) (8/91 – 5/95)**

- Implemented and organized undergraduate teaching laboratories.
- Ensured proper maintenance of the new lab facilities/equipment and implemented safety training/policies for laboratory classes.
- Maintained stock chemical supplies and prepared reagents for laboratories.
- Taught two laboratory classes in organic chemistry each semester.
- Selected and scheduled the experiments to be performed in organic labs.
- Assisted Department Head and Professors in writing/editing technical publications and reports.

**ADDITIONAL TEACHING/ TECHNICAL EXPERIENCE** **INSTRUCTOR for ACS Principles of Polymerization and ACS Polymer Synthesis Short Courses: (VPI & SU) (12/95 to present)**

- Performed demonstrations in polymer synthesis involving solution, melt, interfacial, anionic, suspension and emulsion techniques.

**TEACHING ASSISTANT for Undergraduate Organic Chemistry: VPI & SU (Fall Semesters 1995 & 1998)**

- Taught undergraduate laboratory classes in basic experimental organic chemistry.

### **VPI & SU (Spring Semester 1998)**

- Taught undergraduate problem-solving in basic organic chemistry to supplement the regular lecture course and to assist the supervising professor.

### **INSTRUMENTAL ANALYSIS:**

- Experience in the use of NMR, FT/IR, TGA, DSC, DMA, TMA and Viscometry
- Orientation in the areas of GPC and MS

### **PUBLICATIONS**

"The Synthesis and Characterization of Polyimide Homopolymers Based on 5(6)-amino-1-(4-aminophenyl)-1,3,3-trimethylindane", I. V. Farr, D. Kratzner, T. E. Glass, D. Dunson, Q. Ji and J. E. McGrath, J. Polym. Sci., Part A: Polym. Chem. (Accepted 2000).

"Film Formation in Reactive Oligomeric Polyimides and Polyamic Acids", D. Dunson (presenter), S. J. Mecham, I. V. Farr, Q. Ji and J. E. McGrath, Proc. Am. Chem. Soc. Div. Polym. Mater. Sci. Eng. (PMSE), 81, 201, 1999.

"Synthesis and Characterization of Segmented Polyimide-Polyorganosiloxane Copolymers", J. E. McGrath, D. L. Dunson, S. J. Mecham and J. L. Hedrick, Adv. Polym. Sci., 140, 61, 1999.

"Evaluation of a Novel Polyimide for Use as a Low-Loss, Low Dielectric Constant Interlayer in Electronic Packaging Applications", D. L. Dunson (presenter), M. Sankarapandian, H. Oyama, J. Webster, F. D. Barlow III, A. Elshabini and J. E. McGrath, Intl. Microelectron. Packaging Soc. (IMAPS) Proc., 31<sup>st</sup> Intl. Conf. on Microelectronics, 230, 1998.

"Synthesis and Characterization of Thermosetting Fluorinated Polyimides for Microelectronics Packaging", D. L. Dunson (presenter), M. Sankarapandian, T. E. Glass, H. Oyama, I. V. Farr and J. E. McGrath, Polym. Prepr., Am. Chem. Soc. Div. Polym. Chem., 39(2), 796, 1998.